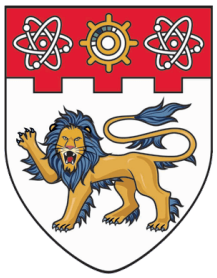

NANYANG TECHNOLOGICAL UNIVERSITY
SINGAPORE

DECELLULARIZATION OF FISH SKIN FOR TISSUE ENGINEERING APPLICATIONS

LAU CHAU SANG

School of Chemical and Biomedical Engineering

2019

DECELLULARIZATION OF FISH SKIN FOR TISSUE ENGINEERING APPLICATIONS

LAU CHAU SANG

(BAppSc (Hons), MSc)

School of Chemical and Biomedical Engineering

A thesis submitted to Nanyang Technological University

in partial fulfilment of the requirement for the degree of

Doctor of Philosophy

2019

Statement of Originality

I hereby certify that the work embodied in this thesis is the result of original research, is free of plagiarised materials, and has not been submitted for a higher degree to any other University of Institution.

06 Mar 2019

Date

Lau Chau Sang

Supervisor Declaration Statement

I have reviewed the content and presentation style of this thesis and declare it is free of plagiarism and of sufficient grammatical clarity to be examined. To the best of my knowledge, the research and writing are those of the candidate except as acknowledged in the Author Attribution Statement. I confirm that the investigations were conducted in accord with the ethics policies and integrity standards of Nanyang Technological University and that the research data are presented honestly and without prejudice.

06 Mar 2019

Date

Professor Teoh Swee Hin

Authorship Attribution Statement

This thesis contains material from one paper published in the following peer-reviewed journal where I was one of the two co-first authors.

Part of Chapter 5 was published as:

[1] C.S. Lau*, A.M. Hassanbhai*, F. Wen, P. Jayaraman, B.T. Goh, N. Yu, S.H. Teoh, In Vivo Immune Responses of Cross-Linked Electrospun Tilapia Collagen Membrane, Tissue Engineering Part A 23(19-20) (2017) 1110-1119.
* Co-first authors

The contributions of the authors are as follows:

[2] I wrote the manuscript drafts and prepared the figures. I also performed the sample preparation, physical characterisation, and analysis of the cytokine assay results.
[3] Dr Ammar Hassanbhai edited and revised the manuscript drafts, coordinated the activities in this study, and performed the *in vitro* characterisation and histological analysis.
[4] Dr Wen Feng revised the manuscript drafts, obtained approval for animal experiments in the NTU Animal Research Facility, and made arrangements for the cytokine assay.
[5] Ms Praveena Jayaraman performed the electrospinning and crosslinking of the collagen membranes.
[6] Dr Goh Bee Tin approved funding for the study and reviewed the manuscript drafts.
[7] Dr Yu Na performed the animal experiments, assisted in the *in vivo* data analysis, and was one of the corresponding authors who liaised with the journal editors.
[8] Prof Teoh Swee Hin provided the initial project direction, reviewed the manuscript drafts, and was the one of the corresponding authors who liaised with the journal editors.

06 Mar 2019

Date

Lau Chau Sang

Acknowledgements

I would like to first express my gratitude to Prof Teoh Swee Hin and Assoc Prof Wang Dongan for their guidance and enthusiasm in these four years. I especially appreciate the freedom that my supervisor Prof Teoh has entrusted in me in making major decisions, the wise advices that he gave at various stages of my project, and his numerous stories and experiences that provided abundant inspirations. I also appreciate the engaging discussions between my co-supervisor Prof Wang and me, and the fact that Prof Wang was one of the firsts who suggested and supported the idea of decellularizing fish skin.

Next, I would like to thank my mentors Dr Wen Feng and Dr Ammar Hassanbhai for their dedicated guidance and encouragement, and for sharing generously their skills, knowledges, experiences, and time with me. I would also like to thank Dr Padmalosini Muthukumaran for tirelessly helping me with the *in vivo* skin studies, and Dr Noreen Ishak for sharing her interesting experiences and being a listening ear to my grumbles.

It was (and still is) an honour to work with my collaborators from National Dental Centre Singapore (NDCS): Assoc Prof Goh Bee Tin, Dr Yu Na, Ms Nur Aishah Binte Ali and Mr Too Jianhui, and I would like to thank them for sharing their experiences from the clinical perspective and for helping me in my research planning and *in vivo* bone studies.

I would also like to thank my thesis advisory committee Asst Prof Xu Chenjie and Assoc Prof Ng Kee Woei for providing valuable inputs on my project, as well as Assoc Prof Chew Sing Yian, Assoc Prof Kathy Luo, Assoc Prof Frank Alexis and Dr Mark Chong for intellectually engaging me during my first year and inspiring me to pursue my research in tissue engineering. I am especially grateful to Dr Mark Chong for giving me an opportunity to contribute to a book chapter and for giving me numerous valuable advices.

I am thankful to my seniors Dr Akhilandeshwari Ravichandran, Dr Padmaja Anand, Dr Madhura Satish Bhave and Dr Asaf Cohen for their helpful guidance, encouragements and suggestions. I am also grateful to my ex-colleague Ms Praveena Jayaraman for her expertise and guidance in electrospinning, my ex-colleague Mr Jin Zhiyao for helping with laboratory purchases, my groupmate Ms Dong Yibing for encouraging me and helping me in administrative matters, and my groupmate Ms Luvita Suryani for her unwavering support and dedication in keeping the laboratory in order, as well as for her cheerful presence.

I am blessed to have the assistance of my school's technical staffs Dr Yu Shucong, Dr Wang Xiujuan, Dr Ong Teng Teng, Ms Chitra Devi D/O Subramaniam, Ms Latifah Binti Abd Rahman and Ms Ella Zhu regarding the school's central equipment and facilities, and I am also grateful to the staffs and students from the laboratories of Assoc Prof Sierin Lim, Prof Mary Chan and Prof Subbu Venkatraman for sharing their equipment and facilities with me.

It was a joy to mentor and work with my students Jian Xiong, Luvita, Cherminn, Joel, Diwa, Jieying, Nindya, Anh Thu, Eiden, Lyna, Dominic and Amanda. Thank you guys for adding colours and noise to my PhD chapter, and for meeting my incessant demands.

I would like to thank the NTU Research Scholarship for supporting my stay in NTU, and the NTU research grant (M4081390), NTU-NDCS joint grant (M4081405), MOE Tier 2 grant (M2016-T2-2-108), NMRC Transition Award (NMRC/TA.0045/2016), A-Star IAF-PP grant (H17/01/a0/0S9) and A-Star AMBM grant (A18A8b0059) for funding the work in this thesis.

Last but not least, I would like to express my deepest gratitude to my family members – my father Mr Andrew Lau, my mother Mdm Wong Lai Ha, and my sister Ms Lau Yu Ching for their unconditional love, support and encouragement which provide me the energy and motivation to pursue my PhD studies.

Table of Contents

Statement of Originality i
Supervisor Declaration Statement ii
Authorship Attribution Statement iii
Acknowledgements iv
Table of Contents vi
List of Publications and Conferences xi
List of Figures xii
List of Tables xviii
List of abbreviations xx
Summary xxiii
1 Introduction 1
1.1 Background 1
1.1.1 Regenerative medicine and tissue engineering 1
1.1.2 Extracellular matrix (ECM) 2
1.1.3 Fish collagen in tissue engineering 3
1.1.4 Decellularized fish tissues in tissue engineering 4
1.2 Objective and specific aims 6
1.3 Hypotheses 6
1.4 Novelty and significance 7
1.5 Scope of thesis 8
2 Literature review 9
2.1 Collagen – Structure, Synthesis & Degradation 9
2.2 Collagen-derived biomaterials 13
2.2.1 Extraction, purification and reconstitution of collagen 13
2.2.2 Decellularization of collagenous tissues 18
2.2.3 Sterilization of biologic scaffolds 22
2.3 Sources of collagen 23
2.3.1 Fish collagen as an alternative to mammalian collagen 25
2.4 Sources of decellularized tissues 27
2.4.1 Fish tissues 29
2.4.2 Reptile and amphibian tissues 31
2.4.3 Avian tissues 32
2.4.4 Current developments 33
2.5 Properties of fish skin 33

2.5.1 Anatomy and physiology of fish skin 34
2.5.2 Fish proteins and peptides 38
2.6 Nile tilapia (*Oreochromis niloticus*) 39
3 Development of crosslinked electrospun tilapia collagen scaffolds 42
3.1 Introduction 42
3.2 Methodology 46
3.2.1 Materials and reagents 46
3.2.2 Characterization with Bioinformatics 47
3.2.3 Collagen extraction 47
3.2.4 Calculation of collagen extraction yield 48
3.2.5 Electrospinning 49
3.2.6 Scanning Electron Microsopy 50
3.2.7 Differential Scanning Calorimetry 50
3.2.8 Sodium dodecyl sulphate−polyacrylamide gel electrophoresis 50
3.2.9 Indirect cytotoxicity 51
3.2.10 Cell adhesion, viability and proliferation 51
3.2.11 Statistical Analysis 52
3.3 Results and Discussion 52
3.3.1 Characterization with Bioinformatics 52
3.3.2 Yield of extracted collagen and 57
3.3.3 Electrospinning of tilapia collagen – optimisation of parameters 58
3.3.4 Fabrication of crosslinked electrospun collagen scaffolds 62
3.3.5 Differential Scanning Calorimetry 64
3.3.6 Sodium dodecyl sulphate−polyacrylamide gel electrophoresis 66
3.3.7 Indirect cytotoxicity 68
3.3.8 Cell adhesion and proliferation 70
3.4 Conclusion 72
4 Decellularization of tilapia skin 73
4.1 Introduction 73
4.2 Methodology 76
4.2.1 Materials 76
4.2.2 Decellularization of fish skin – process optimization 76
4.2.3 Determination of DNA and collagen content 78
4.2.4 Scanning Electron Microsopy 78
4.2.5 Hematoxylin & eosin histology 79
4.2.6 Determination of sodium dodecyl sulphate content 79

4.2.7 Determination of elastin and glycosaminoglycan content 80
4.2.8 Determination of amino acid content 80
4.2.9 Tensile test 80
4.2.10 Differential Scanning Calorimetry 81
4.2.11 Statistical Analysis 81
4.3 Results and Discussion 82
4.3.1 Decellularization of fish skin 82
4.3.2 Determination of sodium dodecyl sulphate content 87
4.3.3 Determination of elastin and glycosaminoglycan content 88
4.3.4 Determination of amino acid content 90
4.3.5 Tensile test 92
4.3.6 Differential Scanning Calorimetry 98
4.4 Electricity – a novel agent to decellularize tilapia skin 99
4.4.1 Introduction 99
4.4.2 Methodology 100
4.4.3 Results and discussion 101
4.5 Conclusion 105
5 Biological evaluation of tilapia scaffolds 107
5.1 Introduction 107
5.2 Methodology 110
5.2.1 Materials 110
5.2.2 Sample preparation 111
5.2.3 Human serum based Immunohistochemical analysis 112
5.2.4 Human serum based ELISA 113
5.2.5 Indirect cytotoxicity 114
5.2.6 Cellular biocompatibility 115
5.2.7 In vivo experiments in rats 115
5.2.8 Cytokine analysis via cage implant system 115
5.2.9 Subcutaneous implantation 116
5.2.10 Statistical Analysis 116
5.3 Results and discussion 117
5.3.1 Immunohistochemical analysis 117
5.3.2 ELISA analysis 118
5.3.3 Indirect cytotoxicity 121
5.3.4 Cellular biocompatibility 122
5.3.5 Cytokine analysis 124

5.3.6 Subcutaneous implantation 128
5.4 Conclusion 131
6 Evaluation of tilapia scaffolds for tissue engineering applications 133
6.1 Introduction 133
6.1.1 Guided bone regeneration 134
6.1.2 Skin wound healing 135
6.2 Methodology 136
6.2.1 Materials 136
6.2.2 Sample preparation 136
6.2.3 Water Contact Angle 138
6.2.4 Porosity 138
6.2.5 Water permeability 139
6.2.6 Degradation 140
6.2.7 In vitro bone regeneration 141
6.2.8 In vivo bone regeneration 142
6.2.9 Acid/alkali treatment of decellularized tilapia skin 143
6.2.10 In vitro skin regeneration 144
6.2.11 In vivo skin regeneration 144
6.2.12 Statistical analysis 145
6.3 Results and discussion 146
6.3.1 Water contact angle, porosity and water permeability 146
6.3.2 Degradation 148
6.3.3 In vitro bone regeneration 150
6.3.4 In vivo bone regeneration 155
6.3.5 Acid/alkali treatment of decellularized tilapia skin 161
6.3.6 In vitro skin regeneration 165
6.3.7 In vivo skin regeneration 167
6.4 Conclusion 173
7 Conclusion and future work 176
7.1 Conclusions 176
7.2 Recommendations for future work 179
7.2.1 Further characterisation of fish skin components 179
7.2.2 Investigation of antimicrobial properties 180
7.2.3 Further optimisation of electric decellularization 182
7.2.4 Decellularization using supercritical carbon dioxide 182
7.2.5 Decellularization of tissues from other fish species 183

7.2.6 Investigation of mechanisms behind enhanced healing.....185
8 Reference.....188

List of Publications and Conferences

Journal publication

[1] C.S. Lau, A.M. Hassanbhai, F. Wen, P. Jayaraman, B.T. Goh, N. Yu, S.H. Teoh, In Vivo Immune Responses of Cross-Linked Electrospun Tilapia Collagen Membrane, Tissue Engineering Part A 23(19-20) (2017) 1110-1119.

[2] C.S. Lau, A.M. Hassanbhai, F. Wen, D. Wang, B.T. Goh, N. Yu, S.H. Teoh, Evaluation of Decellularized Tilapia Skin as a Tissue Engineering Scaffold, Journal of Tissue Engineering and Regenerative Medicine, **accepted for publication in June 2019.**

Book chapter

[1] F. Wen, C.S. Lau, J. Lim, Y. Liao, S.H. Teoh, M.S.K. Chong, Surface Modification of Tissue Engineering Scaffolds, Chapter in "Polymeric Biomaterials for Tissue Regeneration", edited by C. Gao, 2016, Springer, Singapore, pp 123-150

Conference

[1] C.S. Lau, A.M. Hassanbhai, F. Wen, P. Jayaraman, D. Wang, N. Yu, S.H. Teoh, Evaluation of tilapia collagen membrane for guided bone regeneration, Singhealth-NTU Joint Research Day 2016, 29th September 2016, National Dental Centre Singapore, Singapore

[2] C.S. Lau, A.M. Hassanbhai, F. Wen, P. Jayaraman, D. Wang, N. Yu, S.H. Teoh, A comparative study on the use of tilapia collagen membrane for guided bone regeneration, Society for Biomaterials 2017 Annual Meeting, 4th – 8th April 2017, Minneapolis Convention Centre, Minneapolis, USA

[3] C.S. Lau, A.M. Hassanbhai, F. Wen, P. Jayaraman, D. Wang, N. Yu, S.H. Teoh, Collagen scaffolds from tilapia – A comparative study for guided bone regeneration, 9th International Conference on Materials for Advanced Technologies, 18th – 23rd June 2017, Suntec Convention & Exhibition Centre, Singapore

[4] C.S. Lau, A.M. Hassanbhai, F. Wen, P. Jayaraman, D. Wang, N. Yu, S.H. Teoh, Collagen scaffolds from tilapia for guided bone regeneration, Advances in Tissue Engineering 26th Annual Short Course, 8th – 11th August 2018, Rice University, Houston, USA

Award

[1] C.S. Lau, A.M. Hassanbhai, F. Wen, B.T. Goh, S.H. Teoh, N. Yu, Evaluation of fish-derived scaffolds for guide bone regeneration, Singapore General Hospital 23rd Annual Scientific Meeting, 12th April 2019, Singapore General Hospital, Singapore – Best Poster Award: Basic/Translational Research

List of Figures

Figure 2.1	Structure of collagen from the fibre level to the molecule level. Numbers below each term indicates the diameter of the single structure. (Figure adopted from [36] with permission from Elsevier B.V.)	10
Figure 2.2	Simplified schematic drawing of (a) human and (b) fish skin. Major cell types and appendages are represented and listed in the legend. Several cell types such as mast cells or merkel cells are present in human and fish skin but are not shown. [172] (Figure reused with permission from Journal of Investigative Dermatology)	35
Figure 3.1	Schematic diagram of a basic electrospinning process [205] (Figure reused with permission from Elsevier B.V.)	44
Figure 3.2	BLAST analysis of amino acid sequence alignment between human pro-collagen type I α_1 (Query) and tilapia pro-collagen type I α_1 (Sbjct). The row between Query and Sbjct represents identical and positive amino acids between the two sequences. Glycine (G) is highlighted in blue and proline (P) is highlighted in purple.	56
Figure 3.3	SEM images of electrospun mat with optimized parameters: (A) 8% tilapia scale collagen in 50:50 20xPBS:ethanol (1000x), (B) 8% tilapia scale collagen in 40:60 20xPBS:ethanol (1000x), (C) 8% tilapia skin collagen in 50:50 20xPBS:ethanol (1000x), (D) 8% tilapia skin collagen in 40:60 20xPBS:ethanol (1000x), (E) 8% tilapia skin collagen in 40:60 20xPBS:ethanol (5000x), (F) 8% tilapia skin collagen in HFIP (1000x), (G) 8% tilapia skin collagen in HFIP (5000x)	60
Figure 3.4	SEM images (1000x) of tilapia skin collagen scaffolds electrospun with 40:60 20xPBS:ethanol. (A) Tilapia skin collagen scaffold without crosslinking, (B) Tilapia skin collagen scaffold crosslinked by glutaraldehyde vapour for 4 hours, (C) Tilapia skin collagen scaffold crosslinked by EDC/NHS in ethanol for 24 hours	62
Figure 3.5	SDS-PAGE characterization of TSC (tilapia skin collagen), RTC (rat tail collagen), TSC in PBS:EtOH (tilapia skin collagen dissolved in 40:60 20x PBS:ethanol), TSC-ES (electro-spun tilapia skin collagen), TScC (tilapia scale collagen), TSC-GTA (glutaraldehyde crosslinked electro-spun tilapia skin collagen), and TSC-EDC (EDC/NHS crosslinked electro-spun tilapia skin collagen). Molecular markers were added on the leftmost lane and the marker bars indicate the protein's molecular weight in kDa.	67
Figure 3.6	Indirect cytotoxicity studies of TSC-GTA (glutaraldehyde crosslinked electro-spun tilapia skin collagen) and TSC-EDC (EDC/NHS crosslinked electro-spun tilapia skin collagen) by determining the metabolic function of murine fibroblast L929 with AlamarBlue assay. The samples were assayed after 24h incubation and the fluorescence intensity values were normalized against the non-toxic control. *$p < 0.05$ when compared to HDPE (non-toxic control).	69

Figure 3.7 Biocompatibility of TSC-GTA (glutaraldehyde crosslinked electro-spun tilapia skin collagen) and TSC-EDC (EDC/NHS crosslinked electro-spun tilapia skin collagen) with L929 fibroblasts determined by the cellular metabolic function with AlamarBlue assay. No statistical differences ($p < 0.05$) were observed between all groups at each time point, but for every sample, the cellular metabolic activities on Day 3 and 7 were significantly higher ($p < 0.05$) than those on Day 1 and Day 3 respectively. 70

Figure 4.1 Visual appearance of (A) native tilapia skin, (B) tilapia skin treated with 1% SDS in PBS for 6 hours, (C) tilapia skin treated with 1% triton-X in PBS for 6 hours, (D) tilapia skin treated with 2.5U/ml dispase for 3 hours and 1% SDS in PBS for 6 hours. (E) DNA quantitation of treated tilapia skins compared to native samples, $n \geq 3$. Dotted line at 50 ng DNA/mg tissue indicates recommended limit to avoid immunological response [26]. * $p < 0.05$ when compared to native skin. # $p < 0.05$ when compared to skin treated by SDS only. (F) Collagen quantitation of treated tilapia skins compared to native samples, $n \geq 3$. No significant difference ($p < 0.05$) were observed between groups. 83

Figure 4.2 Hematoxylin & Eosin stained histological images of (A) native tilapia skin, sagittal view, (B) decellularized tilapia skin, sagittal view, (C) native tilapia skin, cross-sectional view, and (D) decellularized tilapia skin, cross-sectional view. Cell nuclei are visible in (A) and (C) as blue spots. Scale bars are 100 μm. 86

Figure 4.3 SEM images of (A) inner surface of native tilapia skin, (B) cross-sectional view of native tilapia skin, (C) inner surface of decellularized tilapia skin (treated by dispase, SDS, and nuclease), and (D) cross-sectional view of decellularized tilapia skin. Scale bars are 10 μm. 86

Figure 4.4 SDS concentration in rinse solutions and storage solutions. The rinses were performed after the skin was immersed in 1% SDS for 1 hour, and each rinse was performed for 10 minutes at 100 rpm on an orbital shaker. The rinse solutions were collected at the end of the 10 minute rinse. The storage solution was sampled after the decellularized skin was immersed for 24 hours post-rinsing. * $p < 0.05$ when compared to water. 87

Figure 4.5 (A) Representative diagram of the two locations and two pulling directions for the tensile testing of native tilapia skin, (B) Young modulus of native tilapia skin at two locations under two pulling directions, (C) Maximum tensile stress of native tilapia skin at two locations under two pulling directions, and (D) Maximum strain of native tilapia skin at two locations under two pulling directions. * $p < 0.05$ when compared to D-V. Note: 1 MPa (Mega Pascal) = 1 N/mm2 93

Figure 4.6 Typical stress-strain graph for tensile test. The stress, σ was calculated by dividing the tensile force by the original cross sectional area of the sample, while the strain, ε was calculated by diving the extended length of the sample by the initial length. The Young Modulus, E is defined as the steepest slope on the stress-strain curve and is a measure of the stiffness of a material. The maximum stress, σ_{max} and maximum strain, 94

ε_{max} occur at the point where the sample reached the maximum extension just before failure.

Figure 4.7 (Top) Representative diagram of the alignment of the collagen fibre in the anterodorsal-posteroventral (AD-PV) direction shown in red, and in the anteroventral-posterodorsal (AV-PD) direction shown in blue, with respect to the fish body. (Below) Representation diagram of how the collagen fibres align with the direction of pull when the skin was pulled in a D-V direction, and how the collagen fibres become further apart when then skin was pulled in a A-P direction. 95

Figure 4.8 Circuit diagram of the electroporation set-up. 101

Figure 4.9 (A) DNA content and (B) collagen content in tilapia skin treated with electroporation of varying voltage (V = 10-15V, 23-35V, 55-60V, 80-90V), at f = 1 Hz and t = 60 s. * $p < 0.05$ when compared to control (native tilapia skin). 102

Figure 4.10 (A) DNA content and (B) collagen content in tilapia skin treated with electroporation of varying frequency (f = 0.5 Hz, 1 Hz, 2 Hz), at V = 23-35 V and t = 60 s. * $p < 0.05$ when compared to control (native tilapia skin), # $p < 0.05$ when comparing between 1 Hz and 2 Hz. 102

Figure 4.11 H&E histological images of tilapia skin (A) before and (B) after electroporation. Images taken at 940X magnification by Leica DVM6 microscope (Germany). E = epidermis, Me = melanophores. Electroporation parameters: V = 23-35 V, f = 1 Hz, t = 60 s. 103

Figure 5.1 Cross-sectional immunohistochemical staining of (A) native tilapia skin, (B) decellularized tilapia skin (DTS), (C) native tilapia skin (no primary staining), (D) porcine artery. Tissue samples were fixed in Carnoy buffer, dehydrated, embedded in paraffin, and sectioned to 5 µm. Slides except (C) were treated with human serum as primary antibody. All slides were then treated with peroxidase-linked anti-Ig (G, A, M) antibodies as secondary antibodies, followed by staining with DAB substrate and hematoxylin. Brown areas indicate DAB staining of antigens and purple/blue areas indicate hematoxylin staining of DNA. 117

Figure 5.2 Immunogenic potentials of native tilapia skin, DTS, CETC (crosslinked electrospun tilapia collagen) and porcine artery detected by ELISA. Plates were coated with diluted protein extracts of the samples and blocked with 0.5% fish gelatin. Primary staining was done with human serum, secondary staining was done with peroxidase-linked antibodies, and detection was done with TMB substrate. * $p < 0.05$ when compared to native tilapia skin. # $p < 0.05$ when compared to CETC. 119

Figure 5.3 Metabolic activity of L929 cells after incubation in sample extract determined by AlamarBlue assay, and cell permeability determined by visually checking both sides of the samples with SEM. For metabolic function, the samples were assayed after 24 hours incubation and the fluorescence intensity values were normalised against the non-toxic control. 121

Figure 5.4 Cell viability on CETC (crosslinked electrospun tilapia collagen) and DTS (decellularized tilapia skin), represented by the relative metabolic activity of L929, as determined by direct AlamarBlue assay. No significant differences ($p < 0.05$) were observed between groups at each time-point, but within each group, the metabolic activity at Day 3 or Day 7 was significantly higher ($p < 0.05$) than that at the previous time-point. 123

Figure 5.5 Levels of pro-inflammatory and pro-healing cytokines in rat exudates on 1, 2, 7 and 14 days after subcutaneous implantation of empty cages, cages with Bio-Gide®, cages with crosslinked electrospun tilapia collagen (CETC) and cages with decellularized tilapia skin (DTS). IL = interleukin, TNF-α = tumour necrosis factor alpha, VEGF = vascular endothelial growth factor 125

Figure 5.6 Figure 5.6: Levels of pro-inflammatory/pro-healing and anti-inflammatory/anti-healing cytonkines in rat exudates on 1, 2, 7 and 14 days after subcutaneous implantation of empty cages, cages with Bio-Gide®, cages with crosslinked electrospun tilapia collagen (CETC) and cages with decellularized tilapia skin (DTS). IL = interleukin, MCP-1 = monocyte chemoattractant protein 1 126

Figure 5.7 Histology sections of the subcutaneous implants stained with H&E. Control represents native tissue without any implants. The implants are highlighted with a blue line to indicate their location. Sections are representative of the samples. Scale bars are 100 μm. 129

Figure 6.1 Degradation profile of DTS and CETC in (A) sterile PBS and (B) 200 U/ml collagenase. Samples were incubated in individual sterile tubes at 37°C and the dry weight or hydroxyproline content of each sample was measured before and after the incubation. 148

Figure 6.2 Cell attachment and proliferation were evaluated at Day 1, 3 and 7 after MC-3T3 cells were seeded onto the different membranes. (A) Scanning electron microscopy of membrane surfaces. Micrographs are respective of each sample. (B) AlamarBlue assay with fluorescence as an indication of metabolic activity. Blank = polystyrene well plate. * $p < 0.05$ when compared to blank at each respective time point. # $p < 0.05$ when compared to DTS at each respective time point. DTS- Decellularized tilapia skin; CETC- Cross-linked tilapia collagen. 151

Figure 6.3 RT-PCR of genes related to osteogenic differentiation – BSP, OC and OPN, normalised to the expression of GAPDH. MC-3T3 cells were grown on the membranes and the relative expression of mRNA was quantified at Day 21. * $p < 0.05$ when compared to cells grown in normal growth media (O-). 152

Figure 6.4 The calcium deposition by MC-3T3 cells on DTS and CETC were evaluated after seeding and incubation in osteogenic medium. (A) Samples were Von Kossa stained at Day 7, 14 and 21. Areas that appear dark indicate the presence of phosphate and suggest calcium deposition. (B) Calcium depositions from MC-3T3 cells were quantified and normalized against DNA content at Day 14 and Day 21. The calcium 154

content were compared between cells grown in normal growth media (O-) and cells grown in osteogenic differentiation media (O+). * $p < 0.05$ when compared to cells grown in normal growth media (O-) at same time-point.

Figure 6.5 Rat calvarial defects (10mm) with test membranes. DTS – decellularized tilapia skin; CETC – cross-linked electrospun tilapia collagen. 156

Figure 6.6 Micro-CT analysis of the calvarial defects treated with different membranes at Day 14 and 42. (A) Reconstruction of the defects using micro-CT taken at Day 14 and 42 for each of the test samples. Dotted circle represents initial defect diameter of 10mm, pink colour represents regenerated bone. Images shown here are representative of the samples. (B) Scoring of extent of bone union on the calvarial defects (n=6 per group) after 42 days. Scoring: 0– No bone formation within defect; 1– Few bony spicules dispersed through defect; 2– Bony bridging only at defect borders; 3– Bony bridging over partial length of defect; 4 – Bony bridging entire span of defect at longest point (10 mm) [339] 157

Figure 6.7 H&E staining of cross section of the defect site at Day 14. A) Sham, B) DTS, decellularized tilapia skin C) CETC, cross-linked electrospun tilapia collagen. The region of interest is indicated by a black box and is magnified. Scale bar represents 250μm 159

Figure 6.8 H&E staining of cross section of the defect site at Day 42. A) Sham, B) DTS, decellularized tilapia skin C) CETC, cross-linked electrospun tilapia collagen. The region of interest is indicated by a black box and is magnified. Scale bar represents 250μm 159

Figure 6.9 Cell attachment and proliferation were evaluated with AlamarBlue assay at Day 1, 3 and 5 after human dermal fibroblasts (HDFs) were seeded onto tilapia skins treated in different conditions. The fluorescence level was used as an indication of relative metabolic activity of HDFs. Blank = polystyrene well plate. No significant difference ($p < 0.05$) were observed between groups at each time point and between time points for each group. DTS = Decellularized tilapia skin; DTS-N = Alkali-treated decellularized tilapia skin. 165

Figure 6.10 Cell attachment and viability were evaluated with Live/Dead® cytotoxicity kit at Day 1 and 5 after human dermal fibroblasts (HDFs) were seeded onto tilapia skins treated in different conditions. Live cells were dyed green by calcein-AM, and dead cells were dyed red by ethidium homodimer-1. 166

Figure 6.11 Murine wound healing model. (A) View of the mouse immediately after surgery. (B) View of the same mouse one week later, after sacrifice. In this model two full thickness wounds are created on either side of the midline allowing each mouse to serve as their own control. The left wound was left untreated while the right wound was covered with the sample of interest. Silicone splints are fixed to the wound perimeter by suture to prevent wound contraction, providing a model relevant to that of human wounds. 168

Figure 6.12 Wound healing in BALB/c mice. (A) Representative images of skin wounds after treatment with native tilapia skin, DTS (decellularized tilapia skin), DTS-N (alkali-treated decellularized tilapia skin) or Duoderm, with untreated wounds as control (n = 3). The circular splint has an inner diameter of 6 mm and an outer diameter of 12 mm. For wounds with detached splints, the inner circumference of the splint was indicated with a blue dashed line. (B) Wound area quantified at 1 week and 2 weeks after surgery. 169

Figure 6.13 Representative images of cross-sectional H&E stained sections of mouse skin wounds covered with native tilapia skin, DTS (decellularized tilapia skin), DTS-N (alkali-treated decellularized tilapia skin) or DuoDerm, with untreated wounds as control (n = 3). Scalebar represents 50 μm. 170

Figure 6.14 Wound healing scores of native tilapia skin, DTS (decellularized tilapia skin), DTS-N (alkali-treated decellularized tilapia skin) and DuoDerm, according to the score system listed in Table 6-4. 172

List of Tables

Table 1-1	Number of results based on the following search terms in scientific database Web of Science (https://apps.webofknowledge.com) and biomedical database PubMed (https://www.ncbi.nlm.nih.gov/pubmed). Search was performed on 01 Feb 2019.	5
Table 2-1	Currently applied fabrication techniques and applications for various physical forms of collagen-derived biomaterials [34]	14
Table 2-2	Commonly used methods of decellularization of animal tissues, their modes of action and their effects on ECM [26, 27]	19
Table 2-3	Summary of commercially available decellularized ECM products, arranged by species [25, 56]. At the time of writing there is only one FDA-approved non-mammalian decellularized ECM product – MariGen™ Omega3 from Kerecis. The other decellularized ECM products are all from mammalian sources. (C-link. = crosslinked, DS = dry sheet, HS = hydrated sheet, SIS = small intestinal submucosa)	28
Table 3-1	Theoretical properties and theoretical amino acid content of pro-collagen type 1 chains from human (*Homo sapiens*), Cow (*Bos taurus*), Rat (*Rattus norvegicus*) and Nile Tilapia (*Oreochromis niloticus*) using the Expasy ProtParam tool (https://web.expasy.org/protparam). pI = isoelectric point.	53
Table 3-2	Alignment results of pro-collagen type 1 from human (*Homo sapiens*), Cow (*Bos taurus*), Rat (*Rattus norvegicus*) and Nile Tilapia (*Oreochromis niloticus*) using BLAST. "Identities" refer to amino acids that are identical between the two sequences, "positives" refer to amino acids that are identical or have similar chemical properties between the two sequences, and "gaps" refer to amino acids that are not "identities", not "positives" or missing in either sequence.	56
Table 3-3	Yield of collagen extraction from tilapia skin, tilapia scale and rat tail	57
Table 3-4	Effect of different electrospinning parameters on the diameter of electrospun fibres from 8% (w/v) tilapia skin collagen in 50:50 20xPBS:ethanol.	59
Table 3-5	Fibre diameters of tilapia skin scaffolds electrospun from 8% (w/v) tilapia skin collagen in 40:60 20xPBS:ethanol and crosslinked in different reagents.	62
Table 3-6	Denaturation temperatures of collagen sponges, electrospun collagen scaffolds and crosslinked electrospun collagen scaffolds. Samples were rehydrated to mimic physiological conditions before measurement.	64
Table 4-1	Steps taken during the optimization of the decellularization process	78
Table 4-2	Elastin and GAG content in native and decellularized tilapia skin quantified by Fastin Elastin assay and Blyscan GAG assay.	89

Table 4-3	Amino acid analysis of native tilapia skin, decellularized tilapia skin and lyophilised tilapia collagen. For the theoretical amino acid content, the value for each amino acid were derived by dividing the sum of that amino acid in the α1, α2 and α3 pro-collagen type 1 chains by the sum all all amino acids in all three chains. Asparagine and glutamine are converted to aspartic acid and glutamic acid during the hydrolysis process and therefore counted together with aspartic acid and glutamic acid respectively. Cysteine and tryptophan are unstable during the hydrolysis and cannot be quantified, but their absences do not affect the results due to their low abundance in tilapia collagen (<1% theoretical content). Numbers are expressed as percentage (%) of total number of amino acid residues.	90
Table 4-4	Maximum tensile stress and Young's modulus of native tilapia skin, decellularized tilapia skin and lyophilized & rehydrated decellularized skin (isolated near the head and pulled in the D-V direction). The mechanical properties of porcine acellular dermal matrix (Strattice, Lifecell, USA) and bovine acellular dermal matrix (SurgiMend, TEI Biosciences, USA) reported by Adelman et al.[264], human skin reported by Ni Annaidh et al [265], electrospun tilapia collagen and glutaraldehyde-crosslinked electrospun tilapia collagen reported in Chapter 3, were included for comparison and reference. Note: 1 MPa (Mega Pascal) = 1 N/mm2	96
Table 4-5	Denaturation temperature and denaturation enthalpy of native tilapia skin and decellularized tilapia skin, determined by Differential Scanning Calorimetry (DSC).	98
Table 4-6	Parameters for the electroporation of tilapia skin	101
Table 6-1	RT-PCR primer sets (AIT Biotech, Singapore)	142
Table 6-2	Contact angle, porosity and water permeability of CETC and DTS	146
Table 6-3	Physical, chemical and biological properties of native tilapia skin, DTS, DTS-A and DTS-N. * $p < 0.05$ when compared to DTS.	163
Table 6-4	Definition of terms in the scoring system of wound-healing	172
Table 7-1	The 20 most produced fish species in global aquaculture and their production levels in 2010 and 2016 (in 1000 tonnes) [360]	184

List of abbreviations

3D	Three-dimensional
A-P	Anterior-posterior
AD-PV	Anterodorsal-posteroventral
AMP	Anti-microbial peptide
ARF	Animal Research Facility
AV-PD	Anteroventral-posterodorsal
BHA	Butylated hydroxyanisole
BHT	Butylated hydroxytoluene
BLAST	Basic local alignment search tool
BSE	Bovine spongiform encephalopathy
BSP	Bone sialoprotein
CETC	Crosslinked electrospun tilapia collagen
CSD	Critical size defect
DAB	3,3′-Diaminobenzidine
D-V	Dorsal-ventral
DC	Direct current
DHT	Dehydrothermal
DI	Deionised
DIS	Draft International Standard
DMEM	Dubecco's Modified Eagle's Medium
DNA	Deoxyribonucleic acid
DSC	Differential scanning calorimetry
DTS	Decellularized tilapia skin
DTS-N	Sodium hydroxide-treated decellularized tilapia skin
E	Young Modulus
ECM	Extracellular matrix
EDC	1-ethyl-3-(3-dimethylaminopropyl) carbodiimide
EDTA	Ethylenediaminetetraacetic acid
ELISA	Enzyme-linked immunosorbent assay
ES	Electrospun
FBR	Foreign body reaction

FBS	Fetal bovine serum
FDA	Food and Drug Administration
GAG	Glycosaminoglycan
GAPDH	Glyceraldehyde 3-phosphate dehydrogenase
GBR	Guided bone regeneration
GTA	Glutaraldehyde
H&E	Hematoxylin & eosin
HAR	Hyperacute rejection
HCl	Hydrochloric acid
HDF	Human dermal fibroblast
HDPE	High-density polyethylene
HFIP	Hexafluoroisopropanol
HPLC	High pressure liquid chromatography
IACUC	Institutional Care and Use Committee
Ig	Immunoglobulin
IHC	Immunohistochemcial
IL	Interleukin
IRE	Irreversible electroporation
ISO	International Organization for Standardization
MCP	Monocyte chemoattractant protein
MEM-α	Minimum essential media-alpha
MHC	Major histocompatibility complex
Micro-CT	Microcomputed tomography
MMP	Matrix metalloproteinase
mRNA	Messenger ribonucleic acid
NaCl	Sodium chloride
NACLAR	Singapore's National Advisory Committee for Laboratory Animal Research
NaOH	Sodium hydroxide
NHS	N-hydroxy-succinimide
NTU	Nanyang Technological University
OC	Osteocalcin
OPN	Osteopontin

PBS	Phosphate-buffered saline
PBS-T	Phosphate-buffered saline with 0.05% Tween-20
PCL	Polycaprolactone
pI	Isoelectric point
PLGA	Poly-lactic/co-glycolic acid
PTFE	Polytetrafluoroethylene
RNA	Ribonucleic acid
RT-PCR	Real-time polymerase chain reaction
RTC	Rat tail collagen
SD	Standard deviation
SDS	Sodium dodecyl sulphate
SDS-PAGE	Sodium dodecyl sulphate−polyacrylamide gel electrophoresis
SEM	Scanning electron microscopy
SIS	Small intestinal submucosa
T_d	Denaturation temperature
TMB	3,3',5,5'-Tetramethylbenzidine
TNF-α	Tumour necrosis factor alpha
TS	Tilapia skin
TSC	Tilapia skin collagen
TSc	Tilapia scale
TScC	Tilapia scale collagen
USA	United States of America
UV	Ultraviolet
VEGF	Vascular endothelial growth factor
ZDEC	Zinc diethyldithiocarbamate
α-Gal	Galactose-alpha-1,3-galactose
ε_{max}	Maximum tensile strain
σ_{max}	Maximum tensile stress

Summary

Collagen is a popular biomaterial in tissue engineering due to its natural abundance and excellent biocompatibility. However, most commercial collagen comes from porcine and bovine sources, which have a risk of transmissible diseases and are unsuitable for patients with religious restrictions. Fish-derived collagen scaffolds are gaining attention due to their low immunological risk and the abundance of collagen in fish waste such as skin and scales. Among the various fish types, Nile Tilapia (*Oreochromis niloticus*), a tropical freshwater fish native to Africa, is lauded as a promising source of collagen due to its rapid growth rate and high protein content. Tilapia collagen scaffolds can be formed by reconstituting collagen extracted from tilapia skin, or by removing cells from tilapia skin in a process known as decellularization. While reconstituted tilapia collagen had been studied in tissue engineering, there was very little information on the decellularization of tilapia tissues. This revealed a great potential and novelty for decellularized tilapia skin to be used as a tissue engineering scaffold and to address the growing demand for tissue constructs. In this thesis, we hypothesized that (1) tilapia skin could be decellularized using appropriate treatments to yield an acellular scaffold, (2) the decellularized tilapia skin (DTS) would possess favourable physical and biological properties, and (3) the DTS would be suitable as a scaffold in tissue regeneration.

As collagen accounts for more than 90% of the dry weight of the extracellular matrix (ECM) in most tissues including fish skin, the properties of tilapia collagen was studied via bioinformatics characterisation and development of a crosslinked electrospun tilapia collagen (CETC) scaffold, to facilitate the understanding of tilapia skin ECM in subsequent experiments and to compare the advantages and disadvantages between collagen reconstitution and decellularization. The bioinformatics characterisation revealed a high level of conservation between tilapia collagen and mammalian collagen, suggesting that tilapia collagen would be

well-tolerated by mammals. We also successfully electrospun tilapia skin collagen into well-defined nanofibrous mats using a novel non-toxic PBS/ethanol solvent, and demonstrated that the CETC scaffold was non-cytotoxic and support cellular proliferation.

To develop tilapia skin into a decellularized scaffold suitable for tissue engineering, the decellularization process had to be designed and optimised to maximise the removal of immunogenic cellular materials and to minimize damage to the extracellular matrix. We had demonstrated that a combination of enzyme and detergent treatments were effective in decellularizing tilapia skin, with 99.6% of the DNA removed and 69.3% of the collagen retained. The optimized decellularization protocol did not adversely affect the structural morphology, mechanical properties and denaturation temperature of the decellularized tilapia skin (DTS), although the mechanical properties of tilapia skin were discovered to be dependent on the location of the skin and the direction of pull.

The DTS was demonstrated to have a lower immunogenic potential than native tilapia skin, a low cytotoxicity and a high cellular biocompatibility towards murine fibroblasts L929, which exhibited increasing metabolic activity over time after seeding onto DTS. The DTS also did not induce long-term inflammatory responses after the acute inflammation phase in the rat subcutaneous implant model, as shown by the expression of pro-healing cytokines and the decrease of pro-inflammatory cytokines at the late time-point of Day 14.

To determine the suitability of DTS for tissue engineering, DTS was evaluated as a barrier membrane in guided bone regeneration, a dental surgical procedure to restore bone tissue in an alveolar defect, together with CETC. In osteogenic cell culture studies, both DTS and CETC supported the proliferation, differentiation and mineralization of murine pre-osteoblast cells, while micro-CT results in a rat calvarial defect model revealed that both DTS and CETC led to improved bone regeneration compared with the empty control.

DTS was also evaluated as a wound dressing in full-thickness skin wounds. As DTS was found to be more immunogenic than CETC and inferior to CETC in terms of *in vitro* and *in vivo* osteoinduction in the guided bone regeneration studies, DTS was subjected to an additional alkali treatment in an attempt to improve its biocompatibility. The alkali-treated DTS (termed as DTS-N) was demonstrated to have a lower immunogenic potential and improved cellular biocompatibility to human dermal fibroblasts (HDFs), compared to DTS. Results from the murine full-thickness skin wound model revealed that DTS induced a better healing rate than native tilapia skin, and an additional alkali treatment further improved the wound healing rate, as demonstrated by the smaller mean wound area in the DTS-N group than that of the DuoDerm group on Day 14, as well as the formation of a continuous epidermal layer in the DTS-N group observed in the histological sections.

In summary, this thesis illustrated the functionality of DTS in various tissue engineering applications, supported by *in vitro* and *in vivo* evidences, and the findings of this study proved the hypothesis that tilapia skin can be decellularized to produce an acellular scaffold, the decellularized tilapia skin (DTS) possesses favourable physical and biological properties, and the DTS is suitable as a scaffold in tissue regeneration. Moving forward, we aim to improve the decellularization process by using electricity as a novel decellularization strategy to reduce processing time and reduce chemical waste. We would also like to propose doing further biochemical characterisation of the substances in tilapia skin, investigating the antimicrobial properties of DTS, using supercritical carbon dioxide to achieve decellularization and sterilization in a single treatment, and looking into decellularizing tissues from other fish species. The findings in this thesis and subsequent works would help to meet the increasing need for tissue constructs especially from patients who are unable to take mammalian products, and transform fish waste into useful and valuable biomaterials.

1 Introduction

1.1 Background

1.1.1 *Regenerative medicine and tissue engineering*

Regenerative medicine is a rapidly developing field in the health sciences which aims to restore normal functions in a non-functional tissue or organ [1, 2]. With the incidence rate of tissue failure due to diseases and aging projected to increase worldwide, there is a great demand for regenerative medicine to relieve the burden and improve the quality of life for patients with tissue failure. Tissue engineering, an interdisciplinary field devoted to the manufacture of tissue constructs ex vivo to replace non-functional tissues, serves a vital role in regenerative medicine due to its potential to address the shortage of autologous grafts and donors, as well as the potential to satisfy unmet medical needs [3]. The term "tissue engineering" was first introduced at a panel meeting of the National Science Foundation in 1987 and was further defined by Langer and Vacanti in 1993 [3, 4]. Since then, tissue engineering has progressed into a thriving industry involving over 100 companies, employing 14,000 people and generating nearly 4 billion US dollars in sales as of 2011 [5], and the field is constantly growing due to increasing needs.

In tissue engineering, the development of a successful tissue construct depends on one or a combination of these five tenets: scaffolds, cells, growth factors, bioreactors, and bioimaging [6]. In particular, the scaffold plays an essential role in a tissue construct as it forms the structural framework to facilitate tissue regeneration processes and provide mechanical stability in the implantation site [7]. A scaffold is defined as a three-dimensional porous solid biomaterial designed to perform some or all of these roles: (i) possess physical properties suitable for the intended application, (ii) promote cell proliferation, (iii) allow diffusion of

nutrients and bioactive molecules, (iii) biodegrade at a controllable rate to allow regenerated host tissue to take its space, and (iv) possess minimal toxicity and immunogenicity [8]. Typical tissue engineering scaffolds can be composed of synthetic polymers (e.g. polylactic acid, polyglycolic acid, and polycaprolactone) and/or natural materials (e.g. collagen, alginate, and chitosan). Synthetic polymers offer the advantages of controllable mechanical properties and degradation kinetics, while natural materials have the advantages of inherent bioactivity and low cytotoxicity [9].

1.1.2 *Extracellular matrix (ECM)*

Many tissue engineering scaffolds are designed to mimic the native extracellular matrix (ECM), which is composed of structural and functional molecules organized in a three-dimensional structure unique to each tissue [10]. The ECM give tissues and organs their shapes, and provide a home for the cells that form tissues and organs. The ECM plays a pivotal role in tissue development as it creates the cellular microenvironment, provides structural information and biochemical cues to cells, regulates signalling activities, and influences cell behaviour including cell shape, migration, proliferation and differentiation via cell-ECM interactions [11]. Studies have shown that the ECM can function as an inductive scaffold for tissue regeneration due to the presence of bioactive molecules that support cellular and physiological functions. A number of these bioactive molecules, such as collagen, fibronectin, laminin, and hyaluronic acid, are commonly used in the fabrication of tissue engineering scaffolds [10, 11]. Among these ECM-derived molecules, collagen is the most widely used in tissue engineering as it is the most abundant component of the ECM, making up more than 90% of the dry weight of the ECM in most tissues and organs [12]. Collagen is also the most abundant protein in human and vertebrate animals, making up 25-35% of the total protein mass [13].

1.1.3 *Fish collagen in tissue engineering*

Collagen is a popular biomaterial in tissue engineering due to its excellent biocompatibility and biodegradability. However, most commercial collagen comes from porcine and bovine sources, which may introduce a potential risk of transmissible mammalian diseases such as bovine spongiform encephalopathy (BSE) [14, 15]. Porcine and bovine collagen is also unsuitable for patients with religious or dietary restrictions. In view of the limitations of mammalian collagen, there is a growing interest in alternative sources of collagen, with fish collagen gaining prominence due to the large amounts of fish waste generated by the fish-processing industry [16]. The discarded fish scales and skins often contain a high amount of collagen, which is under-utilized. Among the various type of fishes, Nile Tilapia (*Oreochromis niloticus*), a tropical freshwater fish native to Africa, seems to be a promising source of collagen considering its popularity in modern fish farms, rapid growth rate and high protein content [17]. Ever since tilapia collagen was identified as a potential biomaterial in tissue regeneration, studies has been done to investigate the biological safety and biocompatibility of tilapia collagen. Not only was tilapia collagen proven to be biologically safe, it was also proven to be suitable for tissue engineering applications such as corneal regeneration and skin regeneration [18-20].

In tilapia, type I collagen can be found abundantly in the skin and scales [21]. In order for tilapia collagen to be usable, it needs to be solubilised from the skin or scales with an acid or a proteolytic enzyme. The solubilised collagen can then be converted into tissue engineering scaffolds by the removal of the solvent and the crosslinking of the collagen molecules to form a solid porous structure to support cell attachment and nutrient diffusion. Among the various methods of collagen scaffold production, electrospinning is increasingly employed because the nanofibrous architecture of the electrospun membranes mimics the structure of extracellular matrix (ECM), and the structural morphology and biochemical properties of the electrospun membranes can be easily adjusted by varying the solution composition and spinning parameters

[22]. The nanofiber membrane can be stabilized by physical or chemical crosslinking treatment to preserve its structure and mechanical integrity. There have been numerous studies that reported the use of crosslinked electrospun collagen scaffolds in tissue regeneration, but almost every study utilised mammalian collagen [23, 24]. Prior to this thesis, there was only one study on crosslinked electrospun tilapia collagen, which was reported to improve skin regeneration *in vitro* and *in vivo* [20]. There was limited information on the cytotoxicity and immunogenicity of crosslinked tilapia collagen, as well as its suitability for other clinical applications. In addition, most electrospinning processes involved the use of toxic solvents such as hexafluoro-isopropanol, and there is a motivation to develop greener solvents to reduce the impact on health and environment. In our opinion, obtaining more information on the biological properties of crosslinked tilapia collagen, exploring new clinical applications and improving the safety of scaffold fabrication would allow fish collagen-derived biomaterials to become an attractive alternative to current mammalian collagen products.

1.1.4 *Decellularized fish tissues in tissue engineering*

Another approach to obtain collagen scaffolds from tilapia skin or scales is the removal of cells from the tissue, leaving behind an acellular matrix with a preserved structure consisting of mainly collagen. This method of cell removal, known as decellularization, have been used extensively to derive acellular tissues and organs for a variety of clinical applications, such as reconstruction of damaged/diseased tissues and wound healing [25-27]. Due to a shortage of human donors, animal tissues, especially porcine and bovine tissues, are often used to derive acellular matrix. As mentioned previously, porcine and bovine tissues may be a source of transmissible diseases and are unsuitable for patients with religious restrictions. As a result, fish scales and fish skin, usually discarded by the fish processing industry, are seen as a novel and abundant source of decellularized tissues. Currently, the market of decellularized tissues is

dominated by mammalian sources and the number of studies done on decellularized fish tissues is limited, as shown in the search results in Table 1-1. Hence, there is a great potential for decellularized fish tissues to be used as a non-mammalian alternative in tissue engineering.

Table 1-1: Number of results based on the following search terms in scientific database Web of Science (https://apps.webofknowledge.com) and biomedical database PubMed (https://www.ncbi.nlm.nih.gov/pubmed). Search was performed on 01 Feb 2019.

Search term	Web of Science	PubMed
"Collagen"	219053	209864
"Decellularization"	1697	1422
"Decellularized"	2971	2594
"Collagen" AND "Fish"	2469	2032
"Decellularization" AND "Fish"	2	3
"Decellularized" AND "Fish"	8	8

To obtain an acellular scaffold from fish skin, the skin has to be subjected to a series of physical, chemical and enzymatic treatments to remove as much cellular materials as possible while preserving the native structure of the extracellular matrix (ECM). The presence of contaminants such as nucleic acid, the structural integrity of the ECM, and the biocompatibility and cytotoxicity have to be evaluated before the acellular scaffold can be used for tissue engineering. While decellularized cod skin has been developed by Kerecis, an Icelandic medical device company, and approved for clinical use as a wound dressing by the United States Food and Drug Adminstration (US FDA) [28], there are no other reports on decellularized fish skin to our knowledge. In view of the dramatic decline in cod population globally due to overfishing and the long time required (2 to 4 years) for cod to reach maturity, more sustainable and faster-growing fish species are desired as a source of decellularized tissues [29]. Nile tilapia (*Oreochromis niloticus*) is seen as an attractive and economical alternative, as tilapia is farmed in more than 100 countries and valued for its rapid growth and high protein content. Also, collagen extracted from tilapia skin and scales have been reported to possess numerous benefits, including a high denaturation temperature and favourable

biological properties [30]. While there were already numerous studies on tilapia collagen in food science and a small but increasing number of studies on tilapia collagen for biomedical applications, there was no prior reports on the decellularization of tilapia skin. In the author's opinion, decellularized tilapia skin would be an economical and effective non-mammalian alternative to acellular mammalian matrix for tissue regeneration.

1.2 Objective and specific aims

Given the lack of prior studies on decellularized tilapia skin, the main objective of this thesis was to develop tilapia skin into an acellular scaffold and investigate whether decellularized tilapia skin could serve as an effective scaffold for tissue regeneration. In line with this objective, the thesis focused on the following specific aims:

Specific Aim 1: To investigate the properties of tilapia collagen and to develop a crosslinked electrospun scaffold from tilapia collagen

Specific Aim 2: To develop an acellular scaffold from tilapia skin by decellularization

Specific Aim 3: To evaluate the physical, chemical and biological properties of decellularized tilapia skin (DTS), using crosslinked electrospun tilapia collagen (CETC) as a comparison

Specific Aim 4: To investigate the suitability of DTS for two selected clinical applications - guided bone regeneration (GBR) and full-thickness skin wound regeneration

1.3 Hypotheses

Hypothesis 1: Tilapia collagen can be electrospun and crosslinked into a scaffold which is highly biocompatible.

Hypothesis 2: Tilapia skin can be decellularized using appropriate treatments to yield an acellular scaffold with preserved extracellular matrix.

Hypothesis 3: The decellularized tilapia skin (DTS) possesses favourable physical and biological properties, and is less immunogenic than native tilapia skin.

Hypothesis 4: The DTS is suitable as a scaffold in tissue regeneration, with favourable tissue-scaffold interactions.

1.4 Novelty and significance

While the use of fish collagen has been widely reported in the fields of food science and cosmetics, the use of fish biomaterials in tissue engineering and regenerative medicine is currently overshadowed by the presence of numerous mammalian products, as shown by the search results in Table 1-1. Fish biomaterials have a great potential to replace mammalian biomaterials in medical applications as they offers similar benefits and properties without the limitations faced by mammalian biomaterials. In particular, the novelty of the thesis lies in the development and evaluation of acellular scaffolds from tilapia skin, which has not been reported prior to this thesis. The results from this research would aid in improving our understanding of fish-derived biomaterials, and increase the impact of fish-derived biomaterials in regenerative medicine.

With a substantial amount of fish weight (about 75%) in the form of skins, scales, bones, fins, heads and guts discarded in the fishing industry [16], one significance of my research is the transformation of some of these wastes into useful and safe biomaterials for tissue engineering applications to increase revenue and reduce wastage. For patients who are unable to use mammalian products due to religious or health reasons, fish-derived biomaterials are seen as a

practical and economical alternative. The 1.8 billion Muslims and 1.1 billion Hindus in the world, making up 24.1% and 15.1% of the global population respectively as of 2015 [31], contribute a significant market for fish-derived biomaterials, and so does the small but increasing number of people who have developed allergy to mammalian tissues [32]. The ability to provide a solution to these patients is another significance of my research.

1.5 Scope of thesis

Chapter 1 provides a brief introduction on regenerative medicine and fish biomaterials, and also lists the objectives, hypotheses and scope of this thesis.

Chapter 2 provides a literature review on tissue engineering scaffolds derived from collagen and decellularized tissues, with a focus on fish biomaterials, especially from Nile tilapia.

Chapter 3 focuses on the properties of tilapia collagen and the development of a crosslinked electrospun scaffold from tilapia collagen.

Chapter 4 focuses on the decellularization of tilapia skin, the optimisation of the decellularization process, and the characterisation of the decellularized tilapia skin.

Chapter 5 evaluates the cytotoxicity and immunogenicity of the crosslinked electrospun tilapia collagen (CETC) and decellularized tilapia skin (DTS).

Chapter 6 investigates the suitability of CETC and DTS in selected tissue engineering applications, namely guided bone regeneration (GBR) and skin wound healing.

Chapter 7 presents a conclusion of this thesis with recommendations on future work.

2 Literature review

2.1 Collagen – Structure, Synthesis & Degradation

Collagen, the main structural protein in the ECM of animal tissues, is responsible for maintaining biological and structural integrity of the ECM. Ubiquitously found in various animal species and relatively conserved across species at the gene level, collagen is the most abundant high molecular weight protein in vertebrate organisms, particularly in mammals where collagen can constitute up to 25% of total proteins [33]. Due to its numerous advantages such as good biocompatibility, low immunogenicity, wide availability and biodegradability, collagen is a popular biomaterial for biomedical applications, such as drug delivery, wound healing, and tissue regeneration [34, 35]. There are more than 20 types of collagen, all displaying a typical triple helix structure but there are slight differences in structural and hierarchical organization. Among them, type I collagen is most commonly exploited in biomedical applications due to its abundant distribution in animal skin, bones, tendons, ligaments and cornea [36].

Despite the structural diversity among the different collagen types, all collagen molecules have a common structure, which is a right-handed triple alpha helix consisting of three polypeptide α-chains. For example, mammalian type I collagen consists of two α_1 and one α_2 chains, while teleost fish type I collagen consists of one α_1, one α_2 and one α_3 chains [37]. Each of these chains typically has more than 1000 amino acids and contains at least one series of repeating amino acid sequence Gly-X-Y [38, 39]. Glycine, being the smallest amino acid and being present on the chain at every third position, allow the three chains to pack tightly around a central axis, while the positions X and Y are usually occupied by proline or hydroxyproline [40]. Being a unique amino acid present only in collagen, hydroxyproline is formed by the

post-transcription hydroxylation of proline and possesses a hydroxyl (-OH) group which contributes to intramolecular hydrogen bonding and stabilises the triple helix structure. Another unique amino acid present only in collagen is hydroxylysine, which, like hydroxyproline, is formed by the post-transcription of lysine. The hydroxyl group on hydroxylysine allows the attachment of sugar components to the collagen molecule to form the triple-helical structure [41].

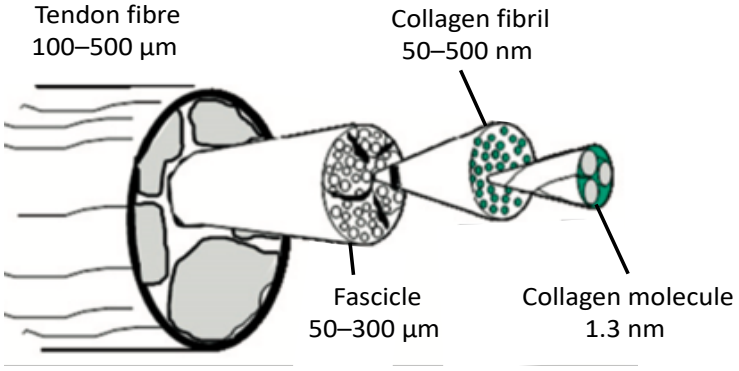

Figure 2.1: Structure of collagen from the fibre level to the molecule level. Numbers below each term indicates the diameter of the single structure. (Figure adopted from [36] with permission from Elsevier B.V.)

A majority of the collagen in connective tissues is produced by the fibroblast, where a unique mRNA is transcribed to form a collagen pro-α chain in the rough endoplasmic reticulum. The pro-α chains are then transported to the Golgi apparatus, where some proline and lysine residues are hydroxylated to introduce hydroxyl groups for intramolecular hydrogen bonding and glycosylation later. As the pro-α chains exit the cell via excretory vesicles, the pro-peptides are cleaved and the collagen chains self-assemble into 10-300 nm diameter fibrils, which then aggregate into 0.5-3 µm diameter fibres [42]. The self-assembly of fibrils is an entropy-driven process where hydrophobic residues are buried within the fibril. The process of self-assembly is referred to as fibrillogenesis and has great importance in ECM pathology and tissue development [43]. The mature collagen molecules are further stabilised by enzymatic crosslinks mediated by lysine hydroxylase and lysyl oxidase, and chemical crosslinks induced

by glycation, oxidation, and disulphide bonding [44]. Although the triple helix is the key feature of collagen, the non-helical domains at the ends of the chains are also important. Before the cleaving of the pro-α chains, the C-terminus pro-peptides are involved in initiating the triple-helix formation and the N-terminus pro-peptides are involved in regulating primary fibril diameters [45]. After the removal of the pro-peptides, the short non-helical telopetides at the ends of the processed collagen chains are involved in intramolecular cross-linking within the fibrils as well as intermolecular cross-linking with other components of the surrounding ECM [46]. In summary, the long amino acid sequences of each chain, the tight packing of the chains due to glycine, the presence of intramolecular hydrogen bonding due to hydroxyproline, and the formation of inter-molecular crosslinks all contribute to collagen's high mechanical strength, one of the main reasons why collagen is a highly valued biomaterial.

Like most biomaterials, collagen can lose its structural integrity via thermal denaturation, chemical reaction or enzymatic degradation. When heat is applied to collagen beyond its denaturation temperature, thermal denaturation occurs as the intramolecular hydrogen bonds break down and the collagen molecules undergo an irreversible kinetic process to form random coiled polymeric chains known as gelatin [47]. The denaturation temperature is the transition point where the ordered triple helix structure switches into a random coil structure. It is known that the denaturation temperature is dependent on the concentration of hydroxyproline since hydroxyproline is responsible for the intramolecular hydrogen bonds within the collagen molecule [48]. The degree of hydroxylation of the proline residues in collagen varies among different animal species, generally with warm-blooded animals and animals living in warm environments having a higher concentration of hydroxyproline in their collagen [15].

Collagen can also undergo denaturation in the presence of acids, alkalis, detergents and organic solvents, which disrupts the intramolecular hydrogen bonds and destabilise the triple helix

structure [34]. In addition, degradation of collagen can occur via chemical hydrolysis of its amino acid chains in the presence of acids and alkalis. Hence, when a collagen-derived material is being processed, it is important to control the temperature and chemical parameters to prevent the premature denaturation or degradation of the collagen, so that the structural integrity of the collagen is maintained [36].

Being a biomolecule, collagen can also undergo biodegradation *in vitro* and *in vivo* by cellular enzymes [49, 50]. In fact, biodegradability is an important aspect of a biomaterial, as the ability of a material to degrade and be replaced by new host tissues prevents the need of a second surgery to remove the implanted material [51]. It is also important for the degradation products and metabolites of a biomaterial to be non-toxic and be easily eliminated from the body or absorbed by the body. Being the most abundant protein in most animals, collagen does not have problems in biodegradability and metabolite toxicity. In humans, collagenases such as matrix metalloproteinase (MMP) are responsible for most *in vivo* degradation of collagen [52]. There are many types of collagenases, each having a different rate of collagen hydrolysis. In general, the proteolytic activity of all collagenases depends on three principles – the ability to bind to collagen, the ability to unwind the triple helix, and the ability to cleave each of the three strands [53]. In addition, collagen can also be degraded by bacterial collagenases and non-specific proteolytic enzymes such as trypsin [41, 54]. Hence, it is important to prevent bacterial contamination during processing and implantation of a collagen-derived scaffold, and it is important to re-evaluate the rate of degradation if the scaffold is going to be implanted at a site with high levels of proteolytic enzymes and/or bacteria, such as the oral cavity or digestive tract [55]. To regulate the rate of degradation in these instances, the collagen may need to be crosslinked or structurally modified. This will be discussed further in the next section.

2.2 Collagen-derived biomaterials

Thanks to its abundance in various animals and its vital role in providing mechanical functions in tissues, collagen is one of the most studied biomolecules and many collagen-derived biomaterials have been developed for various medical applications such as tissue regeneration and drug delivery [41]. There are two fundamental techniques to obtain collagen-derived biomaterials. The first technique is to break down a collagenous tissue to extract collagen molecules, which are then purified and reconstituted into structures resembling the ECM. The second technique is to remove cells from a collagenous tissue leaving behind an acellular collagen matrix with preserved ECM structure, in a process known as decellularization [33]. Each of these techniques would be described in detail below.

2.2.1 *Extraction, purification and reconstitution of collagen*

Despite its high hydrophilicity, native collagen is insoluble in water due to the presence of intra- and intermolecular crosslinks in the collagen matrix. To extract collagen molecules from tissues, the tissues can be treated with acids (e.g. dilute acetic acid), alkalis (e.g. NaOH solutions) or proteolytic enzymes (e.g. pepsin) to break down the crosslinks and release the individual collagen molecules [34, 56]. Being water-soluble at room temperature, the collagen molecules can be purified by precipitation with neutral salts such as sodium chloride, followed by centrifugation and dialysis to obtain a neutral collagen solution. The purification of collagen is important as it removes non-collagenous molecules that can cause cytotoxicity and adverse immune reactions [57].

Solubilised collagen molecules have the ability to polymerise spontaneously *in vitro* into fibrils in a thermodynamically-driven process known as "self-assembly" [58]. However, the assembled fibrils are mobile in solution and therefore do not possess sufficient mechanical

stability. In order to achieve the functions required for clinical applications, the solubilised collagen needs to be reconstituted into physical scaffolds by solvent removal and/or stabilisation with crosslinking or chemical modification [59]. There is a wide number of fabrication techniques to convert solubilised collagen into physical scaffolds, as well as a wide number of crosslinking methods. The choice of physical form, fabrication technique and crosslinking method depends on the requirements of the application.

The physical forms of collagen-derived biomaterials can be broadly categorised into four groups: (i) hydrogels, (ii) microspheres, (iii) sponges and (iv) membranes/films [34]. The currently applied fabrication techniques and applications of each of these physical forms are summarized in Table 2-1.

Table 2-1: Currently applied fabrication techniques and applications for various physical forms of collagen-derived biomaterials [34]

Physical form	Fabrication techniques	Applications
Hydrogels	Physical cross-linking (e.g. UV irradiation), chemical cross-linking (e.g. carbodiimide), blending with other polymers	Injectable scaffolds, 3D printed scaffolds, cell delivery, drug release
Microspheres	Phase separation, emulsification	Drug delivery
Sponges	Freeze-drying, solvent casting, phase inversion, rapid prototyping	Tissue regeneration scaffolds, drug release scaffolds
Membranes/films	Solvent casting, freeze-drying, phase separation, electrospinning	Wound healing, tissue repair, guided tissue regeneration

Due to the hydrophilicity and gelling ability of collagen molecules, collagen can be readily fabricated into a hydrogel, which is defined as a three-dimensional network of hydrophilic polymer chains swollen by water. Collagen hydrogel has been used in a wide variety of applications due to its numerous advantages [60]. Its biocompatibility enables cell encapsulation and proliferation; its high water content facilitates diffusion of nutrients and waste; its fluidity makes it injectable or 3D-printable, allowing high versatility in its applications; and its biodegradability and non-toxicity allow it to be resorbed or eliminated

harmlessly [61]. Beside hydrogel, collagen can also be formed into microspheres for drug delivery [62]. However, collagen hydrogels and microspheres lack mechanical strength at the macro scale and are therefore only suitable for delivery (of cells, drugs, growth factors, antibiotics, etc) and soft tissue regeneration [34].

To enable hard tissue regeneration and wound/defect protection, collagen needs to be formed into a solid physical scaffold, such as sponge, membrane or film. Here are the three most common methods to fabricate physical collagen scaffolds.

- Solvent casting is a fabrication technique where a polymer is dissolved in a solvent, the solution is poured into a mold and the solvent is removed, leaving behind the solid polymer [63]. Solvent casting is one of the simplest fabrication techniques for polymer scaffolds, but such scaffolds are usually dense and compact unless porogens are added to the polymer solution and removed after solvent evaporation to yield a porous scaffold [64]. For collagen, the solvent is usually water or aqueous buffers, as collagen denatures in most organic solvents. The solvent can be removed by evaporation or fluid expulsion [56]. An advantage of using solvent casting is the ability to control the thickness and uniformity of the scaffold [65]. However, as solubilised collagen is heat-sensitive, solvent removal by evaporation has to be done at room temperature or lower temperatures, making this method time-consuming. Solvent removal by fluid expulsion works by the application of a compressive load on the collagen solution to expel the solvent by ultra-filtration via dialysis membrane and/or capillary action via absorbent pads, and the resultant construct is referred to as plastic compressed collagen [66].
- Freeze-drying, or lyophilisation, is a fabrication technique where frozen samples are subjected to high vacuum and the ice sublimes directly into water vapour, resulting in dry samples with intact structures [67]. Freeze-drying can be performed on collagen

solutions to obtain collagen sponges. After the ice sublimes, a porous network of collagen sponge remains. The density and porosity of the sponge can be controlled by varying the concentration of the collagen solution before freeze-drying and the temperature profile of the freezing cycle [68]. One study showed that collagen type I scaffold had larger pore size when frozen at -30°C than at -80°C [69]. The lyophilized sponge can be used in its porous form or further compressed into a membrane or film.

- Electrospinning is a fabrication technique which uses an electric field to deposit polymer fibres onto a target substrate, and the fibre diameter can be controlled to a range from several microns down to 100 nm or less [70]. Electrospinning is increasingly employed in the production of collagen scaffolds because the nanofibrous architecture of the electrospun scaffolds mimics the porous micro-structure of natural ECM and the structural and biochemical properties can be easily adjusted by varying the solution composition and spinning parameters [22]. The principles of electrospinning and the applications of electrospun scaffolds in tissue engineering will be reviewed in more details in section 3.1.

After the reconstitution of solubilised collagen into a physical form, the collagen-derived biomaterial can be crosslinked to stabilise its structure and to enhance its mechanical properties and to control the rate of biodegradation [59]. The principle behind a crosslinking reaction is the formation of intermolecular covalent bonds by modifying the amine and carboxyl groups within the collagen molecules [33]. Crosslinking techniques are broadly categorized into physical, chemical and enzymatic crosslinking, as described in detail below.

- Physical crosslinking usually consists of a thermal source or a high-energy radiation source (e.g. ultra-violet or gamma ray) to induce the formation of covalent bonds. Both irradiation and dehydrothermal (DHT) treatment leads to an increase in tensile strength

but may lead to some fragmentation in the collagen molecules [71]. While irradiation is more time-effective than DHT treatment (15 min for UV irradiation versus 3 days for DHT treatment), UV irradiation only works for thin or transparent scaffolds [72]. Gamma irradiation can penetrate through thick scaffolds but may cause more collagen fragmentation due to its high energy [36, 41].

- Chemical crosslinking consists of a wider variety of techniques compared to physical crosslinking. The most common class of chemical crosslinker is aldehydes, such as formaldehyde and glutaraldehyde. In particular, glutaraldehyde is the most utilised method to crosslink collagen-derived biomaterials [73]. Other classes of commonly used chemical crosslinker include carbodiimides and isocyanates. While chemical crosslinkers are effective in enhancing the mechanical properties of collagen, they are inherently toxic and any trace residues can induce cytotoxicity and adverse immune reactions in the recipient [74, 75]. Genipin, a plant-derived crosslinker, has a potential to replace conventional chemical crosslinkers due to its low toxicity, but its use is limited by its high price [76].
- Enzymatic crosslinking consists of bond-forming enzymes such as transglutaminase. Crosslinking enzymes have the advantage of being less toxic and leaving no chemical residues [77]. However, such enzymes may not be able to assess the interior of dense and thick scaffolds, leading to incomplete or uneven crosslinking. The enzymes may also be difficult to remove from the crosslinked scaffolds and the residual enzymes may provoke adverse immune response [78].

Besides crosslinking, solubilised collagen can also be blended with other polymers to enhance the mechanical properties. One method is to promote the formation of ionic bonds by blending collagen with an ionic polymer such as chitosan and alginate. Chitosan creates ionic bonds between the amine and carboxyl groups of collagen, which are strong enough to provide

mechanical strength [79]. Alginate has the ability to form gel in the presence of calcium ions, and the collagen molecules can be immobilised in the alginate-calcium matrix [80]. Another method is to blend collagen with a strong polymer such as poly-caprolactone and the copolymer mixture can be solvent casted or electrospun to obtain a mechanically strong and yet porous scaffold [81, 82].

2.2.2 *Decellularization of collagenous tissues*

Another way to obtain a collagen-derived biomaterial is decellularization, where cells are removed from a tissue or an organ, leaving behind the ECM which comprises of a complex network of collagen and other structural and functional proteins [27, 83]. This intact acellular matrix can be used as a scaffold to support cell proliferation and eventually tissue regeneration, and would be tolerated well even by xenogenic recipients as the components of the ECM are generally conserved between species [84]. Although individual ECM components such as collagen, fibronectin and laminin have been isolated and applied successfully in tissue engineering, utilizing decellularized ECM has the advantage of having structural and functional molecules in their native three-dimensional arrangements and in similar compositions as in nature [25]. Most tissue engineering scaffolds were designed to mimic the ECM and there has even been attempts to produce ECM analogs with individual ECM components and/or synthetic materials [85, 86], but the complexity of the ECM and the diversity of its component makes the ECM difficult to replicate *in vitro*. Hence, the decellularization of the ECM would be an effective method to obtain scaffolds for tissue engineering applications.

Ideally, the decellularization process should remove all cellular and nuclear materials which can trigger immune reactions in the host recipient, while preserving the architecture, mechanical integrity and biological activity of the remaining ECM . However, any processing step with the aim of removing cells from a tissue will inevitably alter the native structure and

composition of the ECM [87]. The challenge in decellularization is to determine the optimal methods to minimise disruption of the ECM while achieving efficient removal of cellular materials. There are many methods of decellularization, which are categorized into physical, chemical and enzymatic methods. The mode of action and effect on ECM of each method are briefly described in Table 2-2.

Table 2-2: Commonly used methods of decellularization of animal tissues, their modes of action and their effects on ECM [26, 27]

Method	Modes of action	Effects on ECM
Physical		
Freeze-thaw	Disrupts cell membrane via expansion of ice crystals	Can damage ECM by multiple freeze-thaw cycles
Force & pressure	Bursts cell membrane and disperses cellular contents	Can damage ECM by abrasion
Mechanical agitation	Facilitates exposure to chemicals/ enzymes and disperses cellular contents	Can damage ECM by aggressive agitation
Electroporation	Destabilise cell membrane and burst cells with electrical pulses	Slow removal of cellular debris from ECM
Chemical		
Acids & bases	Solubilise cellular components, disrupt nucleic acids	Remove GAGs, can damage collagen
Non-ionic detergents (e.g. Triton X-100)	Disrupt lipid-lipid and lipid-protein interactions but not protein-protein interactions	Variable cell removal, efficiency dependent on time
Ionic detergents (e.g. sodium dodecyl sulfate (SDS), sodium deoxy-cholate)	Solubilise cell membrane and nuclear membrane, disrupt nucleic acids, denature proteins	Tend to damage ECM structure, can denature collagen, can lead to cytotoxicity if not washed away thoroughly
Organic solvents	Dissolve cell membrane, disrupt protein-protein interactions such as hydrogen bonds and hydrophobic interactions	Variable cell removal, can disrupt ECM proteins
Hypotonic/hypertonic solutions	Cause cell lysis by osmotic shock	Does not remove cellular components efficiently
Enzymatic		
Proteases (e.g. dispase, trypsin, collagenase)	Catalyses the hydrolysis of peptide bonds	Can disrupt ECM structure, can remove ECM proteins (e.g. laminin, elastin, etc)
Nucleases	Catalyses the hydrolysis of nucleic acids	Difficult to remove from ECM and can cause cytotoxicity if not removed completely

Physical methods such as freeze-thaw processing and mechanical force can easily disrupt cell membranes but physical methods alone are inefficient in getting cellular materials out of the ECM and can cause damage to the ECM structure and mechanical properties [88]. Chemicals such as ionic solutions and detergents can solubilize and dissociate cellular materials from the ECM, but the chemicals can damage the ECM after long exposures and can cause cytotoxicity if the decellularized tissue is not properly rinsed [87]. Enzymes such as nucleases and proteases offer high specificity in the removal of undesirable residues, but it is difficult to achieve complete cell removal with enzymes alone and residual enzymes left by incomplete washing may trigger adverse immune responses [26]. Enzymes may also be inhibited by native protease inhibitors released from the lysed cells and lose activity over time [89]. Hence, an effective decellularization protocol normally consists of a combination of physical, chemical and enzymatic methods with thorough rinsing after each step to maximise the benefits and minimize the drawbacks of each individual method.

After decellularization, it is important to determine the extent of removal of cellular components in the decellularized tissue, as certain cellular components can contribute to cytotoxicity and cause adverse host responses during implantation [90]. Although it is impossible to remove 100% of cellular components in any decellularization methods, it is generally acceptable for residual cellular materials to fall below the threshold concentration required to elicit adverse cell and host responses. Among the various cellular components, double-stranded DNA (dsDNA) is most commonly quantified as dsDNA is present in all cell types and its quantity is directly proportional to the number of mononuclear cells or the amount of residual cellular materials [91]. DNA can be readily detected quantitatively using commercially available assay kits or qualitatively using routine histologic staining or immunofluorescent methods.

Based on a compilation of findings among scientists performing decellularization processes, the following criteria were established as accepted standards for defining the success of a decellularization process [26, 27]:

- The amount of dsDNA is less than 50 ng per mg ECM (dry weight).
- The length of the DNA fragments was less than 200 base pairs.
- Histological tissue sections stained with hematoxylin & eosin (H&E) or 4',6-diamindino-2-phenylindole (DAPI) show a lack of visible nuclear material.

Besides DNA, antigens such as galactose-alpha-1,3-galactose (alpha-gal) and major histocompatibility complex I (MHC-I) can also be quantified to determine the extent of decellularization of animal tissues, as the purpose of decellularization is to remove antigenic components from a tissue to minimise its immunogenic potential [92, 93]. However, quantifying these antigens may not reveal the actual immunogenic potential of the decelluarized tissues, as there are other antigens that are not detected, and methods to identify unknown antigens can be expensive and time-consuming [94]. To assess the entire immunogenic potential of decellularized tissues rapidly, a novel human serum-based system was developed using a human serum pool, which contains polyclonal antibodies associated with the adaptive immune response [95]. Using the polyclonal antibodies in the serum pool as a primary antibody, antigens in decellularized tissues can be detected and visualized by immunohistochemistry, or quantified by ELISA.

Compared to the extraction, purification and reconstitution of collagen, decellularization has the advantage of being simpler and less time consuming as the decellularized tissue already possess a natural ECM architecture so there is minimal need for reconstitution and crosslinking [96]. The preservation of the ECM also leads to a retention of mechanical strength in decellularized tissues. However, decellularized tissue has a higher immunological risk than

reconstituted collagen as the decellularized tissue consisting of various proteins may retain antigens which can trigger adverse host responses [93]. Large and complex tissues are challenging to decellularize and sterilize, and are likely to trap residual chemicals or enzymes from the decellularization process which can contribute to potential cytotoxicity [27]. Attempts to remove residual contaminants with more thorough treatments and/or washing steps may increase the rate of damage to the ECM. Hence, it is important to select the optimal decellularization methods and evaluate their effectiveness for different types of tissue engineering applications.

2.2.3 *Sterilization of biologic scaffolds*

It is vital to sterilize biologic scaffolds prior to *in vitro* or *in vivo* use to prevent contamination and infection. In the United States, biologic scaffolds including collagen scaffolds and decellularized tissues are typically regulated by the Food and Drug Administration (FDA) as medical devices, and are required to be sterilized according to directed guidelines (e.g. ISO/DIS 1135-1, ISO/DIS 1137-1) [87]. Biologic scaffolds can be sterilized by incubation in acids (e.g. peracetic acid) or antiseptics (e.g. chlorhexidine), which kill microoganisms by disrupting cellular components, but such treatments may not provide sufficient penetration of porous scaffolds or may cause damage to the ECM [97]. Terminal sterilization methods such as gamma irradiation and ethylene oxide exposure are generally more effective as they generate oxidative species that kill microorganisms quickly, but these methods are reported to affect ECM structure and mechanical properties [98, 99]. Of these, ethylene oxide exposure has recently been classified as a mutagen and carcinogen, and residues of ethylene oxide can cause undesirable host immune responses [100]. Gamma irradiation can cause ECM degradation by oxidising ECM components, even at relatively low doses of 5 kGy, and causes residual lipids to become cytotoxic [99, 101].

Recently, supercritical carbon dioxide has become a main method to sterilise food and pharmaceuticals and is currently being investigated as a method to sterilise biologic scaffolds [102]. The time required for supercritical carbon dioxide sterilization was reported to be significantly shorter than ethylene oxide or irradiation methods and similar to steam autoclaving, and the efficacy is due to the rapid diffusion of carbon dioxide into cells and the altering of pH within cells [103]. Supercritical carbon dioxide has also been used for tissue decellularization and it was shown to be compatible with biological materials and leave no toxic residues [104]. Low amount of chemical sterilant can also be mixed with supercritical carbon dioxide to create a very effective and yet gentle medium for sterilization of sensitive biomaterials [105]. Supercritical carbon dioxide shows great potential to be an effective sterilant, but further studies would be necessary to validate its sterilising efficacy on various types of biologic scaffolds.

2.3 Sources of collagen

As the most abundant protein on earth, collagen can be extracted from a wide variety of sources such as mammals (e.g. pigs, cows, sheep) [106, 107], reptiles (e.g. frogs, crocodiles) [108, 109], birds (e.g. chicken, ostrich) [110, 111], and aquatic animals (e.g. fish, sharks, jellyfish) [112-114]. Since ancient times, collagen has been used as a glue, obtained through the boiling of animal skin and collagenous tissues. In fact, the use of collagen as a glue was dated as far as 4000 years ago in ancient Egypt, and the word collagen originates from the Greek word *kolla*, meaning “glue” [115]. In a broader sense, collagen could be seen as the “glue” holding tissues and organs together. In the past two centuries, collagen, especially in its denatured form known as gelatin, has been used in food, photographic, cosmetic and pharmaceutical applications due to its gel-forming and viscoelastic properties [116]. The use of collagen as a scaffold in tissue

engineering emerged in the 1990s, and much progress has been made ever since in the development and application of collagen scaffolds [117].

Traditionally, most of the collagen extracted for industrial applications comes from porcine and bovine tissues as pigs and cows are widely farmed for their meat. While collagen has been used for centuries, the industrial manufacture of collagen only started in the 1930s with pig skin as the first raw material [116]. Even today, porcine and bovine tissues continues to be important materials for large-scale industrial production of collagen. As at 2008, the annual global output of collagen and gelatin is nearly 326,000 tons, with pig skin accounting for the largest source (46%), followed by bovine hides (29,4%), bovine bones (23.1%) and other sources (1.5%) [118]. With a long history of industrial production and a large share in the collagen market, bovine and porcine collagen forms the bulk of collagen scaffolds in tissue engineering.

Although bovine and porcine collagen have a proven record of medical efficacy and are considered safe for clinical use, they still carry a risk of zoonotic diseases, such as bovine spongiform encephalopathy [36]. The cells of non-primate mammals, including pigs and cows, also expresses antigens that can contaminate the extracted collagen and trigger allergic reactions in humans, with galactose-alpha-1,3-galactose (or alpha-gal) being a prominent example of such a xenoantigen [119]. As alpha-gal is present in the saliva of certain tick species, a person bitten by one of these ticks can develop allergic reaction to mammalian products, including meat by oral ingestion [120]. In 2018, tick-induced mammalian tissue allergy had been reported on 6 continents in 17 countries, with the figures expected to increase [121]. For patients with this allergy, bovine and porcine collagen pose a significant risk. In the United States, studies on Zyderm, an implant derived from purified bovine collagen, revealed 3 % of its subjects ($n > 250,000$) experiencing localized hypersensitivity reactions and 1 % of treated

patients demonstrating symptoms of hypersensitivity at treatment sites [122]. If the sample population of this study is representative of the global population, the number of people who are hypersensitive to bovine and porcine collagen would be indeed very high.

Considering the immunological risks of animal collagen, human collagen has also been produced from human cadavers for biomedical applications, but the use of human collagen is limited by the shortage of tissue donors and the complicated process of extraction and purification [123]. To meet the demand for human-collagen and to improve consistency between batches, recombinant human collagen from transgenic plants had been developed, but this new technology is limited by high costs and low yields [124-126].

2.3.1 *Fish collagen as an alternative to mammalian collagen*

In view of the growing global demand for collagen and the limitations of mammalian collagen, alternative sources of collagen such as avian collagen, amphibian collagen and fish collagen are gaining intense interest among consumers and researchers. Avian collagen is abundant in poultry skin, tendons and bones, but despite the high human consumption of poultry, commercial production of avian collagen for biomedical applications is still limited as poultry skin and tendons are also a coveted food source, and occasional episodes of avian flu outbreaks generate concerns about the use of avian collagen in biomedical applications [118]. Collagen from amphibians and reptiles, especially frog skin collagen and turtle collagen, shows promises as a novel biomaterial [127, 128], but the actual use of amphibian and reptile collagen in clinical applications is limited due to the rapid decline of many amphibian and reptile species caused by habitat destruction and unsustainable exploitation [129, 130]. In this regard, fish collagen is seen as a highly attactive alternative to mammalian collagen, especially when fish consumption accounted for almost 20% of the global average per capita intake of animal proteins in 2011 [131]. Fish collagen is highly abundant in fish skin, scales and bones, which makes up a

considerable amount of fish weight (up to 75%) and are often discarded as waste by the fish-processing industry [16]. Exploiting this under-utilized resource would generate value out of unwanted fish parts, and lead to a reduction of waste and pollution. Currently, the production of fish collagen/gelatin is still in its infancy, contributing only about 1% of the annual global collagen/gelatin production [132].

Although fish collagen has been studied since the 1950s and produced by acid extraction since the 1960s, the study of fish collagen has been largely eclipsed by mammalian collagen, and its use has been mainly limited to the food industry until the 1990s, when fish collagen is gaining prominence in the cosmetics and biomedical industries [118]. The use of fish collagen for biomedical applications was traditionally limited because fish collagens generally have low denaturation temperature (T_d), which renders them difficult to process. For example, the T_d of chum salmon collagen is approximately 19 °C, making it unstable at human body temperature and limiting the extraction conditions to low temperatures to avoid denaturation [133]. In comparison, most mammalian collagen has a T_d of more than 40 °C. Fish collagen generally has a low T_d than mammalian collagen due to a lower content of imino acids (proline and hydroxyproline) which contributes to intramolecular hydrogen bonding [134].

To overcome the limitation of low T_d, one approach is to crosslink fish collagen or blend fish collagen with another polymer to enhance its thermal and mechanical stability. For example, chemical crosslinking with carbodiimide brings the T_d of salmon collagen to 55 °C [135]. Another approach is to isolate collagen from warm water fish, as warm water fish collagen has a higher imino acid content than cold water fish collagen and hence higher thermal stability. Among various reported fish collagens, type I collagen from Nile tilapia (*Oreochromis niloticus*), a tropical freshwater fish, has the highest T_d (35 °C) to date, and a high T_d allows

the processing conditions to be less temperature sensitive. Tilapia collagen would be described in more detail in Section 2.6.

2.4 Sources of decellularized tissues

Decellularized tissues can be harvested from a variety of allogeneic or xenogeneic tissue sources, and to date almost all decellularized ECM products approved for clinical applications have been of mammalian origins, particularly from human, bovine, porcine, or equine sources, as shown in Table 2-3. Unlike solubilised collagen which is extracted mostly from skins and tendons, decellularized tissues can be isolated from a wider variety of tissues, including skin [136], small intestine [137], kidney [138], heart [139] and blood vessels [140]. As each tissue type possesses different structures and functions, a diversity of source tissues allows scientists to select an appropriate tissue type to suit a particular clinical application.

As mammalian tissues dominate the decellularized product market, there are strong concerns and a sense of pessimism among consumers and patients due to a risk of transmissible diseases from mammalian tissues to human recipients, such as bovine spongiform encephalopathy (BSE) [14, 15]. Certain patients also tend to avoid bovine and porcine products due to religious restrictions. For example, Muslim and Jewish followers are forbidden to consume porcine products while Hindu followers are forbidden to consume bovine products [118]. There is also a small but increasing number of people who has developed allergy to mammalian tissues [141].

In view of the growing global demand for tissue implants and the limitation of mammalian tissues, alternative sources of decellularized tissues are gaining increasing interest among researchers, clinicians and patients. The rationale of using non-mammalian tissue is that, as the components of the ECM are generally conserved and highly similar between species, a properly decellularized tissue from a non-mammalian invertebrate species would be well-tolerated in a

Table 2-3: Summary of commercially available decellularized ECM products, arranged by species [25, 56]. At the time of writing there is only one FDA-approved non-mammalian decellularized ECM product – MariGen™ Omega3 from Kerecis. The other decellularized ECM products are all from mammalian sources. (C-link. = crosslinked, DS = dry sheet, HS = hydrated sheet, SIS = small intestinal submucosa)

Product	Company	Source tissue	Process	Form	Use
Human origin					
AlloDerm™	Lifecell	Skin	C-link.	DS	Abdominal wall, breast, head and neck reconstruction
AlloPatch™	Musculoskeletal Transplant Foundation	Fascia lata	C-link.	DS	Orthopedic applications
Axis™ Dermis	Mentor	Dermis	Natural	DS	Repair pelvic organ prolapse
FasLata™	Bard	Fascia lata	Natural	DS	Repair soft tissue
GraftJacket™	Wright Medical Tech	Skin	C-link.	DS	Foot ulcers
Suspend™	Mentor	Fascia lata	Natural	DS	Urethral sling
Bovine origin					
Dura-Guard™	Synovis Surgical	Pericardium	C-link.	HS	Spinal/cranial repair
Durepair™	TEI Biosciences	Fetal skin	Natural	DS	Spinal/cranial repair
Peri-Guard™	Synovis Surgical	Pericardium	C-link.	DS	Repair soft tissue
PriMatrix™	TEI Biosciences	Fetal skin	Natural	DS	Wound healing
SurgiMend™	TEI Biosciences	Fetal skin	Natural	DS	Repair damaged soft tissue membranes
TissueMend™	TEI Biosciences	Fetal skin	Natural	DS	Repair soft tissue in rotator cuff
Vascu-Guard™	Synovis Surgical	Pericardium	C-link.	DS	Reconstruct blood vessels in neck, limbs
Veritas™	Synovis Surgical	Pericardium	C-link.	HS	Repair soft tissue
Xenform™	TEI Biosciences	Fetal skin	Natural	DS	Repair pelvic organ prolapse; urethral sling
Porcine origin					
CollaMend™	Bard	Dermis	C-link.	DS	Repair soft tissue
CuffPatch™	Arthrotek	SIS	C-link.	HS	Reinforce soft tissue
Durasis™	SIS	SIS	Natural	DS	Repair dura mater
MatriStem™	ACell	Bladder	Natural	DS	Repair soft tissue, burns
Oasis™	Healthpoint	SIS	Natural	DS	Partial/full thickness wounds, burns
Pelvicol™	Bard	Dermis	C-link.	HS	Repair soft tissue
Permacol™	Tissue Science Laboratories	Skin	C-link.	HS	Repair soft connective tissue
Restore™	DePuy	SIS	Natural	DS	Reinforce soft tissues
Stratasis™	Cook SIS	SIS	Natural	DS	Treat urinary incontinence
Surgisis™	Cook SIS	SIS	Natural	DS	Repair soft tissue
Zimmer Collagen Patch™	Tissue Science Laboratories	Dermis	C-link.	HS	Orthopedic applications
Equine (horse) origin					
DurADAPT™	Pegasus Biologicals	Pericardium	C-link.	DS	Repair dura mater
OrthADAPT™	Pegasus Biologicals	Pericardium	C-link.	DS	Repair soft tissue in orthopedics
Piscine (fish) origin					
MariGen™ Omega3	Kerecis	Cod skin	Natural	DS	Wound healing

human recipients [84]. Compared to decellularized mammalian tissues, the development of decellularized non-mammalian tissues is still at its infancy and current studies suggest that non-mammalian tissues have great potentials in clinical applications.

2.4.1 *Fish tissues*

After mammals, fish is the next most studied class of animals for xenotransplantation into mammalian recipients. Back in the 1970s, piscine islets were demonstrated to be able to survive and function in diabetic rats. Subsequently, piscine islets were shown to exhibit glucose-sensitive insulin release in vitro and in vivo, and islets from Nile tilapia (Oreochromis niloticus) were shown to be able to tolerate mammalian body temperatures and hypoxic conditions in the implant site [142]. Piscine islets have the advantage of being much easier and cheaper to harvest than porcine islets, and functioning immediately after transplantation unlike mammalian islets which take weeks to mature post-transplantation. However, implanted piscine islets can cause hyperacute rejection (HAR) and researchers have to use immunosuppression and islet encapsulation to prolong the life of the piscine implant in mammals [143, 144]. Interestingly, piscine tissues generally take a longer time than mammalian tissue to evoke HAR in rodents as piscine cells do not express α(1,3) gal, an antigen expressed by most mammalian cells that leads to rapid HAR [145].

One of the first cell-free piscine tissues developed for regenerative medicine was an acellular collagen scaffold derived from decellularized and decalcified tilapia scales for corneal regeneration [18]. The tilapia scale-derived scaffold was reported to support proliferation and migration of corneal cells, and in later studies, the scaffold was reported to have good host-implant integration in rat and rabbit models [146-148]. Decellularized and decalcified scales have the advantage of having similar optical and mechanical properties as mammalian cornea, and possessing good biocompatibility and biodegradability due to type I collagen being the

major component. In another study, decellularized fish scales were shown to have similar mechanical properties to mammalian bone and were therefore developed into bio-resorbable bone pins for internal fixation of bone fracture [149].

The first decellularized piscine scaffold approved by FDA and patented for clinical applications is the MariGen™ Omega 3 wound dressing derived from decellularized North Atlantic cod skin [28]. The product, developed in Iceland, was reported to induce wound healing in vitro and in vivo due to the preservation of ECM components such as collagen and the preservation of omega-3 fatty acids which possess antibacterial and anti-inflammatory properties [150]. Unlike mammalian tissues which have risks of viral and prion transmission and therefore require harsh decellularization conditions, piscine tissues do not have such risks and therefore can be processed more gently, preserving most of the beneficial components in the tissue [151]. In another study in Brazil, disinfected tilapia skin was shown to induce skin regeneration in patients with burn injuries [152]. Beside fish skin, decellularized fish swim bladder was also shown to be effective in full thickness skin wound healing in rats [153]. All these studies prove that piscine tissues are safe and effective in regenerative medicine applications, without the disease transmission risk and religious restrictions associated with mammalian tissues.

There are also studies suggesting that fish tissues may facilitate regeneration in damaged mammalian organs with limited regenerative capability, such as hearts, brains and spinal cords [154, 155]. In mammals, the adult cells in these organs lost the ability to proliferate, and any injury would cause inflammatory and fibrotic responses instead of regenerative responses. Fish, being more evolutionary primitive, retain regenerative capability throughout adulthood, and the ECM was suggested to be one of the reasons for this evolutionary difference. To prove the hypothesis that piscine ECM can restore the regenerative capability in mammalian organs, a study was performed to transplant decellularized zebrafish cardiac ECM into adult mouse heart tissues after acute myocardial infarction. The hypothesis was proven when the transplanted

zebrafish ECM increase cell proliferation *in vitro* and enabled cardiac functional recovery *in vivo* [154]. This study brings exciting hopes of using decellularized fish tissues to regenerate organs with limited regenerative capability.

2.4.2 *Reptile and amphibian tissues*

Unlike fish, reptiles and amphibians are not so widely studied for xenotransplantation into mammals. An early study was performed to graft reptile (lizard) and amphibian (tree frog) skin onto nude mice with thymic defect. While the reptile and amphibian skins were not rejected by nude mice, the skins underwent some morphological changes, possibly caused by physiological incompatibility [156]. Meanwhile, no literature has been known on the decellularization of reptile and amphibian tissues.

Reptiles and amphibian tissues hold a similar promise to fish tissues due to the ability of certain reptiles to regenerate lost tail and limbs, with complete restoration of bone, muscle and nerve tissues [157]. However, tissue regeneration in reptiles and amphibians is a very complex process and is not fully understood yet, especially at the cellular and molecular level. Hence, there are still many challenges to translate tissue regeneration in reptiles and amphibians to mammals. Moreover, studies on animal regeneration concur that high regeneration capability is a privilege enjoyed only by evolutionary primitive species. More complex species like mammals may have high regeneration capability during the early phase of life (e.g. embryonic and neo-natal phases) but rapidly lose the capability during growth, due to the introduction of more regulatory pathways to control tissue healing, cell differentiation and cell dedifferentiation [158]. More studies need to be performed to determine whether the ECM contributes to tissue regeneration in reptiles and amphibians, and whether decellularized reptile and amphibian tissues can retain regenerative properties in mammals.

2.4.3 *Avian tissues*

The idea of using avian tissues as xenografts started as early as the 1970s, when chicken skin was grafted onto nude mice with thymic defect, in the same study where lizard and tree frog skin were grafted onto nude mice. While the chicken skin was not rejected by nude mice, the chicken skin caused irritation to the mice due to de novo feather growth [156]. One of the first studies on the decellularization of avian tissues was performed on chicken tendon, with the aim of generating scaffolds suitable for tendon and ligament regeneration. The results showed that the decellularized chicken tendons retained 76-78% of the tensile strength of fresh tendons, and did not induce chronic inflammation when implanted subcutaneously into mice [159].

Among all avian species, ostrich is currently the most popular in terms of deriving decellularized tissues for regenerative medicine applications due to similar organ sizes between ostrich and human. Studies have been performed to evaluate decellularized ostrich skin for wound healing [160], decellularized carotid artery as vascular grafts [161], decellularized ostrich cornea for corneal regeneration [162], and decellularized ostrich tendon for tendon regeneration [163]. Results from these studies showed that decellularized ostrich tissues supported tissue regeneration in mammals (e.g. mice, rabbits and guinea pigs) and are therefore potentially suitable for tissue regeneration in humans.

There was also a study on the decellularization of chicken and emu lungs to generate scaffolds for lung regeneration. The avian lung is known to be superior to the mammalian lung in terms of oxygenation and gas exchange, due to thinner and more uniform walls of avian pulmonary capillaries [164]. By careful preserving the ECM and the architecture of the avian lung during decellularization, it is possible to develop a new class of scaffolds for lung regeneration [165].

2.4.4 *Current developments*

Although decellularized tissues from non-mammalian species show great promises in regenerative medicine, most studies are not yet translated into real clinical applications due to the long and difficult process of passing clinical trials and obtaining regulatory approval. Also, decellularized mammalian tissues are already well-studied and well-established in regenerative medicine, creating an inertia for clinicians to adopt non-mammalian decellularized tissues. To date, there is only one commercially available non-mammalian decellularized ECM product that is approved by the United States Food & Drug Administration (US FDA) for clinical use. It is MariGen™ Omega3, a wound dressing derived from decellularized North Atlantic cod skin, as mentioned in section 2.4.1 [28]. The FDA approval of this cod-derived product for clinical use suggested that decellularized fish tissues can be safe and effective, making them an attractive alternative to decellularized mammalian tissues. The high human consumption of fish and the abundance of ECM in fish waste also makes fish tissues an economical and easily-available source for decellularization. Fish tissues also has the additional advantages of avoiding religious constraints and risk of disease transmission associated with mammalian tissues, and having a lack of galactose-alpha-1,3-galactose (or alpha-gal), a xenoantigen that is present in mammalian tissues and is known to trigger hyperacute rejections and allergic reactions in humans [95, 119]. In the author's opinion, decellularized fish tissues have a lot of untapped potentials to become novel biomaterials for clinical applications, due to the huge diversity of fish species and the very small number of studies that has been done in this field.

2.5 Properties of fish skin

Fish have served as sources of food for humans since ancient times and many species of fish are also kept as ornamental pets or studied in research, especially in the fields of genetics,

developmental biology and pathology. While there are 8000 species of mammals, there are over 25000 species of fish [166]. Among all living fish, 96% belong to the infraclass **teleost**, which is different from the other fish mainly in the structure of the jaw bones [167]. Being the largest group of living vertebrates with the highest number of species, teleost fish come in a variety of shapes, sizes and habitats. Despite its diversity, teleost fish share a similar anatomy and physiology [166]. While there is a large evolutionary distance and many functional differences between teleost fish and mammals, interestingly a long list of human disease models has been successfully established in teleost fish, especially zebrafish, suggesting a substantial level of functional conservation between teleost fish and humans [168]. The success of using teleost fish in the field of pathology can be extrapolated to the field of tissue engineering, where useful biomaterials and bioactive substances can be extracted from teleost fish and applied in humans to facilitate tissue regeneration.

Among the various tissues and organs of a teleost fish, the skin is of the greatest interest to tissue engineers, due to the high amount of type I collagen and the presence of numerous bioactive substances in the skin, as well as the huge amount of fish skin discarded in the fishing industry, accounting for around 30% of fish waste [16, 169]. The structure and function of teleost fish skin would be reviewed in more details in the following section.

2.5.1 *Anatomy and physiology of fish skin*

As in other vertebrates, the skin of a teleost fish is a multifunctional organ and the outermost layer of the body, separating the interior from the environment and serving important functions including protection, sensory perception, communication, ion and osmotic regulation, metabolism, and thermal regulation [170]. Like human skin, teleost fish skin comprises of (i) the epidermis, a relatively thin layer consisting of multiple layers of cells, (ii) the dermis, a dense layer containing blood vessels and nerves, and consisting of mainly fibrous connective

tissue, and (iii) the hypodermis, a fatty layer connecting the dermis to the muscular or skeletal tissues [171]. The main differences between teleost fish and human skin are the lack of a keratinized layer in fish epidermis, the presence of scales and scale-forming osteoblasts instead of hairs, and the presence of mucous glands to protect the skin against pathogen and to provide lubrication instead of sweat glands and sebaceous glands [172], as shown in Figure 2.2.

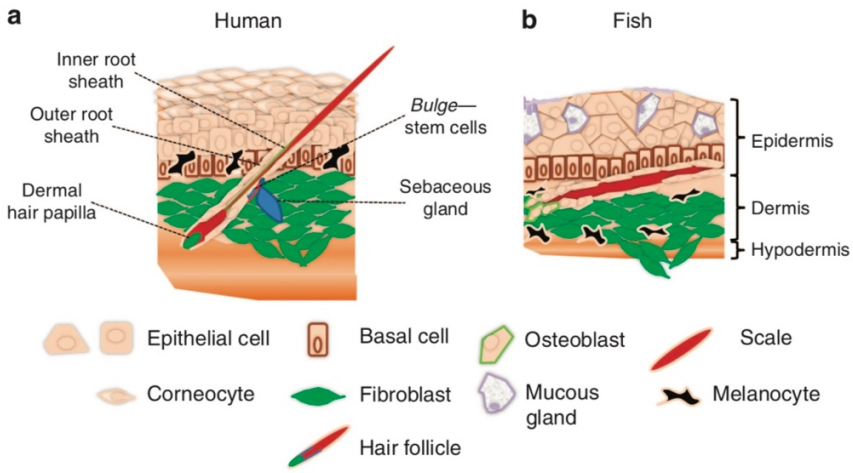

Figure 2.2: Simplified schematic drawing of (a) human and (b) fish skin. Major cell types and appendages are represented and listed in the legend. Several cell types such as mast cells or merkel cells are present in human and fish skin but are not shown. [172] (Figure reused with permission from Journal of Investigative Dermatology)

As fish epidermis lacks a keratinized layer which serves as a waterproof and shear-resistant layer in mammalian skin, teleost fish depends on scales to provide mechanical protection for deeper tissue. Most teleost fish possess elasmoid (bony-ridge) scales consisting of a thin outer layer of hydroxyapatite and a dense inner core of type I collagen fibres with a criss-cross plywood-like arrangement, which provides exceptional tensile strength and penetration resistance, as well as allows for flexibility [173]. The scales overlaps in a staggered arrangement, forming a continuous protective cover, allowing the scales to slide along each other smoothly during the fish's motion and allowing mechanical stress to spread outwards to surrounding scales and soft tissues when a compressive load is applied onto the fish body [174]. The scales, being covered in hydroxyapatite and surrounded by osteoblasts and osteoclasts,

also serves as an internal calcium reservoir and play a vital role in regulating blood calcium levels, similar to the endoskeleton of mammals [175].

While the scales protect the fish from external mechanical forces, the mucous glands on the fish epidermis serve as a chemical shield by producing mucous secretions to keep the skin surface free of pathogens. The mucus is produced and shed from the skin constantly, preventing a build-up of pathogens on the skin surface and helping to keep the skin and gills free of debris in turbid waters [176]. The mucus also helps to reduce friction between overlapping scales during the fish's motion. As the mucosal coating on fish skin is an ideal habitat and colonization target for water-borne pathogens, the mucous secretion contains a cocktail of anti-microbial peptides (AMPs), hydrolytic enzymes such as lysozyme, antibodies and other anti-infection substances to impair the establishment and proliferation of pathogens [177]. Traditionally, fish AMPs have been of interest in the aquaculture industry for the suppression of pathogen growth in fish farms, but due to their antibacterial and immunomodulatory activity, fish AMPs are gaining attention in human medicine as potential antimicrobial agent for treating human pathogens [178]. Fish mucus contains a large variety of AMPs, with each AMP offering selectivity against certain bacteria, fungi, algae, viruses, or parasites [172]. Understanding the mechanisms of fish AMP regulation could lead to a better understanding of AMP regulation in human or other species, and could lead to the design of novel antimicrobial agents.

Epithelial cells, which form the bulk of the fish epidermis, provide a vital form of protection when the skin is wounded. Within seconds or minutes after injury, epithelial cells migrate from the edge of the wound towards the centre in compact groups and rapidly cover the wound to form a barrier against infection by opportunistic pathogens [179]. The wound is closed rapidly by migrating epithelial cells, with the closure complete within a few hours to a few days [171]. In fact, fish epithelial cells are among the fasting moving cells from in vitro studies, moving at

a speed 10 to 20 times faster than mammalian fibroblasts [180]. Due to the high motility, fish epithelial cells has been a subject of interest to study the principles of locomotion in cells [181]. Beside wound coverage, epithelial cells also help to protect the skin from pathogens via proteolytic and phagocytic activities especially during the process of wound healing [182].

The dermis of most fishes is divided into two major layers: the upper layer known as stratum spongiosum, and the lower layer known as stratum compactum. The stratum spongiosum consists of a loose network of collagen and reticulin fibres and is home to fibroblasts, pigment cells, leukocytes and scale-forming osteogenic cells [171]. The stratum compactum consists of a dense matrix of collagen bundles arranged in a series of highly ordered layers, with the angles of the collagen bundles alternating between layers [183]. This criss-cross "plywood" arrangement of the collagen bundles gives the dermis a very high mechanical strength and at the same time offers flexibility by allowing the collagen layers to slide on top of one another during the fish's movement [184]. Beside dermal fibroblasts which are distributed between the collagen fibres, few other cells are present in the stratum compactum. Among the various components of the fish skin, it is the stratum compactum that has received the most attention in tissue engineering, due to the high composition of type I collagen and the high mechanical strength of the ECM. While type I collagen has been extracted from fish skin in the food industry since the 1960s and was gaining prominence in the cosmetics and biomedical industries from the 1990s [118], the utilization of the intact stratum compactum as a biomaterial in tissue engineering is a relatively new concept, with the first fish-skin derived scaffold appearing as recently as 2013, when MariGen™ Omega 3, a wound dressing derived from decellularized North Atlantic cod skin, was introduced [28].

2.5.2 *Fish proteins and peptides*

Beside type I collagen, fish skin also harbours a variety of bioactive substances that could be beneficial for tissue regeneration. Fish protein hydrolysates, produced by the enzymatic hydrolysis of fish collagen or fish skin, have been shown to exhibit potent biological activities beyond their nutritional value, including antioxidant, antimicrobial, antihypertensive and obesity-control properties [185, 186]. The most potent peptides of these fish protein hydrolysates are usually small protein fragments having 2-20 amino acids, with the bioactivity dependent on the amino acid composition of the sequence [187]. Interestingly, these bioactive peptides remain latent within the original protein molecule or ECM and shows bioactivity only after hydrolysis. The most commonly used proteases for the hydrolysis of fish proteins or tissues include pepsin, alcalase, and chymotrypsin [188]. The peptides can be separated using chromatographic methods and further purified by ultrafiltration membranes [189].

One application of fish peptides that has gained wide recognition is cosmetics, due to a number of beneficial properties including high moisturizing action, antioxidant properties and protection against UV radiation [190]. These properties are in high demand in cosmetic products as there is an increasing interest in health and physical appearance. Fish peptides exhibit antioxidant properties owing to their abilities to scavenge free radicals that cause oxidative stress and inflammation, and they do not possess safety concerns associated with synthetic antioxidants traditionally used in food and cosmetics such as butylated hydroxyanisole (BHA), butylated hydroxytoluene (BHT) and propyl gallate [191]. Fish peptides have been shown to inhibit the activity of matrix metalloproteinases (MMPs) and collagenases, which are responsible for aged-related wrinkle formation by degrading collagen and ECM in aging skin [192, 193]. Fish peptides were reported to protect the skin from UV radiation as they are able to reverse and prevent the oxidative damage in the tissue caused by

the UV radiation and inhibit ECM breakdown [194, 195]. Fish peptides that possess cationic moieties have been reported to have antimicrobial properties and are extensively studied in the development of novel antimicrobial agents in cosmeceutical products [196].

2.6 Nile tilapia (*Oreochromis niloticus*)

There is a growing interest in Nile tilapia from the biomedical community, due to the high denaturation temperature (T_d) of its type I collagen, which at 35 °C, is the highest T_d among all reported fish collagen and is close to the T_d of mammalian collagen [30]. Nile tilapia, a tropical freshwater fish native to Africa, had been a food source in ancient Egypt and is now only second to carp as the world's most cultivated fish. Dubbed by fishery experts as the "aquatic chicken", tilapia is farmed in more than 100 countries due to its fast breeding, high protein content, adaptability in a wide range of environments, and high resistance to disease [17]. Due to territorial and sexual competition in its native habitat, tilapia reaches sexual maturation within a short time (usually within 6 months), and has high birth and turnover rates in the absence of predators and competing species [197]. In comparison, the North Atlantic cod takes more than 2 years to mature and has a high mortality rate when farmed, making it an expensive source of food and biomaterials [198].

Originally cultivated on a subsistence level in developing countries to meet local protein needs, tilapia has moved into mainstream seafood markets worldwide due to its mild flavour, affordable price and reliable year-round supply. To meet worldwide demand, the global production of tilapia increased from 1.5 million tonnes in 2003 to 2.5 million tonnes in 2010 and to 3.4 million tonnes in 2013 [17]. The wide geographical distribution and constant availability of tilapia allow tilapia collagen and tilapia-derived biomaterials to be produced on a large scale and at a low price.

The skin and scales of tilapia are rich in Type I collagen, and there have been numerous studies on the extraction, purification and characterisation of tilapia collagen, especially in the field of food science [199-201]. Tilapia collagen was first identified as a potential biomaterial in 2009 by Sugiura et al, who reported that tilapia collagen sponges exhibited similar bioresorption rates and inflammatory responses to porcine collagen sponges [30]. In 2010, Lin et al developed a novel scaffold for corneal regeneration from decellularized tilapia scales, and follow-up *in vivo* studies in rat and rabbit models showed that decellularized tilapia scales had similar optical properties to human cornea, had high biocompatibility and supported function through a long term evaluation of 6 months [18, 147, 148]. In 2014, Yamamoto et al performed a series of in vitro and in vivo biological tests on tilapia collagen to evaluate its sterility, toxicity and immunogenicity. The sterility tests showed an absence of bacteria and viruses, and all evaluations of cell toxicity, sensitization, chromosomal aberrations, intracutaneous reactions, acute systemic toxicity, pyrogenic reactions, and hemolysis were negative according to ISO criteria, proving that tilapia collagen is biologically safe for biomedical applications [19]. In 2015, Tang et al performed an in vitro study with rat odontoblast-like cells on tilapia scale collagen, and reported that tilapia collagen has similar biocompatibility to porcine collagen, suggesting that tilapia collagen might be a potential alternative to mammalian collagen for oral-maxillofacial regeneration [202]. In 2016, Zhou et al developed crosslinked electrospun tilapia collagen nanofibers for skin wound dressing, and reported that the electrospun tilapia nanofibers supported proliferation of human dermal fibroblasts and human keratinocytes, and accelerated *in vivo* wound healing in rats effectively [20]. In 2017, a team in Brazil reported that disinfected tilapia skin was able to induce skin regeneration in patients with burn injuries, and there was minimal scarring due to the high amount of type I collagen in tilapia skin [152].

To the author's knowledge, the study of decellularized tilapia skin has not been reported, so the work in this thesis is expected to contribute valuable information in the field of

decellularized fish tissues for clinical applications. Extrapolating from the successes of the previous studies on tilapia collagen and decellularized tilapia scales, we can hypothesize that tilapia derived collagen and decellularized tilapia skin would be able to play a constructive role in a variety of clinical applications and would become an economical, religiously sensitive and biologically safe alternative to mammalian collagen products.

3 Development of crosslinked electrospun tilapia collagen scaffolds

3.1 Introduction

Collagen from the Nile tilapia (*Oreochromis niloticus*) has been extracted as a food additive for several decades but its potential as a tissue engineering biomaterial was only identified as recently as 2009 by Sugiura *et al* [30]. The biological safety of Tilapia collagen was validated by Yamamoto et al in 2014 [19], and tilapia collagen has been proven to support a variety of tissue regeneration including corneal regeneration [18], oral-maxillofacial regeneration [202] and chondrogenesis [203]. However, in some of these studies, tilapia collagen was evaluated as a coating on tissue culture dishes, which may be useful for assessing cell biocompatibility but is not representative for *in vivo* and clinical applications. For tilapia collagen to be successfully translated into clinical applications, it has to be processed into a scaffold capable of being handled and implanted into a target site with ease.

As mentioned in chapter 2, there are two approaches to convert tilapia collagen into useable scaffolds. The first approach is to extract collagen molecules from a tissue, purify them and reconstitute them into solid structures, while the second approach is to decellularize a collagenous tissue leaving behind an acellular collagen matrix [33]. The first approach was attempted by Sugiura *et al* in 2009 when they subjected lyophilised tilapia collagen sponges to physical or chemical crosslinking to produce crosslinked collagen sponges for *in vitro* and *in vivo* evaluations. In 2015, Zhang *et al* successfully fabricated fibrous scaffolds from tilapia collagen and polycaprolactone (PCL) by electrospinning, and the scaffolds supported the growth of L929 fibroblasts, although the composition of collagen in the composite scaffold was relatively low (accounting for only 4-10% of the scaffold by weight) [82]. In 2016, Zhou

et al developed an electrospun membrane comprising entirely of tilapia collagen and crosslinked by glutaraldehyde vapour [20]. The membrane, which supported the proliferation of human skin cells and accelerated wound healing in rats, generated an intense interest in tilapia collagen scaffolds, as this study was one of the first to report on an electrospun scaffold made of 100% collagen from one of the world's most cultivated fish species.

Decellularization, the other approach to produce collagen scaffolds, had been attempted by Lin et al in 2010, when they successfully decellularize and demineralize tilapia scales into acellular scaffolds for corneal regeneration [18]. Beside tilapia scales, no other parts of the tilapia has been reported for decellularization prior to this thesis. In the author's opinion, tilapia skin would be a novel and useful source of decellularized tissue due to its high composition of type I collagen and its high mechanical strength. Due to a lack of information on decellularized tilapia skin and the success of crosslinked electrospun tilapia collagen in the study by Zhou et al, the first objectives of this thesis would be to investigate the properties of tilapia collagen on the basis that collagen accounts for more than 90% of the dry weight of the ECM in most tissues, including fish skin [12], and to develop a crosslinked electrospun tilapia collagen scaffold to pave the way for evaluating the decellularized tilapia skin scaffolds developed subsequently. Knowing the properties of tilapia collagen would help in the understanding of tilapia ECM during the development of decellularized tilapia skin scaffolds, as tilapia collagen is the major component of tilapia skin ECM. Developing a crosslinked electrospun tilapia collagen scaffold would also allow us to compare the advantages and disadvantages between scaffolds formed by the reconstitution of collagen and scaffolds formed by decellularization.

Electrospinning, a fabrication technique using an electric field to deposit polymer fibres onto a target substrate, is increasingly employed in tissue engineering to reconstitute biomaterials from solutions to fibrous membranes [204]. Electrospinning is valued for its simple operation,

low-cost setup, high performance in nanofiber production, and most importantly, its ability to mimic the porous micro- and nano-structure of natural ECM, as the fibre diameter and pore size can be controlled to a range from several microns down to 100 nm or less [22]. The process is easily reproducible, and the structural and biochemical properties of the electrospun scaffold can be adjusted by varying the solution composition and spinning parameters [20, 81, 82]. The main principle of electrospinning is the electrostatic interaction driven by the high voltage difference between the needle and the collector, causing the polymer solution at the end of the needle to form a Taylor cone towards the collector, as shown in Figure 3.1 [205]. The positively charged polymer solution, drawn by the negatively charged collector, would leave the needle and accelerate towards the collector. As the polymer solution approaches the collector, it becomes thinner due to molecular cohesion, and the solvent evaporates, leaving the residual polymer fibres collecting randomly on the collector to form a fibrous mat [206].

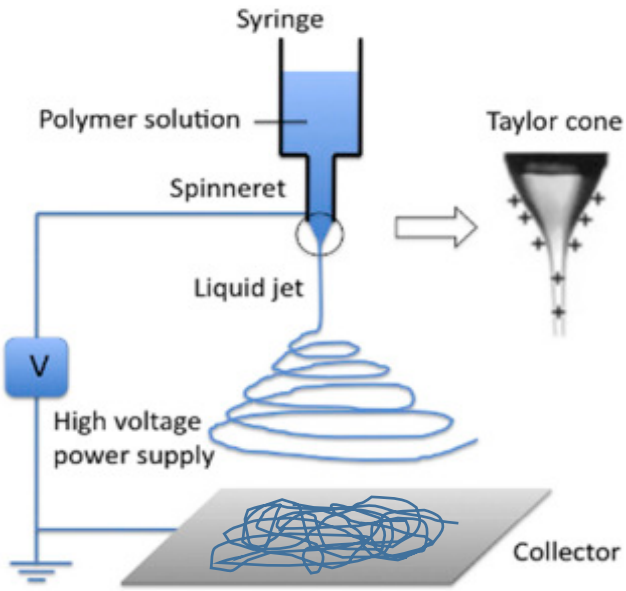

Figure 3.1: Schematic diagram of a basic electrospinning process [205] (Figure reused with permission from Elsevier B.V.)

Originally reported in 1934 for spinning artificial fibres in the textile industry [207], electrospinning was used mainly for the production of air filters, adsorbent pads, and protective

clothings [208]. The potential applications of electrospun mats in tissue engineering only began to be examined in the 1970s, when Annis and Bornat reported the use of electrospun polyurethane mats as vascular prosthesis [209]. As the volatility of the solvent can affect the quality of the electrospun fibres, early electrospun scaffolds were mostly made of synthetic polymers that are soluble in volatile solvents [70]. Collagen is hydrophilic, so it was a challenge to find a suitable solvent that is able to dissolve collagen and yet volatile. It was only in 2002 when Matthews et al successfully electrospun calf-skin collagen using hexafluoro-isopropanol (HFIP) as the solvent [210]. HFIP is a volatile solvent that is able to solubilise collagen by breaking the hydrophobic interactions via its two trifluoromethyl groups and by breaking hydrogen bonds via its mildly acidic hydroxyl group. Also, HFIP is able to dissolve collagen to form a viscous solution without the aid of carrier polymers. While collagen is soluble in aqueous solutions, aqueous collagen solutions are often too fluid and require carrier polymers to achieve the required viscosity and volatility for electrospinning [211]. As a result, HFIP has become the solvent of choice for the electrospinning of collagen, and was adopted in many studies involving electrospun collagen, including the study by Zhou et al in 2016, where electrospun tilapia collagen scaffolds were reported to accelerate would healing [20].

Despite its exceptional ability to dissolve collagen and form electrospun fibres, HFIP is toxic and corrosive. HFIP in its liquid form can cause severe skin burns and eye damage, while HFIP vapour is toxic if inhaled [212]. As the solvent is evaporated during the electrospinning process, the HFIP vapour would become a health hazard to surrounding personnel or an environmental hazard if released into the atmosphere. For electrospinning to become a viable and sustainable method to produce collagen scaffolds, there is a motivation to develop greener electrospinning solvents to reduce the impact on health and environment. A number of studies have been conducted on the use of benign solvents for the electrospinning collagen, but all the studies focused on bovine and porcine collagen [213-215]. Some of these studies use acetic acid or

formic acid as the solvent. Although acetic acid and formic acid are less toxic than HFIP, they are also corrosive and dangerous to handle in high concentrations. Among the numerous studies on benign solvents, the use of a phosphate-buffered saline/ethanol solvent reported by Dong et al [216] and Bak et al [217] appears highly promising, as both phosphate-buffered saline (PBS) and ethanol are non-toxic, non-corrosive, cheap, and easily available. This PBS/ethanol system has been attempted on the electrospinning of bovine collagen and porcine collagen, and bead-free electrospun fibres could be obtained by lowering the humidity level and increasing the amount of ethanol in the solvent. The author of this thesis assumed that this PBS/ethanol system would work well for the electrospinning of tilapia collagen too.

At the time of writing, there was limited information on the use of benign solvents for the electrospinning of fish collagen, particularly tilapia collagen. Since one objective of this thesis is to develop a tilapia collagen scaffold as a model to investigate the biocompatibility of tilapia collagen, it would be beneficial and novel to use a benign solvent which is biologically and environmentally friendly to electrospin tilapia collagen.

3.2 Methodology

3.2.1 *Materials and reagents*

Fresh tilapia was purchased from a local supermarket and processed on the same day. Phosphate-buffered saline (PBS), penicillin-streptomycin, Dubecco's Modified Eagle's Medium (DMEM), fetal bovine serum (FBS), and AlamarBlue assay kit were obtained from Life Technologies (Grand Island, NY, USA). The reagents and apparatus for sodium dodecyl sulphate−polyacrylamide gel electrophoresis (SDS−PAGE) were obtained from Bio-Rad (Hercules, CA, USA). All other chemicals were obtained from Sigma Aldrich (St Louis, MO, USA) unless otherwise stated.

3.2.2 *Characterization with Bioinformatics*

The theoretical properties of the type I collagen chains from human (*homo sapiens*), cow (*bos taurus*), rat (*Rattus norvegicus*) and tilapia (*oreochromis niloticus*) were characterized and compared using currently available bioinformatics tools. The amino acid sequences and the sequence ID of the collagen type I chains from various species were retrieved from the Universal Protein Resource (UniProt) website (https://www.uniprot.org) provided by the European Bioinformatics Institute. The theoretical properties and theoretical amino acid content of the collagen chains were characterized with the ExPASy ProtParam tool (https://web.expasy.org/protparam) provided by the Swiss Institute of Bioinformatics. The amino acid sequence homology between two different collagen chains were analysed with the Basic local alignment search tool (BLAST) (http://blast.ncbi.nlm.nih.gov/Blast.cgi) provided by the National Center for Biotechnology, USA.

3.2.3 *Collagen extraction*

Collagen was extracted from tilapia skin and scales according to the methods reported by Zhou et al [20] and Pati et al [218], with slight modifications. The fish skin and scales were removed from freshly obtained tilapia, weighed separately, and immersed in PBS with 1% penicillin/streptomycin for 1 hour to remove blood and debris. The skin and scales were then rinsed in DI water, lyophilised, and weighed. The dried skin was cut into smaller pieces and each piece was weighed. The skin and scales were stirred in 0.1 M NaOH solution (in separate containers) for 6 hours with a change of solution every 2 hours to remove non-collagenous proteins. The skin and scales were rinsed with deionised (DI) water until the pH was below 8. The skin was stirred in 10% 1-butanol and 20% isopropanol in water for 24 hours to remove fats and fat-soluble pigments, while the scales were stirred in 0.5M EDTA for 48 hours with a change of solution every 24 hours to remove the superficial hydroxyapatite. The skin and scales

were rinsed with DI water again. Afterwards, the scales and skin were stirred in 0.5 M acetic acid for 48 hours to solubilize the collagen. The crude collagen extracts were separated from the solid residue by centrifugation at 10000g for 20 minutes, and 5 M NaCl solution was added to the supernatant to a final concentration of 1 M to precipitate the collagen. After centrifugation at 10000 g for 1 hour, the precipitate was re-dissolved in 0.5 M acetic acid. The solution was filtered through Whatman no. 1 filter paper, dialyzed using dialysis tubes with a molecular weight cutoff of 14 kDa in DI water overnight, and lyophilized to obtain collagen sponges. The whole process was performed at room temperature (23°C ± 1°C).

Collagen was also extracted from rat tail collagen according to the methods reported by Timpson et al [219] with some modifications. Rat tails were obtained from the Animal Research Facility (ARF) of Nanyang Technological University (NTU) and were stored in 70% ethanol at -20°C until ready for processing. The tendons from the rat tails were removed and immersed in PBS with 1% penicillin/streptomycin for 1 hour to remove blood and debris. The tendons were rinsed with DI water, lyophilised, and weighed. The subsequent collagen extraction and purification steps were identical to those for tilapia collagen mentioned above, except that the whole process for rat tail collagen was performed at 4°C.

3.2.4 *Calculation of collagen extraction yield*

The yield of the collagen extraction was calculated to quantify the amount of collagen obtained from each batch of animal tissue. After the lyophilization, the collagen spongers were weighed. The weight of the collagen sponge was divided by the dry weight of the starting material to determine the percentage yield.

$$\text{Percentage yield} = \frac{Weight\ of\ lyophilized\ collagen}{Dry\ weight\ of\ animal\ tissues}\ X\ 100\%$$

3.2.5 *Electrospinning*

Electrospinning was performed according to the methods reported by Zhou et al [20] and Bak et al [217] with some modifications. Lyophilised collagen was dissolved in hexafluoro-isopropanol, a 20xPBS:ethanol solution at 50:50 ratio, or a 20xPBS:ethanol solution at 40:60 ratios. The collagen solutions were centrifuged at 5000 g for 3 minutes to separate solid debris and each solution was drawn into a 3 ml syringe with a needle (inner diameter 0.25 mm). The syringe was mounted on a syringe pump with the needle tip 10 cm above the aluminum foil collector. The set-up was conducted in a hermetically sealed glove box (Kiyon, Korea) with the inner atmosphere maintained by nitrogen gas, the temperature maintained within (24 ± 2) °C and the relative humidity maintained in the range of (30 ± 5) %. A voltage of 10 kV was applied between the needle and the collector, and the pump flow rate initially set at 0.6 mL/h. To optimise the electrospinning process, each parameter (voltage, flow rate or distance) was adjusted, and electrospun nanofibers were collected on microscopic glass slides and observed under a microscope. The fibre diameters were then measured by ImageJ analysis software (National Institute of Health, USA). After the process was optimized, the electrospinning was left to continue for 3 hours, with the collector rotated every 15 minutes to ensure all areas of the collector was covered. The electrospun mats were then crosslinked in glutaraldehyde vapour for 4 hours or in 200 mM 1-ethyl-3-(3-dimethylaminopropyl) carbodiimide (EDC) + 200 mM N-hydroxy-succinimide (NHS) in ethanol for 24 hours. The glutaraldehyde-crosslinked mats were vacuum-dried overnight, while the EDC/NHS-crosslinked mats were rinsed in absolute ethanol to remove residual EDC/NHS before being vacuum-dried overnight. The whole process was performed at room temperature.

3.2.6 *Scanning Electron Microsopy*

The morphology of the membranes was analysed by scanning electron microscopy (SEM). Each sample were cut into 3 mm × 3 mm pieces, fixed on carbon tape,and dried in vacuum overnight. The dry samples were sputter-coated for 200 seconds at 10 mA using a platinum ion coater (JFC-1600, JEOL, Japan) and analysed with the SEM machine (JSM-6700F, JEOL, Japan).

3.2.7 *Differential Scanning Calorimetry*

The denaturation temperature of the collagen sample was determined by differential scanning calorimetry (DSC) with the Diamond DSC system (PerkinElmer, MA, USA). The lyophilised collagen were rehydrated with 0.05M acetic acid with a weight:volume ratio of 1:40, while crosslinked membranes were pre-wetted to mimic physiological conditions, tapped with tissue paper to remove excess water and cut into 3 mm × 3 mm pieces. After weighing, each piece was placed into an aluminium sample pan, which was then sealed with a pan cover. The sample pan and reference pan were inserted into the DSC system and the denaturation temperature and denaturation enthalpy of the samples were determined with a heating rate of 10 °C per minute. The test was performed at least three times for each set of samples.

3.2.8 *Sodium dodecyl sulphate−polyacrylamide gel electrophoresis*

The composition and molecular weight of the individual proteins in the collagen samples were visually analysed using sodium dodecyl sulphate−polyacrylamide gel electrophoresis (SDS−PAGE). Lyophilised collagen was dissolved in 1x PBS to form a 2 mg/ml collagen solution, 50 µl of which was mixed with equal volume of Laemmli sample buffer (Bio-Rad, USA). Crosslinked membranes were cut into 3 mm × 3 mm pieces and dissolved in 50 µL of 10% SDS and 50 µL of Laemmli sample buffer. The samples were heated at 95 °C for 30

minutes. 10 μL of each sample solution and the protein ladder solution were added into the wells of a SDS-PAGE gel containing a 4% polyacrylamide stacking gel (upper portion) and 7.5% polyacrylamide resolving gel (lower portion). The loaded gel was connected to a constant voltage of 110-120V until the blue tracking dye was reaching the bottom of the gel. The gel was then stained for 1 hour with CBB Stain One (Nacalai Tesque, Japan) and destained with DI water several times until the background was clear. The gel was scanned and analysed.

3.2.9 *Indirect cytotoxicity*

Indirect cytotoxicity studies were performed in accordance to ISO 10993-5 protocols. Murine fibroblasts L929 (ATCC®, VA, USA) were cultured in DMEM + GlutaMAX supplemented with 10% FBS and 1% penicillin-streptomycin. Cells were incubated at 37 °C and medium was changed every 2 days until seeding. Samples were sterilized with 70% ethanol for 2 hours and washed with DMEM + GlutaMAX, before being individually incubated in DMEM (6 cm^2 per ml media) at 37°C for 24 hours to obtain an extract of the test sample. Simultaneously, L929 cells were seeded into 24-well plates (Corning, USA) at a density of 2×10^4 cells/well and grown overnight. The culture media were then replaced by the sample extracts and after 24 hours incubation, cells were visualised by light microscopy and cell viability determined using AlamarBlue assay (Invitrogen, USA). Polyurethane film containing 0.1% zinc diethyldithiocarbamate (ZDEC) was used as positive (toxic) control and high-density polyethylene (HDPE) was used as negative (non-toxic) control.

3.2.10 *Cell adhesion, viability and proliferation*

The biocompatibility of the membranes were evaluated with L929 fibroblasts. Samples were cut into 10 × 10 mm squares, sterilized as previously described and placed into a 24 well plate (Corning, USA). L929 cells were seeded onto the samples at a density of 2×10^4 cells/well. After 1, 3, 7 days, cell proliferation was evaluated by AlamarBlue assay.

3.2.11 *Statistical Analysis*

Quantitative results are expressed as mean ± standard deviation (SD) and differences between mean values were evaluated using a two-tailed Student's t-test. A p-value of <0.05 was considered to be statistically significant.

3.3 Results and Discussion

3.3.1 *Characterization with Bioinformatics*

Before using tilapia collagen in tissue engineering applications, it is useful to understand the basic properties of tilapia collagen and the similarities and differences between tilapia collagen and mammalian collagen. Thanks to information technology, many of the physical and molecular properties of proteins can be predicted and analysed in a short time using a wide array of bioinformatics tools. As the goal of this thesis is to utilise tilapia collagen biomaterials in tissue engineering applications, it would be appropriate to investigate the properties of tilapia collagen and compare tilapia collagen with mammalian collagen, in order to predict the physical properties of tilapia collagen and the biocompatibility of tilapia collagen towards other species *in vitro* and *in vivo*.

Among the various types of collagen, type I collagen is the most abundant in animal skin and bones and is the most common type of collagen in collagen biomaterials, so the attention of the bioinformatics characterization would be on type I collagen. In particular, tilapia type I collagen would be compared with human type I collagen because of the goal of using tilapia collagen in human patients, with bovine type I collagen because of its popularity in current commercial products, and with rat type I collagen because of the widespread use of rats in animal testing of biomaterials. The theoretical properties and theoretical amino acid content of the pro-collagen type I chains from the four species were presented in Table 3-1.

Table 3-1: Theoretical properties and theoretical amino acid content of pro-collagen type 1 chains from human (*Homo sapiens*), Cow (*Bos taurus*), Rat (*Rattus norvegicus*) and Nile Tilapia (*Oreochromis niloticus*) using the Expasy ProtParam tool (https://web.expasy.org/protparam). pI = isoelectric point.

Species	Human (*Homo sapiens*)		Cow (*Bos taurus*)		Rat (*Rattus norvegicus*)		Nile Tilapia (*Oreochromis niloticus*)		
Collagen Name	Type I α1	Type I α2	Type I α1	Type I α2	Type I α1	Type I α2	Type I α1	Type I α2	Type I α3
Gene Name	COL1A1	COL1A2	COL1A1	COL1A2	COL1A1	COL1A2	COL1A1	COL1A2	COL1A3
Sequence ID	P02452	P08123	P02453	P02465	P02454	P02466	G9M6I5	G9M6I6	G9M6I7
Number of Amino Acids	1464	1366	1463	1364	1453	1372	1447	1350	1444
Molecular Weight (Da)	138942	129314	138938	129064	137953	129564	137283	126477	136079
Theoretical pI	5.60	9.08	5.60	9.23	5.71	9.39	5.64	9.18	5.68
Amino acid content (Number of amino acid in protein, percentage of total number of amino acids)									
Alanine (A)	139 (9.5%)	129 (9.4%)	143 (9.8%)	126 (9.2%)	130 (8.9%)	128 (9.3%)	157 (10.9%)	145 (10.7%)	137 (9.5%)
Arginine (R)	71 (4.8%)	72 (5.3%)	70 (4.8%)	73 (5.4%)	67 (4.6%)	74 (5.4%)	73 (5.0%)	73 (5.4%)	68 (4.7%)
Asparagine (N)	28 (1.9%)	41 (3.0%)	29 (2.0%)	43 (3.2%)	32 (2.2%)	41 (3.0%)	28 (1.9%)	36 (2.7%)	27 (1.9%)
Aspartic acid (D)	66 (4.5%)	43 (3.1%)	64 (4.4%)	43 (3.2%)	61 (4.2%)	40 (2.9%)	63 (4.4%)	47 (3.5%)	66 (4.6%)
Cysteine (C)	18 (1.2%)	9 (0.7%)	18 (1.2%)	9 (0.7%)	18 (1.2%)	9 (0.7%)	18 (1.2%)	8 (0.6%)	17 (1.2%)
Glutamine (Q)	49 (3.3%)	33 (2.4%)	51 (3.5%)	36 (2.6%)	49 (3.4%)	39 (2.8%)	43 (3.0%)	30 (2.2%)	38 (2.6%)
Glutamic acid (E)	75 (5.1%)	66 (4.8%)	76 (5.2%)	64 (4.7%)	74 (5.1%)	63 (4.6%)	78 (5.4%)	58 (4.3%)	69 (4.8%)
Glycine (G)	391 (26.7%)	381 (27.9%)	389 (26.6%)	380 (27.9%)	389 (26.8%)	382 (27.8%)	387 (26.7%)	385 (28.5%)	396 (27.4%)
Histidine (H)	9 (0.6%)	15 (1.1%)	9 (0.6%)	12 (0.9%)	9 (0.6%)	12 (0.9%)	7 (0.5%)	16 (1.2%)	10 (0.7%)
Isoleucine (I)	24 (1.6%)	32 (2.3%)	25 (1.7%)	35 (2.6%)	26 (1.8%)	32 (2.3%)	26 (1.8%)	24 (1.8%)	31 (2.1%)
Leucine (L)	48 (3.3%)	61 (4.5%)	50 (3.4%)	60 (4.4%)	50 (3.4%)	62 (4.5%)	44 (3.0%)	53 (3.9%)	41 (2.8%)
Lysine (K)	57 (3.9%)	50 (3.7%)	57 (3.9%)	50 (2.75)	57 (3.9%)	49 (3.6%)	57 (3.9%)	46 (3.4%)	55 (3.8%)
Methionine (M)	13 (0.9%)	10 (0.7%)	13 (0.9%)	9 (0.7%)	15 (1.0%)	10 (0.7%)	26 (1.8%)	14 (1.0%)	20 (1.4%)
Phenylalanine (F)	27 (1.8%)	22 (1.6%)	24 (1.6%)	23 (1.7%)	26 (1.8%)	22 (1.6%)	29 (2.0%)	22 (1.6%)	26 (1.8%)
Proline (P)	278 (19.0%)	232 (17.0%)	279 (19.1%)	236 (17.3%)	275 (18.9%)	230 (16.8%)	252 (17.4%)	228 (16.9%)	252 (17.5%)
Serine (S)	60 (4.1%)	52 (3.8%)	58 (4.0%)	54 (4.05)	68 (4.7%)	64 (4.7%)	52 (3.6%)	63 (4.7%)	81 (5.6%)
Threonine (T)	45 (3.1%)	42 (3.1%)	44 (3.0%)	43 (3.2%)	44 (3.0%)	44 (3.2%)	53 (3.7%)	49 (3.6%)	49 (3.4%)
Tryptophan (W)	6 (0.4%)	5 (0.4%)	6 (0.4%)	5 (0.4%)	6 (0.4%)	4 (0.3%)	6 (0.4%)	5 (0.4%)	6 (0.4%)
Tyrosine (Y)	13 (0.9%)	16 (1.2%)	16 (1.1%)	13 (1.0%)	14 (1.0%)	14 (1.0%)	10 (0.7%)	15 (1.1%)	13 (0.9%)
Valine (V)	47 (3.2%)	55 (4.0%)	42 (2.9%)	50 (3.7%)	43 (3.0%)	53 (3.9%)	38 (2.6%)	33 (2.4%)	42 (2.9%)
Instability index *	30.43	23.38	31.64	24.35	33.20	22.46	27.03	23.21	26.42
Aliphatic index **	37.98	47.67	38.09	47.03	37.93	47.25	37.33	40.07	37.37
Number of RGD peptide	0	0	0	1	0	0	2	0	0

* Instability index – An estimate of the stability of the protein in aqueous solution based on statistical analysis of 12 unstable and 32 stable proteins

** Aliphatic index – Relative volume occupied by aliphatic side chains (Ala, Val, Ile, Leu)

As the amino acid sequences from the Universal Protein Resource (UniProt) website are derived from the genome of each species, the amino acid sequences of collagen actually reflect the sequences of pro-collagen, which is formed immediately after mRNA transcription and has not undergone post-translational modifications. Hence, the amino acids hydroxyproline and hydroxylysine, which are present in collagen and are formed by the hydroxylation of proline and lysine during post-translational modifications, are reflected as proline and lysine on the sequences of pro-collagen. Also, the pro-peptides at the end of the chains, which are cleaved off during post-translational modifications, are reflected in the pro-collagen sequence. Nevertheless, using the pro-collagen sequences allow us to compare the sequences at the genetic level, and evaluate the degree of genetic conservation of type I collagen between species.

From Table 3-1, it was observed that the number of amino acids, molecular weight and isoelectric point (pI) differ between the α_1 and α_2 chains in every species, but are generally similar in the α_1 chains between species and similar in the α_2 chains between species. One major difference between mammalian and tilapia type I collagen is that mammalian type I collagen composes of two α_1 chains and one α_2 chains, while fish type I collagen composes of 3 different chains – α_1, α_2 and α_3 [37]. For all species, the α_2 chain is shorter than the α_1 chains by 80-100 amino acid residues, and for tilapia, the α_1 and α_3 chains have similar lengths, with the α_1 chain longer than the α_3 chain by just 3 amino acid residues. One interesting observation is that the α_1 chains in all species, as well as the α_3 chain in tilapia, have a theoretical isoelectric point (pI) of 5.6 to 5.7, while the α_2 chains in all species have a theoretical pI of 9.0 to 9.4. The isoelectric point (pI) of a protein is the pH where the protein acquires a zero net charge, and is also the pH where the protein has minimum solubility in water and would precipitate out of solution [21]. The lower pI values of the α_1 and α_3 chains are due to a higher composition of

aspartic acid and glutamic acid residues in the sequences. At neutral pH (pH 7), the α_1 and α_3 chains would carry a negative charge while the α_2 chain would carry a positive charge. This charge difference creates an electrostatic attraction between the α_1/α_3 and α_2 chains, which explains the ability for collagen molecules to self-assemble readily in solution. In reality, the pI of collagen is lower, with the actual pI values of bovine gelatin reported to be 4.7 and 7.7 [220]. This is because some of the proline (pI = 6.3) and lysine (pI = 9.5) residues are hydroxylated during post-translational modification to hydroxy-proline (pI = 5.7) and hydrolysine (pI = 9.2), leading to a drop of pI [221]. Extrapolating from this observation, we expected the actual pI values of tilapia collagen to be lower than those reported in Table 3-1.

Another observation was that the amino acids glycine and proline make up a significant portion of the pro-collagen chains in all species, accounting for almost 30% and 20% respectively. As mentioned in section 2.1, glycine, being the smallest amino acid and being present on the chain at every third position, allow the three chains to pack tightly around a central axis, while the other two positions are usually occupied by proline or hydroxyproline (reflected as proline in the pro-collagen sequence) to provide stabilisation of the triple helix and hydrogen bonding between the three chains. The arrangement of the amino acids can be visualised in Figure 3.2. However, it was observed that tilapia pro-collagen has a slightly lower number of proline residues than mammalian pro-collagen, suggesting that tilapia collagen may have a lower mechanical and thermal stability than mammalian collagen. All the pro-collagen chains are predicted to be stable and hydrophilic, as indicated by the low values in the instability index and the aliphatic index. To further appreciate the similarities and differences of the type I collagen between tilapia and other animal species, sequence alignments were conducted with the Basic Local Alignment Tool (BLAST) and shown in Table 3-2. The sequence alignment between human pro-collagen type I α_1 chain and tilapia pro-collagen type I α_1 chain was also visualised in Figure 3.2.

Table 3-2: Alignment results of pro-collagen type 1 from human (*Homo sapiens*), Cow (*Bos taurus*), Rat (*Rattus norvegicus*) and Nile Tilapia (*Oreochromis niloticus*) using BLAST. "Identities" refer to amino acids that are identical between the two sequences, "positives" refer to amino acids that are identical or have similar chemical properties between the two sequences, and "gaps" refer to amino acids that are not "identities", not "positives" or missing in either sequence.

Query Sequence	Subject Sequence	Identities	Positives	Gaps
Human type I α1	Human type I α2	888/1467 (61%)	1007/1467 (68%)	104/1467 (7%)
	Bovine type I α1	1426/1464 (97%)	1442/1464 (98%)	1/1464 (0%)
	Rat type I α1	1347/1464 (92%)	1388/1464 (94%)	11/1464 (0%)
	Tilapia type I α1	1152/1465 (79%)	1240/1465 (84%)	19/1465 (1%)
Human type I α2	Bovine type I α2	1269/1366 (93%)	1303/1366 (95%)	2/1366 (0%)
	Rat type I α2	1245/1372 (91%)	1287/1372 (93%)	6/1372 (0%)
	Tilapia type I α2	957/1367 (70%)	1059/1367 (77%)	18/1367 (1%)
Tilapia type I α1	Tilapia type I α2	857/1447 (59%)	987/1447 (68%)	97/1447 (6%)
	Tilapia type I α3	1130/1451 (78%)	1232/1451 (84%)	11/1451 (0%)
	Bovine type I α1	1154/1464 (79%)	1243/1464 (84%)	18/1464 (1%)
	Rat type I α1	1131/1457 (78%)	1227/1457 (84%)	14/1457 (0%)
Tilapia type I α2	Tilapia type I α3	855/1446 (59%)	990/1446 (68%)	98/1446 (6%)
	Bovine type I α2	960/1367 (70%)	1053/1367 (77%)	20/1367 (1%)
	Rat type I α2	937/1375 (68%)	1044/1375 (75%)	28/1375 (2%)
Tilapia type I α3	Human type I α1	1078/1466 (74%)	1201/1466 (81%)	24/1466 (1%)
	Bovine type I α1	1083/1465 (74%)	1204/1465 (82%)	23/1465 (1%)
	Rat type I α1	1053/1457 (72%)	1183/1457 (81%)	17/1457 (1%)

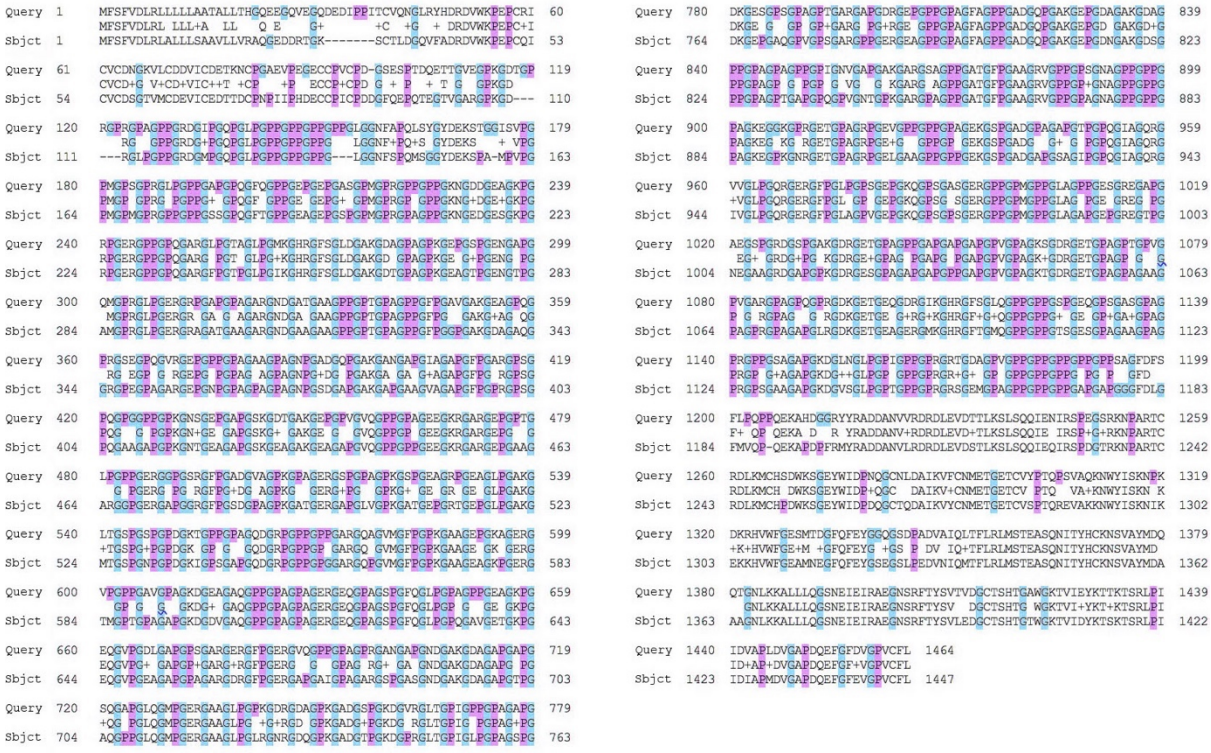

Figure 3.2: BLAST analysis of amino acid sequence alignment between human pro-collagen type I α_1 (Query) and tilapia pro-collagen type I α_1 (Sbjct). The row between Query and Sbjct represents identical and positive amino acids between the two sequences. Glycine (G) is highlighted in blue and proline (P) is highlighted in purple.

From the alignment results, a high degree of genetic conservation was observed tilapia collagen and mammalian collagen, with the sequence of the tilapia pro-collagen type I α_1 being 79% identical and 84% positive to human or bovine pro-collagen type I α_1, and having less than 2% gaps with the pro-collagen type I α_1 of any other species. In figure 4, human and tilapia pro-collagen type I α_1 chains were observed to share multiple regions of identical domains, and both sequences show the characteristic repeating Gly-X-Y sequence where many of the X and Y are occupied by proline. Interestingly, among the 4 species, bovine collagen has the closest sequence to human collagen with the highest number of identities and positives, indicating the close evolutionary distance between cows and humans. In tilapia, the α_3 chain is more similar to α_1 than α_2, and the α_1/α_2 alignment yields similar results as the α_2/α_3 alignment (59% identities, 68% positives, 6% gaps). This similarity between α_1 than α_3 suggested that the genes for both proteins probably originated from the duplication of an ancestor α_1 gene during the evolution of teleost fish 320 million years ago [222].

In view of the high degree of genetic conservation was observed tilapia collagen and mammalian collagen, it was predicted that tilapia collagen would have similar biochemical properties as mammalian collagen and would be biocompatible to mammalian cells and tissues.

3.3.2 *Yield of extracted collagen and*

The dry weight yield of the collagen extraction is presented in Table 3-3.

Table 3-3: Yield of collagen extraction from tilapia skin, tilapia scale and rat tail

Tilapia skin	Tilapia scale	Rat tail
16.6 % ± 3.5 %	0.41 % ± 0.11 %	32.0% ± 2.8 %

The yield of collagen from tilapia skin reported here is close to the value of 20.7% reported by Potaros et al, who also extracted collagen from tilapia skin at 22-23°C [223]. Our yield is

slightly lower than the reported value because of an additional filtration step to remove solid debris after the resolubilization of the salt-precipitated collagen in 0.5 M acetic acid. The yield of collagen from tilapia scale is close to the yield from grey mullet scales (0.43%), flying fish (0.72%) and horse mackerel scale (0.64%) reported by Minh Thuy et al [113], but lower than the yield from tilapia scales (2%) reported by Ikoma et al, who used 0.01M HCl instead of 0.5M acetic acid for the collagen extraction [224]. The yield of collagen from tilapia scale is much lower than the yield from tilapia skin, because the collagen fibres in scales is much more tightly packed than the collagen in skin, making solubilisation of collagen from scales much slower [201]. The yield of collagen from rat tail is much higher than the yield from tilapia skin because rat tail tendons contain a higher concentration of collagen than other tissues and do not contain non-collagenous proteins, blood, lipids and appendages which are present in skin [57].

3.3.3 *Electrospinning of tilapia collagen – optimisation of parameters*

While there is a plethora of data from the electrospinning of fish collagen with HFIP as the solvent, there was no prior reports of using PBS/ethanol as a solvent to electrospin fish collagen. As a result, some process optimisation was necessary to ensure the formation of fine and consistent fibres without beads. Generally, there are three main parameters during the electrospinning process that can affect the diameter and consistency of the fibres, and they are (i) voltage, (ii) flow rate and (iii) distance from needle to collector. In addition, the temperature and humidity can also affect the quality of the electrospun mat, but these parameters were kept in a constant range: (24 ± 2) °C and (30 ± 5) % relative humidity to maintain a consistent environment. Using a 8% (w/v) fish collagen in 50:50 20xPBS:ethanol solution, electrospinning was attempted with the following initial parameters: voltage = 10 kV, flow rate = 0.6 ml/h, distance from needle to collector = 10 cm. The fibre diameter after the adjustment of each parameter was presented in Table 3-4.

Table 3-4: Effect of different electrospinning parameters on the diameter of electrospun fibres from 8% (w/v) tilapia skin collagen in 50:50 20xPBS:ethanol.

Constant flow rate = 0.6 ml/h Constant distance = 10 cm Varying voltage		Constant voltage = 10 kV Constant distance = 10 cm Varying flow rate		Constant voltage = 10 kV Constant flow rate = 0.6 ml/h Varying distance	
Voltage (kV)	Diameter (μm)	Flow rate (ml/h)	Diameter (μm)	Distance (cm)	Diameter (μm)
12	1.70 ± 0.06	0.3	1.89 ± 0.32	10	1.80 ± 0.24
15	1.98 ± 0.19	0.4	1.81 ± 0.30	12	1.75 ± 0.18
18	1.70 ± 0.45	0.6	1.70 ± 0.10	15	1.77 ± 0.24

As the target of the optimization was to get fine and consistent fibres, the spinning parameters that produce fibres with smaller diameters and smaller standard deviation were chosen. From the results presented in Table 3-4, the following operating parameters were chosen: voltage = 12 kV, flow rate = 0.6 ml/h, distance from needle to collector = 12 cm. These parameters were adopted for the subsequent electrospinning processes with the following solutions: (i) 8% tilapia scale collagen in 50:50 20xPBS:ethanol, (ii) 8% tilapia scale collagen in 40:60 20xPBS:ethanol, (iii) 8% tilapia skin collagen in 50:50 20xPBS:ethanol, and (iv) 8% tilapia skin collagen in 40:60 20xPBS:ethanol. As each solution has slightly different viscosities, the conditions of the electrospun fibres were monitored for the first 5 minutes of electrospinning by collecting the fibres on a glass slide and observing it under the microscope, and the flow rate was adjusted accordingly. After 1 hour of electrospinning, the electrospun mats were analysed by SEM and shown in Figure 3.3.

To compare between the traditional solvent HFIP and the novel PBS:ethanol solvent, tilapia skin collagen was also electrospun using HFIP as the electrospinning solvent. The spinning parameters for tilapia skin collagen in HFIP was optimized to: voltage = 11 kV, flow rate = 0.7 ml/h, distance from needle to collector = 10 cm. The electrospun mats after 1 hour of electrospinning with HFIP were also analysed by SEM and shown in Figure 3.3.

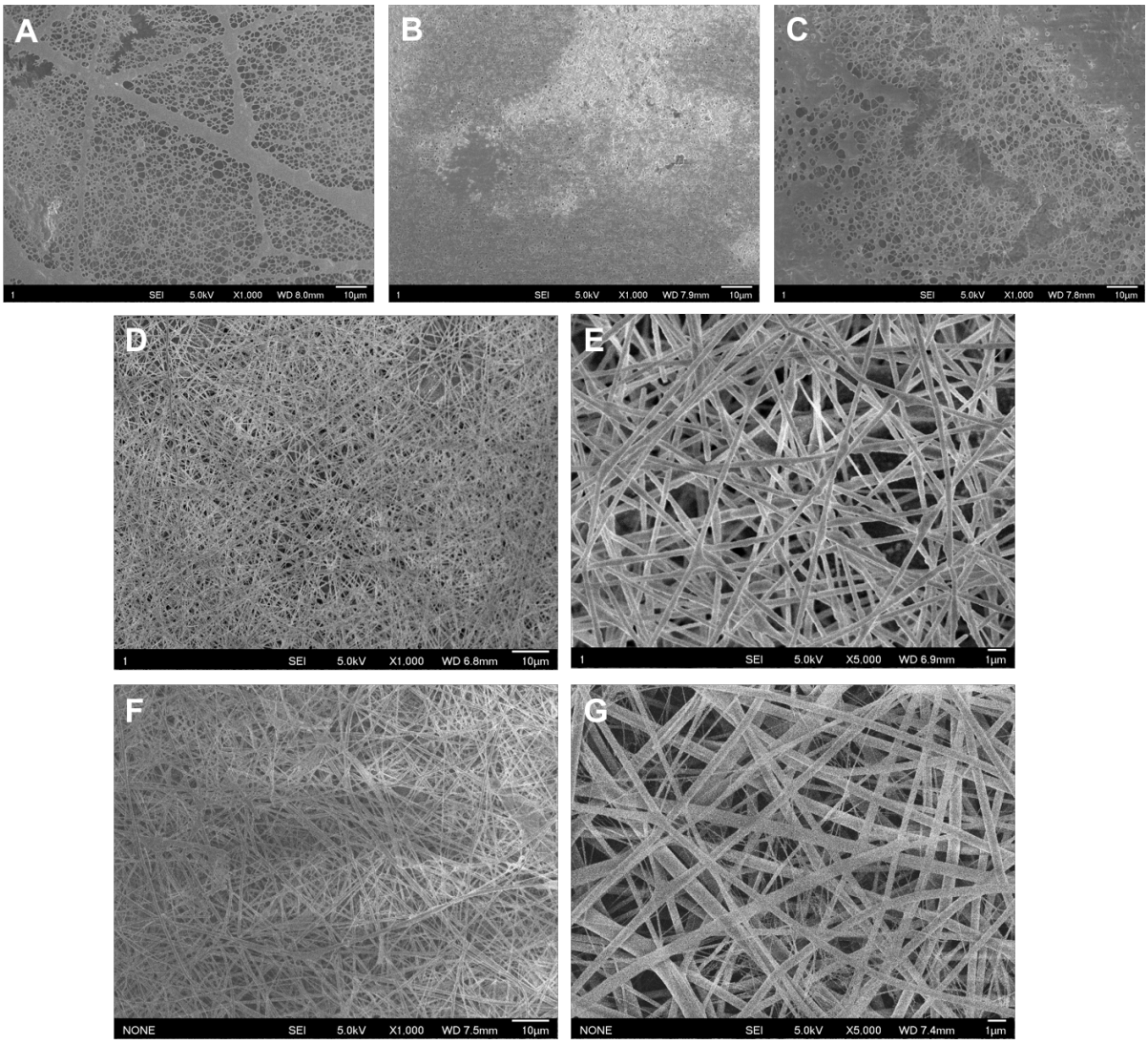

Figure 3.3: SEM images of electrospun mat with optimized parameters: (A) 8% tilapia scale collagen in 50:50 20xPBS:ethanol (1000x), (B) 8% tilapia scale collagen in 40:60 20xPBS:ethanol (1000x), (C) 8% tilapia skin collagen in 50:50 20xPBS:ethanol (1000x), (D) 8% tilapia skin collagen in 40:60 20xPBS:ethanol (1000x), (E) 8% tilapia skin collagen in 40:60 20xPBS:ethanol (5000x), (F) 8% tilapia skin collagen in HFIP (1000x), (G) 8% tilapia skin collagen in HFIP (5000x)

Among the four samples electrospun from PBS:ethanol, 8% tilapia skin collagen in 40:60 20xPBS:ethanol (Figure 3.3D & E) produced the best-looking fibres as the nanofibers were continuous, were mostly straight, had a narrow distribution of diameters ranging from 200 to 400 nm, and had minimal bead formation. The fiber morphology and consistency in 8% tilapia skin collagen in 40:60 20xPBS:ethanol were similar to those in 8% tilapia skin collagen in HFIP (Figure 3.3F & G), thus proving 40:60 20xPBS:ethanol as an effective electrospinning solvent for tilapia skin collagen.

On the other hand, 8% tilapia scale collagen in 50:50 20xPBS:ethanol (Figure 3.3A) and 8% tilapia skin collagen in 50:50 20xPBS:ethanol (Figure 3.3C) produced similar-sized fibres but most of the fibres ended up merging or breaking. A number of beads were also formed and merged with the fibres. This could be due to the incomplete evaporation of the solvent, as 50:50 20xPBS:ethanol contained more water than 40:60 20xPBS:ethanol and was less volatile as a result. As the deposited fibres were still wet on the collector, they merged with one another before the solvent evaporates.

Lastly, 8% tilapia scale collagen in 40:60 20xPBS:ethanol (Figure 3.3B) did not form continuous fibres like 8% tilapia skin collagen in 40:60 20xPBS:ethanol. When tilapia scale collagen was dissolved in 40:60 20xPBS:ethanol, the solution was noticed to be less viscous than the tilapia skin collagen solutions. Viscosity was reported to be one factor affecting fibre quality, as surface tension is a dominant factor in the formation of the Taylor cone at the end of the needle, and a solution with low viscosity leads to weak surface tension, resulting in the deposition of droplets instead of fibres [225]. Even though tilapia scale collagen and tilapia skin collagen are both type I collagen, studies have shown that the same type of collagen from different parts of the same animal may have different degrees of hydroxylation, leading to slight variations in properties [226]. Hence, to obtain good electrospun mat from tilapia scale collagen, it would be necessary to re-optimize the spinning parameters, as well as adjusting the collagen concentration and solvent composition of the spinning solution.

In summary, 8% tilapia skin collagen in 40:60 20xPBS:ethanol was chosen for subsequent experiments due to the formation of smooth and consistent fibres. As the fibre morphology and consistency in 8% tilapia skin collagen in 40:60 20xPBS:ethanol are similar to those in 8% tilapia skin collagen in HFIP, we had shown that 40:60 20xPBS:ethanol is a good alternative of HFIP for the electrospinning of tilapia skin collagen, without the toxicity of HFIP.

3.3.4 *Fabrication of crosslinked electrospun collagen scaffolds*

To evaluate the biocompatibility of tilapia collagen scaffolds electrospun with the benign PBS:ethanol solvent, 8% tilapia skin collagen in 40:60 20xPBS:ethanol was electrospun for 3 hours. One set of electrospun scaffold was crosslinked in glutaraldehyde vapour and the second set of scaffold was crosslinked in EDC/NHS in ethanol to evaluate the effect of the crosslinkers on the biocompatibility of the scaffolds. The crosslinked electrospun scaffolds were analysed by SEM (Figure 3.4) and the fibre diameters are measured by ImageJ (Table 3-5).

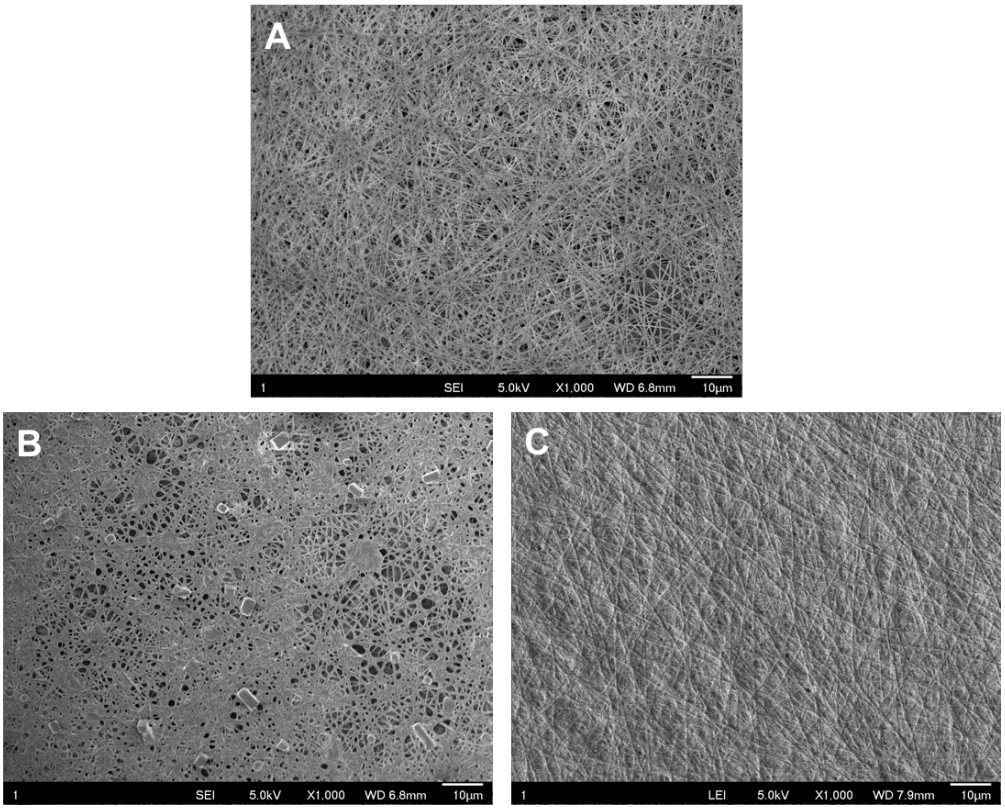

Figure 3.4: SEM images (1000x) of tilapia skin collagen scaffolds electrospun with 40:60 20xPBS:ethanol. (A) Tilapia skin collagen scaffold without crosslinking, (B) Tilapia skin collagen scaffold crosslinked by glutaraldehyde vapour for 4 hours, (C) Tilapia skin collagen scaffold crosslinked by EDC/NHS in ethanol for 24 hours

Table 3-5: Fibre diameters of tilapia skin scaffolds electrospun from 8% (w/v) tilapia skin collagen in 40:60 20xPBS:ethanol and crosslinked in different reagents.

Scaffold		Abbreviation	Fibre diameter (nm)
Electrospun tilapia skin collagen	non-crosslinked	TSC-ES	318.0 ± 73.6
	crosslinked by glutaraldehyde	TSC-GTA	505.0 ± 143.5
	crosslinked by EDC/NHS	TSC-EDC	534.6 ± 80.2

Electrospun tilapia skin collagen (TSC-ES) showed straight and consistent fibres (Figure 3.4A) with a mean diameter of 318.0 nm (Table 3-5). When TSC-ES was crosslinked, the fibre diameters generally increased as the fibres merged, with EDC/NHS generating thicker fibres and exhibiting more merging (Figure 3.4C). Although the fibre diameter increased, shrinking was observed in all crosslinked collagen films, and the contraction and merging of the collagen fibers led to a decrease in porosity, as observed in the SEM images.

After crosslinking in glutaraldehyde vapour for 4 hours, the crosslinked tilapia skin collagen (TSC-GTA) showed the formation of crystals (Figure 3.4C & D), which were very likely salt crystals precipitated from PBS, which comprises of sodium chloride, potassium chloride, sodium hydrogen-phosphate and potassium dihydrogen-phosphate [227]. As the electro-spinning solvent used was 40:60 20xPBS:ethanol, the evaporation of the solvent would leave the PBS salts immobilised within the electrospun fibres, with the salts presumably stabilized by the hydrophilic groups of the collagen molecules. During the crosslinking in glutaraldehyde vapour, the formation of new covalent bonds made the collagen fibres shrink and merge, causing the destabilisation between the salt and collagen molecules and leading to the crystallization of the salt. One set of electrospun collagen were crosslinked in glutaraldehyde vapour for 24 hours, but the results were not shown as the 24 hour glutaraldehyde crosslinked sample showed excessive shrinkage and cracks.

The EDC/NHS crosslinked samples (TSC-EDC) exhibited a higher degree of shrinking and fibre merging, but there was no formation of salt crystals, as the crosslinking was done in a solution of EDC/NHS in ethanol and the PBS salts were presumably removed by the solvent. The duration of the EDC/NHS crosslinking was chosen to be 24 hours, as electrospun collagen samples crosslinked in EDC/NHS for 4 hours, 8 hours and 12 hours were found to be too fragile to be handled. From literature, glutaraldehyde is reported to be a highly potent, fast-acting and

inexpensive crosslinker that reacts with free amino groups of proteins to create new covalent bonds, and is widely used as a crosslinking agent despite reports on its cytotoxicity [228]. In view of glutaraldehyde's toxicity, carbodiimides including EDC were viewed as a less toxic alternative. EDC works by activating the carboxylic acid groups in proteins, and NHS serves as a catalyst to covalently join the carboxylic acid groups to free amine groups in the protein [229]. EDC has limited cross-linking ability due to its short molecular structure and slower reaction time, but is not as cytotoxic as glutaraldehyde [75].

3.3.5 *Differential Scanning Calorimetry*

A biomaterial intended for *in vivo* applications must be thermally stable at body temperature to ensure that it would not undergo thermal degradation rapidly upon implantation. Hence, it is important to measure the denaturation temperature (T_d) of the material using differential scanning calorimetry (DSC), which is a popular instrument to measure the T_d of biomaterials. The denaturation temperatures of the collagen sponges, electrospun collagen scaffolds and crosslinked electrospun collagen scaffolds were presented in Table 3-6.

Table 3-6: Denaturation temperatures of collagen sponges, electrospun collagen scaffolds and crosslinked electrospun collagen scaffolds. Samples were rehydrated to mimic physiological conditions before measurement.

Scaffold		Abbreviation	Denaturation temperature (°C)
Tilapia scale		TSc	76.0 ± 2.0
Tilapia scale collagen		TScC	36.5 ± 0.1
Tilapia skin		TS	68.1 ± 1.0
Tilapia skin collagen		TSC	37.2 ± 0.7
Electrospun tilapia skin collagen	non-crosslinked	TSC-ES	34.3 ± 0.6
	crosslinked by glutaraldehyde	TSC-GTA	56.3 ± 0.5
	crosslinked by EDC/NHS	TSC-EDC	54.5 ± 3.1
Rat tail tendon		RT	63.2 ± 1.4
Rat tail collagen sponge		RTC	40.0 ± 0.9

The T_d of the native tissues were found to be much higher than the extracted collagen. Tilapia scale has the highest T_d of among all native tissues, because of the tight packing of collagen

fibrils within the scale and the outer coating of hydroxyapatite, a inorganic material known for its high thermal stability [149]. The T_d of tilapia skin is also surprisingly high, and this high T_d could be attributed to the extensive crosslinking between collagen molecules and between collagen and other structural components of the ECM. The thermal properties of tilapia skin would be discussed in more details in section 4.3.6 of Chapter 4. Rat tail tendon was also analysed as a comparison and was observed to have a high T_d, which could be attributed to the high level of crystallinity and structural alignment of the collagen fibrils within the tendon, as reported by Zeugolis et al [230].

After acid solubilisation and purification, the T_d of the extracted collagen became lower. The T_d of tilapia scale collagen (36.5°C) and tilapia skin collagen (37.2°C) determined in this study were close to that of tilapia scale collagen (36°C) reported by Ikoma et al [224], while the T_d of rat tail collagen (40.0°C) was close to that (38.6°C) reported by Ozecelikkale & Han [231]. Rat tail collagen is expected to have a higher T_d than tilapia collagen, because to cope with higher body temperatures, the collagen in warm-blooded animals has a higher composition of hydroxyproline which contributes to intramolecular hydrogen bonding and stabilisation of the triple helix in the collagen molecules [232]. Among the collagen of all fish species, tilapia collagen was reported to have the highest T_d due to its warm native habitat [30].

After electrospinning, the T_d of tilapia skin collagen dropped, suggesting that the collagen molecules became unstable during the electrospinning process. Zeugolis et al reported a loss of up to 99% of triple-helical collagen when collagen was electrospun in HFIP, with the T_d of porcine tendon collagen and bovine dermal collagen dropping more than 10°C after electrospinning [230]. Zeugolis et al also proved by circular dichroism that HFIP caused the denaturation of collagen by dissociating the triple-helix molecule into three randomly coiled α-chains. Although HFIP was not used as the solvent in our study, the presence of ethanol in

the electrospinning solvent might play a role in destabilising the collagen. Gopinath et al reported that collagen retains its triple helix in the presence of ethanol at low temperature (5°C) but becomes thermodynamically unstable at elevated temperature (~34°C), as ethanol has a dehydrating effect and disrupts the inter-peptide and water-mediated hydrogen bonds in collagen [233]. Although the PBS/ethanol solvent caused a drop in T_d of tilapia skin collagen, the drop was not as drastic as that reported by Zeugolis et al, suggesting that PBS/ethanol has a less destabilising effect than HFIP, with the ionic salts in PBS presumably reducing the dehydrating effect of ethanol by preserving the hydrogen bonds in the collagen.

Both glutaraldehyde and EDC/NHS increased the T_d of electrospun tilapia skin collagen due to the formation new covalent bonds between the collagen molecules, but the T_d of the crosslinked electrospun collagen still could not match the T_d of native tissues, as native tissues possess other structural components that stabilise the tissue integrity while the crosslinked electrospun collagen lack these non-collagenous structural molecules. Nevertheless, the increased T_d makes the crosslinked membranes stable at body temperature and suitable for *in vivo* applications.

3.3.6 *Sodium dodecyl sulphate−polyacrylamide gel electrophoresis*

Collagen, like any proteins, can undergo degradation in the presence of heat, chemicals, or enzymes. To determine the effect of processing parameters on the stability and structural integrity of the collagen chains, collagen samples can be denatured in the detergent sodium dodecyl sulphate (SDS) and analysed by sodium dodecyl sulphate-polyacrylamide gel electrophoresis (SDS-PAGE), which is a technique to separate protein mixtures by molecular weight. Here, the protein composition and molecular weights of the collagen samples were analysed SDS-PAGE (Figure 3.5).

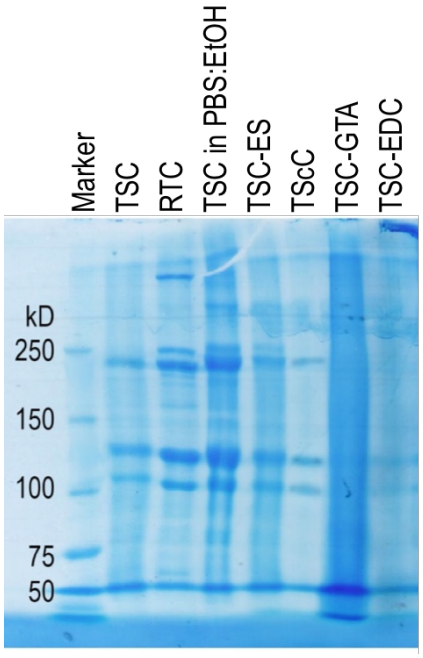

Figure 3.5: SDS-PAGE characterization of TSC (tilapia skin collagen), RTC (rat tail collagen), TSC in PBS:EtOH (tilapia skin collagen dissolved in 40:60 20x PBS:ethanol), TSC-ES (electro-spun tilapia skin collagen), TScC (tilapia scale collagen), TSC-GTA (glutaraldehyde crosslinked electro-spun tilapia skin collagen), and TSC-EDC (EDC/NHS crosslinked electro-spun tilapia skin collagen). Molecular markers were added on the leftmost lane and the marker bars indicate the protein's molecular weight in kDa.

The electrophoresis patterns showed that the extracted collagens from tilapia skin, rat tail and tilapia scales were mainly composed of α-chains (approximately 110 kDa and 130 kDa) and crosslinked β and γ chains (approximately 240 kDa, 250 kDa and 350 kDa). From the bioinformatics characterisation results (section 3.2.2), the molecular weight of pro-α_1, pro-α_2, pro-α_3 chains are 137 kDa, 126 kDa and 136 kDa respectively. When the pro-collagen chains undergoes post-translational modification, despite the addition of hydroxy groups to proline and lysine residues, the molecular weight drops slightly due to the removal of the pro-peptides at the end of the chains [234]. Hence, in the SDS-PAGE gel, the 130kDa band corresponds to the α_1 and α_3 chains and the 110 kDa band corresponds to the α_2 chain. As the α_1 and α_3 chains have similar molecular weights, the 2 bands overlap to form a more intense band at 130kDa. The 240 kDa and 250 kDa bands correspond to β chains, which are crosslinked dimers of α chains, while the 350 kDa bands correspond to γ chains, which are crosslinked trimers of α

chains. The presence of α, β and γ chains indicates that the structural integrity of the collagen molecules is preserved. An absence of the α, β and γ bands and the appearance of bands corresponding to lower molecular weights would indicate the degradation of the collagen.

The electrophoresis patterns showed that PBS/ethanol-electrospun tilapia skin collagen retain the α, β and γ bands, while Zeugolis et al reported extensive denaturation of the collagen molecules in HFIP-electrospun collagen and the disappearance of bands for HFIP-electrospun collagen in SDS-PAGE gels [230], indicating that PBS/ethanol is less damaging to the structure of collagen molecules than HFIP. However, glutaraldehyde cross-linking caused the α, β and γ bands to disappear, while EDC/NHS crosslinking retained the α bands to a small extent but caused the β and γ bands to disappear. As chemical crosslinkers form new covalent bonds between collagen molecules, the crosslinked collagen chains become immobile and could not travel down the SDS-PAGE gel during electrophoresis. As mentioned in section 3.3.4, EDC was reported to have a slower reaction time and lower crosslinking efficiency [75], hence the cross-linking might not be complete and some unbound collagen molecules could travel down the SDS-PAGE gels, giving rise to the α bands.

3.3.7 *Indirect cytotoxicity*

Before a biomaterial is used for any in vitro or in vivo applications, it is crucial to check whether the material is toxic and has the potential to induce unfavourable immune responses. Indirect cytotoxicity assay, which is the determinination of cell viability after incubation in the sample extract, is a relatively simple method to evaluate the toxicity of a material and is an accepted standard method in ISO-10993-5 [235]. Here, the cell viability of L929 fibroblasts after incubation in the sample extract was evaluated quantitatively in term of the cellular metabolic function by AlamarBlue assay (Figure 3.6).

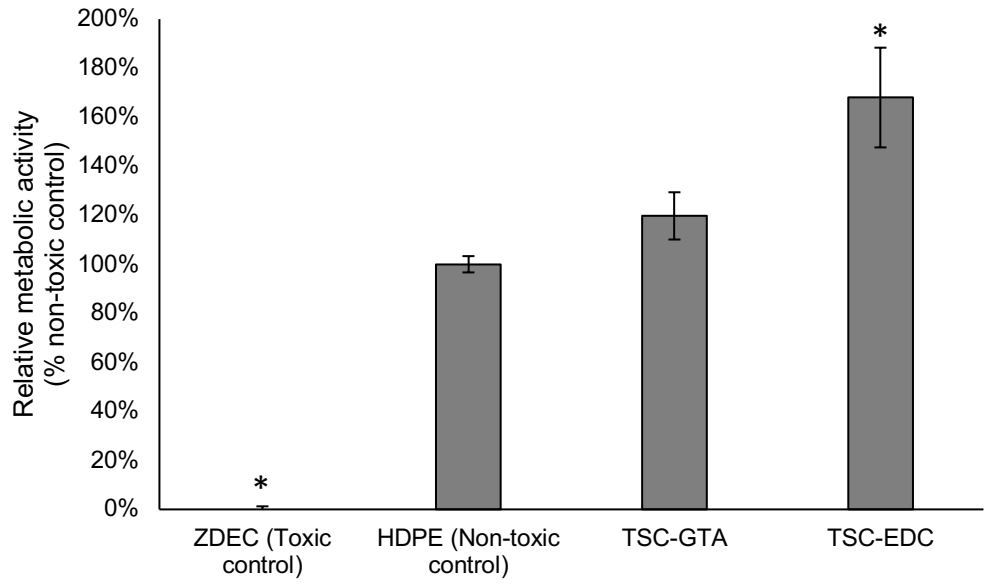

Figure 3.6: Indirect cytotoxicity studies of TSC-GTA (glutaraldehyde crosslinked electro-spun tilapia skin collagen) and TSC-EDC (EDC/NHS crosslinked electro-spun tilapia skin collagen) by determining the metabolic function of murine fibroblast L929 with AlamarBlue assay. The samples were assayed after 24h incubation and the fluorescence intensity values were normalized against the non-toxic control. *$p < 0.05$ when compared to HDPE (non-toxic control).

The results indicated that both crosslinked electrospun collagen scaffolds were non-toxic, as L929 cells incubated in the extracts of the 4 scaffolds exhibited higher metabolic activities than the non-toxic control HDPE. Although glutaraldehyde is reported to be cytotoxic, the glutaraldehyde-crosslinked scaffolds did not exhibit any cytotoxicity, suggesting that the amount of residual glutaraldehyde was negligible. It was assumed that the free glutaraldehyde molecules had been removed by vacuum drying or had totally reacted with the collagen molecules. On the other hand, EDC/NHS-crosslinked scaffolds were found to be even less toxic than the glutaraldehyde-crosslinked scaffolds, with the cellular metabolic activities in their extracts significantly higher than that of the non-toxic control. This confirmed that EDC is a less cytotoxic crosslinker than glutaraldehyde. Between the two scaffolds, TSC-EDC showed the least cytotoxicity, as evident by the highest metabolic activity exhibited by the L929 cells incubated in the extract of TSC-EDC. Looking at the SDS-PAGE results, it was possible that the crosslinking was incomplete in EDC/NHS-crosslinked scaffolds, leading to

the unbound collagen molecules leaching into the sample extract and improving the viability of the L929 cells. As the indirect cytotoxicity assay evaluates the cytotoxicity of a material by the toxic substances released into the sample extract, any water-soluble biocompatible substances may interfere with the toxicity of the dissolved toxins. To assess the cytotoxicity of a material more accurately, it would be necessary to conduct experiments where cells have direct contact with the material.

3.3.8 *Cell adhesion and proliferation*

The biocompatibility of a scaffold and its integration with the host tissues depend on its surface properties, which play a role in influencing cell attachment and proliferation. Here, the biocompatibility of the four crosslinked electrospun collagen scaffolds were assessed by seeding L929 fibroblasts onto the scaffolds and evaluating the biological behaviour at selected time-points (1, 3 and 7 days) (Figure 3.7). The blank in this study referred to the polystyrene culture dish, where cells were directly seeded onto the dish without any scaffolds.

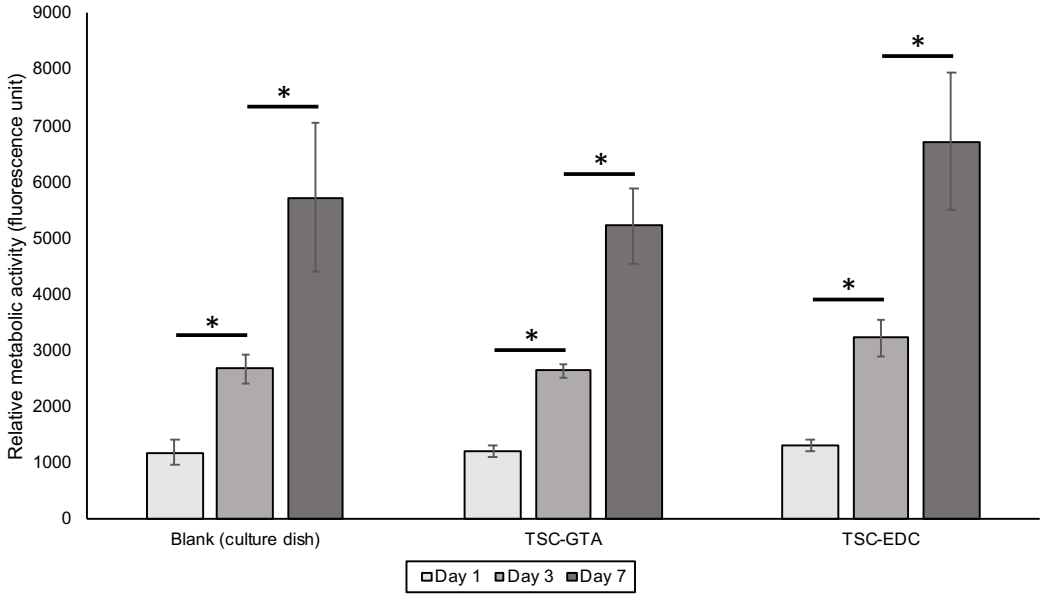

Figure 3.7: Biocompatibility of TSC-GTA (glutaraldehyde crosslinked electro-spun tilapia skin collagen) and TSC-EDC (EDC/NHS crosslinked electro-spun tilapia skin collagen) with L929 fibroblasts determined by the cellular metabolic function with AlamarBlue assay. No statistical differences ($p < 0.05$) were observed between all groups at each time point, but for every sample, the cellular metabolic activities on Day 3 and 7 were significantly higher ($p < 0.05$) than those on Day 1 and Day 3 respectively.

Once again, the results indicated that both crosslinked electrospun collagen scaffolds were non-toxic, as the metabolic activities of L929 cells seeded on both scaffolds increased exponentially and significantly at each time point. The increase in L929 cellular metabolic activities suggested that the L929 cells adhered onto the scaffolds rapidly and began to proliferate and reproduce shortly after adhesion. Between the 2 scaffolds, TSC-EDC induced a higher metabolic activity than TSC-GTA on Day 3 and Day 7, supporting the fact that EDC is a less toxic crosslinking agent and EDC/NHS-crosslinked scaffolds are less cytotoxic. Nevertheless, the glutaraldehyde-crosslinked scaffolds showed similar performance to the blank (polystyrene culture dish), indicating that the glutaraldehyde-crosslinked scaffolds are also not cytotoxic, despite reports on the cytotoxicity of glutaraldehyde. Due to the potency of glutaraldehyde, crosslinking with glutaraldehyde vapour is a much quicker process, and the shorter processing time may make glutaraldehyde crosslinking a more attractive option when the production of crosslinked collagen scaffolds is scaled up.

The fact that L929 cells which are from a murine origin could grow well on tilapia skin collagen scaffolds showed that tilapia collagen could be well tolerated by mammalian cells due to the high level of functional and structural conservation between tilapia collagen and mammalian collagen (with 78% identities and 84% positives between tilapia and rat collagen type I α_1 as revealed in section 3.3.1). Looking at the biocompatibility of tilapia skin collagen scaffolds towards murine cells, we could hypothesize that tilapia skin collagen scaffolds would also be well-tolerated by human cells and human tissues.

3.4 Conclusion

In this study, type I collagen was successfully extracted and purified from the skin and scales of Nile tilapia, a tropical fish that is widely cultivated as food and valued for its type I collagen with high denaturation temperature. Tilapia skin collagen was then successfully electrospun into well-defined nanofibrous mats using a novel benign PBS/ethanol solvent which had been attempted on bovine and porcine collagen but not on fish collagen. While there was some degree of collagen instability during the electrospinning, the PBS/ethanol solvent was shown to have a less adverse effect on the structure of collagen than HFIP, a fluoro-alcohol which is a popular solvent for collagen electrospinning. The fibre morphology and consistency of electrospun tilapia skin collagen were similar between PBS/ethanol and HFIP. More importantly, PBS/ethanol is non-toxic and more environmentally friendly than HFIP. The electrospun tilapia skin scaffolds were crosslinked with glutaraldehyde vapour or EDC/NHS, and all crosslinked scaffolds were shown to be non-cytotoxic and support adhesion and proliferation of L929 fibroblasts. The high level of conservation between tilapia collagen and mammalian collagen revealed in the bioinformatics characterisation suggests that tilapia collagen would be well-tolerated by mammals.

Extrapolating from the results of the bioinformatics characterisation and the characteristics of the tilapia collagen scaffolds reported in this chapter, the author would expect decellularized tilapia tissues to be biocompatible in mammals and have similar, if not superior, physical and biological performances as decellularized mammalian tissues. The experimental methods reported in this chapter would also serve as a guideline to characterise and evaluate the decellularized tilapia skin in the subsequent chapters.

4 Decellularization of tilapia skin

4.1 Introduction

Biologic materials derived from the extracellular matrix (ECM) of human or animal tissues are commonly used as scaffolds to support the regeneration of damaged or missing tissues or organs [10]. Such biologic materials are obtained from a process known as decellularization, where cells are removed from a tissue or an organ, leaving behind the ECM which comprises of a complex network of structural and functional proteins. This acellular ECM can be used as a scaffold to support cell proliferation and eventually tissue regeneration [25].

Ideally, the decellularization protocol should remove all cellular and nuclear materials which can trigger immune reactions in the host recipient, while preserving the structure, mechanical integrity and biological activity of the remaining ECM. However, any processing step with the aim of removing cells from a tissue will inevitably alter the native structure and composition of the ECM [27]. The challenge in decellularization is to determine the optimal methods to preserve the ECM while achieving high removal of cellular materials [83].

Currently, many decellularized ECM products are employed in various fields of regenerative medicine, including dermatologic applications (e.g. wound-healing), soft tissue repair, urethral reconstruction, spinal repair and orthopaedic applications [26]. Most of these decellularized ECM products are from human, bovine or porcine origins. Examples of approved and commercially available decellularized ECM products are AlloDerm® (Lifecell) derived from human skin, Matristem® (ACell) derived from porcine urinary bladder, Oasis® (Healthpoint) derived from porcine small intestinal submucosa, and PriMatrix® (TEI Biosciences) derived from fetal bovine skin [25, 56].

Recently, there is a growing interest in decellularized tissues from non-mammalian sources due to the avoidance of porcine and bovine products by patients with religious constraints and the risk of disease transmission from mammals to humans, as seen in the cases of bovine spongiform encephalopathy, swine influenza and foot-and-mouth disease [14, 15]. In this regard, the use of decellularized tissues of piscine origin is considered to be an attractive alternative, due to the similarity of the physical structure, chemical composition and physiological functions of the ECM between piscine and mammalian tissues [170]. Fish is traditionally an accepted food source in most religions, including Islam, Judaism and Hinduism [236, 237], so fish tissues avoid the religious constraints associated with mammalian tissues. Also, zoonoses from fish to humans are rare and are restricted to a small number of opportunistic bacterial pathogens, which can be eliminated with proper decellularization and sterilisation, unlike mammalian zoonoses caused by viruses or prions, which are difficult to eliminate [238]. Another motivation to use fish tissues is the huge amount of waste generated by the seafood industry. In the case of fish, about 75% of the fish weight is discarded in the form of skins, scales, bones, and internal organs [16]. Conversion of these largely untapped resources into valuable products would concurrently generate more revenue and reduce wastage in the seafood industry .

The use of decellularized fish skin for wound care and other tissue healing applications was described in U.S. Patent Number 8,613,957 B2 by Kerecis, an Icelandic medical device company, in 2013 [28]. Kerecis had successfully developed the “Kerecis™ Omega3”, an acellular graft product derived from the skin of farmed North Atlantic cods. At the time of writing, Kerecis is only one company in the world which has received approval from the Food and Drug Administration (FDA) in the United States for the use of decellularized fish tissues in medical treatments. Other studies involving decellularized fish tissue included the development of a collagen matrix from tilapia fish scales for corneal reconstruction [18], the

fabrication of a bioabsorable bone pin from decellularized fish scales for bone regeneration [149], and the development of scaffolds from decellularized fish swim bladder for skin wound healing and soft tissue regeneration [153, 239]. Other than the works mentioned above, there are very few reported works on the use of decellularized fish tissues in regenerative medicine.

Among the various organs in teleost fish, the skin is of the greatest interest to tissue engineers as the skin has a high composition of type I collagen and possess numerous bioactive substances whose benefits have not been fully explored. In addition, a huge amount of fish skin is discarded in the fishing industry, accounting for around 30% of fish waste [16, 169]. These factors, together with the fact that there were few reported works on decellularized fish tissues, generated a motivation to study the decellularization of fish skin and investigate the suitability of decellularized fish skin in tissue engineering. In this thesis, Nile tilapia was chosen as the species of interest due to its popularity as a food source and the high denaturation temperature of its type I collagen.

Hence, the next objective of this thesis would be to develop an acellular scaffold from tilapia skin by decellularization. Since there was no prior studies on the decellularization of tilapia skin, another objective would be to investigate the effects of different decellularization methods on tilapia skin and to optimise the decellularization process in order to maximise removal of cellular components while preserving the ECM structure.

In Chapter 3 of this thesis, it was reported that tilapia skin collagen and rat tail collagen were successfully electrospun into well-defined nanofibrous scaffolds using a novel benign PBS/ethanol solvent, and after crosslinking, the scaffolds were shown to be non-cytotoxic and support adhesion and proliferation of L929 fibroblasts. The similar biological performances between tilapia collagen scaffolds and rat collagen scaffolds suggests that tilapia collagen would be well-tolerated by mammals. Moving from the molecular level to the tissue level, the

degree of functional and structural conservation between tilapia and mammals should be similar and one hypothesis in this thesis was that decellularized tilapia skin might be thermally stable in vivo, biocompatible to mammals, non-toxic, biodegradable, and not immunogenic. This chapter would focus on the process optimisation for the decellularization of tilapia skin, and physical and biochemical characterization of decellularized tilapia skin, while Chapter 5 and 6 would focus on the biological characterization and clinical assessment of decellularized tilapia skin, using crosslinked electrospun tilapia collagen as a comparison biomaterial.

At the end of this chapter, a short section would be devoted to the introduction of electricity as a novel decellularization medium. Some preliminary data from the electric decellularization of tilapia skin would be presented, with suggestions for future work.

4.2 Methodology

4.2.1 *Materials*

Fresh tilapia was purchased from a local supermarket and processed on the same day. Phosphate-buffered saline (PBS), Pierce Universal Nuclease, Dispase and PicoGreen DNA quantification kit were obtained from Life Technologies (Grand Island, NY, USA). Sircol collagen assay kit, Fastin elastin assay kit and Blyscan glycosaminoglycan assay kit were obtained from BioColor (Carrickfergus, UK). Other chemicals were obtained from Sigma Aldrich (St Louis, MO, USA) unless otherwise stated.

4.2.2 *Decellularization of fish skin – process optimization*

The scales and skin were removed from fresh tilapia. The skin was cleaned, cut into smaller pieces (4cm × 4cm), and stored in PBS with 1% antibiotics at 4°C until ready for processing. As there is no prior studies on the decellularization of tilapia skin, a series of studies were

performed using various chemical and enzymatic treatments to optimize the decellularization process. The optimization of the decellularization process was carried out in two phases. In the first phase, two groups of tilapia skin were placed separately into two detergents, 1% sodium dodecyl sulphate (SDS) in PBS and 1% Triton-X in PBS, and shaken on an orbital shaker at 100 rpm for 6 hours. The skins were then rinsed with DI water and characterized to evaluate the effectiveness of each detergent treatment. In the second phase, one group of tilapia skin was shaken in 2.5 U/mL dispase in PBS for 3 hours to detach the epidermis before the 6 hour detergent treatment. Another group of tilapia skin was shaken in 25 U/mL Pierce Universal Nuclease in PBS for 3 hours to break down the nucleic acids after the 6 hour detergent treatment. All the skins were rinsed with water thoroughly after each detergent treatment or enzymatic treatment. The skins were then characterized to assess the effectiveness of the additional enzymatic treatment.

Finally, the optimized decellularization process was carried out as followed. The skin was shaken in 2.5 U/mL dispase in PBS for 3 hours to detach the epidermis. The skin was rinsed with DI water, and shaken in 1% SDS in PBS for 6 hours to lyse the cells and release cellular contents. The skin was then gently scrapped to physically remove the epidermis. The skin was rinsed with DI water, and shaken in 25 U/mL Pierce Universal Nuclease in PBS for 3 hours to break down the nucleic acid. Finally, the skin was rinsed with DI water, and shaken in 1% sodium dodecyl sulphate (SDS) in PBS again for 1 hour to remove the nuclease and residual contaminants. The skin was rinsed with DI water and lyophilized in a freeze-dryer for 24 hours. The lyophilized skin was further dried in a vacuum chamber for 1 hour to remove any condensation. The whole process was performed at room temperature (23 ± 1 °C). This final product is termed decellularized tilapia skin (DTS) and was stored dry at room temperature until further use. The optimization of the decellularization process is summarized in Table 4-1.

Table 4-1: Steps taken during the optimization of the decellularization process

Step	Duration	Phase 1	Phase 2		Optimized
2.5 U/mL dispase in PBS Water rinse	3 hours 5 min × 4 times		Yes		Yes
Detergent (1% SDS in PBS or 1% Triton in PBS) Water rinse	6 hours 5 min × 4 times	The detergent with better performance would be used in the next phase	Yes	Yes	Yes
25 U/mL nuclease in PBS Water rinse	3 hours 5 min × 4 times			Yes	Yes

4.2.3 *Determination of DNA and collagen content*

Fresh tilapia skin and decellularized tilapia skin were tapped dry with tissue paper and cut into 5 mm × 5 mm pieces. Each piece was weighed and placed into a 1.5 mL sample tube. For DNA content quantification, the DNA was extracted from the sample with the Favorprep™ Tissue Genomic DNA Extraction Mini Kit (Favorgen, Taiwan) and then quantified with the PicoGreen® dsDNA assay kit (Life Technologies, USA) according to the manufacturer's instructions. For collagen content quantification, the collagen in the sample was solubilised and quantified with the Sircol Collagen Assay kit (Biocolor, UK) according to the manufacturer's instructions. For plotting of the standard curve for the collagen assay, standards were prepared from tilapia collagen (extracted and purified as per section 2.2.1) instead of the porcine collagen provided by the Sircol Collagen Assay kit.

4.2.4 *Scanning Electron Microsopy*

The morphology of the membranes was analysed by scanning electron microscopy (SEM). Bio-Gide®, CETC and DTS were cut into 3 mm × 3 mm pieces. The samples were fixed in 2.5% glutaraldehyde in PBS for 1 hour at room temperature, washed twice with water, dehydrated with increasing concentrations of ethanol (i.e. 50%, 70%, 90%, 100%), and dried in vacuum overnight. The dry samples were sputter-coated using a platinum ion coater (JFC-1600, JEOL, Japan) and analysed with the SEM machine (JSM-6700F, JEOL, Japan)

4.2.5 *Hematoxylin & eosin histology*

The structural morphology and the presence of DNA in the samples were visually analysed by hematoxylin & eosin (H&E) histology. The samples were cut into small pieces, fixed in 10% neutral-buffered formalin solution overnight, dehydrated through increasing concentrations of ethanol (i.e. 50%, 70%, 90%, 100%) and xylene, and embedded in paraffin wax at 60 °C. The embedded samples were then sliced perpendicularly to the skin surface at a thickness of 5 μm with a rotary microtome (RM2255, Leica, Germany) to obtain cross-sectional sections of the samples. The sections were stained with hematoxylin and eosin, and observed with light microscopy. Areas stained blue or purple indicated the presence of DNA, while areas stained pink represent the proteins [240].

4.2.6 *Determination of sodium dodecyl sulphate content*

The concentration of sodium dodecyl sulphate (SDS) in the rinse and storage solutions was quantified by a stains-all reagent according to the method reported by Rusconi et al [241]. First, 1 mg of stains-all was dissolved in 1 mL of isopropanol:water (50:50 v/v) to produce the reagent stock. Then, 1 mL of the reagent stock and 1 mL of formamide were mixed with 18 mL of water to produce the reagent. A series of standards from 0 % to 0.2 % SDS were prepared by diluting various amount of 1 % SDS solution with water. A 6 cm^2 piece of decellularized tilapia skin was immersed in 1% SDS solution for more than 1 hour, and then rinsed in PBS or water 4 times, each time for 10 minutes at 100 rpm on an orbital shaker. At the end of each rinse, a small amount of the rinse solution was collected. After the 4 rinses, the skin was immersed in a storage solution (PBS) and a small amount of the storage solution was collected after 24 hours. 1 μL of the standard, the rinse solution or the storage solution was added into each well in a clear 96 well plate, followed by 200 μL of reagent. The plate was read for

absorbance at 438 nm and the SDS concentration in the sample was calculated from the standard curve.

4.2.7 *Determination of elastin and glycosaminoglycan content*

Fresh tilapia skin and decellularized tilapia skin were tapped dry with tissue paper and cut into 5 mm × 5 mm pieces. Each piece was weighed and placed into a 1.5 mL sample tube. For elastin quantification, the elastin in the sample was solubilised in 0.25M oxalic acid and quantified with the Fastin Elastin Assay kit (Biocolor, UK) according to the manufacturer's instructions. For glycosaminoglycan (GAG) quantification, the sample was digested in a papain extraction reagent (400 mg sodium acetate, 200 mg EDTA disodium salt, 40 mg cysteine hydrochloride and 5 mg papain in 50 ml of 0.2 M sodium phosphate pH 6.4) and the GAG in the supernatant was quantified with the Blyscan GAG assay (Biocolor, UK) according to the manufacturer's instructions.

4.2.8 *Determination of amino acid content*

Fresh tilapia skin, decellularized tilapia skin and lyophilised tilapia collagen were separately homogenized into fine powder at cryogenic temperature for 10 cycles at 10 minutes per cycle with the 6970EFM Freezer Mill (SPEX SamplePrep, USA). 1 milligram of each homogenized sample was sent to Proteomics International, Australia, where the samples underwent 24 hours gas phase hydrolysis with 6 M hydrochloric acid at 110 °C and the amino acids in the hydrolysates were analysed in duplicate using the Waters AccQTag Ultra chemistry.

4.2.9 *Tensile test*

The mechanical strength of the tilapia skin was determined by uniaxial tensile testing. Pre-wetted membranes were tapped with tissue paper to remove excess water, cut into 30 mm × 5

mm strips, and secured onto the tensile tester (Instron 5543, Instron, USA) with clamps in a 100 N load cell. The dimensions of the sample was measured with a micrometer and recorded in the tensile testing software. The load cell of the tensile tester was calibrated and the sample was pulled with an extension rate of 10 mm/min until the sample broke. The maximum tensile stress and Young's modulus, derived from the tensile testing software, were recorded and compiled. Five samples from each group were tested and the results were expressed as the mean and standard deviation.

4.2.10 *Differential Scanning Calorimetry*

The denaturation temperatures of the skin samples were determined by differential scanning calorimetry (DSC) with the Diamond DSC system (PerkinElmer, MA, USA). Lyophilised skins were pre-wetted to mimic physiological conditions. Wet skins were then tapped with tissue paper to remove excess water and cut into 3 mm × 3 mm pieces. After weighing, each piece was placed into an aluminium sample pan, which was then sealed with a pan cover. The sample pan and reference pan were inserted into the DSC system and the denaturation temperature and denaturation enthalpy of the samples were determined with a heating rate of 10 °C per minute. Three samples from each group were tested and the results were expressed as the mean and standard deviation.

4.2.11 *Statistical Analysis*

Quantitative results are expressed as mean ± standard deviation (SD) and differences between mean values were evaluated using a two-tailed Student's t-test. A p-value of <0.05 was considered to be statistically significant.

4.3 Results and Discussion

4.3.1 *Decellularization of fish skin*

As there were no prior studies on the decellularization of tilapia skin, several methods encompassing different combinations of detergents and enzymes were tested and evaluated based on their effectiveness of removing cellular materials and preserving structural components. In this study, DNA content was used to assess the extent of decellularization due to its correlation to immunogenic reactions and its ease of isolation and quantification, while collagen content was used to assess the preservation of the ECM due to the role of collagen as the main structural component of the ECM [26]. The visual appearance of the epidermal layer was also used to assess the extent of decellularization as the epidermal layer of tilapia skin is rich in mucous cells, pigment-forming melanophores, scale-forming osteoblasts and immune cells, all of which are highly likely to cause adverse immune responses in the xenograft recipient [242].

In the first phase of the decellularization process optimization, two detergents were assessed – SDS, a strong ionic detergent, and Triton-X, a non-ionic detergent. Detergent treatment is commonly employed in decellularization as detergents solubilize cell membranes and dissociate cellular components from one another [26, 27]. In the second phase of the decellularization process optimization, two enzymes were assessed – dispase, which is a protease commonly used to dissociate epithelial cells from tissues, and nuclease, which cleave nucleic acids and aid in DNA removal after cell lysis [26]. The effects of the different detergents and enzymes on the visual appearance of the skin and the DNA and collagen content in the skin were presented in Figure 10.

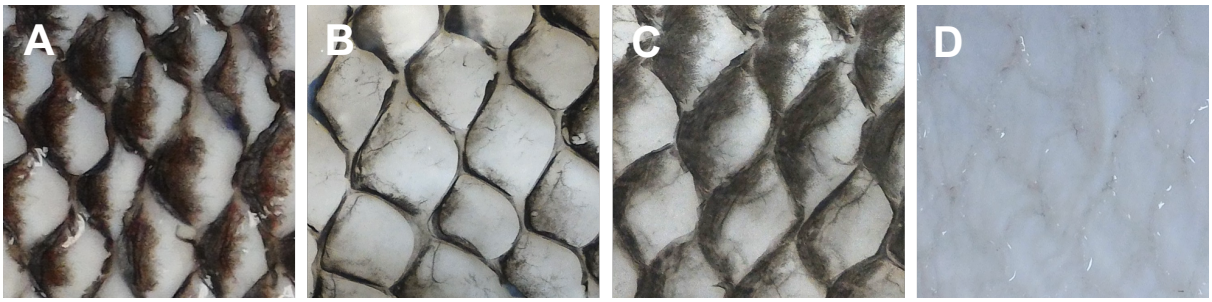

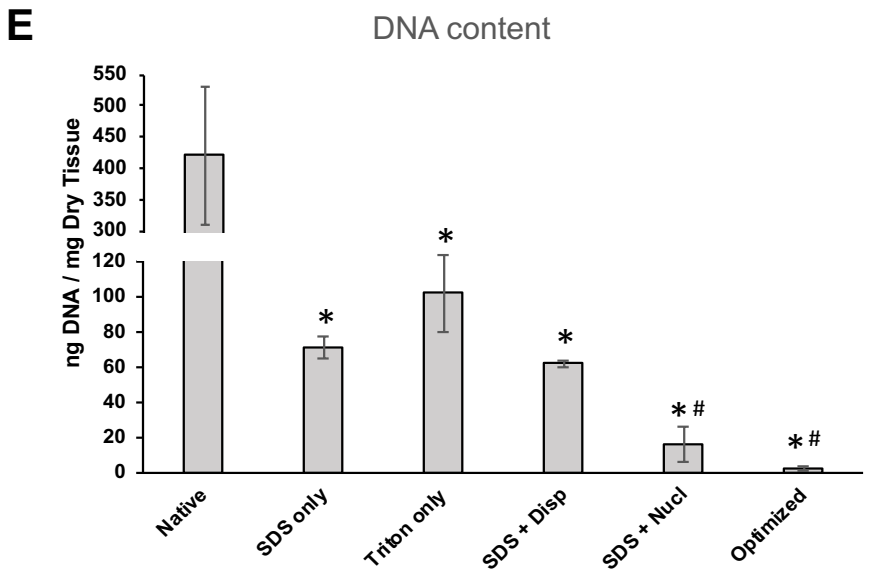

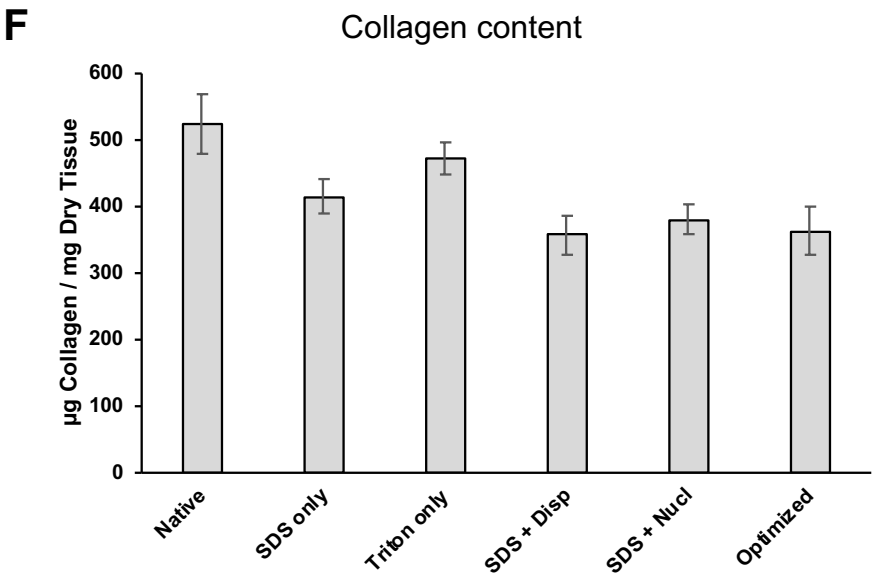

Figure 4.1: Visual appearance of (A) native tilapia skin, (B) tilapia skin treated with 1% SDS in PBS for 6 hours, (C) tilapia skin treated with 1% triton-X in PBS for 6 hours, (D) tilapia skin treated with 2.5U/ml dispase for 3 hours and 1% SDS in PBS for 6 hours. (E) DNA quantitation of treated tilapia skins compared to native samples, $n \geq 3$. Dotted line at 50 ng DNA/mg tissue indicates recommended limit to avoid immunological response [26]. * $p < 0.05$ when compared to native skin. $^{\#}$ $p < 0.05$ when compared to skin treated by SDS only. (F) Collagen quantitation of treated tilapia skins compared to native samples, $n \geq 3$. No significant difference ($p < 0.05$) were observed between groups.

In the first phase of optimizing the decellularization process, 1% SDS in PBS was shown to be a more effective decellularizing agent than 1% Triton-X in PBS, as upon visual inspection, the SDS-treated skin has less remaining black pigment (Figure 10B) than the native skin (Figure 10A) and Triton-treated skin (Figure 10C). The SDS-treated skin also has less residual DNA (71.2 ± 6.8 ng/mg tissue) than the native skin (419.9 ± 109.5 ng/mg tissue) and Triton-treated skin (102.4 ± 22.0 ng/mg tissue) as shown in Figure 10E. The results demonstrated that SDS was more effective than Triton-X in wearing down the epidermal layer and reducing the amount of DNA significantly ($p < 0.05$) while retaining a high amount of collagen and maintaining the morphology of the dermis. However, SDS alone is insufficient to remove the epidermal layer completely and reduce the DNA content to below 50 ng DNA/mg tissue, the recommended maximum limit to avoid adverse immune responses [26].

In the second phase of optimizing the decellularization process, an additional 3 hour treatment in 2.5 U/mL dispase in PBS causes a complete disappearance of the epidermal layer, leaving behind a white tissue (Figure 10D). However, the dispase treatment was unable to bring the DNA content (61.9 ± 2.3 ng/mg tissue) to below 50 ng/mg tissue. On the other hand, an additional 3 hour treatment in 25 U/mL Pierce Universal Nuclease in PBS had no effect on the visual appearance of the skin, but significantly reduced the DNA content (15.5 ng/mg tissue) to below 50 ng/mg tissue. The results demonstrated that the dispase treatment, when carried out in a combination with SDS treatment, was effective in removing the epidermal layer. Dispase and trypsin are two of the most commonly used proteolytic enzymes in decellularization protocols, but in this study, dispase was selected over trypsin because dispase specifically targets the proteins in the basement membrane between the epidermis and dermis with minimal degradation of type I collagen [243], and is effective at a low concentration of 2.5U/mL [244]. Although trypsin is effective in cleaving proteins responsible for cell adhesion, it may also degrade type I collagen and other ECM proteins with prolonged exposure [26].

Dispase is also chosen because of its bacterial origin, unlike trypsin which is isolated from porcine pancreas [243]. As the aim of this study is to develop scaffolds from tilapia as non-mammalian alternatives, mammalian substances should be avoided during the scaffold fabrication. It is the same reason that Pierce Universal Nuclease, with its bacterial origin, was selected over other nucleases. Pierce Universal Nuclease has an additional advantage over other nucleases, as it targets all kinds of nucleic acids, including ribonucleic acid (RNA), while most other nucleases are selective for either DNA or RNA [245]. As both DNA and RNA are known to induce antigenicity, it is useful to have a single nuclease that can degrade both DNA and RNA [246, 247].

When the dispase treatment, SDS treatment and nuclease treatment were combined into an optimised process, the resultant product, which we termed as DTS (decellularized tilapia skin), had only 1.8 ± 0.9 ng DNA per mg tissue, or 0.4% of the native DNA content (Figure 10E). The DTS also retained 362.5 ± 35.6 μg collagen/mg tissue, or 69.3% of the native collagen content (Figure 10F).

The extensive removal of DNA by the optimized decellularization protocol can also be observed by comparing the histological sections of the native and decellularized tilapia skin where cellular and nucleic materials are visibly absent in the decellularized skin (Figure 4.2). The SEM images show that the native tilapia skin has a smooth continuous inner surface and a compact layered structure (Figure 4.3A & B). The decellularization seemed to have no visible effect to the inner surface of the skin (Figure 4.3C). The layered structure was maintained but the interior layers became more porous (Figure 4.3D). In general, the structural integrity of the skin was retained after the decellularization.

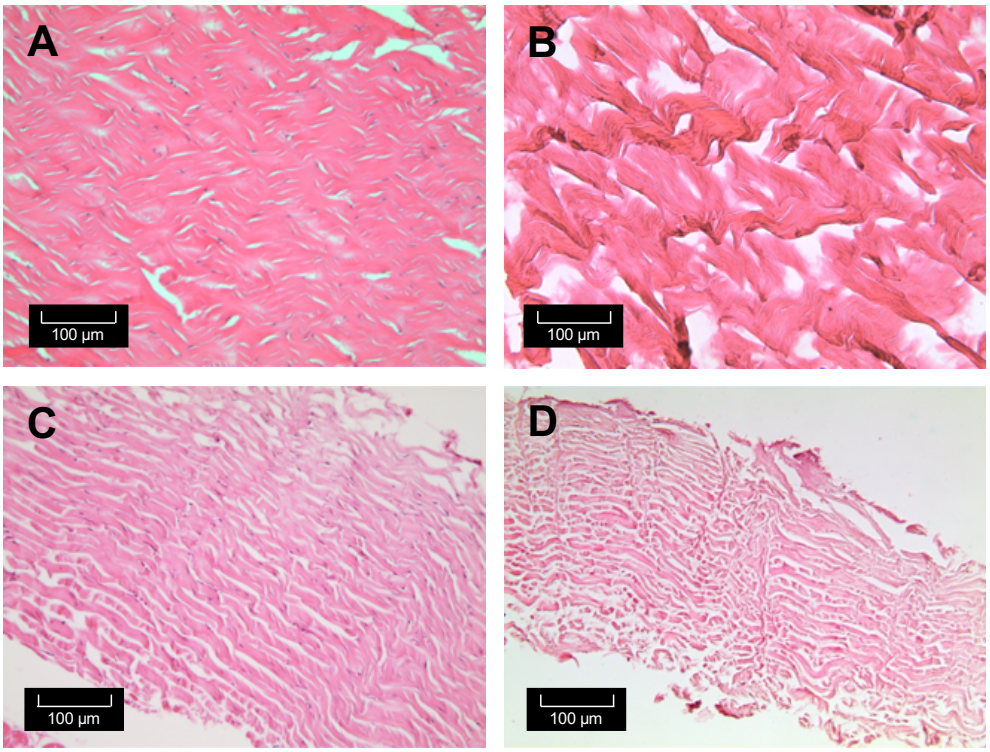

Figure 4.2: Hematoxylin & Eosin stained histological images of (A) native tilapia skin, sagittal view, (B) decellularized tilapia skin, sagittal view, (C) native tilapia skin, cross-sectional view, and (D) decellularized tilapia skin, cross-sectional view. Cell nuclei are visible in (A) and (C) as blue spots. Scale bars are 100 µm.

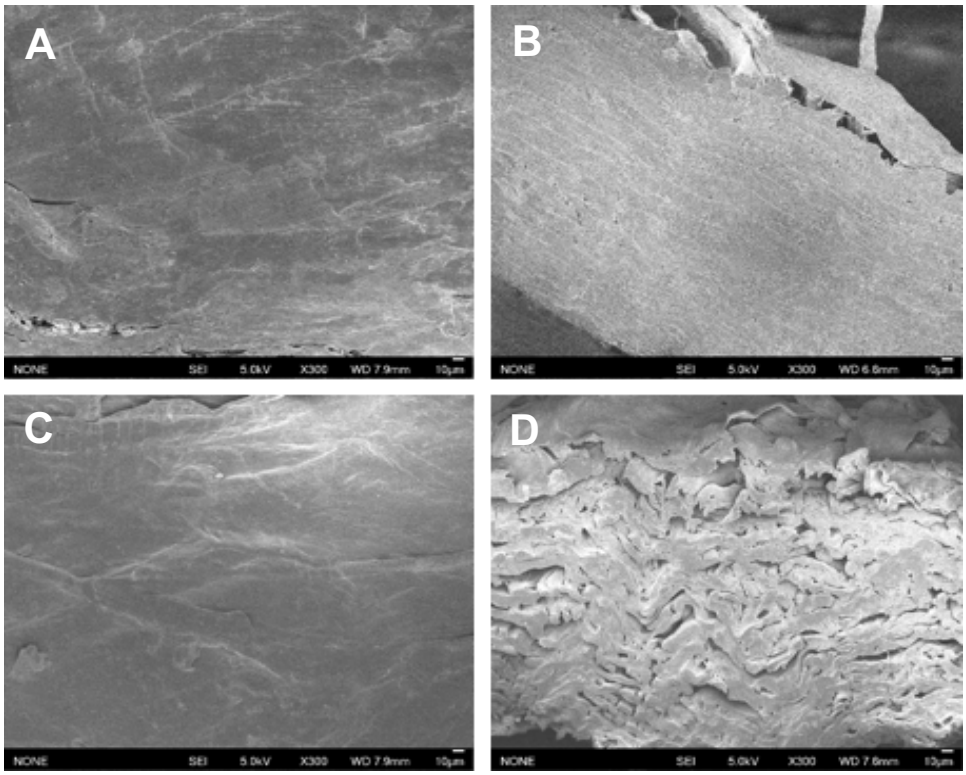

Figure 4.3: SEM images of (A) inner surface of native tilapia skin, (B) cross-sectional view of native tilapia skin, (C) inner surface of decellularized tilapia skin (treated by dispase, SDS, and nuclease), and (D) cross-sectional view of decellularized tilapia skin. Scale bars are 10 µm.

4.3.2 *Determination of sodium dodecyl sulphate content*

As SDS is cytotoxic, it is important to quantify the amount of residual SDS in the decellularized skin after the rinsing step and during storage, so as to minimise the introduction of SDS into the host recipient [241]. As PBS and DI water are the two most common rinsing agents in decellularization protocols [248, 249], the two agents were compared for their ability to remove SDS during the rinsing phase. The concentration of SDS in the rinse solutions and storage solution was quantified with the Stains-All reagent and shown in Figure 4.4.

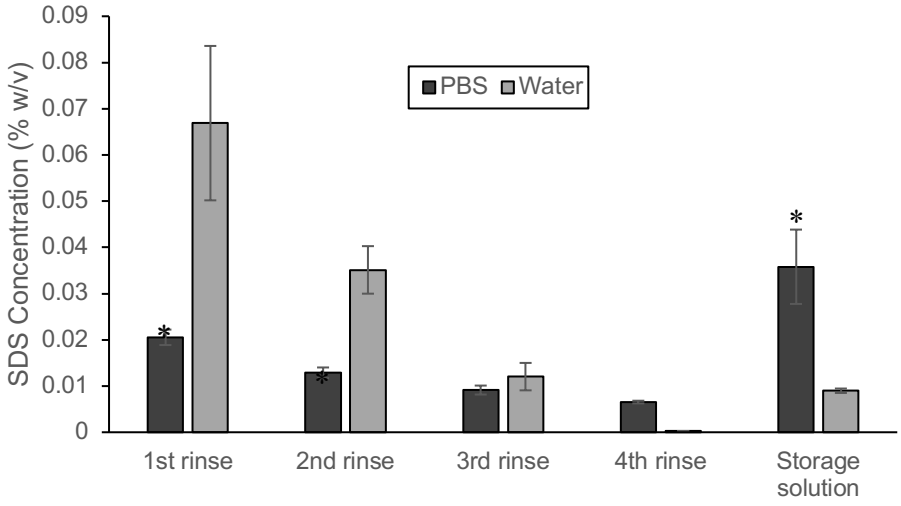

Figure 4.4: SDS concentration in rinse solutions and storage solutions. The rinses were performed after the skin was immersed in 1% SDS for 1 hour, and each rinse was performed for 10 minutes at 100 rpm on an orbital shaker. The rinse solutions were collected at the end of the 10 minute rinse. The storage solution was sampled after the decellularized skin was immersed for 24 hours post-rinsing. * $p < 0.05$ when compared to water.

In a previous study, the lower cytotoxic threshold for residual SDS in tissue was reported to be about 10 µg/mg dry tissue [250]. As the volume of rinse solution used to wash the tilapia skin in this study was 40 times the dry weight of tilapia skin, the lower cytotoxic threshold for residual SDS in the rinse solution should be 10 µg SDS / 40 ml solution, or 0.025 % w/v. From the results (Figure 4.4), although the SDS concentrations in the PBS rinses were below the 0.025% w/v threshold, the SDS concentration in the storage solution was much higher than the threshold, indicating that a substantial amount of SDS remained in the tilapia skin despite 4

rounds of PBS rinses. On the other hand, the SDS concentrations were high in the first 2 water rinses, and the SDS concentration dropped below the 0.025% w/v threshold in the third rinse and remained below the threshold in the fourth rinse and in the storage solution. One possible reason is that water has a greater osmotic pressure than PBS, so water is able to penetrate into the tilapia skin ECM more deeply and force the SDS out of the skin more quickly. This presumption was supported by the higher amount of SDS in the first three water rinses. As more SDS was present in the rinses, less SDS remained in the skin. Water also has the advantage of being hypotonic, and therefore is able to cause cell lysis by hypoosmotic shock [251]. Due to the observations, it was decided that all rinses in the decellularization protocol would be performed with water, and every rinsing phase would consist of at least 4 rinses, each time for 10 minutes, so as to maximise the removal of cytotoxic detergents, enzymes, and cellular contaminants. To ensure minimal contamination by SDS or any residual reagents, the storage solution would be changed 24 hours after the skin was rinsed and immersed in the storage solution.

4.3.3 *Determination of elastin and glycosaminoglycan content*

While collagen is the main component of ECM, there are other substances in the ECM that has important structural and functional roles. One of them is elastin, a key ECM protein that is responsible for the elasticity and resilience of many vertebrate tissues including arteries, lung, tendon and skin [252]. Elastin fibres, made up of an outer layer of microfibrils and an inner core of tropoelastin molecules, form a highly crosslinked network that contributes to the tissue's structural integrity through persistent flexibility, allowing the tissue to retain its shape after repeated stretch and relaxation cycles [253]. Another important component of the ECM is glycosaminoglycans (GAGs), a family of polysaccharide chains composed of specific disaccharide units. Due to the numerous negatively charged carboxyl and sulphate groups on

the GAG chains, GAGs are responsible for water retention, providing a gel-like environment in the ECM, and the binding and releasing of growth factors and bioactive substances [254].

Like any ECM components, elastin and GAGs may degrade when exposed to chemicals and enzymes used for decellularization. To investigate the effect of decellularization on these two components, quantification assays were performed on native and decellularized tilapia skin and the results were presented in Table 4-2.

Table 4-2: Elastin and GAG content in native and decellularized tilapia skin quantified by Fastin Elastin assay and Blyscan GAG assay.

Sample	μg elastin / mg tissue	μg GAG / mg tissue
Native tilapia skin	59.4 ± 4.6	3.9 ± 0.1
Decellularized tilapia skin	5.3 ± 1.2	2.2 ± 0.1
	% elastin retained	% GAG retained
	9.0 % ± 2.1 %	55.1 % ± 1.4 %

The results indicated that tilapia elastin was not stable during decellularization, with only 9.0% being retained after decellularization. One possible explanation is that, in physiological conditions, elastin is highly insoluble due to the presence of multiple hydrophobic domains in the tropoelastin molecules, but in the presence of SDS, a strong ionic detergent, the tropoelastin molecules became solubilized by the hydrophobic tails of SDS, causing the elastin fibers to denature [255]. Moreover, elastin is formed by the coacervation of tropoelastin, which is the reversible and thermodynamically-controlled self-aggregation of tropoelastin molecules by hydrophobic interaction [256]. Detergents and organic solvents can easily destabilise elastin by disrupting the hydrophobic interaction between tropoelastin.

On the other hand, GAGs are more stable than elastin, with 55.1% being retained after decellularization. Unlike elastin, GAGs are highly hydrophilic and form strong hydrogen bonds with other hydrophilic ECM components, making them unlikely to be affected by SDS. Many GAGs are also covalently bonded to proteins via glycosylation, forming proteoglycans which

are important in regulating cellular pathways [257]. Proteoglycans are huge molecules and are often anchored within the ECM, making them unlikely to be removed during decellularization.

4.3.4 *Determination of amino acid content*

Proteins such as collagen, elastin, fibronectin and laminin form the bulk of the ECM and contribute to the mechanical and biochemical properties of tissues and organs. As the decellularization process differentially removes some proteins while leaving other proteins mostly intact, the protein composition in a tissue would change after decellularization [258]. As amino acids are the building blocks of all proteins, analysing the amino acid content before and after decellularization is a simple way to quantify and evaluate the change in protein composition in a tissue. The amino acid analysis results are presented in Table 4-3.

Table 4-3: Amino acid analysis of native tilapia skin, decellularized tilapia skin and lyophilised tilapia collagen. For the theoretical amino acid content, the value for each amino acid were derived by dividing the sum of that amino acid in the α1, α2 and α3 pro-collagen type 1 chains by the sum all all amino acids in all three chains. Asparagine and glutamine are converted to aspartic acid and glutamic acid during the hydrolysis process and therefore counted together with aspartic acid and glutamic acid respectively. Cysteine and tryptophan are unstable during the hydrolysis and cannot be quantified, but their absences do not affect the results due to their low abundance in tilapia collagen (<1% theoretical content). Numbers are expressed as percentage (%) of total number of amino acid residues.

	Native TS	DTS	Tilapia collagen	Theoretical amino acid content from Table 3-1
Alanine	11.8	12.1	12.0	11.0
Arginine	5.3	5.3	5.3	5.4
Aspartic acid	5.4	5.0	4.9	4.4
Glutamic acid	7.4	7.2	7.2	5.2
Glycine	32.0	33.5	33.1	29.4
Histidine	0.6	0.5	0.6	0.8
Hydroxylysine	0.7	0.7	0.7	-
Hydroxyproline	7.6	8.1	8.1	-
Isoleucine	1.2	0.9	1.0	2.0
Leucine	2.8	2.4	2.4	3.5
Lysine	2.7	2.6	2.6	4.0
Methionine	0.9	0.8	0.9	1.5
Phenylalanine	1.5	1.4	1.4	1.9
Proline	11.4	11.8	11.8	18.4
Serine	3.4	3.2	3.3	4.9
Threonine	2.6	2.4	2.5	3.8
Tyrosine	0.5	0.3	0.4	1.0
Valine	2.2	1.9	2.0	2.8
Total	100.0	100.0	100.0	100.0

The results showed a high degree of similarity in the amino acid content between tilapia collagen and tilapia skin (both native and decellularized), confirming that collagen is the dominant component in tilapia skin. There is also a high degree of similarity in the amino acid content between native and decellularized tilapia skin, suggesting that the decellularization process did not cause considerable changes to the overall amino acid composition. Glycine makes up close to one-third of all amino acids in tilapia collagen and tilapia skin, due to its presence at every third position in the collagen molecules as mentioned in section 3.3.1. The abundance of glycine and alanine, the two smallest amino acids, allow the three collagen chains to pack tightly around a central axis in the collagen molecules. There is also a high abundance of hydroxyproline and proline, which provide stabilisation of the triple helix by forming hydrogen bonds between the three chains.

While the theoretical contents and actual contents for most amino acids are similar (with differences of less than 2%), the actual glycine content is higher than the theoretical glycine content. This is because the theoretical content is derived from the amino acid sequences of pro-collagen, which is formed immediately after mRNA transcription and has not undergone post-translational modifications. In Figure 3.2, it is obvious that most glycine residues are concentrated in the central portion and not in the pro-peptides at the end of the chains. Hence, after the pro-peptides are cleaved off during post-translational modifications, the concentration of glycine increases. Also, during the post-translational modifications of collagen, a portion of proline and lysine residues undergoes hydroxylation (attachment of hydroxy groups), leading to the formation of hydroxyproline and hydroxylysine, which were absent in the theoretical content but present in the actual content.

Another interesting observation is the small increase of glycine, hydroxyproline and proline content in tilapia skin after decellularization (from 32.0 to 33.5% for Gly, from 7.6% to 8.1% for Hyp, from 11.4 to 11.8% for Pro). As glycine, hydroxyproline and proline are abundant in

collagen, the increase in glycine, hydroxyproline and proline content indicated the removal of non-collagenous proteins during the decellularization process, leaving behind an acellular tissue which is richer in collagen.

4.3.5 *Tensile test*

One of the factors that influence the effectiveness of a tissue engineering scaffold is its mechanical property. A scaffold serving as a protective membrane for tissue defects should possess these suitable biomechanical properties – strong enough to resist tearing during processing, suturing and *in vivo* movements, and soft enough to fit and cover the wound, and not cause irritation to surrounding soft tissue. Uniaxial tensile testing is one of the simplest methods to determine the mechanical properties of a biomaterial, and comparing the mechanical strength of a material before and after a process would enable us to determine whether the material undergoes degradation during the process.

Before performing mechanical evaluation on skin, it is important to consider the variations in mechanical behaviour of skin at different locations, in order to avoid random errors during data collection. According to Naresh et al, the mechanical properties of shark skin differed at different regions and different direction of test due to differences in histological characteristics and functional roles [259]. This variation in mechanical behaviour was also reported in skin from a variety of species, including humans [260], rats [261] and seals [262], and therefore would be expected for tilapia skin as well. To obtain a reliable and reproducible comparison of native and decellularized tilapia skin, it would be appropriate to study the intrinsic variations in mechanical properties in tilapia skin, and then standardize the region of skin and direction of pull for subsequent tensile experiments. To study the mechanical variations of tilapia skin, tensile test was performed in two directions, anterior-posterior (A-P) and dorsal-ventral (D-V),

on native tilapia skin isolated from two different parts of the body – one near the head and the other near the tail. The schematic diagram and results were presented in Figure 4.5.

For each tensile test performed, a force-displacement curve was obtained where the maximum stress, σ_{max}, maximum strain, ε_{max}, and Young Modulus, E, were determined. A typical curve is illustrated with the terms explained in Figure 4.6.

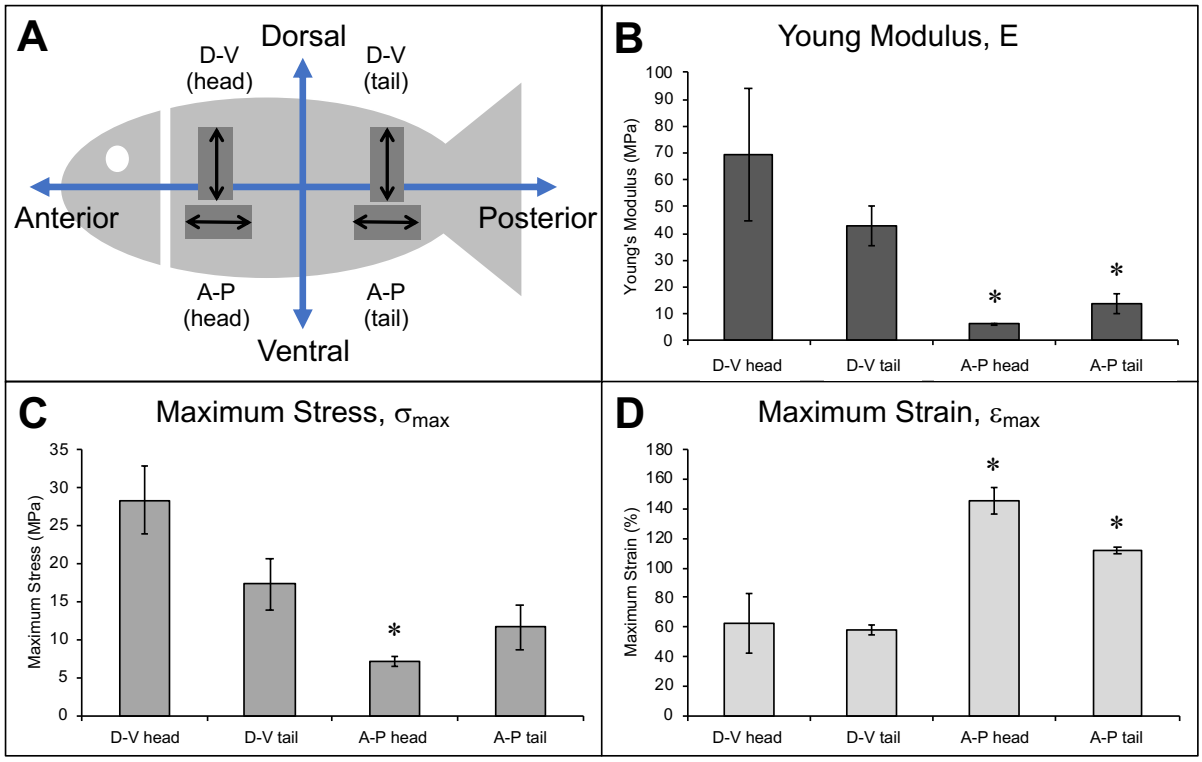

Figure 4.5: (A) Representative diagram of the two locations and two pulling directions for the tensile testing of native tilapia skin, (B) Young modulus of native tilapia skin at two locations under two pulling directions, (C) Maximum tensile stress of native tilapia skin at two locations under two pulling directions, and (D) Maximum strain of native tilapia skin at two locations under two pulling directions. * $p < 0.05$ when compared to D-V. Note: 1 MPa (Mega Pascal) = 1 N/mm^2

The tensile data indicated that native tilapia skin samples pulled vertically in the D-V direction exhibited notably stiffer and stronger tensile responses compared to skin samples pulled horizontally in the A-P direction, at both locations. When pulled in the D-V direction, the skin near the head was stiffer and stronger than the skin near the tail. However, when pulled in the A-P direction, the skin near the tail was stiffer and stronger than the skin near the head.

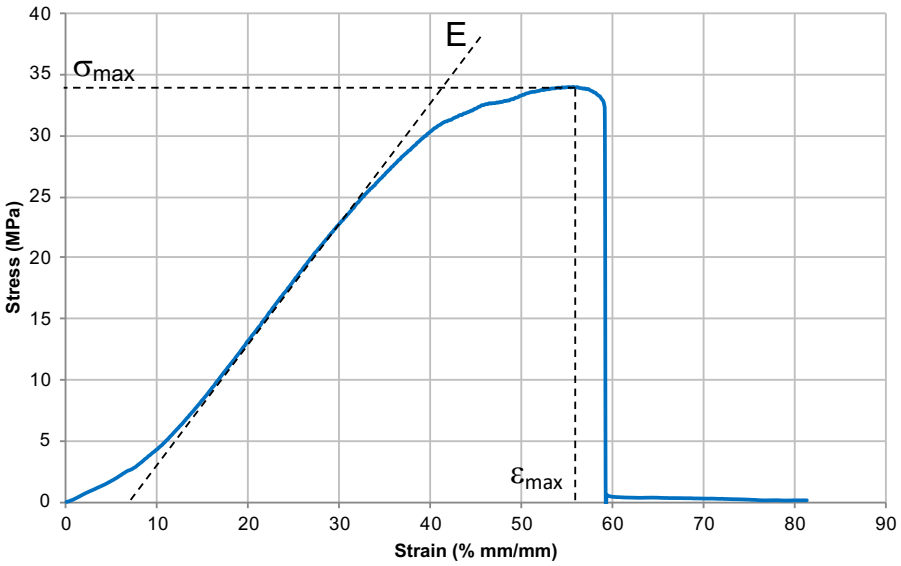

Figure 4.6: Typical stress-strain graph for tensile test. The stress, σ was calculated by dividing the tensile force by the original cross sectional area of the sample, while the strain, ε was calculated by diving the extended length of the sample by the initial length. The Young Modulus, E is defined as the steepest slope on the stress-strain curve and is a measure of the stiffness of a material. The maximum stress, σ_{max} and maximum strain, ε_{max} occur at the point where the sample reached the maximum extension just before failure.

The higher stiffness of the skin near the head could be due to a higher concentration of collagen fibres, while the higher stiffness of the skin in the D-V direction could be attributed to the arrangement of the collagen fibres in the stratum compactum layer of the skin. A study by Szewciw & Barthelat revealed that the collagen fibres in the stratum compactum of striped bass (*Morone saxatilis*) are aligned to two axis - the anterodorsal-posteroventral (AD-PV) axis and the anteroventral-posterodorsal (AV-PD) axis [184]. As teleost fish share a similar physiology, the findings by Szewciw & Barthelat could apply here to tilapia skin. The fibres in two directions are arranged in a criss-cross plywood like layered structure, with the directions of the collagen fibres alternating between layers. When a tensile force is applied to the skin, the collagen fibers slide on top of one another and align to the direction of the applied load, as illustrated in Figure 4.7.

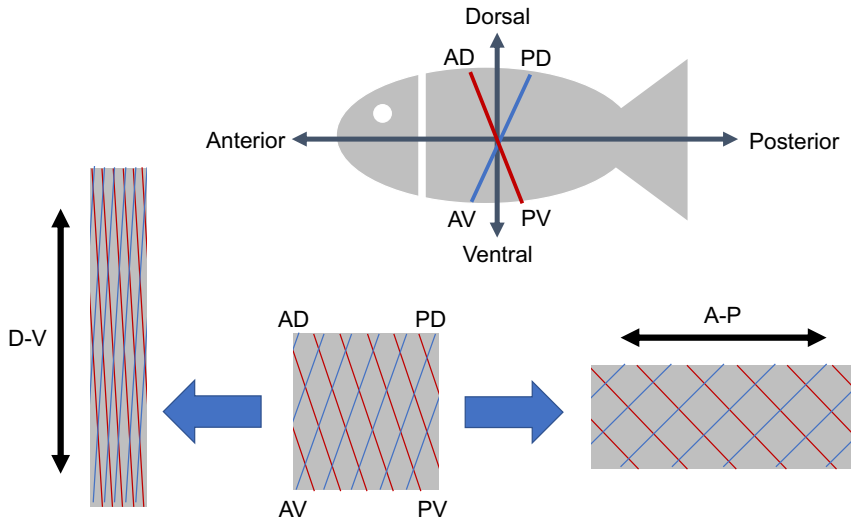

Figure 4.7: (Top) Representative diagram of the alignment of the collagen fibre in the anterodorsal-posteroventral (AD-PV) direction shown in red, and in the anteroventral-posterodorsal (AV-PD) direction shown in blue, with respect to the fish body. (Below) Representation diagram of how the collagen fibres align with the direction of pull when the skin was pulled in a D-V direction, and how the collagen fibres become further apart when then skin was pulled in a A-P direction.

As most of the collagen fibres are continuous from the dorsal to the ventral side of the fish, when the skin is pulled in the D-V direction, the collagen fibres become parallel to the tensile force. When the collagen fibres are fully extended, the skin stiffens and behaves like tendon. On the other hand, as there are very few collagen fibres that are continuous from the anterior to the posterior side of the fish, when the skin is pulled in the A-P direction, the collagen fibers, which are perpendicular to the tensile force, tend to get further apart, making the skin more elastic and less stiff. Szewciw & Barthelat also reported that the angle between the collagen fibres and the A-P axis decrease from the head to the tail. This explains why the skin near the tail was stiffer and stronger than the skin near the head when pulled in the A-P direction.

From literature, it was also reported that the collagen density in a tissue is also dependent on the age, diet and health of the animal, and therefore can vary among individuals [263]. To reduce the effect of variability among skin samples, we only chose tilapia with a weight of 500 ± 50 g, and we only used the skin near the head for decellularization. (Other parts of the skin was used for collagen extraction.) Subsequent tensile tests of tilapia skin were done in the D-

V direction, to reduce random errors and to allow effective comparison of the skin before and after decellularization by focusing on the mechanical strength of the load-bearing collagen fibres.

The mechanical properties of the native and decellularized skin (isolated near the head of the fish and pulled in the D-V direction) were determined by uniaxial tensile testing and shown in Table 4-4, together with the data for porcine and bovine acellular dermal matrices from a previous study [264] as well as data for human skin [265]. The mechanical properties of electrospun tilapia collagen and glutaraldehyde-crosslinked electrospun tilapia collagen (from Chapter 3) were also measured and included in the table.

Table 4-4: Maximum tensile stress and Young's modulus of native tilapia skin, decellularized tilapia skin and lyophilized & rehydrated decellularized skin (isolated near the head and pulled in the D-V direction). The mechanical properties of porcine acellular dermal matrix (Strattice, Lifecell, USA) and bovine acellular dermal matrix (SurgiMend, TEI Biosciences, USA) reported by Adelman et al.[264], human skin reported by Ni Annaidh et al [265], electrospun tilapia collagen and glutaraldehyde-crosslinked electrospun tilapia collagen reported in Chapter 3, were included for comparison and reference. Note: 1 MPa (Mega Pascal) = 1 N/mm^2

	Maximum tensile stress (MPa)	Young's modulus (MPa)
Fresh tilapia skin	28.4 ± 4.4	69.4 ± 24.6
DTS	24.0 ± 10.2	56.2 ± 14.4
Lyophilized & rehydrated DTS	22.8 ± 2.7	64.9 ± 17.6
Porcine acellular dermal matrix	11.8 ± 2.5	49.4 ± 19.2
Bovine acellular dermal matrix	18.5 ± 5.1	55.7 ± 18.5
Human skin (from the back of body)	21.6 ± 8.4	83.3 ± 34.9
Electrospun tilapia collagen	Disintegrates when wetted	Disintegrates when wetted
Crosslinked electrospun tilapia collagen	0.44 ± 0.05	1.30 ± 0.11

A slight drop of mechanical strength in tilapia skin was observed after decellularization, which could be attributed to the increase in porosity in the dermis, as seen in the SEM images of DTS (Figure 4.3D). As the dermis became more porous, the collagen fibres could slide more easily, causing the skin to be less stiff. Despite the drop in mechanical strength, DTS (when pulled in the D-V direction) was found to have a higher maximum tensile stress than porcine and bovine acellular dermal matrices (ADMs). One explanation is that the dermis of tilapia skin lacks appendages such as hair glands and sebaceous glands, which are common in mammalian

dermis [171]. This lack of appendages allows the collagen fibers to be packed more tightly in tilapia skin, contributing to a higher density of load-bearing collagen fibers per cross-sectional area.

The results demonstrated that tilapia skin possessed a high mechanical strength, and even after decellularization, acellular tilapia skin (when pulled in the D-V direction) has a higher mechanical strength than acellular porcine and bovine dermal matrix. Tilapia skin was also found to be stronger than human skin, although not as stiff. This suggested that the decellularization process did not adversely affect the structural integrity of tilapia skin. It was also noted that the lyophilisation and rehydration of decellularized tilapia skin did not have any adverse effects on its mechanical strength. This suggests that freeze-drying is an effective method to obtain dried decellularized skin for long-term storage and the skin can be simply rehydrated and applied without loss of mechanical integrity.

The mechanical properties of electrospun tilapia collagen and crosslinked electrospun tilapia collagen were also investigated. From the results, it can be deduced that the crosslinking process strengthened the mechanical properties of electrospun tilapia collagen. Before crosslinking, the electrospun membrane disintegrated when wetted. After crosslinking, the membrane remained intact when wetted and it was able to withstand a uniaxial tensile stress of 0.44 ± 0.05 MPa. This value is lower than that for DTS, but it was proposed that an increase of the membrane thickness or crosslinking time would allow the mechanical properties of CETC to match those of decellularized tissues [266, 267]. The results also showed that scaffolds obtained from decellularization are generally mechanically stronger than scaffolds obtained from the extraction and reconstitution of collagen, due to the preservation of native ECM architecture and collagen fibre alignment in the decellularized skin as observed from the histology images (Figure 11) and SEM images (Figure 12).

4.3.6 *Differential Scanning Calorimetry*

Before a biomaterial is utilised for *in vivo* applications, it is important to check the denaturation temperature (T_d) of the material to ensure that the material is thermally stable and does not undergo thermal degradration rapidly at body temperature. For decellularization, the T_d of the native and decellularized tissue could also reveal the effects of the decellularization treatments on the structural integrity of the tissue. The denaturation temperatures of the native and decellularized tilapia skins, determined by differential scanning calorimetery (DSC), were presented in Table 4-5.

Table 4-5: Denaturation temperature and denaturation enthalpy of native tilapia skin and decellularized tilapia skin, determined by Differential Scanning Calorimetry (DSC).

Sample	Denaturation temperature (°C)	Denaturation enthalpy (J/g)
Native tilapia skin (head)	68.1 ± 1.0	18.0 ± 0.9
Native tilapia skin (tail)	67.8 ± 0.9	19.9 ± 1.1
Decellularized tilapia skin (head)	64.2 ± 0.6	19.1 ± 1.0

It could be deduced from the results that the decellularization protocol did not adversely the thermal stability of the tilapia skin, as the DTS retained a high T_d of 64.2°C. In fact, the T_d of DTS was higher than the T_d of the glutaraldehyde-crosslinked and EDC/NHS-crosslinked electrospun tilapia collagen scaffolds (56.3°C and 54.5°C) reported in Chapter 3, agreeing with the tensile test results that scaffolds obtained from decellularization are generally stronger than scaffolds obtained from the extraction and reconstitution of collagen. The ECM is an intricate interlocking mesh of collagens, elastic fibers and glycoproteins, with covalent crosslinks joining many of the structural components [268]. This complex interlocking network, together with the dense packing of the collagen fibers, makes the ECM resistant to mechanical stress and thermal degradation. On the other hand, the collagen fibers in electrospun scaffolds are oriented randomly, hence even with crosslinking between the molecules, the thermal stability of the electrospun scaffolds cannot match that of decellularized tissues.

Although the skin near the head and the skin near the tail exhibited different mechanical properties, they have similar thermal stability, with no significant differences in the denaturation temperature and denaturation enthalpy. From this observation, we hypothesized that the denaturation temperature depends more on the bonds and interactions of the ECM components at the molecular level and less on the structural arrangements of the ECM components at the macro level.

4.4 Electricity – a novel agent to decellularize tilapia skin

4.4.1 *Introduction*

Current decellularization protocols involving physical, chemical and enzymatic methods have the limitations of long processing time, irreversible changes to the ECM structure, and in the case for chemical and enzymatic methods, toxicity caused by residual chemicals/enzymes and huge amount of chemical waste generated [26]. In view of these limitations, electricity can be a novel method to decellularize tissues in a short period of time through disruption of cells but not affecting the ECM structure and protein content.

Electric decellularization works mainly on the principle of electroporation, where the application of an electric field to a cell causes an increase in permeability of the cell membrane through the formation of nanopores. At low electric fields, the cell membrane is temporarily permeable and the cell reverts to its original state upon removal of the electric field, in a process known as “reversible electroporation”. This process is commonly used to deliver molecules such as drugs or DNA into cells. However, once the applied electric field exceeds a critical threshold, the cell membrane is unable to recover and cell death occurs, in a process known as “irreversible electroporation (IRE)” [269]. As IRE does not involve any drugs, chemicals, or enzymes, cells can be efficiently killed and removed from a tissue without affecting the ECM

structure and protein content, provided that the duration and strength of the electric field are controlled to avoid thermal heating of the tissue [270].

While electricity has been used as a bactericical process in the food industry since the early 19th century, the idea of using electricity for decellularization is still in its infancy as most studies in the biomedical application of electricity focus on tumour ablation and bioburden reduction [271]. To date, there were no known prior studies on the use of electricity to decellularize marine tissues. In our preliminary study, electroporation was attempted on tilapia skin and was found to be an effective method to decellularize tissues, with an efficient removal of cellular remnants and minimal damage to the tissue structure.

4.4.2 *Methodology*

Fresh tilapia was obtained from a local market and the skin was removed from both sides of the fish. After the scales were removed with a fish-scaler and the attached muscle tissues were scrapped away with a surgical blade, the skin was stored in PBS with 1% penicillin/streptomycin at 4°C for at least 1 hour before the experiment. A piece of moist tilapia skin (2 cm × 2 cm) was sandwiched between two stainless steel plates, which were connected to an electric circuit consisting of a DC power supply with voltage booster (MPS-3003S, Matrix, Spain) and a 4-pin relay (HR-CR313DC012, China) operated by an arbitrary function generator (AFG-3051, Instek, Taiwan). The function generator was set to output pulsed square-wave current of uniform pulse size. The set-up is illustrated in Figure 4.8.

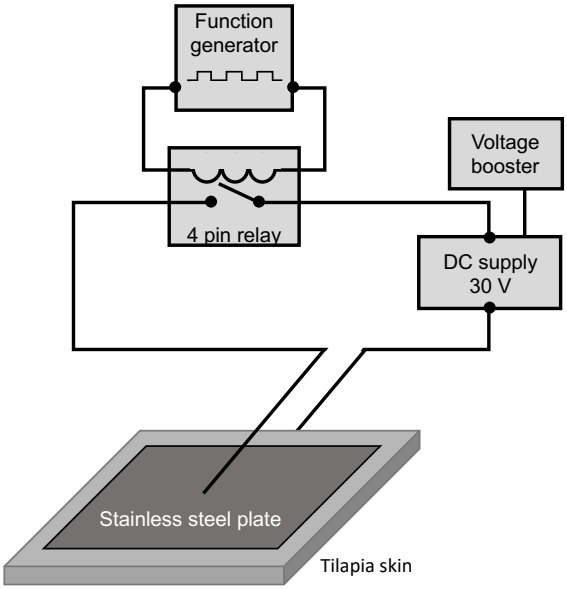

Figure 4.8: Circuit diagram of the electroporation set-up.

The DC power supply could be adjusted to give a voltage of 0-30V, while a voltage booster could increase the voltage to between 30V and 80V. The function generator could be set to turn the relay switch on and off to generate square-wave pulse with a frequency of 0.5-2 Hz. To study the effect of voltage and frequency on the electroporation of tilapia skin, the parameters were varied according to Table 4-6.

Table 4-6: Parameters for the electroporation of tilapia skin

	Duration (s)	Voltage (V)	Frequency (Hz)
Set 1 (varied voltage)	60	<10, 20-35, 50-60, 70-80	1
Set 2 (varied frequency)	60	20-35	0.5, 1, 2

4.4.3 *Results and discussion*

The DNA content and collagen content of tilapia skin after the electroporation treatment are presented in Figure 4.9 and Figure 4.10. At high voltage (above 30V), the voltage from the DC power supply and voltage booster could not be maintained at a stable voltage, hence a voltage range was used for each group of samples.

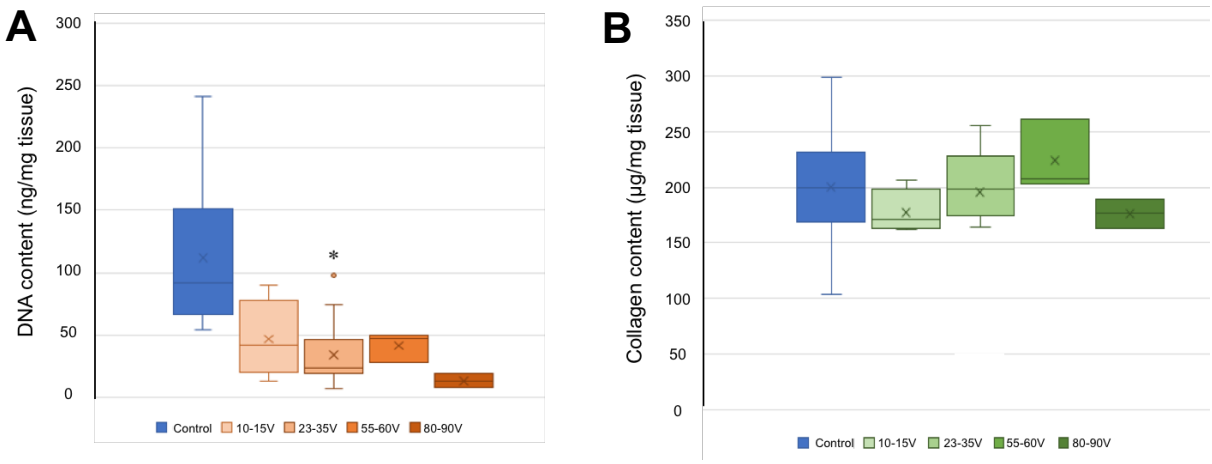

Figure 4.9: (A) DNA content and (B) collagen content in tilapia skin treated with electroporation of varying voltage (V = 10-15V, 23-35V, 55-60V, 80-90V), at f = 1 Hz and t = 60 s. * $p < 0.05$ when compared to control (native tilapia skin).

The results of varying voltage indicated that the DNA content in tilapia skin decreased with increasing voltage, and the collagen content was not affected significantly with increasing voltage, indicating that electricity can efficiently remove DNA while preserving the collagen in the skin. In fact, by using a voltage of 23-35V, the amount of residual DNA of all samples decreased to below 50 ng / mg tissue, the recommended maximum limit to avoid adverse immune responses [26].

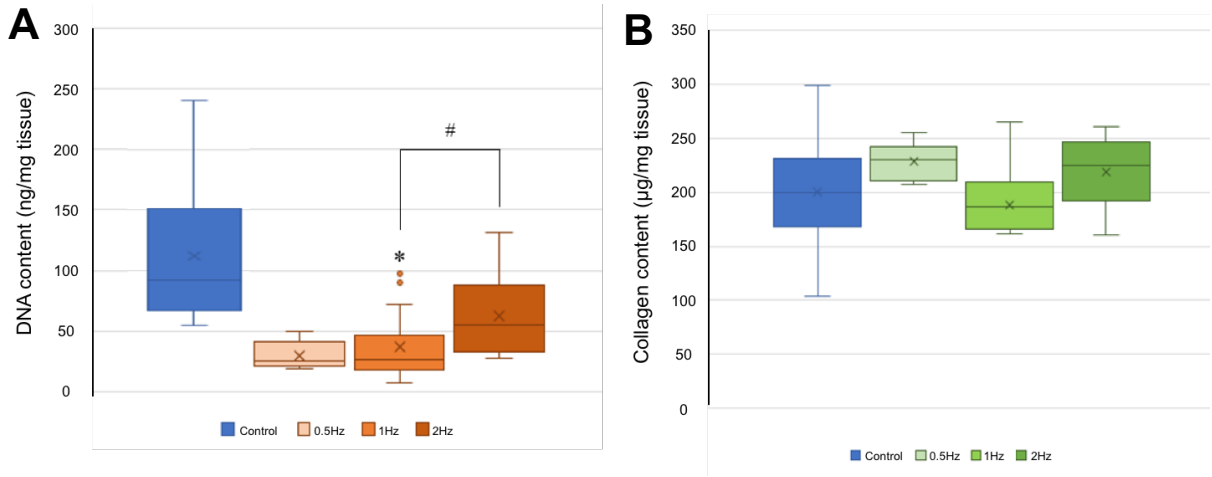

Figure 4.10: (A) DNA content and (B) collagen content in tilapia skin treated with electroporation of varying frequency (f = 0.5 Hz, 1 Hz, 2 Hz), at V = 23-35 V and t = 60 s. * $p < 0.05$ when compared to control (native tilapia skin), # $p < 0.05$ when comparing between 1 Hz and 2 Hz.

The results of varying frequency showed that there was no clear correlation between frequency and DNA content, while there was no significant changes in collagen content at all frequencies. However, for high frequency (f = 2 Hz), the DNA content was significantly higher than that at f = 1 Hz. One presumption is that if the frequency was too high, the membrane of the cells could not charge up to the critical voltage required to create irreversible pores on the membrane. At f = 0.5 Hz or 1 Hz, the amount of residual DNA decreased to below 50 ng / mg tissue, the recommended maximum limit to avoid adverse immune responses.

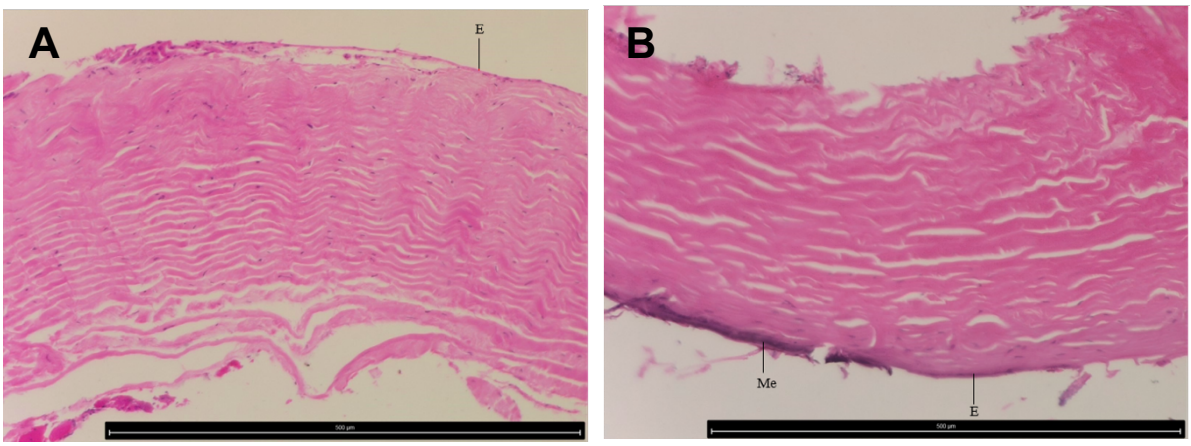

Figure 4.11: H&E histological images of tilapia skin (A) before and (B) after electroporation. Images taken at 940X magnification by Leica DVM6 microscope (Germany). E = epidermis, Me = melanophores. Electroporation parameters: V = 23-35 V, f = 1 Hz, t = 60 s.

The extensive removal of DNA was also observed in the H&E histological images (Figure 4.11), as DNA, represented by purple dots and visible in the native skin (Figure 4.11A), were no longer visible in the bulk of the skin after electroporation (Figure 4.11B). The ECM structure also looked preserved and unaffected by the treatment.

During the electroporation, it was observed that heat was generated after electroporation for more than 60 s. Also, as the voltage gets higher, the amount of heat generated increased. To prevent thermal denaturation of the tilapia skin, it was recommended that the duration should be kept to 60 s and the voltage was set at 23-35 V. Based on the results, the optimal parameters

were established to be time = 60 s, V = 23-35V, f = 1 Hz. Compared to the decellularization protocol reported in section 4.2.2, electroporation is a much quicker method to decellularize tilapia skin, as the detergent and enzymatic treatments took more than 12 hours while electroporation took only 1 minute.

In summary, the results of this preliminary study suggested that electroporation was effective in removing DNA from tissues while preserving the ECM. However, this study only focused on DNA content, collagen content and histology to assess the effectiveness of the treatments. Also, there are many parameters that can affect the effectiveness of the treatment but only a few parameters were studied here. To evaluate and understand the effect of electricity on the treated tissues more comprehensively, the tissues have to be subjected to more varying parameters, and be further characterized for properties such as mechanical strength and thermal stability. As the aim of decellularization is to produce acellular scaffolds for tissue engineering, biological properties such as cytotoxicity and biocompatibility have to be investigated too.

In this study, the tissue of interest was tilapia skin, which is a thin tissue and is more easily decellularized than thicker tissues such as tendons and muscles, as well as whole organs. For large tissues or organs, electroporation may have insufficient effectiveness in decellularization due to the limited contact area between the tissue and the electrodes. Hence, for every tissue type it is essential to investigate and optimise the process parameters to ensure maximal removal of cellular content with minimal disruption to the ECM.

Nevertheless, electricity is an attractive and novel decellularization medium, as electrical treatments generate little chemical waste, and offer substantial time savings compared to current physical, chemical and enzymatic methods. When optimized, electric decellularization can also be easily scaled up to process large amount of tissues in short times. As the demand on biologic scaffolds increases worldwide, electric decellularization is expected to serve as a

novel and rapid method to generate acellular tissue scaffolds to meet the needs of clinicians and patients.

4.5 Conclusion

Tilapia skin was successfully decellularized via a series of chemical and enzymatic treatments. After optimization of the decellularization protocol, it was determined that a combination of SDS, dispase and nuclease treatments was effective in decellularizing tilapia skin with almost all DNA (99.6%) removed and relatively high amount of collagen (69.3%) retained. However, the optimized decellularization process removed a large amount of elastin (91%), although glycosaminoglycans (GAGs) were less affected, with 55.1% retained. It was also found that water is a more effective rinsing agent than PBS, as the amount of residual SDS is lower in water-rinsed samples than in PBS-rinsed samples. The skin decellularized by the optimized process was termed DTS (decellularized tilapia skin). The physical properties of DTS were investigated in this chapter, while its biological properties would be investigated in the next two chapters.

Tensile tests performed on tilapia skin revealed that the mechanical properties of skin are dependent on the location of the skin and the direction of pull. When pulled in the dorsal-ventral (D-V) direction, tilapia skin exhibited higher mechanical strength than bovine and porcine acellular matrix, and the mechanical strength of tilapia skin remained high even after decellularization, lyophilisation and rehydration. The high mechanical strength of tilapia skin was attributed to the highly-ordered arrangements of the collagen fibres, which align with the direction of pull and make the skin stiffen like tendon when the skin is pulled in the D-V direction. As the mechanical and thermal properties are related, both native and decellularized tilapia skin possessed high denaturation temperatures (> 64°C). On the other hand, crosslinked

electrospun tilapia collagen had a much lower mechanical strength and denaturation temperature, as the collagen molecules were no longer in their native tightly packed arrangements and were randomly aligned instead.

Lastly, electricity was introduced as a novel decellularization medium. Electroporation was attempted on tilapia skin, and preliminary results suggested that electroporation was effective in the removal of DNA and the preservation of the ECM. In the author's opinion, more studies are needed to validate the effectiveness of electric decellularization. As electric decellularization generates little chemical waste, works much more rapidly compared to current decellularization methods, and easy to scale up, it would be a novel and promising technique to meet the increasing needs in tissue engineering.

5 Biological evaluation of tilapia scaffolds

5.1 Introduction

In tissue engineering, a scaffold can be described as an artificial structure used to support tissue regeneration. An ideal scaffold should provide a suitable 3-dimensional support, possess biological signals to induce cell proliferation and differentiation, and degrades over time to allow regenerated host tissue to take its space [1]. Over the years, a variety of biomaterials from natural and synthetic sources has been developed to fulfil the purposes of an ideal scaffold, but there are still some important challenges to be overcome to translate these biomaterials into real clinical applications *in vivo*. While there are many factors that contributes to the fate and effectiveness of a scaffold, including its mechanical and physical properties, it is the tissue-material interactions that dominantly determines the ultimate success of the scaffold [272]. As the body is equipped with a comprehensive defence system to detect and reject any intruding object, any material that is destined to be implanted into the body must be chosen and evaluated meticulously in order to survive this hostile and sensitive environment. Failure to address this issue may result in the loss of functionality of the implanted material, or in a more serious case, would lead to health complications in the patient and might even lead to death.

All materials, when introduced into a living tissue, would cause local injury to the tissue and provoke the body of the recipient to initiate an inflammatory reaction, known as the foreign body reaction (FBR), to protect the body from the foreign object [273]. The FBR typically comprises of an initial acute phase and a subsequent chronic phase. The acute phase, which can last from hours to days, is mostly responsible for the cleaning of the wound site and is characterized by the presence of leukocytes and the formation of a provisional matrix. The chronic phase, which is caused by persistent inflammatory stimuli, is generally characterized

by the presence of monocytes, macrophages, and lymphocytes, with the proliferation of blood vessels and connective tissues [274]. When the implanted material no longer poses a threat, the healing response is initiated by monocytes and macrophages, leading to vascularization and the formation of granulation tissue by fibroblasts.

For degradable scaffolds, the FBR will generally continue to be chronic, until complete degradation of the scaffold. For nondegradable or non-biocompatible scaffolds, a collagenous fibrous capsule may form around the scaffold to isolate it from the host tissue [275]. In large tissue defects or in sites with extensive loss of cells, native tissues may not be regenerated in time, leading to fibroblasts forming excessive fibrous tissue to fill up the space. This formation of excessive fibrous tissue, known as fibrosis, can lead to the loss of functionality of the encapsulated material, hinder tissue regeneration, and lead to formation of scars [276]. While it is impossible for a scaffold to avoid FBR as any foreign object would evoke an inflammatory reaction, a good scaffold should minimise the negative impact of FBR by being biocompatible to host cells, supporting angiogenesis, and degrading in a timely manner to allow the host tissue to regenerate in its place.

Thankfully, there is a variety of methods to predict the biocompatibility and the immunogenic potential of a biomaterial. For biomaterials of natural origin, especially decellularized tissues, the detection of antigens is a common approach to evaluate the immunogenic potential of the scaffold. Although xenogenic tissues contain many structural and functional molecules that are biocompatible and well-tolerated due to the high degree of conservation between species, they also harbour a number of antigens that would provoke adverse immune reactions in the recipient [277]. Based on the assumption that cell removal equals antigen removal, the quantification of antigens becomes a standard approach to evaluate the effectiveness of a decellularization protocol [95]. A number of methods are available to detect known antigens, such as DNA, galactose-alpha-1,3-galactose (alpha-gal) and major histocompatibility complex

I (MHC-I) [92, 93], but quantifying these antigens may not reveal the actual immunogenic potential of the decelluarized tissues as there are other antigens that may not be detected. To assess the entire immunogenic potential of decellularized tissues rapidly, Daugs et al developed a novel human serum-based detection system using a human serum pool, which contains polyclonal antibodies associated with the adaptive immune response [95]. Using the polyclonal antibodies in the serum pool as a primary antibody, antigens in decellularized tissues can be detected and visualized by immunohistochemistry, or quantified by ELISA.

Beside immunogenic potential, cytotoxicity is another important biological parameter that is included in safety assessments of biomaterials. Cytotoxicity testing, a primary requirement for the regulatory approval of biomaterials and medical devices, uses *in vitro* cell culture systems to evaluate the health of cells exposed to the test material or the extract of the test material [278]. As most mammalian cell types react similarly to toxic substances, materials that are toxic to cells would also be toxic to humans, so potentially toxic materials can be identified rapidly prior to *in vivo* or clinical testing, saving time and resources, as well as preventing unnecessary sufferings of laboratory animals [279]. To establish a uniform system to evaluate cytotoxicity in a variety of biomaterials and environments, the international standards for medical devices ISO 10993-5 has been published by the International Organization for Standardization (ISO), and is now used by regulatory agencies worldwide to assess the toxicity of biomaterials and to approve/reject their uses for *in vivo* and clinical applications [235].

Even if a biomaterial is found to have a low immunogenic potential and a low cytotoxicity, the biological evaluation of a biomaterial would not be complete without an in vivo assessment, as the complexity of the mammalian immune system and the mechanisms of the FBR from the molecular level to the cellular level and tissue level are extremely difficult to replicate *in vitro*. In the body, multiple cell types contribute to the FBR by secreting cytokines and growth factors that act as molecular messengers to promote inflammatory events such as macrophage

recruitment, as well as healing events such as vascularization [280]. Since many of these cellular and molecular pathways in immune response are similar between mammals, animal testing using a mammalian model is an effective approach to predict the FBR to a biomaterial in humans [281]. Among various mammals, rodents such as mice and rats are commonly used in biomedical research. Despite a number of differences between mouse and human immune systems and the presence of genomic gaps, rodents are still the foundation of biomedical research as they are easy to keep, they breed rapidly and their genomes can be easily manipulated [282]. By monitoring the cell populations and quantities of molecular messengers after implantation of a biomaterial in a rodent, one can interpret the *in vivo* FBR to the material and accordingly predict the immune responses in humans.

In view of the importance of establishing the biological safety of novel biomaterials and the lack of prior studies on the biological properties of decellularized tilapia skin, the next objective of the thesis would be to evaluate and characterise the immunogenic potential, cytotoxicity, and *in vivo* immune response of decellularized tilapia skin (DTS), using crosslinked electrospun tilapia collagen (CETC) and a porcine collagen product as a comparison. The hypotheses of the biological evaluations would be that DTS and CETC would have low immunogenicity, low cytotoxicity and favourable in vivo immune response. Results from the biological evaluations would reveal the suitability of tilapia-derived biomaterials for tissue engineering applications.

5.2 Methodology

5.2.1 *Materials*

Fresh tilapia was purchased from a local supermarket and processed on the same day. Fresh porcine artery was obtained from a local abattoir and stored in -20°C until use. Phosphate-

buffered saline (PBS), Dubecco's Modified Eagle's Medium (DMEM), fetal bovine serum (FBS), penicillin-streptomycin, AlamarBlue assay kit and PicoGreen DNA quantification kit were obtained from Life Technologies (Grand Island, NY, USA). The Milliplex® Rat Cytokine assay kit were obtained from Merck (Darmstadt, Germany). Other chemicals were obtained from Sigma Aldrich (St Louis, MO, USA) unless otherwise stated.

5.2.2 *Sample preparation*

Decellularized tilapia skin (DTS) was prepared according to the methods mentioned in section 4.2.2 of this thesis. In summary, freshly obtained tilapia skin was cleaned, cut into smaller pieces (4cm × 4cm), and stored in PBS with 1% penicillin/streptomycin at 4°C for 1 hour to remove blood and debris. The skin was shaken in 2.5 U/mL dispase in PBS for 3 hours to detach the epidermis. The skin was rinsed with DI water, and shaken in 1% SDS in PBS for 6 hours to lyse the cells and release cellular contents. The skin was then gently scrapped to physically remove the epidermis. The skin was rinsed with DI water, and shaken in 25 U/mL Pierce Universal Nuclease in PBS for 3 hours to break down the nucleic acid. Finally, the skin was rinsed with DI water, and shaken in 1% sodium dodecyl sulphate (SDS) in PBS again for 1 hour to remove the nuclease and residual contaminants. The skin was rinsed with DI water and lyophilized in a freeze-dryer for 24 hours. The lyophilized skin was further dried in a vacuum chamber for 1 hour to remove any condensation. This final product is termed decellularized tilapia skin (DTS) and was stored dry at room temperature until further use.

Crosslinked electrospun tilapia collagen (CETC) membranes were prepared according to the methods reported by Zhou et al [20] and mentioned in section 3.2.3 and 3.2.5 of this thesis, with slight modifications. In brief, freshly obtained tilapia skin was immersed in PBS with 1% penicillin/streptomycin for 1 hour to remove blood and debris, stirred in 0.1 M NaOH solution for 6 hours to remove non-collagenous proteins, rinsed with deionised (DI) water, stirred in 10%

1-butanol and 20% isopropanol in water for 24 hours to remove fats and fat-soluble pigments, rinsed with DI water again, and stirred in 0.5 M acetic acid for 48 hours to solubilize the collagen. The crude collagen extracts were separated from the solid residue by centrifugation at 10000g for 20 minutes, and 5 M NaCl solution was added to the supernatant to a final concentration of 1 M to precipitate the collagen. After centrifugation at 10000 g for 1 hour, the precipitate was re-dissolved in 0.5 M acetic acid. The solution was filtered through Whatman no. 1 filter paper, dialyzed in DI water overnight, and lyophilized to obtain collagen sponges, which were dissolved in hexafluoro-isopropanol to make a 8% (w/v) solution. The collagen solution was centrifuged at 5000 g for 3 minutes to separate solid debris and each solution was drawn into a 3 ml syringe with a needle (inner diameter 0.25 mm). The collagen was electrospun for 3 hours with a voltage of 10 kV, a flow rate of 0.6 ml/h and a distance of 10 cm between the needle tip and the aluminum foil collector, with the collector rotated every 15 minutes to ensure all areas were covered. The electrospun mat was crosslinked in glutaraldehyde vapour (50% solution in water) for 2 hours and vacuum-dried overnight. The whole process was performed at room temperature (23 °C).

5.2.3 *Human serum based Immunohistochemical analysis*

Immunohistochemical (IHC) analysis was performed according to the method reported by Daugs et al [95], with slight modifications. Native tilapia skin, DTS and porcine arteries were fixed for 16 hours in Carnoy buffer (60% ethanol, 30% chloroform, 10% acetic acid), dehydrated using increasing ethanol concentrations, and embedded in paraffin. The embedded samples were then sliced at a thickness of 5 μm with a rotary microtome (RM2255, Leica, Germany) to obtain cross-sectional sections of the samples. The sections were dried at 62°C for 2 hours, incubated two times for 10 minutes in xylene and rehydrated in decreasing ethanol concentrations. After rinsing with DI water, endogenous peroxidases in the samples were

inactivated in 0.3% hydrogen peroxide in PBS for 10 minutes. Slides were washed in PBS-T (PBS with 0.05% Tween-20) for 5 minutes and were treated with blocking buffer (0.5% fish gelatin (Virico, Singapore) in PBS-T) at room temperature. Slides were then incubated at 4°C with the primary antibody solution (human serum pool (PAN-Biotech, Germany)) for 2 hours, rinsed in PBS-T, and incubated with the secondary antibody solution (Goat-anti-human Ig(G, A, M)-peroxidase (Sigma-Aldrich, USA) diluted to 1:6000 with PBS) for 1 hour at room temperature. Slides were rinsed and incubated with the UltraVision Quanto HRP DAB Detection System (Thermo Scientific, USA) for 10 minutes. After rinsing with DI water, cell nuclei were stained with hematoxylin for 3 minutes, which were blued in warm water for 10 minutes. Finally, sections were dehydrated with increasing ethanol concentrations, washed in xylene, embedded in tissue mounting medium (Leica, Germany), dried, and analysed by light microscopy (DVM6, Leica, Germany).

5.2.4 *Human serum based ELISA*

Native tilapia skin, DTS, CETC and porcine arteries were separately homogenized into fine powder at cryogenic temperature for 10 cycles at 10 minutes per cycle with the 6970EFM Freezer Mill (SPEX SamplePrep, USA). One hundred milligrams of the powder were dissolved in 1 ml TE-buffer (10 mM Tris-HCl, 1 mM EDTA, pH 7.2), followed by 15 minutes of vortex and 15 minutes of ultrasonification. The mixture was centrifuged at 5000 g for 10 minutes to remove insoluble debris, and the total protein content of the supernatant was determined using the Pierce BCA protein assay kit (Thermo Scientific, USA).

The protein extracts were then used for enzyme-linked immunosorbent assay (ELISA) according to the method reported by Daugs et al [95], with slight modifications. Each protein extract was diluted to 1:10, 1:100 and 1:1000 with TE buffer, and 100 µL of every original and diluted extract were added in duplicate to wells of high-binding 96-well plates (Corning, USA).

After 1 hour of incubation with the protein extracts, the wells were rinsed 3 times for 5 minutes with PBS-T (PBS with 0.05% Tween-20), treated with 150 µl blocking buffer (0.5% fish gelatin (Virico, Singapore) in PBS-T) for 30 minutes, incubated with 100 µl primary antibody solution (human serum pool (PAN-Biotech, Germany)) for 2 hours, rinsed in PBS-T 3 times, incubated with 100 µl secondary antibody solution (Goat-anti-human Ig(G, A, M)-peroxidase (Sigma-Aldrich, USA) diluted to 1:6000 with PBS), rinsed in PBS-T 3 times, and finally incubated in 100 µl Ultra TMB Reagent (Thermo Scientific, USA) for 20 minutes. The reaction was stopped with 100 µl stop reagent (2M sulphuric acid) and the plate was read at 450/620 nm absorbance. The whole process was performed at room temperature (23°C ± 1°C).

5.2.5 *Indirect cytotoxicity*

Indirect cytotoxicity studies were performed in accordance to ISO 10993-5 protocols. Murine fibroblasts L929 (ATCC®, VA, USA) were cultured in DMEM + GlutaMAX supplemented with 10% FBS and 1% penicillin-streptomycin. Cells were incubated at 37 °C and passaged every 2-3 days until seeding. Samples were sterilized with 70% ethanol for 2 hours and washed with DMEM + GlutaMAX, before being individually incubated in DMEM (6 cm^2 per ml media) at 37°C for 24 hours to obtain an extract of the test sample. Simultaneously, L929 cells were seeded into 24-well plates (Corning, USA) at a density of 2×10^4 cells/well and grown overnight. The culture media were then replaced by the sample extracts and after 24 hours incubation, cells were visualised by light microscopy and cell viability determined using AlamarBlue assay (Invitrogen, USA). Polyurethane film containing 0.1% zinc diethyldithiocarbamate (ZDEC) was used as positive (toxic) control and high-density polyethylene (HDPE) was used as negative (non-toxic) control.

5.2.6 *Cellular biocompatibility*

Cellular biocompatibility studies were performed with murine fibroblast L929. Samples were cut into 10 × 10 mm squares, sterilized as previously described and placed into a 24 well plate (Corning, USA). L929 cells were seeded onto the samples at a density of 2×10^4 cells/well. After 1, 3, 7 days, cell proliferation was evaluated by AlamarBlue assay.

5.2.7 *In vivo experiments in rats*

All animal experiments were performed in the Animal Research Facility (ARF), Nanyang Technological University (NTU) under the rules and regulation of NTU's Institutional Care and Use Committee (NTU-IACUC) and Singapore's National Advisory Committee for Laboratory Animal Research (NACLAR).

5.2.8 *Cytokine analysis via cage implant system*

The implantation of cages and the subsequent analysis of extracted exudate were performed according to the procedures described by Schutte et al. with slight modification [283]. Surgical-grade stainless steel mesh was cut and formed into cylindrical cages (2 cm × Ø 1 cm). The cages were autoclaved and divided into 4 groups; empty, Bio-Gide®, CETC and DTS. Bio-Gide® (Geistlich, Switzerland) is a commercial porcine collagen membrane used in guided bone regeneration. Membranes of 1 cm × 1 cm inserted aseptically into each cage and one cage from each group was implanted subcutaneously into the back of a male adult Sprague-Dawley rat (n = 3) under anaesthesia with isofluorane. On days 1, 2, 7 and 14 after implantation, the rats were anesthetized and the exudate fluid in each cage was drawn and centrifuged (300g) for 10 minutes at 4°C, before the supernatants were frozen at -80 °C for later analysis.

After the last time-point (14 days after implantation), the exudate samples were assayed for cytokines with a Milliplex® Map Rat Cytokine / Chemokine assay kit (Merck Millipore,

Germany). Cytokines interleukin-1beta (IL-1β), IL-2, IL-4, IL-6, IL-10, 1L-13, monocyte chemoattractant protein 1 (MCP-1), tumour necrosis factor alpha (TNF-α) and vascular endothelial growth factor (VEGF) were measured according to the manufacturer's protocol. In brief, the working standards were prepared with the Assay Buffer provided in the kit. The samples and standards were added into a 96-well plate, followed by the addition of antibody coupled magnetic beads. The plate was incubated with agitation followed by addition of Streptavidin-Phycoerythrin. The beads were resuspended in the provided Sheath Fluid and analysed on a Luminex Magpix machine (Luminex Corporation, USA). The cytokine concentrations (pg/mL) were determined from mean fluorescence intensities (MFI) with respect to standard curves using the Cubic Spline curve fitting method to analyze the data.

5.2.9 *Subcutaneous implantation*

Samples were implanted subcuteaneously through a 2 cm skin incision into the back of a male adult Sprague-Dawley rat (n = 3 per time point) under anesthesia with isofluorane. The samples (1 × 2 cm) were implanted in the subcutaneous space on the back of the animals. On days 7 and 14 after implantation, the rats were sacrificed and the tissue around each sample was harvested *en block*. Paraffin-embedded sections were slices along the longitudinal axis into 5 μm thick sections with a microtome (RM2255; Leica, Germany), stained with hematoxylin and eosin, and observed with light microscopy (BX51; Olympus, Japan). The inflammatory response around the implant was determined by counting the number of cell layers surrounding the implant.

5.2.10 *Statistical Analysis*

Quantitative results are expressed as mean ± standard deviation (SD) and differences between mean values were evaluated using a two-tailed Student's t-test. A p-value of <0.05 was considered to be statistically significant.

5.3 Results and discussion

5.3.1 *Immunohistochemical analysis*

In vitro detection of antigens such as DNA, alpha-Gal or MHC-I is often used to evaluate the extent of decellularization and the immunogenicity of xenografts based on the assumption that cell removal is equal to antigen removal, but a lot of unknown tissue components are able to activate the immune system. The aim of this analysis was to use a novel human-serum based detection system that allows the qualitative and quantitative determination of a xenograft's immunogenic potential *in vitro* without focusing on individual antigens. Here, immunohistochemical (IHC) staining of tissue sections was established to visualise and identify antigenic tissue components.

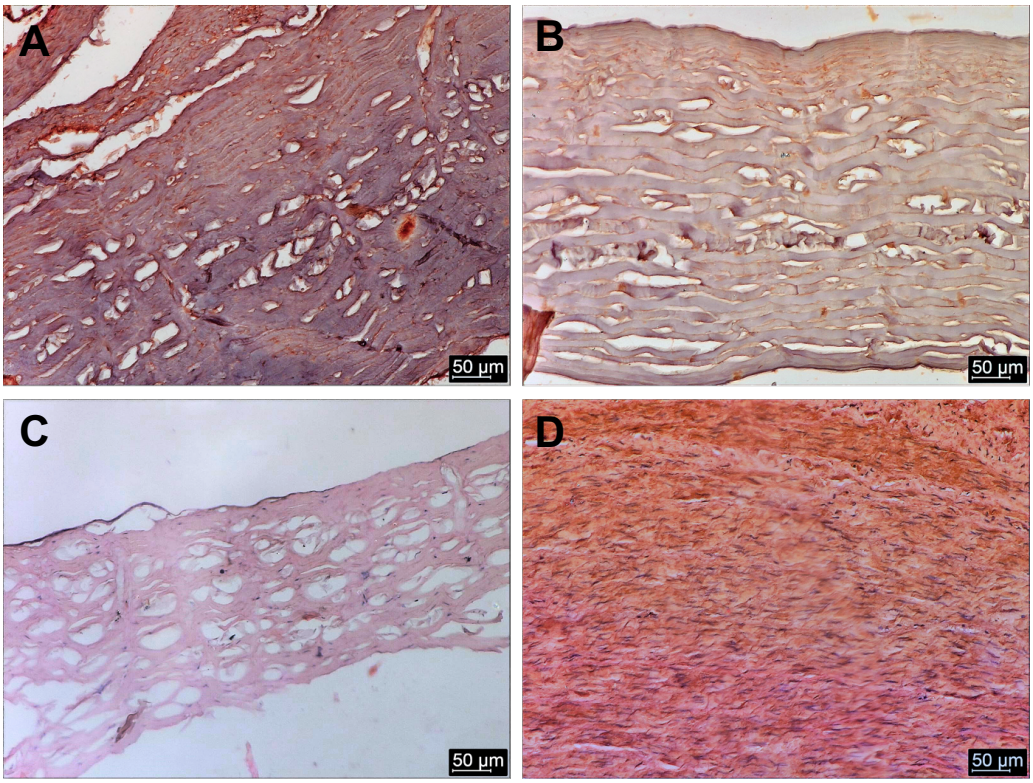

Figure 5.1: Cross-sectional immunohistochemical staining of (A) native tilapia skin, (B) decellularized tilapia skin (DTS), (C) native tilapia skin (no primary staining), (D) porcine artery. Tissue samples were fixed in Carnoy buffer, dehydrated, embedded in paraffin, and sectioned to 5 µm. Slides except (C) were treated with human serum as primary antibody. All slides were then treated with peroxidase-linked anti-Ig (G, A, M) antibodies as secondary antibodies, followed by staining with DAB substrate and hematoxylin. Brown areas indicate DAB staining of antigens and purple/blue areas indicate hematoxylin staining of DNA.

In the IHC section of the native tilapia skin with no primary staining (Figure 5.1C), cell nuclei were clearly visible as blue spots due to the staining of DNA by hematoxylin. With primary staining, a strong detection of antigens was observed as brown stains in the epidermis, at the outer layers of the dermis and in the gaps between the collagen layers within the dermis (Figure 5.1A). Decellularization greatly reduced the intensity of the brown stains and eliminate blue spots (Figure 5.1B), indicating a significant removal of antigens and a thorough removal of DNA by the decellularization protocol. Some antigens were still visible in decellularized tilapia skin (DTS), and were mostly concentrated in the gaps between the collagen layers. The collagen layers were not stained brown, an indication that collagen is less antigenic. The IHC section of the porcine artery showed a high density blue spots in a brown-stained background, indicating that porcine artery has a high density of cells and the ECM has high amounts of antigens. While IHC staining allows us to visualise the antigens and pinpoint them to certain locations or cells, it does not provide quantitative data and does not reveal the identities of the antigens [284]. Hence, further tests would be required to determine the immunogenicity of the samples more accurately.

5.3.2 *ELISA analysis*

To detect and quantify potential antigens in native and decellularized tilapia skin, the tissues were homogenized and dissolved in TE buffer to extract the tissue proteins. The extracts were screened for antigens by ELISA with a human serum pool containing polyclonal IgG, IgA and IgM antibodies associated with primary immune response and hyperacute graft rejection [285]. The quantity of antigens in the sample was expressed as the immunogenic potential, and normalised to the value for native tilapia skin. (Native tilapia skin represents 100%.) The immunogenic potentials of the samples are illustrated in Figure 5.2.

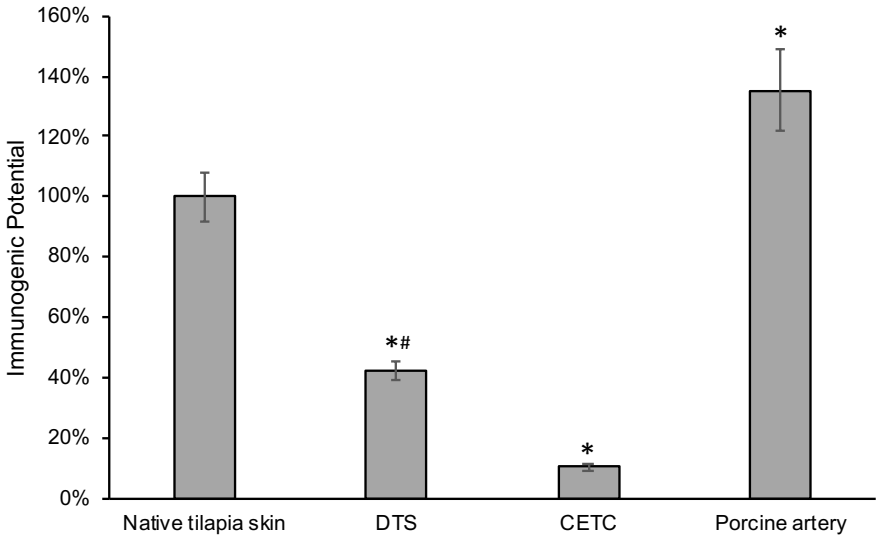

Figure 5.2: Immunogenic potentials of native tilapia skin, DTS, CETC (crosslinked electrospun tilapia collagen) and porcine artery detected by ELISA. Plates were coated with diluted protein extracts of the samples and blocked with 0.5% fish gelatin. Primary staining was done with human serum, secondary staining was done with peroxidase-linked antibodies, and detection was done with TMB substrate. * $p < 0.05$ when compared to native tilapia skin. # $p < 0.05$ when compared to CETC.

From the ELISA, it was evident that decellularization resulted in a significant reduction ($p < 0.05$) of immunogenic potential of 57.4% in tilapia skin, which agrees with the immunohistochemical staining data. Crosslinked electrospun tilapia collagen (CETC) was included in this assay to investigate the immunogenicity of crosslinked collagen scaffolds, and CETC was found to have a significantly lower immunogenic potential ($p < 0.05$) than both native tilapia skin and DTS, with only 10.6% potential compared to native tilapia skin. As CETC is fabricated from purified collagen only from tilapia skin, it does not have any other substances beside collagen and glutaraldehyde. Collagen is a protein abundant in the ECM and highly conserved between species, so it is expected to have a low immunogenic potential. Although glutaraldehyde is reported to be cytotoxic, the crosslinking time for this batch of CETC was relatively short (2 hours) and the CETC samples were thoroughly vacuum-dried to remove residual glutaraldehyde. Therefore the CETC has a low immunogenic potential.

On the other hand, porcine artery was found to have a significantly higher immunogenic potential than native tilapia skin, with its value 35.4% higher than that of native tilapia skin,

suggesting that native mammalian tissues are immunogenic than native fish tissues. It was reported that fish tissues are generally less immunogenic than mammalian tissues as fish tissues do not have certain antigens that are common in mammalian tissues, such as galactose-alpha-1,3-galactose (or α-gal), a xenoantigen that is expressed on the surface of all cells in non-primate mammals [286]. Alpha-gal is known to trigger hyperacute rejections and allergic reactions in humans [95, 119] as continuous exposure to gut bacteria expressing α-gal leads to the generation of xenoreactive antibodies against α-gal [287]. In fact, anti-α-gal antibodies make up 1-8% of human immunoglobulin M (IgM) and 1-2.4% of human immunoglobulin G (IgG) antibodies, making α-gal the dominant antigen causing hyperacute rejections of mammalian xenografts in humans [288]. As fish cells do not express α-gal, fish tissues have an immunogenic advantage over mammalian tissues.

With human serum-based IHC staining and ELISA, it is possible to compare and evaluate tissues of different origin and tissues processed by various decellularization methods for their immuno-compatibility. It is also possible to predict FBR at an early stage so that highly immunogenic samples can be identified *in vitro*, reducing unnecessary sufferings in animal testing [95]. However, this approach has some limitations, one of which is the inability to predict acute and chronic rejection caused by formation of new antibodies in the recipient's body, which usually occurs weeks after implantation. Another limitation is the inability to identify the individual substances responsible for the antigenicity, as this human serum-based approach only reveals the immunogenicity at the macro-scale. To predict the immune-compatibility with more certainty, *in vivo* testing would be required.

5.3.3 *Indirect cytotoxicity*

The cytotoxicity of the samples was evaluated quantitatively by determining the cell viability of L929 cells in term of the cellular metabolic function by AlamarBlue assay. The relative metabolic activity of the cells exposed to the sample extract was normalised to the value of the non-toxic control. (Non-toxic control represents 100%.) The results are shown in Figure 5.3.

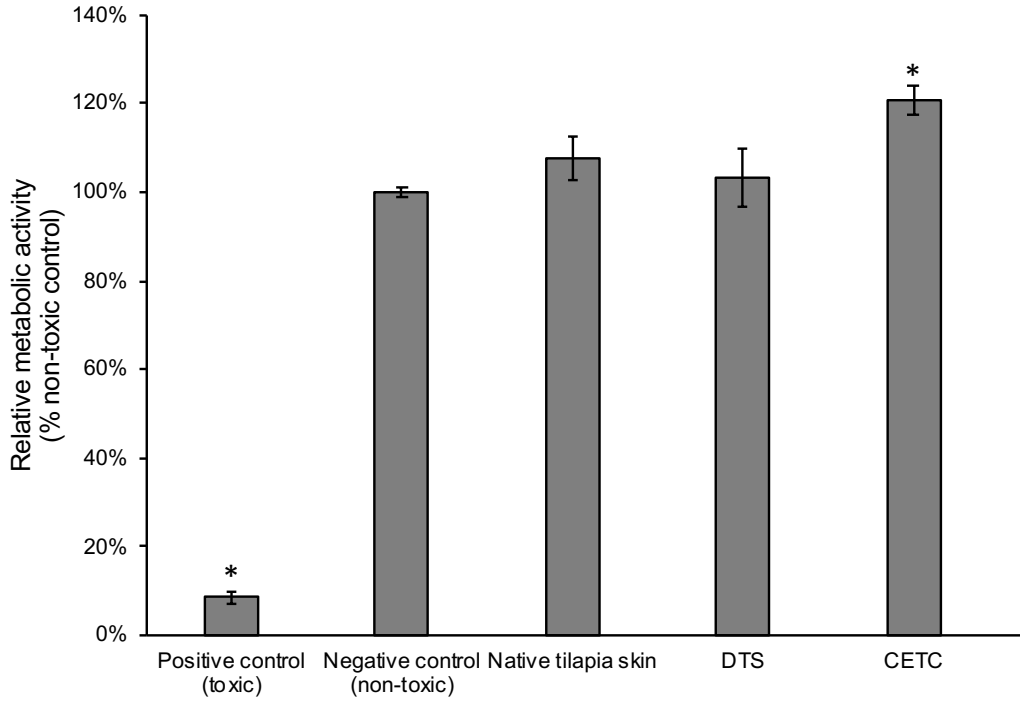

Figure 5.3: Metabolic activity of L929 cells after incubation in sample extract determined by AlamarBlue assay, and cell permeability determined by visually checking both sides of the samples with SEM. For metabolic function, the samples were assayed after 24 hours incubation and the fluorescence intensity values were normalised against the non-toxic control.

Before the implantation of a biomaterial, it is important to check whether the material is toxic. Determining the cell viability after incubation in the sample extract is a simple way to evaluate the toxicity of a material [235]. When cells proliferate, innate metabolic activity results in a chemical reduction of the AlamarBlue dye, changing the dye from the oxidized (non-fluorescent) form to the reduced (fluorescent) form [289]. If the sample contains soluble toxic components, the toxic substances would leach into the extract, causing the cells exposed to the

extract to be affected, and the reduced metabolic activity would be reflected by a drop of fluorescence intensity in the assay.

From the results, it was observed that all samples have similar or higher values than the non-toxic control, indicating that the materials are all non-cytotoxic. Hence, it could be presumed that cytotoxic chemicals and enzymes used in the decellularization of tilapia skin had been successfully washed away from DTS and residual glutaraldehyde was also successfully removed from CETC.

Among all samples, CETC was observed to support the highest metabolic activity of L929 in its extract, with its value significantly higher ($p < 0.05$) than that of the non-toxic control. As the indirect cytotoxicity assay evaluates the cytotoxicity of a material by the toxic substances released into the sample extract, any water-soluble biocompatible substances may reduce or mask the toxicity of the dissolved toxins. Observing the high metabolic activity of L929 in the CETC extract, we hypothesized that the crosslinking was incomplete in CETC, leading to the unbound collagen molecules leaching into the sample extract and increasing the metabolic activity of the L929 cells.

5.3.4 *Cellular biocompatibility*

To evaluate the direct cytotoxicity and cellular biocompatibility of DTS and CETC, the scaffolds were seeded with murine fibroblast L929 and the cellular activity were measured at selected time-points with AlamarBlue assay. The fluorescence values of the metabolite were converted to the relative cellular metabolic activity. The result is shown in Figure 5.4.

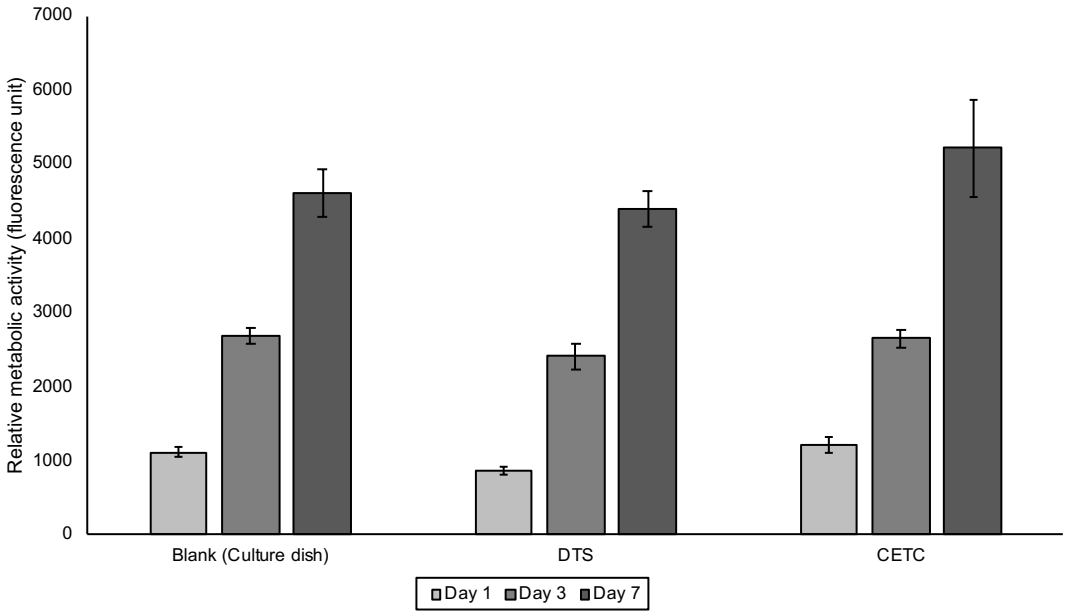

Figure 5.4: Cell viability on CETC (crosslinked electrospun tilapia collagen) and DTS (decellularized tilapia skin), represented by the relative metabolic activity of L929, as determined by direct AlamarBlue assay. No significant differences ($p < 0.05$) were observed between groups at each time-point, but within each group, the metabolic activity at Day 3 or Day 7 was significantly higher ($p < 0.05$) than that at the previous time-point.

The results showed increasing growth of L929 cells with time on both scaffolds, indicating that both CETC and DTS were not cytotoxic and exhibited good cellular biocompatibility towards L929 cells. Between CETC and DTS, CETC possessed better cellular biocompatibility due to the higher number of cells observed on CETC at Day 3 and Day 7. CETC was also found to have a lower immunogenic potential in the human-serum ELISA and low cytotoxicity in the indirect cytotoxicity assay. Although CETC is mechanically weaker than DTS as reported in section 4.3.5, it has better biological performances as indicated in the human-serum ELISA, indirect cytotoxicity and cellular biocompatibility assays. In terms of cytotoxicity and cellular biocompatibility, DTS was found to have similar performances to Bio-Gide®, suggesting that DTS and CETC would be suitable candidates for tissue engineering applications.

5.3.5 *Cytokine analysis*

In this study, subcutaneous cage implants in rats were used to examine the *in vivo* immune response of our tilapia-derived scaffolds, based on the experimental design reported by other groups [290-292]. Exudate samples were extracted from the empty and sample-containing stainless steel mesh cages implanted subcutaneously in rats. The quantities of nine cytokines – IL-1β, IL-2, IL-4, IL-6, IL-10, 1L-13, MCP-1, TNF-α and VEGF – in the exudate were measured with a multiplex magnetic bead array system and shown in

Figure 5.5.

In this study, Bio-Gide®, a commercially available porcine collagen membrane use, was included as a reference. As Bio-Gide® has been approved for clinical use in guided bone regeneration [293], any scaffolds that has similar or better immunological performances than Bio-Gide® would be highly likely to be suitable for tissue engineering applications.

Among the tested cytokines, IL-2 (interleukin-2), IL-6 (interleukin-6), and TNF-α (tumour necrosis factor alpha), promote inflammation [294-296]. Pro-inflammatory/pro-wound healing cytokines, which include IL-1β (interleukin-1 beta) and MCP-1 (monocyte chemoattractant protein 1), can activate both inflammatory cells and wound healing cells while anti-inflammatory/anti-wound healing cytokine IL-10 (interleukin-10) does the opposite by suppressing both cells [297-299]. Anti-inflammatory/pro-wound healing cytokines, which include IL-4 (interleukin-4) and IL-13 (interleukin-13), inhibit inflammation and promote wound healing [300]. Another important cytokine VEGF (vascular endothelial growth factor) promotes the formation of blood vessels to support growth of new tissue [301].

The results (

Figure 5.5 and Figure 5.6) indicated a high production of pro-inflammatory cytokines such as IL-1β, IL-6, IL-10 and MCP-1 at the early time-points and a decrease in production with time. Notably on Day 1, Bio-Gide®, CETC and DTS induced a higher production of IL-1β than the empty cage, and CETC and DTS induced a significantly higher

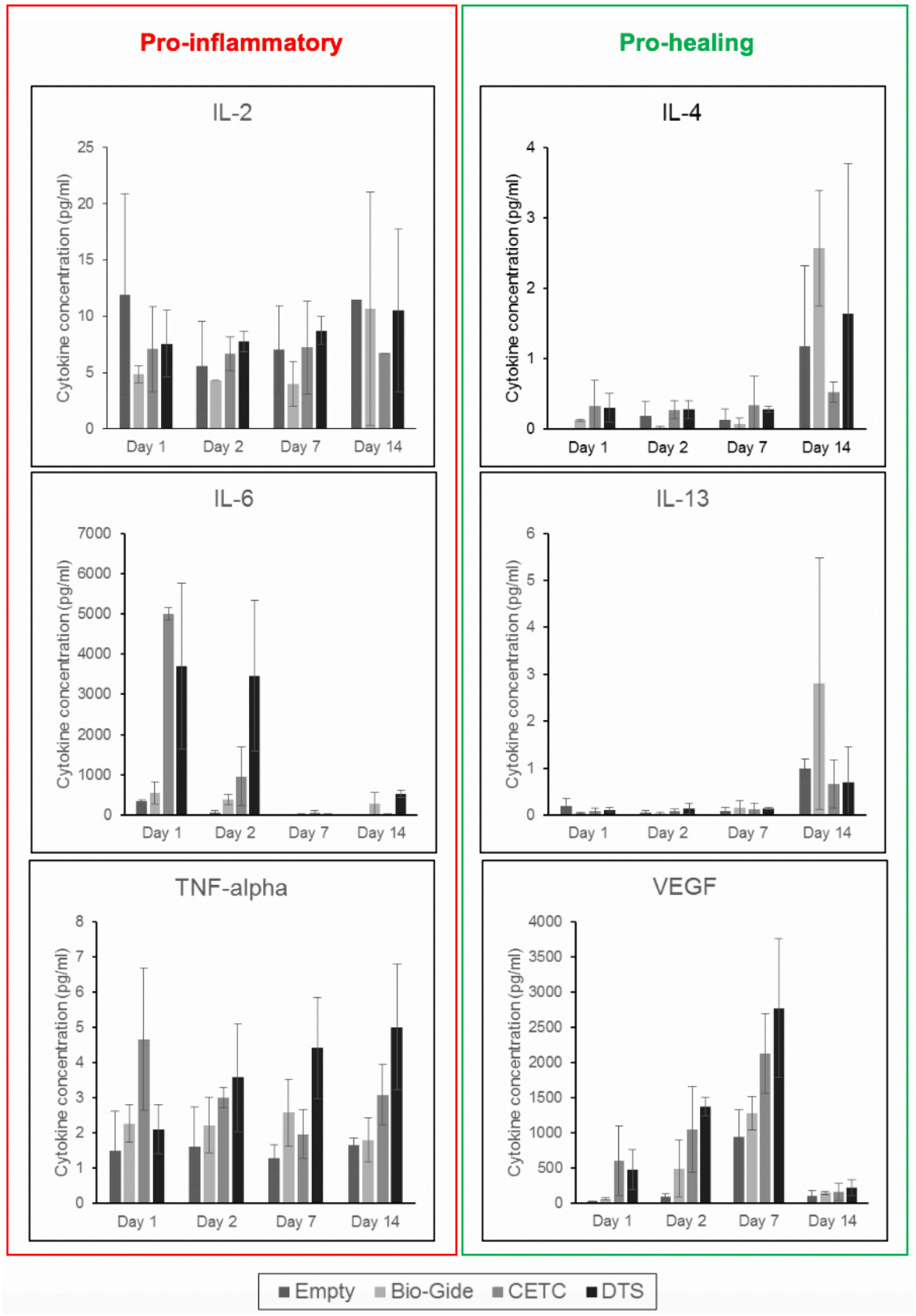

Figure 5.5: Levels of pro-inflammatory and pro-healing cytokines in rat exudates on 1, 2, 7 and 14 days after subcutaneous implantation of empty cages, cages with Bio-Gide®, cages with crosslinked electrospun tilapia collagen (CETC) and cages with decellularized tilapia skin (DTS). IL = interleukin, TNF-α = tumour necrosis factor alpha, VEGF = vascular endothelial growth factor

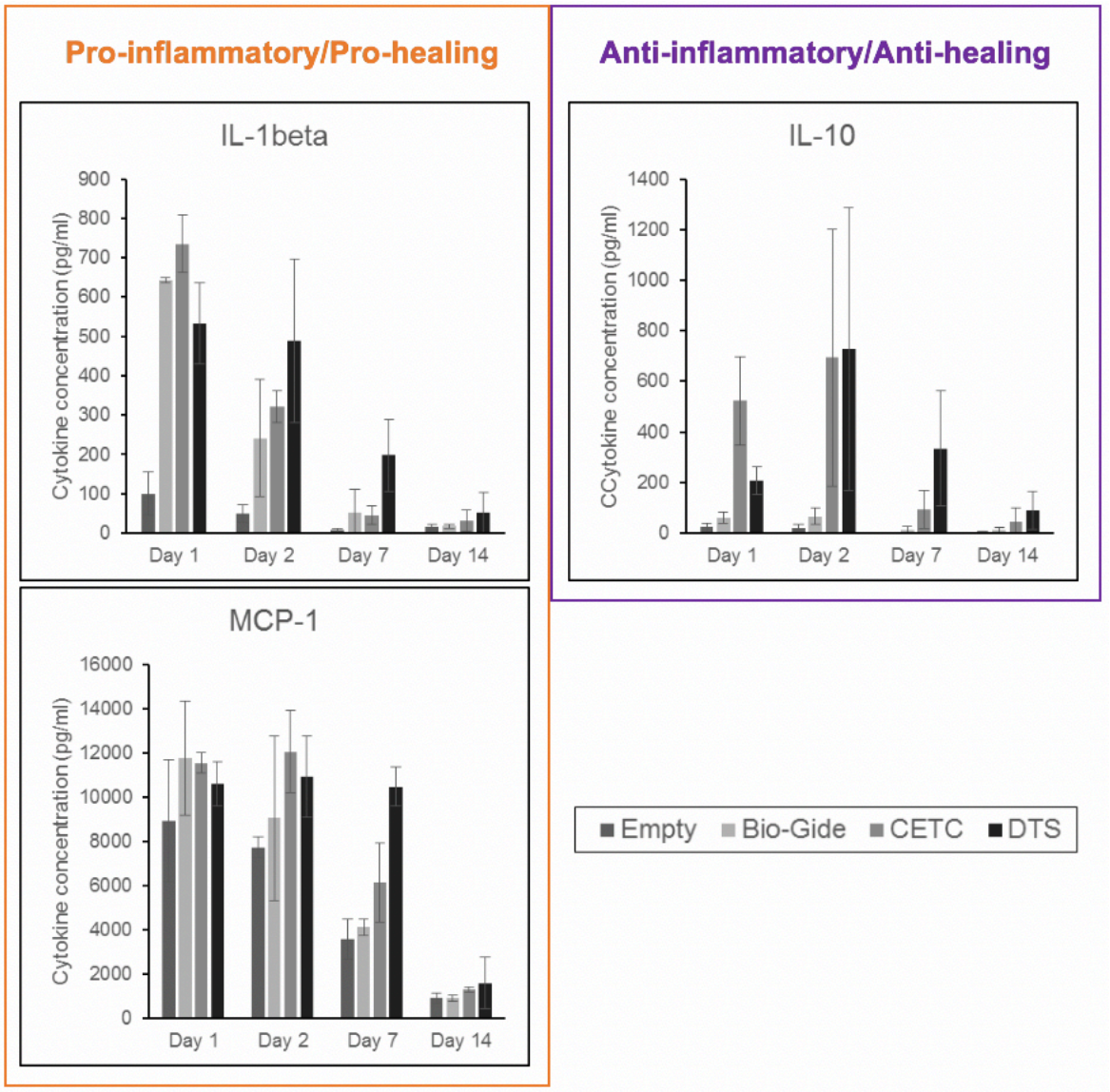

Figure 5.6: Levels of pro-inflammatory/pro-healing and anti-inflammatory/anti-healing cytonkines in rat exudates on 1, 2, 7 and 14 days after subcutaneous implantation of empty cages, cages with Bio-Gide®, cages with crosslinked electrospun tilapia collagen (CETC) and cages with decellularized tilapia skin (DTS). IL = interleukin, MCP-1 = monocyte chemoattractant protein 1

production of IL-6 and IL-10 than the empty cage and Bio-Gide®. Such a difference diminished after 7 days. The results also showed a comparable production of cytokines at all time-points with little or no differences between the empty cage, Bio-Gide® and CETC for IL-2 and TNF-α. The pro-healing cytokines IL-4, IL-13 and VEGF were observed in low production at the early time-points and the production increased with time. For IL-4 and IL-13,

cytokine production was only noticeable on Day 14. For VEGF, cytokine production increased with time and peaked on Day 7, before dropping to very low levels on Day 14.

A more detailed analysis revealed some general trends among all the groups. Firstly, all implantation groups including the empty group induced a strong expression of MCP-1 and a mild expression of IL-1β, IL-2, IL-6 and TNF-α after 1 day post-implantation, indicating that the stainless steel cages alone caused inflammation. MCP-1 had a high production after 1 and 2 days post-implantation and its production decreased after 7 and 14 days, indicating the accumulation of monocytes in the acute inflammation phase and the clearance of monocytes in the wound healing phase respectively [297]. Pronounced production of IL-1β in the collagen containing groups was found in the first 2 days of implantation, which was not noticeable after 7 days. Secondly, the expression of IL-4 and IL-13 for all the groups only became evident after 14 days post-implantation indicating the implantation sites progressed from the acute inflammation phase into the wound healing phase. Thirdly, the concentration of VEGF increased with time and reached a peak after 7 days post-implantation for all samples, before dropping back to low levels. This suggested that the implantation site was undergoing vascularization for the first 7 days, and once a network of blood vessels was formed to supply oxygen, nutrients and soluble factors into the cages, VEGF was no longer produced in high amounts.

As tilapia collagen and mammalian collagen are reported to have similar properties [30], we expected CETC and DTS to have similar cytokine responses as Bio-Gide®, which is derived from porcine collagen. Indeed it was found that CETC, DTS and Bio-Gide® had comparable cytokine profiles in terms of pro-inflammatory cytokines IL-1β, IL-2, MCP-1 and TNF-α. For IL-6, CETC and DTS had a higher cytokine response at earlier time-points, but later, CETC and DTS had comparable responses as Bio-Gide® and the empty cage. One possible explanation for the high response at the earlier time points is that certain portions of the tilapia

collagen molecules might be considered foreign by the rat immune system and therefore triggered the high expression of IL-6. As the tilapia collagen molecules get degraded, the cytokine response at the later time-points became similar to that of the empty cage. The low concentrations of pro-inflammatory cytokines at late time-points showed that the tilapia collagen membranes are not cytotoxic and do not cause chronic inflammation, suggesting that the tilapia collagen membranes were resorbed or well tolerated by the body.

5.3.6 *Subcutaneous implantation*

To further investigate the *in vivo* immunological effects of our tilapia-derived scaffolds, the host tissue response was evaluated at 1 and 2 weeks after the samples were subcutaneously implanted into the back of male adult rats. The histological sections were stained with hematoxylin and eosin and shown in Figure 5.7.

Host reactions following biomaterial implantation may include fibrous capsule formation, foreign body reaction, injury, blood-material interactions, provisional matrix formation and inflammation to name a few [275, 302]. After 1 week of implantation, Bio-Gide and DTS samples demonstrated thin localized fibrous tissue encapsulation. No obvious granulomatous reactive tissue or inflammatory cells seen in all groups while CETC samples did not show any fibrous tissue encapsulation. After 2 weeks, the encapsulation was more distinct and thicker in the Bio-Gide® and DTS samples while that of the CETC still had a lack of an encapsulating layer of cells.

From the histology data (Figure 5.7), it is evident that the CETC membrane elicits a lower tissue response from the host as indicated by the lack of / thin biomaterial encapsulation as compared to that of Bio-Gide® and DTS. In general, biomaterials that have cross-linking may in some cases result in the non-incorporation and graft failure, also the preclusion of immune cell penetration, making such grafts unable to participate in normal remodelling [303, 304].

However, despite chemical cross-linking of the collagen membrane, no increase in cellular encapsulation was observed after 2 weeks.

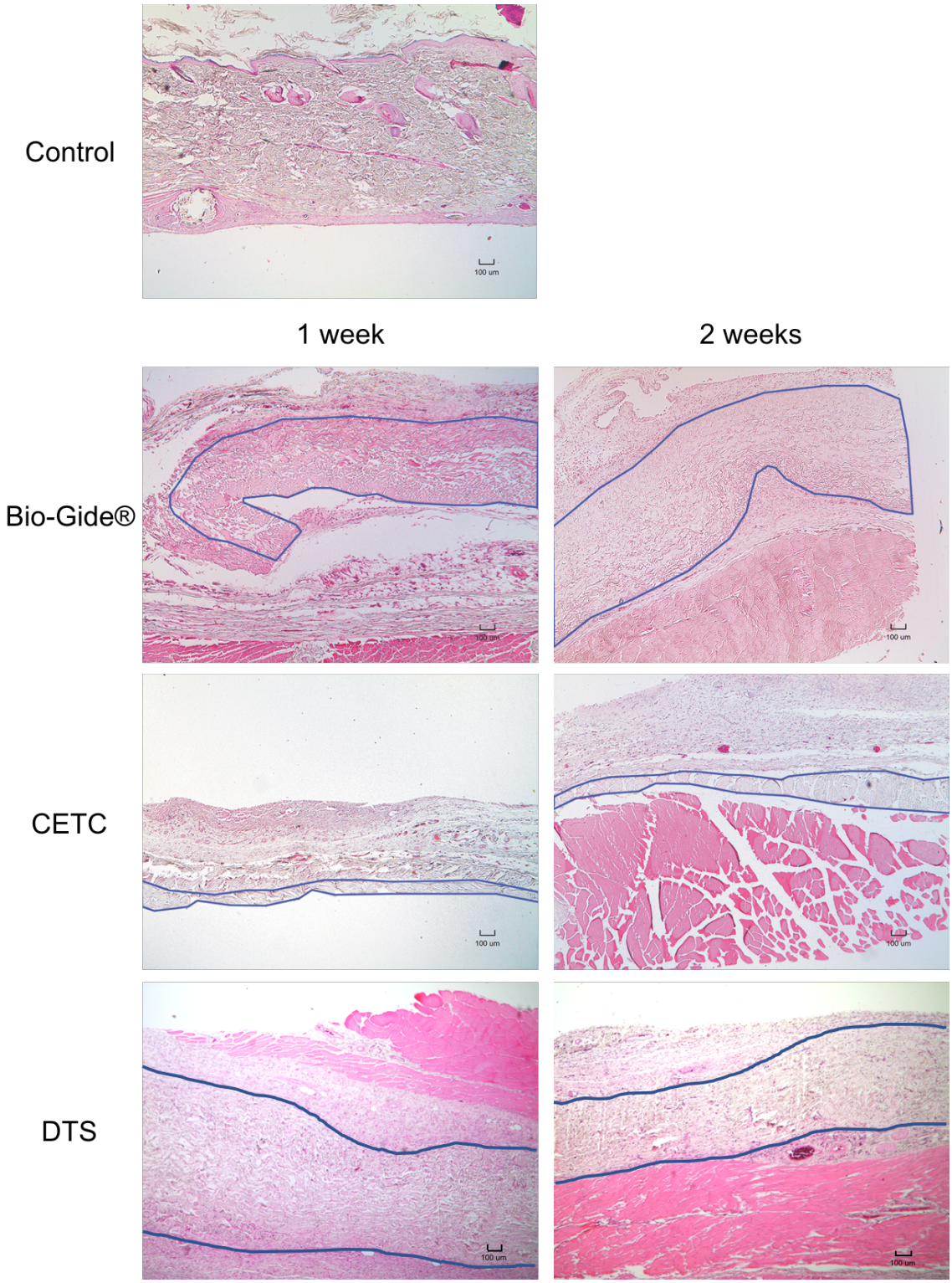

Figure 5.7: Histology sections of the subcutaneous implants stained with H&E. Control represents native tissue without any implants. The implants are highlighted with a blue line to indicate their location. Sections are representative of the samples. Scale bars are 100 µm.

Typically, a foreign body response occurs under normal physiological conditions and is based on nonspecific protein adsorption, and interaction between the implant and inflammatory cells, which protect the body from the foreign objects [273]. Importantly, in this inflamed environment, the immune cells contribute to the development of a dense layer of fibrotic connective tissue which is detrimental to the implants' function, safety, and biocompatibility [273-275]. The lack of encapsulation suggests that the host does not mount a typical foreign body response to CETC and this observation is in agreement with the results from the cytokine assay.

On the other hand, thin localized fibrous tissue encapsulation was observed for Bio-Gide® and DTS one week after implantation and the encapsulation became thicker two weeks after implantation. The presence of a fibrous capsule indicated that the FBR was still in the chronic phase, as the scaffolds have not been completely degraded. Bio-Gide® was designed to be a protective barrier membrane that prevents the entry of epithelial cells into the bone defect site, to allow osteogenic cells inside the defect to proliferate and generate bone tissues. As a result, Bio-Gide® was designed to have a controlled degradation so as to provide protection and mechanical support to the defect site for an extended time [293]. As the subcutaneous implants were harvested two weeks after implantation, it was unlikely that the Bio-Gide® samples would have degraded by then. Based on the high mechanical strength of DTS, it was also unlikely that the DTS samples would have degraded in 2 weeks. For degradable scaffolds, the FBR will generally continue to be chronic, until complete degradation of the scaffold [275]. Hence it would be expected that the fibrous capsule would last until the complete biodegradation of Bio-Gide® and DTS.

The FBR is also influenced by the surface topography and surface chemistry of the implant, as the tissue-implant interface manipulates macrophage adhesion and activation in the early phase

of inflammation. High surface-to-volume implants, such as porous materials will have higher ratios of macrophages than smooth-surface implants, which will result in fibrosis being a significant component of the implant site [305]. From the human-serum ELISA, it was observed that DTS still had some degree of immunogenicity even after decellularization. Indeed, both *in vitro* and *in vivo* studies have shown that persistent antigens remain in decellularized tissues, and scaffold acellularity does not guarantee the elimination of inflammatory and immune responses towards decellularized scaffolds [306]. The porous nature of the scaffolds and the presence of residual antigens are likely factors that contribute to the formation of fibrous encapsulation for Bio-Gide® and DTS. Despite the presence of fibrous encapsulation, which is a sign of chronic FBR and will last until the complete degradation and resorption of the scaffold, no obvious granulomatous reactive tissue or inflammatory cells were observed after 1 week and 2 weeks, indicating that Bio-Gide® and DTS were not cytotoxic, did not release toxic metabolites and did not induce chronic inflammation. This observations were in agreement with the results of the cytokine assay.

5.4 Conclusion

In this chapter, two forms of tilapia-derived scaffolds – DTS (decellularized tilapia skin) and CETC (crosslinked electrospun tilapia collagen) were subjected to a series of biological assessments to evaluate their biological safety and performance. The immunogenic potential of the scaffolds were assessed with human serum based immunohistochemical staining and human serum based ELISA. The results indicated that decellularization significantly reduced the immunogenic potential of tilapia skin, but DTS still possessed some degree of immunogenicity. CETC had a significantly lower immunogenic potential than DTS, as CETC comprised of pure collagen only. Porcine artery, included in the assay as a reference, had a significantly higher immunogenic potential than native tilapia skin. As fish cells do not express

antigens expressed by mammalian cells such as α-gal, fish tissues are seen as less immunogenic than mammalian tissues.

The cytotoxicity and cellular biocompatibility of the scaffolds were assessed with murine fibroblasts L929. Both DTS and CETC were observed to be non-cytotoxic to cells, with cells in the CETC group exhibiting higher metabolic activity than the cells in the DTS group. An increase of cellular metabolic activity of L929 cells was also observed on both DTS and CETC with increasing duration, indicating that both scaffolds are biocompatible to L929 cells.

Lastly, the *in vivo* immune responses of the scaffolds were assessed with a cytokine assay of the exudate extracted from subcutaneously implanted cages, and H&E stained sections of subcutaneously implanted scaffolds. All samples induced the expression of inflammatory cytokines at early time points (Day 1 and Day 2), which is a sign of acute inflammation. The level of inflammatory cytokines decreased and the level of pro-healing cytokines increased at late time points (Day 7 and Day 14), suggesting that inflammation had given way to wound healing and there was no chronic inflammation. CETC was found to have exceptional *in vivo* immune responses and biocompatibility due to the lack of fibrous encapsulation, while DTS and Bio-Gide® was observed to be surrounded by a thin fibrous encapsulation, which was attributed to the slow degradation and porous nature of the scaffolds. The formation of fibrous encapsulation is a part of the chronic phase in the FBR, and the fibrous tissue would persist until complete degradation of the implanted scaffold. Despite the presence of fibrous encapsulation, there were no granulomatous tissue or inflammatory cells after 2 weeks, indicating that DTS and Bio-Gide® were non-toxic and did not induce chronic inflammation.

As CETC had better biological performance than Bio-Gide® and DTS has similar performances to Bio-Gide®, it was expected that CETC and DTS would be suitable scaffolds in tissue engineering applications.

6 Evaluation of tilapia scaffolds for tissue engineering applications

6.1 Introduction

Organ shortage has been reported as a growing problem globally due to the increasing prevalence of tissue failure caused by diseases, aging and trauma [307]. The dire shortage of organs and long waiting time for organ transplantation have necessitated a rising demand for tissue-engineered constructs to restore structural and functional attributes in the impaired or missing organ. Among the numerous types of tissue-engineered constructs, collagen scaffolds are widely used due to the abundance of collagen in humans and animals and its essential role as a structural protein in the extracellular matrix (ECM) [56]. Currently dominated by mammalian products, the collagen scaffold market is gradually shifting to non-mammalian sources to mitigate the risk of disease transmissions and religious constraints associated with mammalian products, with fish tissues being identified as a promising alternative [186]. In this thesis, we focused on Nile tilapia (*Oreochromis niloticus*) due to its popularity as a food source and the favourable characteristics of its type I collagen.

The preceding chapters of this thesis have highlighted the development and characterisation of two types of tilapia-derived scaffolds: crosslinked electrospun tilapia collagen (CETC) and decellularized tilapia skin (DTS). CETC was fabricated by the extraction and purification of collagen from tilapia skin, followed by the reconstitution of the collagen by electrospinning and crosslinking, while DTS was fabricated by subjecting tilapia skin to a series of chemical and enzymatic treatments to remove cellular materials and antigens from the tissue. The two scaffolds were found to be non-cytotoxic and biocompatible to cells. For DTS, the optimized decellularization process removed most of the DNA and significantly reduced the antigen

content, while preserving the collagen content, ECM structure and physical properties. While CETC has been previously reported to support *in vitro* and *in vivo* skin regeneration [20], there was no prior studies on DTS, making this study one of the first to investigate the properties of DTS and the potential of DTS as a tissue engineering material.

Considering the small number of studies done on crosslinked electrospun tilapia collagen and the lack of prior studies on decellularized tilapia skin in tissue engineering applications, the next objective of the thesis would be to explore the suitability of CETC and DTS for selected clinical applications using appropriate *in vitro* and *in vivo* models. As there are numerous collagen scaffolds derived from mammalian tissues already approved and marketed for clinical use, the hypothesis of this investigation would be that CETC and DTS would also be structurally and functionally suitable as tissue engineering scaffolds in clinical settings. Collagen scaffolds are currently utilised in many types of medical and cosmetic applications, but due to a limited time-frame, this thesis focused on two applications introduced below.

6.1.1 *Guided bone regeneration*

Following tooth loss or extraction, the alveolar bone would undergo irreversible resorption, and the resultant inadequate bone volume poses challenges to the placement of dental implants [308]. To promote bone growth and restore bone tissue in the alveolar defect, a dental surgical procedure known as guided bone regeneration (GBR) is performed with the help of a barrier membrane [309, 310]. The ideal GBR membrane should prevent epithelial cells from entering the defect so as to allow time for bone cells to grow and bone tissue to regenerate. In addition, the membrane should also support bone cell attachment and promote osteo-induction within the defect. The membrane should also provide mechanical support to protect the defect, allow nutrition diffusion and vascularization, and be bioresorbable (ideally after 2 months) so as to prevent the need for a secondary operation to remove the membrane [311, 312].

Historically, non-resorbable materials such as PTFE (polytetrafluoroethylene) and resorbable materials such as PLGA (poly-lactic/co-glycolic acid) have been developed as barrier membranes for GBR, but recently collagen membranes are gaining popularity for GBR applications due to its abundance in tissues, good biocompatibility and bioresorbability [293]. Current commercial barrier membranes are derived from bovine or porcine collagen, and their uses are limited due to high prices and religious restrictions associated with bovine and porcine products. Hence, tilapia-derived collagen scaffolds may offer an attractive and economical non-mammalian alternative. In this chapter, the suitability of CETC and DTS as GBR membranes would be evaluated using osteogenic cell culture and a rat calvarial defect model.

6.1.2 *Skin wound healing*

The skin is the largest organ of the human body and it acts as a barrier to protect the host from the foreign environment [313]. In addition, the skin helps to regulate body temperature and support sensory functions. Given the importance of the skin, any damage to the skin's structure or function must be treated quickly in order to prevent complications or infections. However, patients with severe skin damages (e.g. burns) or chronic diseases (e.g. diabetes) may not have skin regeneration capability and will require wound dressing to cover their wounds [314, 315].

Current wound dressing products fall mainly into two categories – "traditional wound care products" which are simple hemostatic dressings acting as a physical barrier between the wound and the environment, and "advanced wound care products" which possess unique properties to enhance wound healing, such as antimicrobial properties and the ability to release bioactive molecules [315]. Among the advanced wound care products, skin substitutes are the dressing of choice for burn wounds and chronic wounds that extend into the deep dermis or through the entire dermis [316]. Autografts are the gold standard for skin substitutes but are limited by inadequate supply, damage to donor sites and scar formation. Allografts and

xenografts are more readily available but there are risks of disease transmission and immunological rejection [317]. To eliminate such risks, decellularization may be the solution to produce acellular scaffolds that mimic the native skin environment and offer biocompatibility and bioresorbability. Due to limited supply of human skin to be used as allografts and religious restrictions associated with porcine and bovine xenografts, decellularized fish skin may become an attractive alternative as a wound dressing to protect the wound from the external environment and support skin regeneration. In this chapter, the suitability of DTS as a skin wound dressing would be evaluated using fibroblast cell culture and a murine full-thickness skin defect model.

6.2 Methodology

6.2.1 *Materials*

Fresh tilapia was purchased from a local supermarket and processed on the same day. Phosphate-buffered saline (PBS), Dubecco's Modified Eagle's Medium (DMEM), minimum essential media-alpha (MEM-α), fetal bovine serum (FBS), penicillin-streptomycin, AlamarBlue assay kit and PicoGreen DNA quantification kit were obtained from Life Technologies (Grand Island, NY, USA). Other chemicals were obtained from Sigma Aldrich (St Louis, MO, USA) unless otherwise stated.

6.2.2 *Sample preparation*

Decellularized tilapia skin (DTS) was prepared according to the methods mentioned in section 4.2.2 of this thesis. In summary, freshly obtained tilapia skin was cleaned, cut into smaller pieces (4cm × 4cm), and stored in PBS with 1% penicillin/streptomycin at 4°C for 1 hour to remove blood and debris. The skin was shaken in 2.5 U/mL dispase in PBS for 3 hours to

detach the epidermis. The skin was rinsed with DI water, and shaken in 1% SDS in PBS for 6 hours to lyse the cells and release cellular contents. The skin was then gently scrapped to physically remove the epidermis. The skin was rinsed with DI water, and shaken in 25 U/mL Pierce Universal Nuclease in PBS for 3 hours to break down the nucleic acid. Finally, the skin was rinsed with DI water, and shaken in 1% sodium dodecyl sulphate (SDS) in PBS again for 1 hour to remove the nuclease and residual contaminants. The skin was rinsed with DI water and lyophilized in a freeze-dryer for 24 hours. The lyophilized skin was further dried in a vacuum chamber for 1 hour to remove any condensation. This final product is termed decellularized tilapia skin (DTS) and was stored dry at room temperature until further use.

Crosslinked electrospun tilapia collagen (CETC) membranes were prepared according to the methods reported by Zhou et al [20] and mentioned in section 3.2.3 and 3.2.5 of this thesis, with slight modifications. In summary, freshly obtained tilapia skin was immersed in PBS with 1% penicillin/streptomycin for 1 hour to remove blood and debris, stirred in 0.1 M NaOH solution for 6 hours to remove non-collagenous proteins, rinsed with deionised (DI) water, stirred in 10% 1-butanol and 20% isopropanol in water for 24 hours to remove fats and fat-soluble pigments, rinsed with DI water again, and stirred in 0.5 M acetic acid for 48 hours to solubilize the collagen. The crude collagen extracts were separated from the solid residue by centrifugation at 10000g for 20 minutes, and 5 M NaCl solution was added to the supernatant to a final concentration of 1 M to precipitate the collagen. After centrifugation at 10000 g for 1 hour, the precipitate was re-dissolved in 0.5 M acetic acid. The solution was filtered through Whatman no. 1 filter paper, dialyzed in DI water overnight, and lyophilized to obtain collagen sponges, which were dissolved in hexafluoro-isopropanol to make a 8% (w/v) solution. The collagen solution was centrifuged at 5000 g for 3 minutes to separate solid debris and each solution was drawn into a 3 ml syringe with a needle (inner diameter 0.25 mm). The collagen was electrospun for 3 hours with a voltage of 10 kV, a flow rate of 0.6 ml/h and a distance of

10 cm between the needle tip and the aluminum foil collector, with the collector rotated every 15 minutes to ensure all areas were covered. The electrospun mat was crosslinked in glutaraldehyde vapour (50% solution in water) for 2 hours and vacuum-dried overnight. The whole process was performed at room temperature (23 °C).

6.2.3 *Water Contact Angle*

The water contact angle, which corresponds to the hydrophilicity of the material surface, was measured using a contact angle goniometer (FTA200, First Ten Angstroms, VA, USA). Prior to measurement, the membranes were gently tapped dry with a tissue and placed flat on a glass slide. A drop of water (approx 1 – 2 μL) was introduced onto the surface and an image of the drop of water on the membrane surface was captured within three seconds after contact. The angle between the solid surface and the liquid-vapour interface was determined by analysing the image with the software connected to the contact angle goniometer.

6.2.4 *Porosity*

The porosity of the membranes, which is the volume in the membrane occupied by empty space, was determined by an ethanol intrusion method reported by Pham et al [318]. Dry Bio-Gide® membrane, dry CETC and freeze-dried DTS were cut into 1 cm × 1 cm pieces, weighed, and immersed in ethanol overnight on a shaker to allow the void volume to be filled by ethanol. The scaffolds were taken out, tapped with a Kimwipe to remove excess ethanol, and reweighed. The dimensions of the membranes (length, width, thickness) were also measured. The change in mass after the intrusion was multiplied by the density of ethanol (0.789 g/mL) to obtain the volume of the ethanol occupying the void, and the porosity was determined by dividing the volume of the ethanol by the volume of the membrane (length × width × thickness).

6.2.5 *Water permeability*

Membrane permeability was measured using a device and method adapted from the work of Sell et al [319]. In the device, a 5 ml pipette is placed horizontally on a shelf 160 cm above the ground. The pipette tip was connected to a 3-way valve, which was connected to a funnel on one outlet and the sample holder 10 cm above the ground (or 150 cm below the pipette) on the other outlet. Clear rubber tubing was used for the connections. An open/close valve was installed along the tubing between the 3-way valve and the sample holder. The sample holder consisted of two silicone gaskets with an inner diameter of 4 mm, secured by a metal cage. The membrane, with its thickness measured, was placed between the two silicone gaskets. The 5 ml pipette, rubber tubing and sample holder were filled with water via the funnel, and then water was passed through the membrane from the 5 ml pipette. Fluid flow was measured via the markings in the 5 ml pipette at selected time-points, and the membrane permeability was determined by the Darcy equation:

$$\tau = \frac{Q.\eta.h_m}{F.t.(\rho.g.h)}$$

where τ is the membrane permeability in darcy unit (D), Q is the volume of water passing through the membrane in time t, η is the viscosity of water (0.89 cp at 25°C), h_m is the membrane thickness, F is the membrane's cross sectional area, and ($\rho.g.h$) is the applied pressure head defined by the density of water ρ (1 g/mL at 25°C), the gravitational force g and the height of the system from the pipette to the sample h (1.5 m). The applied pressure head has to be converted from pascals (Pa) to atmosphere (atm) for use in the Darcy equation.

6.2.6 *Degradation*

The degradation profile of the membranes was measured according to the procedure described by Zhang *et al.* [82] and the other according to the procedure described by Ma *et al*. [79], both with some modifications. In the first method, each 1 cm × 1 cm sample was freeze-dried, accurately weighed, and placed in 2 ml PBS under aseptic conditions. The tubes were sealed and incubated at 37 °C for 7, 14, 21 and 28 days. After each time-point, samples were taken out and rinsed in DI water, freeze-dried and weighed. The degree of degradation of each sample is defined as the weight loss percentage calculated by the following equation:

$$Weight\ loss\ (\%) = \frac{W_0 - W_t}{W_0} \times 100$$

where W_0 represents the initial weight (g) of the dried sample before incubation and W_t represents the weight of the degraded sample after the respective time-points.

In the second method, each 1 cm × 1 cm sample was freeze-dried, accurately weighed, and placed in 200 U/ml collagenase type I to simulate *in vivo* enzymatic degradation [79]. The tubes were sealed and incubated at 37 °C for 1, 2 and 3 days. After each time-point, the degradation was stopped by incubating the tubes on ice. After centrifugation at 10,000 g for 10 min, 50 µl of the clear supernatant were hydrolysed with 200 µl of 6 M HCl at 120°C for 6 hours. The amount of collagen released by the sample during degradation was quantified by measuring the amount of hydroxyproline in the hydrolysate with a hydroxyproline assay kit (MAK008, Sigma-Aldrich, USA). The degree of degradation is defined as the percentage of released hydroxyproline from the sample at a certain time-point to the completely degraded sample with same composition and weight.

6.2.7 *In vitro bone regeneration*

Murine-derived pre-osteoblast cell line MC3T3-E1 Subclone 4 (ATCC® CRL2593, VA, USA) was used in this study. MC3T3-E1 cells were cultured in MEM-α and supplemented with 10% FBS and 1% penicillin-streptomycin. Cells were incubated at 37 °C and passaged every 2-3 days. All samples for the *in vitro* studies were sterilized with 70% ethanol for 2 hours and washed with MEM-α (for MC3T3-E1) prior to use in cell culture. Osteogenic induction medium was prepared by supplementing the culture media with 0.2 mM ascorbic acid, 10 mM β-glycerophosphate and 10^{-8} M dexamethasone and sterile filtered prior to use. These supplements were added to the culture medium and culture medium replaced every 3–4 days.

MC3T3-E1 cells were seeded on the membranes at a density of 2 x 10^4 cells/well in 24-well plates. Cells seeded directly into the well without any samples were used as a control. After culturing for 1, 2 and 3 weeks, the seeded samples were harvested to determine osteogenic gene expression, calcium deposition and distribution of mineralized ECM.

The calcium deposited by MC3T3-E1 cells after osteogenic differentiation was quantified by a calcium assay. After each time-point, the samples were digested in 0.25 mg/mL Proteinase K (Invitrogen, USA) at 50 °C for 3 hours. The mixtures were further frozen and thawed 3 times to lyse the cells. The lysates were centrifuged at 10,000 g for 5 min. For each sample, the supernatant was analysed with the PicoGreen assay kit to quantify the DNA content, while the pellet was dissolved in 400 µl of 0.5 M acetic acid and analysed with the Quantichrom Calcium Assay Kit (BioAssay Systems, USA) to quantify the calcium content. The calcium content was then divided by the DNA content to give the normalised calcium content.

The mineralized extracellular matrix secreted by the MC3T3-E1 cells was examined by Von Kossa staining. After each time-point, samples were fixed with 4% paraformaldehyde and

thereafter washed thrice in distilled water. Samples were stained with 2% silver nitrate for 10 minutes in the dark and then exposed to bright light for 15–30 minutes. The exposed samples were soaked in 5 % (w/v) sodium thiosulphate solution to prevent further darkening. The stained samples were then observed with light microscopy (Leica DVM6, Germany).

The gene expression of osteogenic markers was quantified by Real-time polymerase chain reaction (RT-PCR). After each time-point, RNA was extracted using the RNeasy extraction kit (Qiagen, Germany) and reverse-transcribed into cDNA using the iScript cDNA synthesis kit (Bio-Rad, USA). The expression of genes related to osteogenic differentiation - bone sialoprotein (*BSP*), osteocalcin (*OC*), and osteopontin (*OPN*) was determined with the iQ SYBR Green Supermix (Bio-Rad, USA) on a CFX Connect Real-Time PCR System (Bio-Rad, USA). The RT-PCR data were normalised to the values of the housekeeping gene GAPDH and calculated via the $2^{-\Delta\Delta Ct}$ method [320]. The RT-PCR primers (AIT Biotech, Singapore) are listed in Table 6-1.

Table 6-1: RT-PCR primer sets (AIT Biotech, Singapore)

Gene/Oligo Name	Oligo Sequence
BSP forward	5'-TTTATCCTCCTCTGAAACGGT-3'
BSP reverse	5'-GTTTGAAGTCTCCTCTTCCTCC-3'
OC forward	5'-CCGGGAGCAGTGTGAGCTTA-3'
OC reverse	5'-TAGATGCGTTTGTAGGCGGTC-3'
OPN forward	5'-GATGAACAGTATCCTGATGCC-3'
OPN reverse	5'-TTGGAATGCTCAAGTCTGTG-3'
GAPDH forward	5'-AACGACCCCTTCATTGAC-3'
GAPDH reverse	5'-TCCCACGACATACTCAGCAC-3'

6.2.8 *In vivo bone regeneration*

Animal experiments were approved by NTU-IACUC and conducted in accordance to its guidelines and procedures. The rat calvarial defect model was used to evaluate the suitability of the tilapia scaffolds for *in vivo* bone regeneration, based on the protocol adapted from Spicer *et al.* [321]. In our study, a 10 mm defect was created in the calvarial bone of 10 week-old male

Sprague-Dawley rats. The rats (n=36) were divided into three groups: sham (no sample, blank), DTS and CETC. Samples were sterilised in hydrogen peroxide vapour and rinsed in PBS before implantation into the calvarial defect. Samples were harvested at two time points of 14 and 42 days post implantation, with n=6 per group per time point.

At designated time points, the animals were euthanized and the cranium containing the implant was harvested and fixed in 10% formalin (Sigma, USA). The samples were first evaluated using microcomputed tomography (micro-CT) (Shimadzu SMX90-CT, Japan) and images were rendered (VGStudio 3). Thereafter, samples were decalcified in 10% ethylenediamine-tetraacetic acid (EDTA) for 3 weeks to prepare for histology analysis. The paraffin-embedded samples were sectioned along the longitudinal axis into 5 μm thick slides with a microtome (Leica RM2255, Germany), stained with hematoxylin and eosin and observed with light microscopy (Leica DVM6, Germany).

6.2.9 *Acid/alkali treatment of decellularized tilapia skin*

In an attempt to modify the surface properties of the decellularized tilapia skin (DTS), an additional acid or alkali treatment was added to the optimised decellularization protocol reported in section 4.2.2 and 6.2.2. In summary, after freshly obtained tilapia skin was washed in PBS with 1% penicillin/streptomycin, the skin was shaken in 0.025 M ascorbic acid for 15 minutes or 0.5 M sodium hydroxide for 3 hours. The acid or alkali-treated skin was then subjected to the normal decellularization protocol consisting of dispase, SDS and nuclease treatments, following by rinsing and lyophilsation. The acid/alkali treated skin was then characterised with DNA assay (section 4.2.3), collagen assay (section 4.2.3), DSC (section 4.2.10), tensile test (section 4.2.9), water contact angle (section 6.2.3), indirect cytotoxicity (section 5.2.5), human serum based ELISA (section 5.2.4), elastin assay (section 4.2.7) and GAG assay (section 4.2.7).

6.2.10 *In vitro skin regeneration*

Primary human dermal fibroblast (HDF) (Invitrogen, USA) was used in this study. HDF cells were cultured in DMEM + GlutaMAX supplemented with 10% FBS and 1% penicillin-streptomycin. Cells were incubated at 37 °C and passaged every 2-3 days until seeding. Samples were cut into 10 × 10 mm squares, sterilized with 70% ethanol for 2 hours, washed with DMEM and placed into a 24 well plate (Corning, USA). HDF cells were seeded onto the samples at a density of 2×10^4 cells/well. After 1, 3, 5 days, cell proliferation was evaluated by AlamarBlue assay and picogreen assay. The cell morphology and viability was also evaluated by Live/Dead® cytotoxicity kit after 1 and 5 days according to the manufacturer's instructions.

6.2.11 *In vivo skin regeneration*

Animal experiments were approved by NTU-IACUC and conducted in accordance to its guidelines and procedures. The splinted murine wound model was used to evaluate the suitability of tilapia skin for *in vivo* wound healing, based on the method reported by Dunn et al [322]. In our study, two 6 mm full-thickness skin defects were created on the back of 6 week old BALB/c mice. A circular silicone splint with 6 mm inner diameter and 12 mm outer diameter was fixed over the wound with sutures to prevent the wound from contracting. The mice (n=24) were divided into four groups: Native fish skin, decellularized tilapia skin (DTS), decellularized tilapia skin with NaOH treatment (DTS-N), and Duoderm (positive control), an established hydro-colloid dressing used in the management of chronic wounds [323].

Samples were sterilised in hydrogen peroxide vapour and rinsed in PBS before implantation onto the wound. The left defect was left empty as the negative control while the right defect was covered with the sample held in position by the splint. The two wounds were covered with

a transparent dressing. Samples were harvested at two time points of 1 week and 2 weeks post implantation, with n=3 per group per time point.

At designated time points, the animals were euthanized and the splints were removed to reveal the wounds. After photos were taken, the whole area around the wound was harvested *en block* and fixed in 10% formalin. The samples were embedded and sectioned cross-sectionally into 5 μm thick slides with a microtome (Leica RM2255, Germany), stained with hematoxylin and eosin and observed with light microscopy (Leica DVM6, Germany).

6.2.12 *Statistical analysis*

All quantitative data are expressed as mean ± standard deviation and differences between mean values were analyzed using a two-tailed Student's *t* test. A *p* value of less than 0.05 was considered statistically significant.

6.3 Results and discussion

6.3.1 *Water contact angle, porosity and water permeability*

A major factor contributing to the success of a tissue engineering scaffold is the surface properties of the scaffold, as unique microenvironments of the biomaterial surfaces can influence tissue-scaffold interactions and affinities of bioactive molecules on the surface [324]. One surface property that can be easily quantified is the water contact angle, which is a measure of the hydrophilicity of the surface. Beside surface properties, the porosity and permeability of the scaffold is also important factors defining the success of a scaffold, as the scaffold should be micro-porous to transport nutrients and waste products [325]. The water contact angle, porosity and water permeability of CETC and DTS were measured and the results were summarized in Table 6-2.

Table 6-2: Contact angle, porosity and water permeability of CETC and DTS, using Whatman filter paper No. 4 (GE Healthcare, USA) as the control

	Filter paper (control)	CETC	DTS
Contact angle	Water droplet absorbed instantly	Inner: 29.2° ± 2.9° Exposed: 33.9° ± 4.4°	Inner: 54.1° ± 4.5° Outer: 57.0° ± 2.5°
Porosity	35.4 % ± 1.7 %	53.5 % ± 9.4 %	33.5 % ± 2.1 %
Permeability	0.36 ± 0.01 Darcy	$(4.6 \pm 0.5) \times 10^{-5}$ Darcy	$(3.1 \pm 0.6) \times 10^{-5}$ Darcy

The water contact angle is related to the surface tensions at the liquid-vapour, solid-vapour and solid-liquid interfaces. A low contact angle represents a stronger attraction between the liquid (water) and the solid surface, meaning that the surface is more hydrophilic. For biomaterials, surfaces with a contact angle of more than 90° are generally defined as hydrophobic. The results show that CETC and DTS are hydrophilic as their contact angles are all below 90°. As hydrophilic surfaces tend to better support cell attachment, it was predicted that CETC would support cell attachment better than DTS. There was a slight difference between the two sides of CETC because the crosslinking took place when the electrospun membrane was still attached

to the collector plate, leading to the exposed side being more crosslinked than the inner side. Before decellularization, the outer surface of fresh tilapia skin has a contact angle of as high as 90° (experimental value = 90.4° ± 3.2°) which helps to repel impurities and microorganisms when the fish is in water. After decellularization, the contact angle dropped to 57°, as the decellularization removed the hydrophobic epidermal layer from the skin.

From the porosity results, it was observed that CETC was relatively porous, having more of their volume as void spaces, while DTS is relatively compact. In DTS, the low porosity is most likely be due to the compact stacking of the collagen layers, as observed in the SEM images of DTS (Figure 4.3 C & D). The high porosity values for CETC may be due to the higher hydrophilicity of the collagen, as deduced from the contact angle results. The high hydrophilicity may lead to more retention of ethanol, which is a polar solvent and is attracted to hydrophilic surfaces. A non-polar liquid may reduce the effect of liquid-material attraction, but its high volatility may lead to inaccurate readings during the weighing step.

From the water permeability results, CETC and DTS had very low permeability, compared to the control (filter paper). From the SEM images in Figure 4.3, DTS appeared to have stacked layers of tightly packed collagen fibres. This tight packing of the collagen fibres in each layer and the stacking of multiple such layers contribute to the low permeability. On the other hand, although electrospinning usually produces porous membranes, the permeability of CETC was low presumably because of the effect of cross-linking, which caused the fibres to contract and merge, making the material less permeable. Although a low permeability may affect nutrient diffusion, it is a benefit in applications where water retention and the maintenance of a moist environment is desired, such as skin wound healing [326]. A low permeability is also desirable in applications where the purpose of the scaffold is to prevent penetration of cells and/or microbes, such as guided bone regeneration [309].

6.3.2 *Degradation*

The degradation rates of CETC and DTS were evaluated and compared after the samples were incubated in PBS or 200 U/ml collagenase at 37 °C (Figure 6.1).

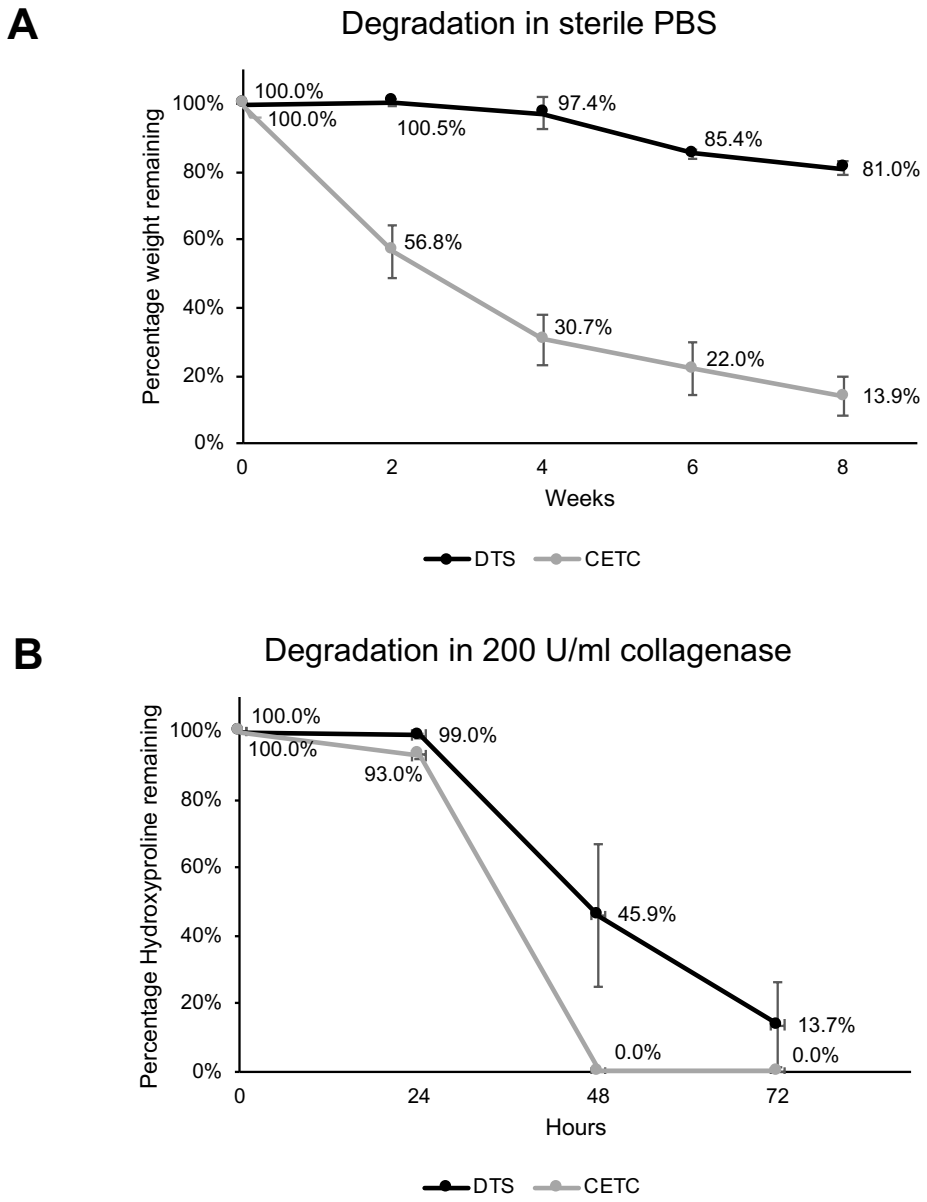

Figure 6.1: Degradation profile of DTS and CETC in (A) sterile PBS and (B) 200 U/ml collagenase. Samples were incubated in individual sterile tubes at 37°C and the dry weight or hydroxyproline content of each sample was measured before and after the incubation.

The degradation rate of DTS was evaluated and compared with CETC by two methods. In the first method where samples were incubated in sterile PBS at 37°C (Figure 6.1A), DTS samples

retained (97.4 ± 4.7) % after 4 weeks and (81.0 ± 2.1) % of their weight after 8 weeks, while CETC samples only retained (30.7 ± 7.4) % of their weight after 4 weeks and (13.9 ± 6.0) % of their weight after 8 weeks. In the second method where samples were incubated in 200 U/ml collagenase (Figure 6.1B), DTS samples retained (99.0 ± 1.0) % after 24 hours, (45.9 ± 21.1)% after 48 hours and (13.7 ± 12.6) % of their weight after 72 hours, while CETC samples only retained (93.0 ± 1.1) % of their weight after 24 hours and negligible amount of the samples remained after 48 hours.

If the degradation profiles of the 2 materials were compared with their mechanical strength, a trend was observed where a material with higher mechanical strength had a slower degradation. One explanation is that a material with higher mechanical strength had a more tightly packed and more crosslinked structure, which takes a longer time to break down. The compactness of the collagen fibres, observed in the SEM images of DTS (Figure 4.3), is one factor that contributed to the slow degradation rate of DTS in PBS. However, in the presence of collagenase, DTS degrades rapidly. We hypothesized that the tightly packed collagen fibres are resistant to hydrolysis and the low water permeability of the outer layers protects the inner layers from bulk degradation. On the other hand, collagenase causes the collagen fibres on the outer layer to break up and separate, thus exposing the inner layers to further degradation. The collagenase concentration in this study is much higher than the actual concentration in real physiological conditions [327], but it allowed us to accelerate the biodegradation and observe the effects in a shorter time.

In guided bone regeneration, current collagen-based membranes exhibit good biocompatibility but have the problem of easy collapse and rapid degradability in vivo, compromising the formation of new bone tissue [311]. Ideally, a GBR membrane should last for more than 6 months to support new bone formation and maturation, but Bio-Gide®, a commercial porcine

collagen membrane, was shown to lose 60% of its initial collagen content at 4 weeks and 80% at 9 weeks after implantation in Wistar rat calvarial defects [56]. A study to implant two layers of Bio-Gide® to control its degradation has also been attempted but the degradation rate was similar to that of one layer [328]. From the results of this project, DTS appears to be a promising material for GBR due to its slow degradation, but further studies are needed to determine the long term *in vivo* biodegradability of DTS.

6.3.3 *In vitro bone regeneration*

In tissue engineering, the scaffold plays an important role due to its effect on cell behaviour. One major requirement of any tissue engineering scaffold is biocompatibility, which is the ability to support normal cellular activity without any toxic effects to the host tissue [329]. The biocompatibility of DTS and CETC to osteogenic cells were evaluated using MC3T3-E1 cells, an immortalized pre-osteogenic cell-line derived from murine calvaria and commonly used to assess *in vitro* osteogenic development [330].

The ability of MC3T3-E1 cells to adhere onto the surface of DTS and CETC was evaluated qualitatively by SEM on Day 1, Day 3 and Day 7 (Figure 6.2A). SEM images showed the cells could attach well to both membranes by Day 1 and a 'layer' of cells can be observed after 1 week. The proliferation of the cells was also evaluated quantitatively on Day 7, 14 and 21 by AlamarBlue assay (Figure 6.2B), which showed increasing cell metabolic activity from Day 7 to Day 14. Cells grown on DTS showed higher metabolic activity than cells on the blank (polystyrene well plate) on Day 14 and 21, while cells grown on CETC were metabolically more active than cells grown on DTS and the blank at all time points. The SEM images and metabolic data indicated that the DTS and CETC membranes are able to promote MC3T3-E1 attachment and the cells remain metabolically active for up to 3 weeks.

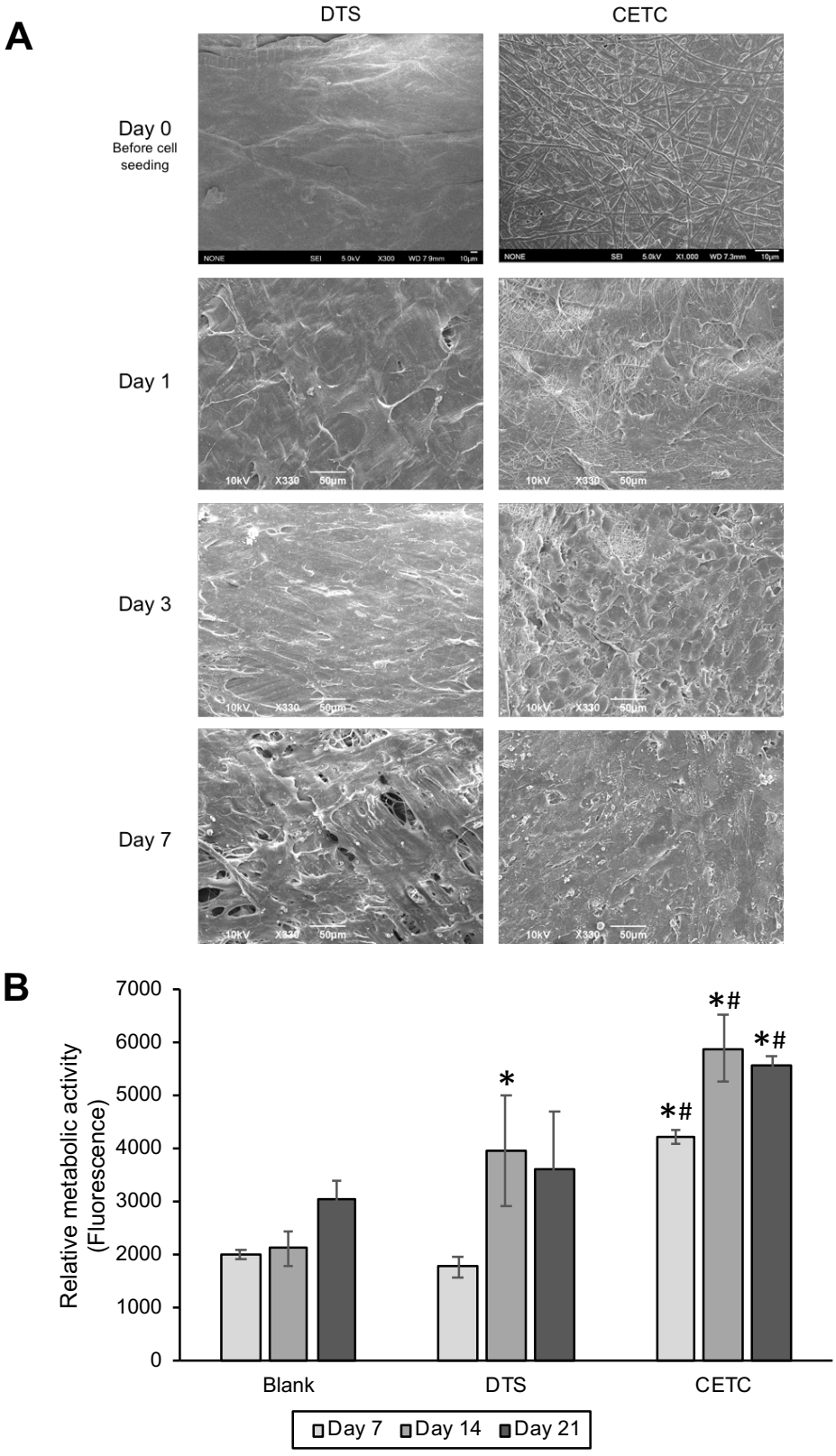

Figure 6.2: Cell attachment and proliferation were evaluated at Day 1, 3 and 7 after MC-3T3 cells were seeded onto the different membranes. (A) Scanning electron microscopy of membrane surfaces. Micrographs are respective of each sample. (B) AlamarBlue assay with fluorescence as an indication of metabolic activity. Blank = polystyrene well plate. * $p < 0.05$ when compared to blank at each respective time point. $^{\#}$ $p < 0.05$ when compared to DTS at each respective time point. DTS- Decellularized tilapia skin; CETC- Cross-linked tilapia collagen.

To assess the osteogenic differentiation of MC3T3-E1 cells on DTS and CETC membranes, gene expression involved with osteogenesis (*BSP*, *OC*, and *OPN*) was determined by performing quantitative RT-PCR on the cells cultured for 21 days. In osteogenic media, MC3T3-E1 cells would undergo osteogenic differentiation, which involves the phases of proliferation, maturation and mineralization [331]. These phases could be identified by the up-regulation of osteogenic genes, the increased production of osteogenic proteins, and the production of mineralized matrix [330]. Among the various osteogenic genes, BSP, OC and OPN were used as markers to investigate osteogenic differentiation in this study. Bone sialoprotein (BSP) facilitates the crystallization of hydroxyapatite in mineralized matrix [332]. Osteocalcin (OC) binds calcium in mineralized matrix and is used as a late-stage marker of osteogenic differentiation [333]. Osteopontin (OPN) facilitates the attachment of osteoblasts and osteoclasts to the ECM [334].

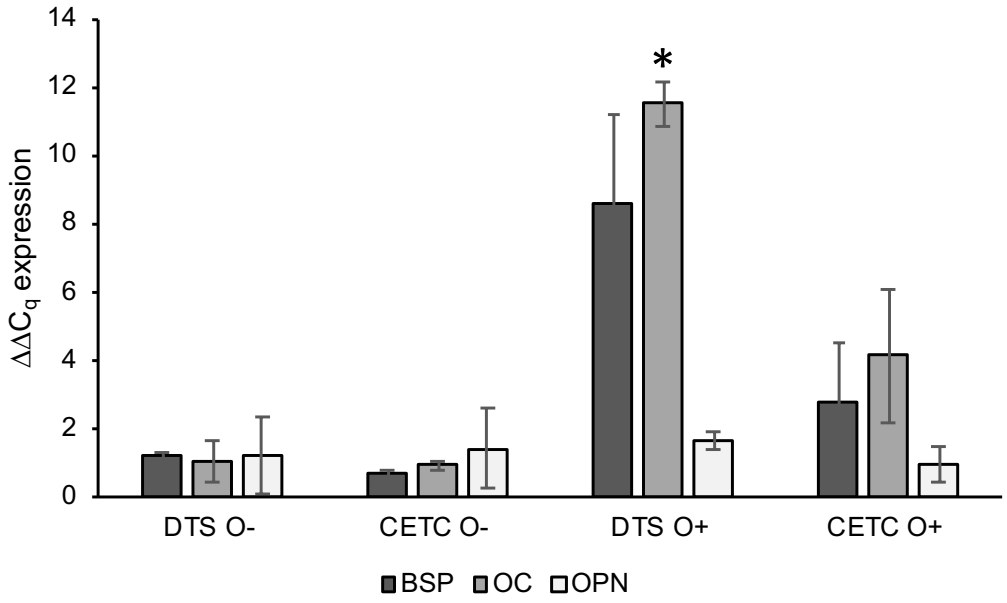

Figure 6.3: RT-PCR of genes related to osteogenic differentiation – BSP, OC and OPN, normalised to the expression of GAPDH. MC-3T3 cells were grown on the membranes and the relative expression of mRNA was quantified at Day 21. * $p < 0.05$ when compared to cells grown in normal growth media (O-). BSP = Bone sialoprotein, OC = osteocalcin, OPN = osteopontin, GAPDH = Glyceraldehyde 3-phosphate dehydrogenase

From the RT-PCR results, basal levels of gene expression were observed for cells grown in non-osteogenic media (O-) but an increased expression of BSP and OC could be observed for cells grown on both DTS and CETC in osteogenic media (O+). Remarkably, DTS induced a 7-fold and 11-fold increase in the expression levels of BSP and OC. On the other hand, we did not observe an increase in expression of OPN. We hypothesized that the expression of OPN only occurs in the early stages of osteogenic differentiation due to its role of facilitating the attachment of osteoblasts.

To further verify the osteogenic differentiation of cells on different substrates, Von Kossa staining and calcium assay were performed to visualize and quantify the mineral deposition by MC3T3-E1 cells. Von Kossa staining, which indicates the presence of hydroxyapatite, was performed on the samples on Day 7, Day 14 and Day 21 to allow visualization of mineralization nodules. The images (Figure 6.4A) showed an observable increase in the mineralization over time. At Day 14, DTS showed some mineralization nodules while CETC was observed to have more. At Day 21, there was an increase in mineralization nodules for both membranes with those on CETC covering almost the entire membrane.

The calcium deposition was also quantitatively analysed on Day 14 and 21, and normalized against the DNA content to account for the variation in cell numbers. From the graph (Figure 6.4B), calcium deposition was observed at Day 14 and increased proportionally at Day 21 on both membranes incubated in osteogenic differentiation media, while little calcium deposition was observed on membranes incubated in normal growth media. In fact, the osteogenic differentiation media induced significantly higher calcium deposition ($p < 0.005$) than normal growth media at all time points for both membranes, and the proportional increase of calcium deposition observed in the quantitative data is in alignment with the Von Kossa results (Figure 6.4A).

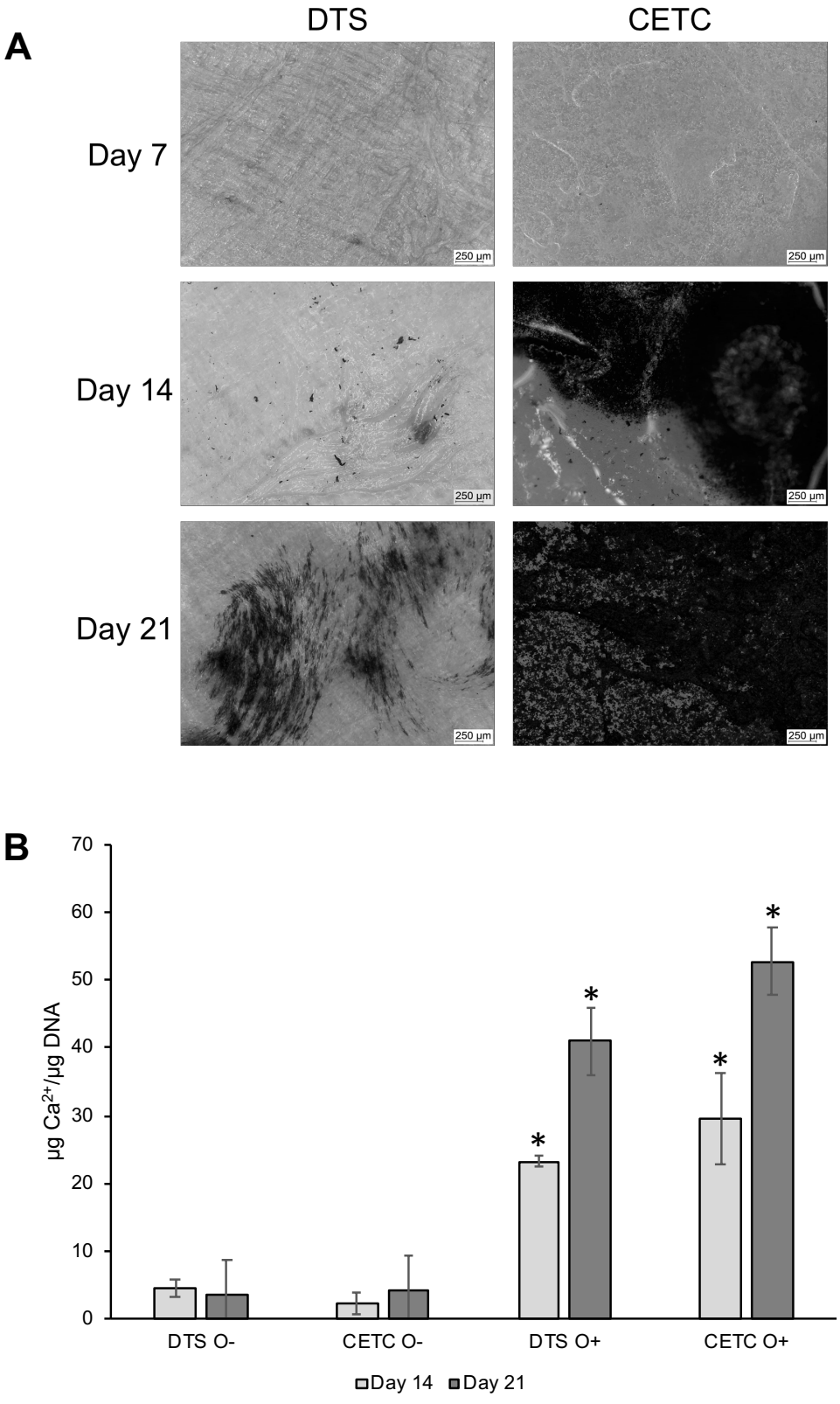

Figure 6.4: The calcium deposition by MC-3T3 cells on DTS and CETC were evaluated after seeding and incubation in osteogenic medium. (A) Samples were Von Kossa stained at Day 7, 14 and 21. Areas that appear dark indicate the presence of phosphate and suggest calcium deposition. (B) Calcium depositions from MC-3T3 cells were quantified and normalized against DNA content at Day 14 and Day 21. The calcium content were compared between cells grown in normal growth media (O-) and cells grown in osteogenic differentiation media (O+). * $p < 0.05$ when compared to cells grown in normal growth media (O-) at same time-point.

We observed an increase of stained areas on both DTS and CETC in Von Kossa staining, and an increase of calcium content over time in the calcium assay. This indicated that the MC3T3-E1 cells underwent differentiation and mineral deposition on both DTS and CETC in osteogenic media, in agreement to the RT-PCR data. There is no mineralization in the normal growth media (O-), indicating that the materials do not induce osteogenic cellular differentiation automatically. Interestingly, mineralization nodules were observed as localized patches on DTS but appeared continuously and extensively on CETC. Collagen molecules contain some functional peptide sequences such as Arg-Gly-Asp (RGD) which can promote cell proliferation and differentiation [335]. We hypothesized that in CETC, the collagen molecules are separated and dispersed randomly, causing the functional peptide sequences to be homogenously distributed and exposed. Hence the osteogenic differentiation and mineral deposition occurred uniformly across the membrane. In DTS, the collagen molecules are bundled together and crosslinked tightly in the ECM with other structural molecules, hence only some of the functional peptide sequences are exposed, leading to localised osteogenic differentiation on the exposed collagen bundles.

6.3.4 *In vivo bone regeneration*

As the aim of this study is to evaluate the suitability of DTS and CETC for guided bone regeneration, an appropriate animal model is necessary to simulate a physiological bone defect and evaluate the therapeutic effects of our sample materials. Critical size defects (CSDs) in small animals are commonly used in preclinical studies due to the reproducibility of the defect's shape and size, and feasibility of operation and evaluation [336]. A CSD is defined by Schmitz and Hollinger as "the smallest size defect which will not heal on its own during the lifetime of the animal" and its size is dependent on the animal species used [337]. Rats are one of the most common model for CSDs due to their manageable size, fast healing time and

relatively low cost [338], and the rat calvarial model was chosen in this study to evaluate the *in vivo* performance of our scaffolds.

As the generally accepted size for rat calvarial defect is 8 mm [321], we chose a defect of 10 mm to ensure that the defect would not heal on its own. After the creation of a 10 mm critical defect in the rats, the membranes were placed to cover the defect (Figure 6.5). At Day 14 (2 weeks) and 42 (6 weeks), the rats were sacrificed and the extent of new bone formation was examined. To evaluate DTS and CETC for bone regeneration *in vivo*, we used microcomputed tomography (micro-CT) and H&E histology to visualise the volumetric and spatial density of mineralized tissue in the defect.

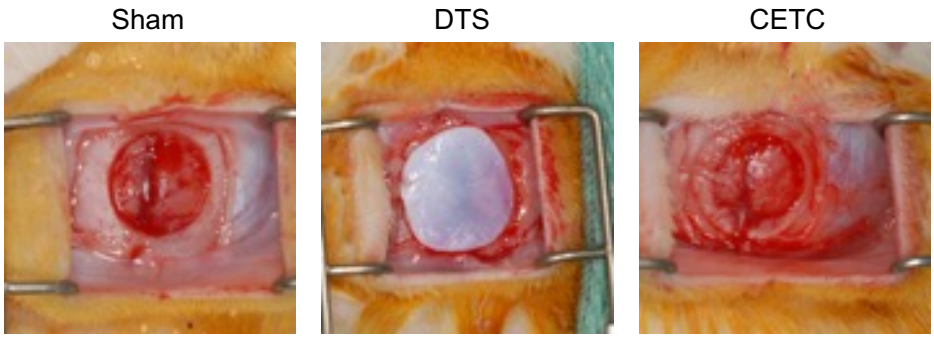

Figure 6.5: Rat calvarial defects (10mm) with test membranes. DTS – decellularized tilapia skin; CETC – cross-linked electrospun tilapia collagen.

Micro-CT was performed to obtain 3D rendering of the calvarial defect site (Figure 6.6). The sham, DTS and CETC groups had minimal bone regeneration at Day 14 post-surgery (Figure 6.6A). After 42 days, the images revealed varying degrees of bone union with the sham group being the poorest while the DTS and CETC having observable bone coverage at the defect site. To better classify these observations, we used a scoring system of 1 (no bone formation) to 4 (bony bridging covering defect at largest length) that has been previously reported [339]. The animals from the DTS and CETC group had higher scores than the sham group at Day 42, indicating that the membranes promote bone formation (Figure 6.6B).

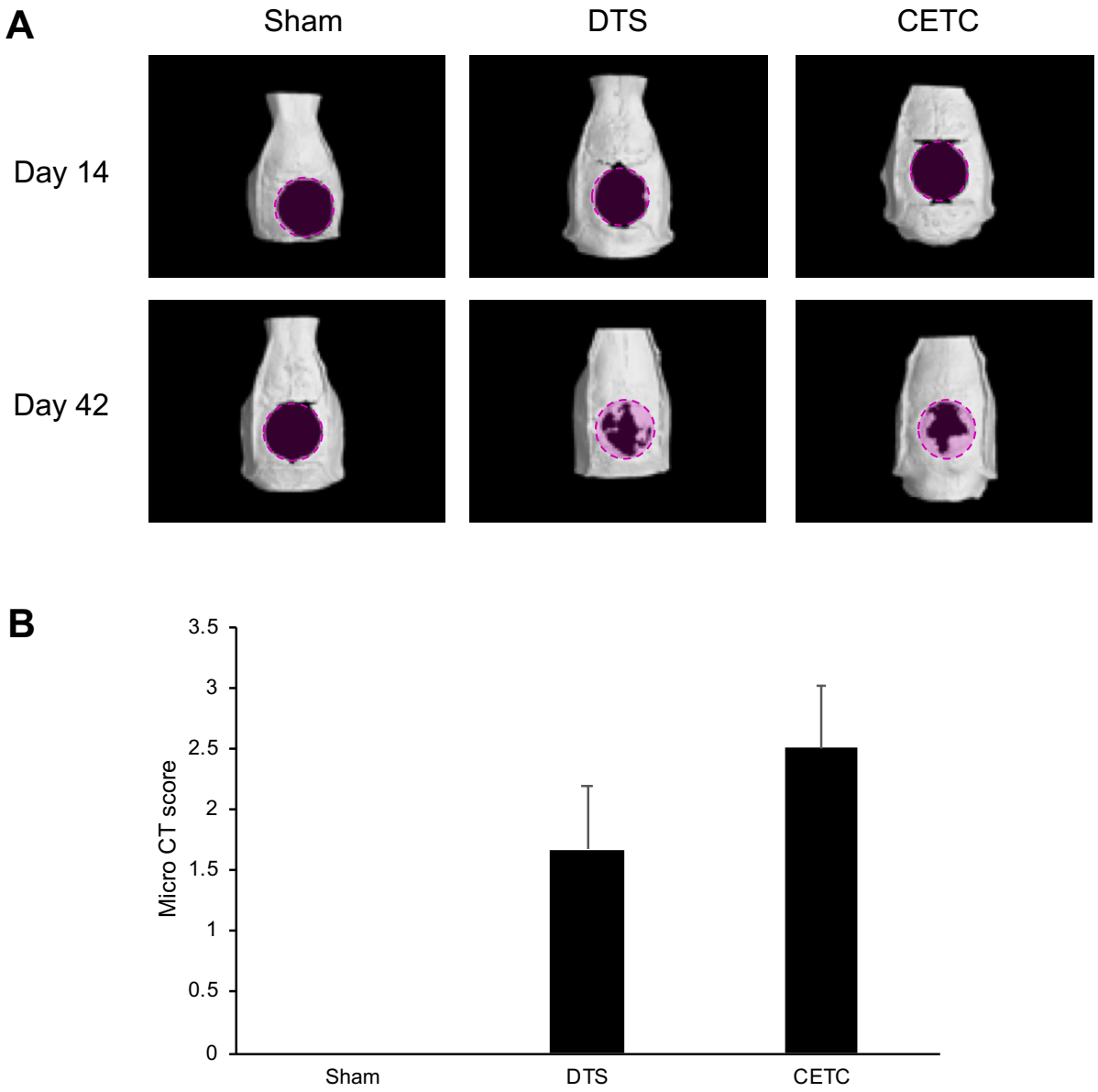

Figure 6.6: Micro-CT analysis of the calvarial defects treated with different membranes at Day 14 and 42. (A) Reconstruction of the defects using micro-CT taken at Day 14 and 42 for each of the test samples. Dotted circle represents initial defect diameter of 10mm, pink colour represents regenerated bone. Images shown here are representative of the samples. (B) Scoring of extent of bone union on the calvarial defects (n=6 per group) after 42 days. Scoring: 0– No bone formation within defect; 1– Few bony spicules dispersed through defect; 2– Bony bridging only at defect borders; 3– Bony bridging over partial length of defect; 4 – Bony bridging entire span of defect at longest point (10 mm) [339]

Figure 6.7 shows an overview of histological sections of different groups after 2-week implantation. Surgical created margin of bone plate is visible as a cement line where newly formed bone and original bone meet. In the control group (Sham) the defect area was mainly occupied by unsupported soft tissues (Figure 6.7A). Dura mater was extruding from defect area and adherent to the soft tissue originating from skin side. Very limited bony matrix can be

found along the surgically created defect margin. For the DTS group, stratified structure of the residual DTS was present within the defect (Figure 6.7B). There is obvious infiltration of lymphocytes and plasma cells in the cerebral side of the defect. At the skin side of the defect, it is filled with structured fibro-collagenous stroma with less inflammatory cells but without obvious mineralized matrix. For the CETC group, in 4 out of 6 samples, unsupportive fibrous connective tissue was present in the defect without obvious mineralized matrix (Figure 6.7C). Notable infiltration of lymphocytes and plasma cells was present in the area of defect as well. In 2 samples from the CETC group, the defect was filled with maturing woven bone structure at the cerebral side. Lining osteoblasts present surround the mineralized osteoid. There is inflammatory cell infiltrate in the soft tissue with presence of dark stained multinucleate cells.

Figure 6.8 shows an overview of histological sections of different groups after 6-week implantation. In the control group (Sham) the defect area was still occupied by unsupported soft tissues and exhibited no sign of tissue regeneration (Figure 6.8A). For the DTS group, similar to the 2-week results, the presence of stratified structure of the residual DTS within the defect is consistent among all samples in the group (Figure 6.8B). There is now a lower density of cells due to the subsided acute cellular response including lymphocytes and plasma cells, especially at the cerebral side of the defect. Instead, the population of cells now contain an elevated level of macrophages, multinucleated cells and active fibroblasts. Some samples from this group showed island shape matrix deposition which could be found in between the stratified collagen structure. For the CETC group, unsupportive fibrous connective tissue is present in the defect (Figure 6.8C). Newly formed bone was observed with more mature structure on the cerebral side than the skin side. Grey stratified residual material could be found in the defect area, with bone matrix. The residual stratified material is still present at one side of bone margin, which is surrounded by inflammatory (neutrophilic, histiocytic, multinucleated) cells.

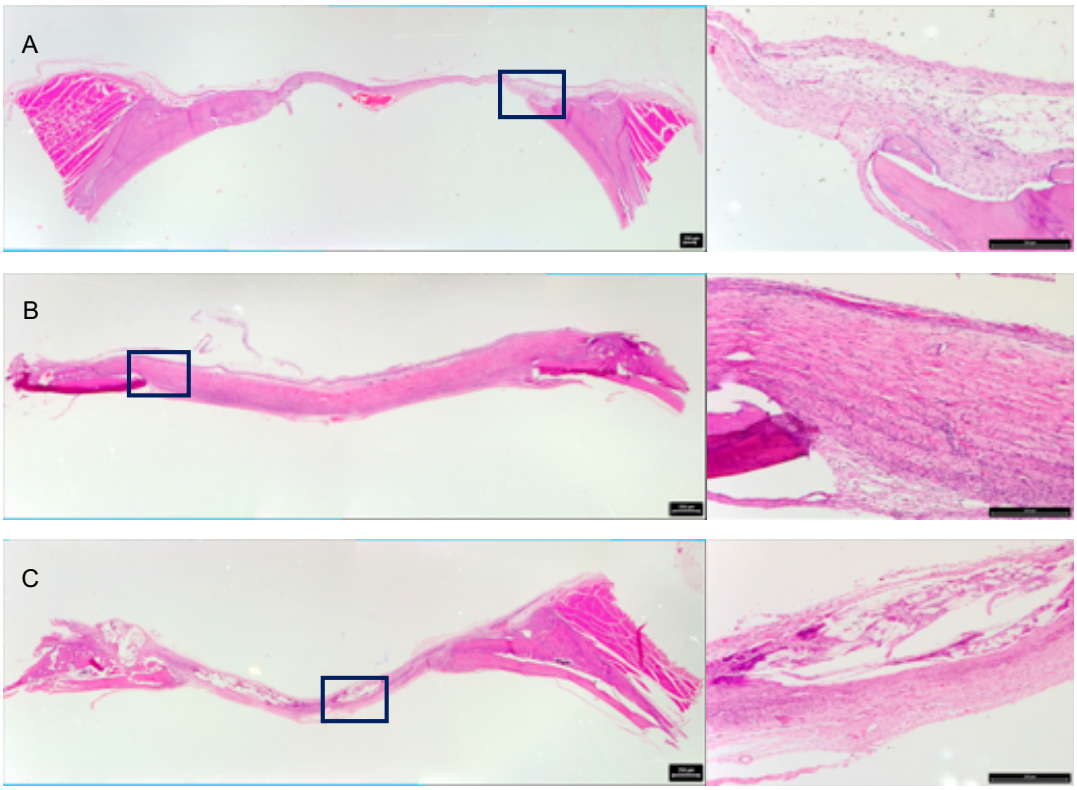

Figure 6.7: H&E staining of cross section of the defect site at Day 14. A) Sham, B) DTS, decellularized tilapia skin C) CETC, cross-linked electrospun tilapia collagen. The region of interest is indicated by a black box and is magnified. Scale bar represents 250µm

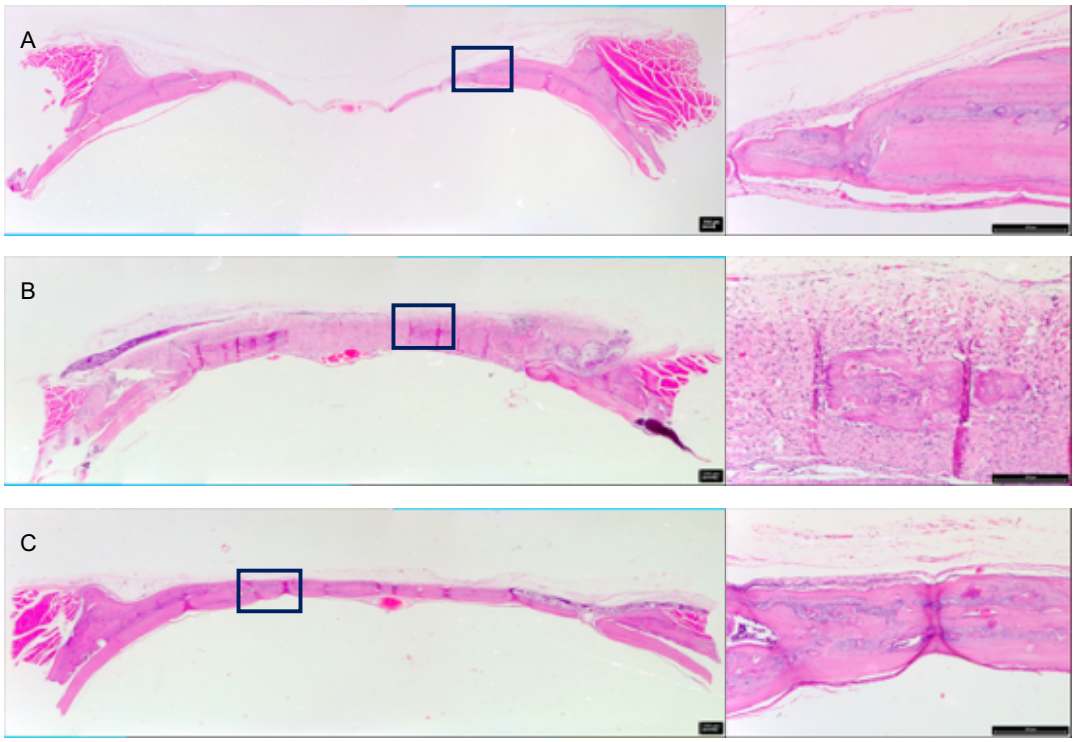

Figure 6.8: H&E staining of cross section of the defect site at Day 42. A) Sham, B) DTS, decellularized tilapia skin C) CETC, cross-linked electrospun tilapia collagen. The region of interest is indicated by a black box and is magnified. Scale bar represents 250µm

In normal bone healing, tissue regeneration generally occurs in the defect in three phases: hematoma formation, where extracellular matrix is produced by mesenchymal, endothelial and immune cells; soft callus phase, where osteogenic progenitor cells migrate to the defect; and hard callus phase, where mineralization and bone maturation occurs [338]. At Day 14 post-surgery, no mineralized tissues were observed for all samples, suggesting that the defects were still in the hematoma formation phase and soft callus phase, where newly formed cartilage and fibrous tissues were abundant and mineralization had not started. Interestingly, osteoblasts and mineralized osteoids were observed in some defects in the CETC group, indicating that CETC catalyses the migration of osteoblasts to the defect and supports osteoinduction.

At Day 42 post-surgery, a reduction of immune cells in all samples indicated that the hematoma formation phase had ended and the defect was filled with newly formed extracellular matrix from the host. For the DTS and CETC groups, the appearance of mineralized tissues along the defect edge in the micro-CT images and the presence of island shape matrix depositions in the histology images suggested that tissue regeneration has progressed to the hard callus phase, where osteoblasts had migrated to the defect and initiated mineralization to form new bone. In DTS, the matrix deposition occurred within the stratified collagen structure, indicating that DTS was degrading to allow cells to migrate into the interior of DTS, and the biocompatible environment within DTS promoted the formation of new matrix by osteoblasts. However, in the CETC group, fibrous connective tissues were observed in addition to the newly formed bone. Given that the degradation rate of CETC was rapid (Figure 6.1), it was likely that the CETC managed to prevent epithelial cell ingrowth and support osteoinduction in the first 2 weeks, but degraded *in vivo* between 2 weeks and 6 weeks, allowing external fibroblasts to enter the defect site and form fibrous tissues. Alternatively, the fibrous tissues may be formed as an immune response to the CETC from the host's immune system. Nevertheless, the DTS

and CETC groups exhibited superior performance to the empty group where minimal or no mineralization was observed.

The role of a barrier membrane in guided bone regeneration (GBR) is to prevent the entry of epithelial cells into the bone defect and provide mechanical support and promote osteoinduction in the defect space. This requires the barrier membrane to be thermally stable at the recipient's body temperature, possesses sufficient mechanical strength, be permeable to nutrients but not to cells; and have a controlled degradation rate where the membrane degrades at the same rate of host tissue regeneration [309, 311]. We have demonstrated that DTS and CETC have high thermal stability, low permeability, and good biocompatibility. DTS has an advantage of high mechanical strength and slow degradation rate, while CETC exhibited better *in vitro* osteogenic support than DTS but has a limitation of poor mechanical strength and fast degradation. To overcome the limitations of DTS and CETC, the two membranes could be combined to form a bi-layer membrane for GBR, where DTS provides mechanical support to the defect space and prevents the entry of fibroblasts and microbes, while CETC provides a biocompatible surface for osteogenic cell adhesion and proliferation and supports osteoinduction. The outer DTS layer would also protect the inner CETC from rapid degradation, allowing the CETC layer to serve its function for a longer time. We proposed to develop and evaluate this bilayer membrane for GBR in our future work.

6.3.5 *Acid/alkali treatment of decellularized tilapia skin*

In previous sections, DTS was reported to be biocompatible to murine fibroblasts L929 and murine osteogenic cells MC3T3-E1, but when compared to CETC, DTS appeared to be less biocompatible. In summary, DTS was found to be inferior to CETC in terms of immunogenic potential, *in vivo* immune responses, cellular biocompatibility to MC3T3-E1 cells, mineralization of MC3T3-E1 cells, and *in vivo* bone regeneration. One possible explanation

for the inferior biological performances of DTS was its relatively higher water contact angle compared to CETC. As hydrophilic surfaces have been reported to be more biocompatible [324], it was hypothesized that a reduction of water contact angle of DTS would improve its biocompatibility. Another possible explanation for the inferior biological performances of DTS was the presence of antigens. Despite a drop of 57.4% in immunogenic potential after decellularization, there was still a substantial amount of antigens remaining in DTS. Hence, it was hypothesized that a further reduction of immunogenic potential would improve the biocompatibility of DTS.

To reduce the water contact angle and immunogenic potential, an additional step was added into the decellularization protocol. The tilapia skin was subjected to 0.025 M ascorbic acid for 15 minutes or 0.5 M sodium hydroxide for 3 hours, before being processed according to the optimized protocol reported previously. Ascorbic acid was chosen due to its antioxidant properties and its ability to improve cellular biocompatibility [340], and sodium hydroxide was chosen due to its ability to dissociate non-collagen proteins and its established role as a sanitization agent of chromatography columns [341, 342]. The acid-treated skin was labelled as DTS-A and the alkali-treated skin was labelled as DTS-N. The effects of the additional acid/alkali treatment on the physical and biological properties of DTS were investigated and presented in Table 6-3.

The results indicated that, while an additional treatment of ascorbic acid or sodium hydroxide did not affect the DNA removal rate, the ascorbic acid treatment significantly reduced the collagen content in the tissue. In fact, the duration of the ascorbic acid treatment was limited to 15 minutes and the concentration was limited to 0.025 M, because when the duration exceeded 20 minutes or when the concentration was 0.05 M and above, the tilapia skin disintegrated into a gel-like substance. As collagen solubilises rapidly in acidic conditions, the

presence of ascorbic acid might have caused the collagen in the tilapia skin to solubilise, leading to a reduction of collagen content in the skin. The loss of collagen also explained the huge loss in mechanical strength of DTS-A, although the denaturation temperature and water contact angle were not significantly affected.

Table 6-3: Physical, chemical and biological properties of native tilapia skin, DTS, DTS-A and DTS-N. * $p < 0.05$ when compared to DTS. TS = tilapia skin, DTS = decellularized tilapia skin, DTS-A = ascorbic acid treated decellularized tilapia skin, DTS-N = sodium hydroxide treated decellularized tilapia skin.

Property	Native TS	DTS	DTS-A	DTS-N
DNA content (ng/mg tissue)	419.9 ± 109.5	6.3 ± 0.9	6.3 ± 2.5	7.0 ± 1.1
Collagen content (µg/mg tissue)	522.9 ± 45.0	362.5 ± 35.6	166.7 ± 130.1 *	339.2 ± 50.9
Denaturation temperature (°C)	68.1 ± 1.0	64.2 ± 0.6	62.1 ± 3.3	62.8 ± 1.1
Maximum tensile stress (MPa)	28.4 ± 4.4	24.0 ± 10.2	0.39 ± 0.37 *	4.7 ± 2.1 *
Young's Modulus (MPa)	69.4 ± 24.6	56.2 ± 14.4	1.5 ± 2.1 *	30.0 ± 12.0
Water contact angle (outer surface)	90.4° ± 3.2°	57.0° ± 2.5°	50.7° ± 6.3°	59.8° ± 9.1°
Indirect cytotoxicity (relative metabolic activity of L929, 100% = non-toxic control)	107.6 % ± 5.1 %	103.1 % ± 7.0 %	60.0% ± 5.5 % *	101.7 % ± 14.2 %
Immunogenic potential (determined by human-serum ELISA, 100% = native tilapia skin)	100.0 % ± 7.9 %	42.6 % ± 3.1 %	Not measured	35.3 % ± 2.1 %
Elastin content (µg/mg tissue)	59.4 ± 4.6	5.3 ± 1.2	Not measured	5.2 ± 3.2
GAG content (µg/mg tissue)	3.9 ± 0.1	2.2 ± 0.1	Not measured	2.0 ± 0.5

From the indirect cytotoxicity results, DTS-A had a 40% reduction of relative metabolic activity compared to native tilapia skin. According to ISO-10993-5, a reduction of more than 30% in the relative metabolic activity means that the material is cytotoxic [235]. The cytotoxicity was presumed to be contributed by residual ascorbic acid in the treated skin, as ascorbic acid was reported to react with DMEM (the medium used for the culture of L929 cells) to generate hydrogen peroxide that induces apoptosis in cells [343]. As the ascorbic acid treatment greatly reduced the collagen content and mechanical strength, and induced *in vitro* cytotoxicity, DTS-A was removed from subsequent evaluations.

On the other hand, the sodium hydroxide treatment did not adversely affect the properties of tilapia skin. The collagen content, denaturation temperature, water contact angle and indirect

cytotoxicity did not experience a significant change after the skin was exposed to 0.5 M sodium hydroxide for 3 hours. 0.5 M sodium hydroxide has an additional advantage of removing pathogens from the tilapia skin, as 0.5 M sodium hydroxide is a validated sanitization agent for protein-based affinity chromatography columns [341, 342] and is effective in the inactivation of viruses [344]. However, sodium hydroxide was reported to reduce mechanical properties in decellularized tissues due to the cleavage of collagen fibrils and disruption of collagen crosslinks [97], which explained the drop of maximum tensile stress from 24.0 ± 10.2 MPa in DTS to 4.7 ± 2.1 MPa in DTS-N. Nevertheless, the loss of mechanical properties in DTS-N was not as drastic as that in DTS-A and the collagen content in DTS-N was similar to that in DTS, suggesting that the collagen molecules did not solubilise in the sodium hydroxide treatment and most of the collagen molecules were retained in DTS-N. Contrary to our belief, the sodium hydroxide treatment did not reduce the water contact angle of the skin, suggesting that the surface chemistry and hydrophilicity of the skin were not affected by the sodium hydroxide treatment. The elastin content and GAG content in DTS-N were also observed to be similar to those in DTS, indicating that elastin and GAG were not affected by the sodium hydroxide treatment and the decline in elastin and GAG contents was most likely contributed by the SDS treatment.

Interestingly, the sodium hydroxide treatment led to a further reduction in the immunogenic potential. As sodium hydroxide was known to remove non-collagenous proteins from tissues [345], it was likely that some antigens were removed by the sodium hydroxide treatment. In subsequent experiments, the biological performances of native tilapia skin, DTS and DTS-N would be evaluated and compared to investigate the effect of 2 decellularization protocols on tilapia skin.

6.3.6 *In vitro skin regeneration*

In the skin, fibroblasts and keratinocytes are two key types of cells responsible for maintaining skin homeostasis and for orchestrating skin tissue regeneration [346, 347]. Fibroblasts, in particular, serve an important role in forming ECM components and secreting proteinases and proteinase inhibitors to remodel the ECM [347]. In damaged tissues, fibroblasts become activated and differentiate into myofibroblasts, which generate contractions and produce ECM proteins to facilitate wound closure [348]. Therefore, scaffolds intended for wound healing and skin regeneration should possess low cytotoxicity and good biocompatibility towards fibroblasts. In this study, primary human dermal fibroblasts (HDFs) were used to evaluate the cellular biocompatibility of tilapia skin to skin cells. AlamarBlue assay was performed to investigate the cell attachment and proliferation of HDFs on native tilapia skin, DTS (decellularized tilapia skin), and DTS-N (alkali-treated decellularized tilapia skin).

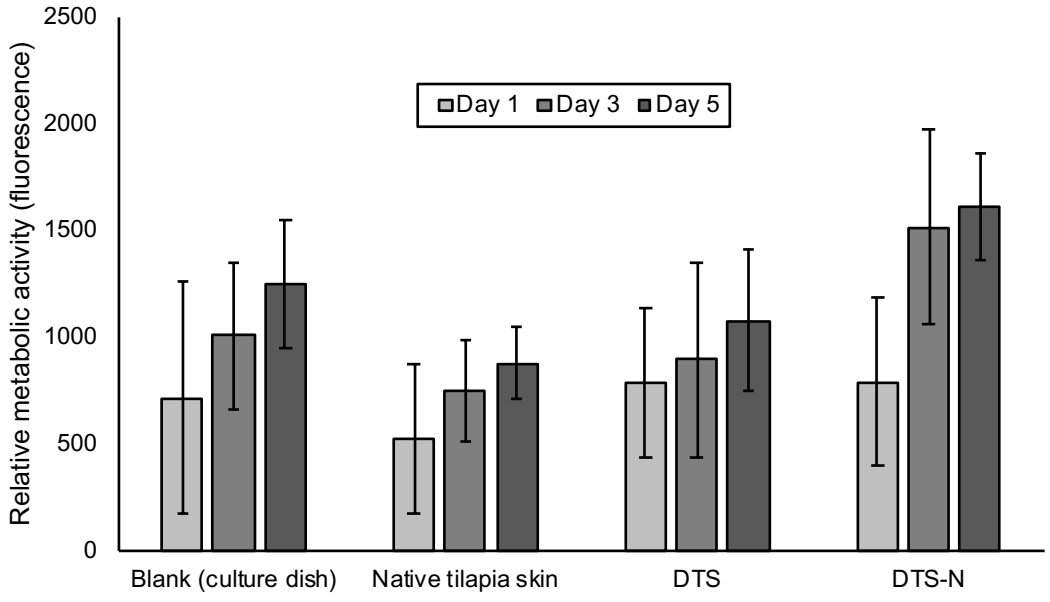

Figure 6.9: Cell attachment and proliferation were evaluated with AlamarBlue assay at Day 1, 3 and 5 after human dermal fibroblasts (HDFs) were seeded onto tilapia skins treated in different conditions. The fluorescence level was used as an indication of relative metabolic activity of HDFs. Blank = polystyrene well plate. No significant difference ($p < 0.05$) were observed between groups at each time point and between time points for each group. DTS = Decellularized tilapia skin; DTS-N = Alkali-treated decellularized tilapia skin.

The ability of HDFs to adhere onto the native tilapia skin, DTS and DTS-N was evaluated quantitatively by AlamarBlue assay on Day 1, Day 3 and Day 5 (Figure 6.9), and qualitatively by Live/Dead® cytotoxicity kit (Figure 6.10). Live/dead stained images showed that the HDFs were able to attach to all three skin samples and had high viability on Day 5, as indicated by the numerous live cells dyed green by calcein-AM and the low number of dead cells dyed red by ethidium homodimer-1. Some areas were stained red in the live/dead images of native tilapia skin, because of the presence of residual tilapia DNA in the untreated skin. After staining, the HDFs were observed to be spindle-shaped, indicating good cell attachment and favourable cellular biocompatibility of the surface. (On incompatible or toxic surfaces, fibroblasts would not attach well and would appear rounded.) For DTS on Day 1, no cells were observed, suggesting that the cells had not attached securely to the skin and were washed away during the staining steps.

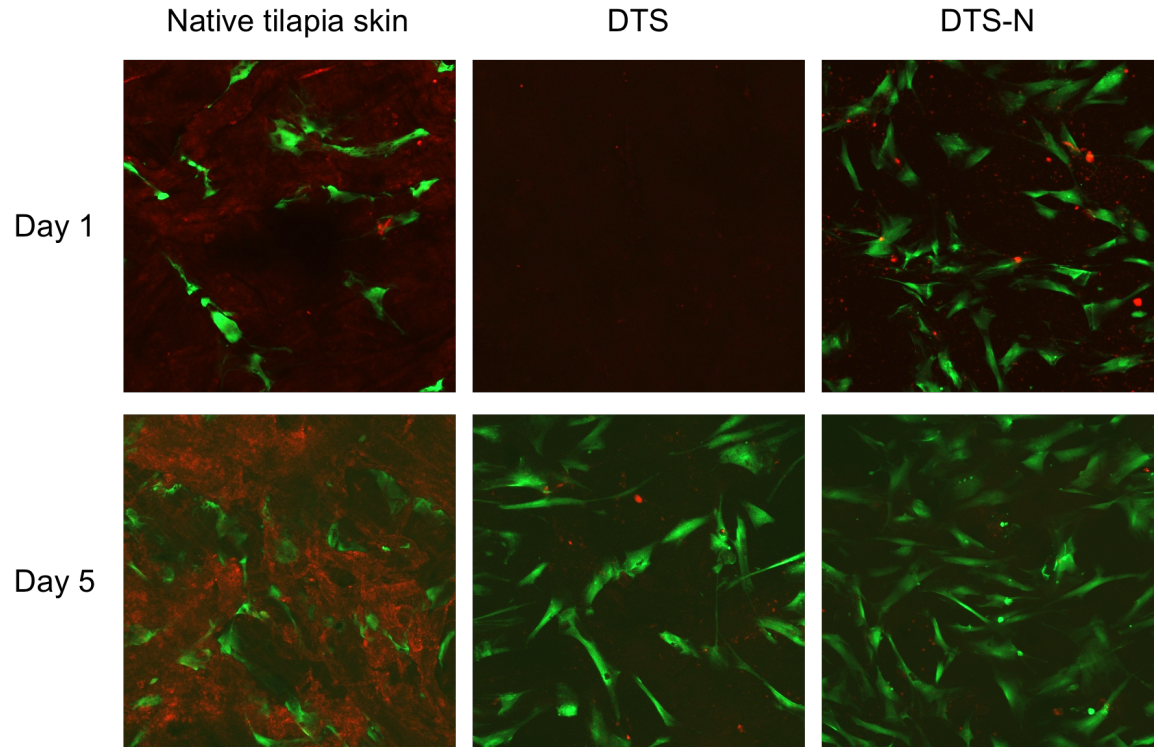

Figure 6.10: Cell attachment and viability were evaluated with Live/Dead® cytotoxicity kit at Day 1 and 5 after human dermal fibroblasts (HDFs) were seeded onto tilapia skins treated in different conditions. Live cells were dyed green by calcein-AM, and dead cells were dyed red by ethidium homodimer-1.

From the AlamarBlue results (Figure 6.9), it was observed that all three samples supported HDF proliferation, with the metabolic activity of the HDFs increasing over time. Among the three samples, DTS-N exhibited the best cellular biocompatibility, indicating that an additional sodium hydroxide treatment helped to improve the biocompatibility of tilapia skin. The observation in this study was similar to the results in another study where rat lungs decellularized by sodium hydroxide solution exhibited better recellularization than rat lungs decellularized by SDS [349]. The reason why sodium hydroxide leads to better cellular biocompatibility in tilapia skin was unclear, but we could rule out the hypothesis that the improved biocompatibility was caused by a reduction of water contact angle as the sodium hydroxide treatment did not reduce the contact angle of DTS-N.

On the other hand, DTS-N was observed to have a lower immunogenic potential than DTS, and this could be a possible reason for the better cellular biocompatibility of DTS-N. However, more experiments, especially *in vivo* studies, would be needed to prove the hypothesis that a reduction of antigen content in the sodium hydroxide treated tilapia skin would improve its biocompatibility.

6.3.7 *In vivo skin regeneration*

Impaired wound healing is responsible for considerable morbidity and mortality globally, especially for diabetic patients and immunosuppressed patients [322]. In mammals including humans, wound healing is a continuous process involving four overlapping phases – (i) hemostasis, where blood vessels were constricted and blood clots were formed by the activation of platelets to prevent further blood loss; (ii) inflammation, where neutrophils and macrophages are recruited to the wound to prevent infection; (iii) proliferation, where the fibroblasts and epithelial cells contribute to wound repair by collagen deposition, wound retraction and

angiogenesis; and (iv) remodelling, where development of normal epithelium and maturation of the scar tissue takes place [350, 351].

The complexity of wound healing is impossible to be replicated *in vitro* and therefore necessitates the use of animal models. Among various mammals, the laboratory mouse are commonly used in biomedical research due to easy housekeeping and easy genetic manipulations [282]. However, murine wounds heal differently to human wounds as a subcutaneous striated muscle layer present in murine skin but not in human skin causes rapid contraction of murine skin after wounding. To overcome this limitation, a splint was incorporated around the wound so that the repair process was dependent on epithelialization, cellular proliferation and angiogenesis, closely mirroring the human wound healing process.

Figure 6.11: Murine wound healing model. (A) View of the mouse immediately after surgery. (B) View of the same mouse one week later, after sacrifice. In this model two full thickness wounds are created on either side of the midline allowing each mouse to serve as their own control. The left wound was left untreated while the right wound was covered with the sample of interest. Silicone splints are fixed to the wound perimeter by suture to prevent wound contraction, providing a model relevant to that of human wounds.

Here, two 5 mm full-thickness defects were created on the back of 6 week old mice and fixed with circular silicone splints (Figure 6.11A). One defect was covered with the sample of interest and the other defect was left uncovered as the control. At 1 week and 2 weeks after

implantation, the mice were sacrificed (Figure 6.11B). The morphology of the wounds was examined and H&E histology was performed to evaluate the extent of tissue regeneration in the defect. The covered defect was then compared with the uncovered defect to determine the effect of the sample on *in vivo* skin regeneration.

The morphology of the wounds were captured on photograph and presented in Figure 6.12A, and the area of each wound was quantified, with the mean and standard deviation represented in Figure 6.12B. The H&E stained histological sections of the wound are shown in Figure 6.13.

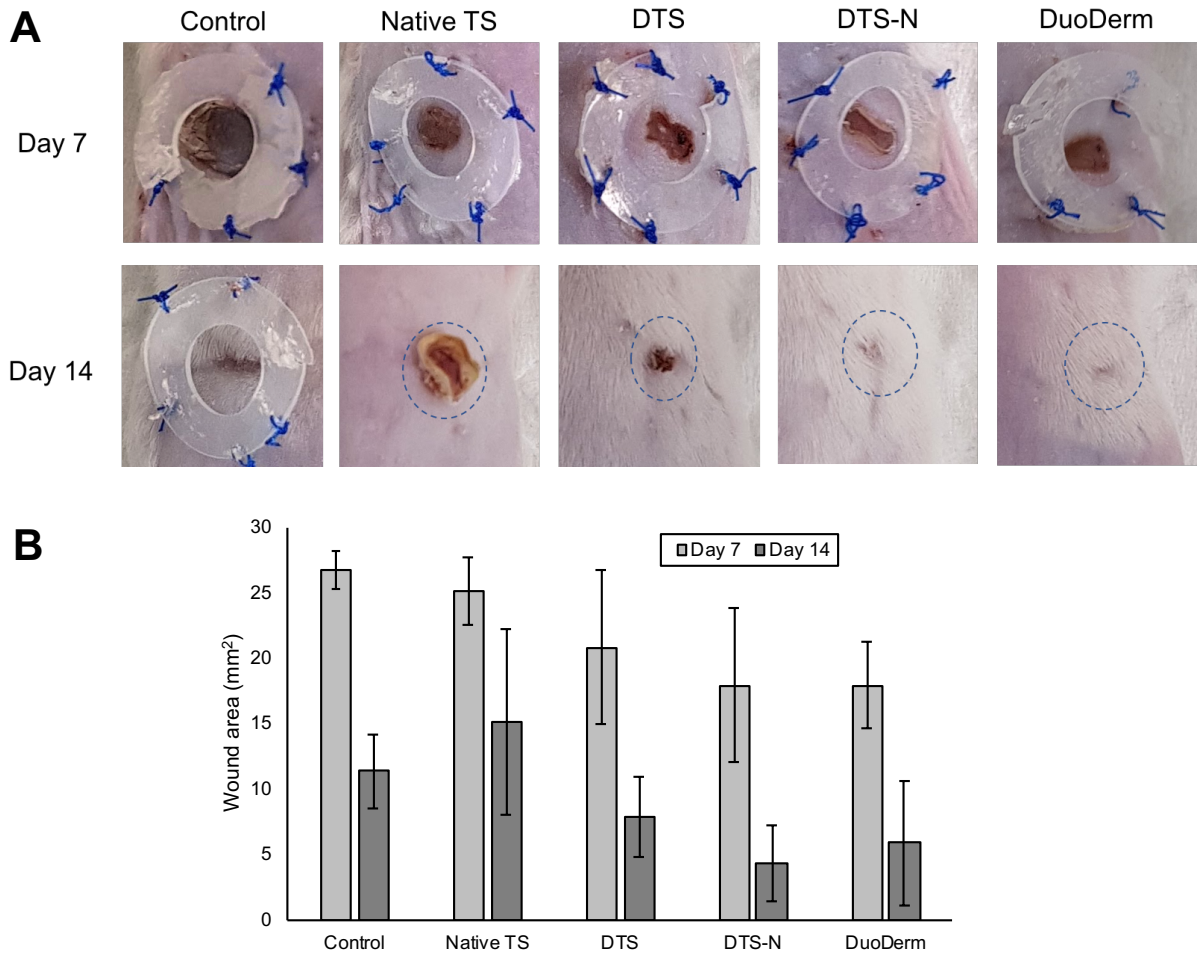

Figure 6.12: Wound healing in BALB/c mice. (A) Representative images of skin wounds after treatment with native tilapia skin, DTS (decellularized tilapia skin), DTS-N (alkali-treated decellularized tilapia skin) or Duoderm, with untreated wounds as control (n = 3). The circular splint has an inner diameter of 6 mm and an outer diameter of 12 mm. For wounds with detached splints, the inner circumference of the splint was indicated with a blue dashed line. (B) Wound area quantified at 1 week and 2 weeks after surgery.

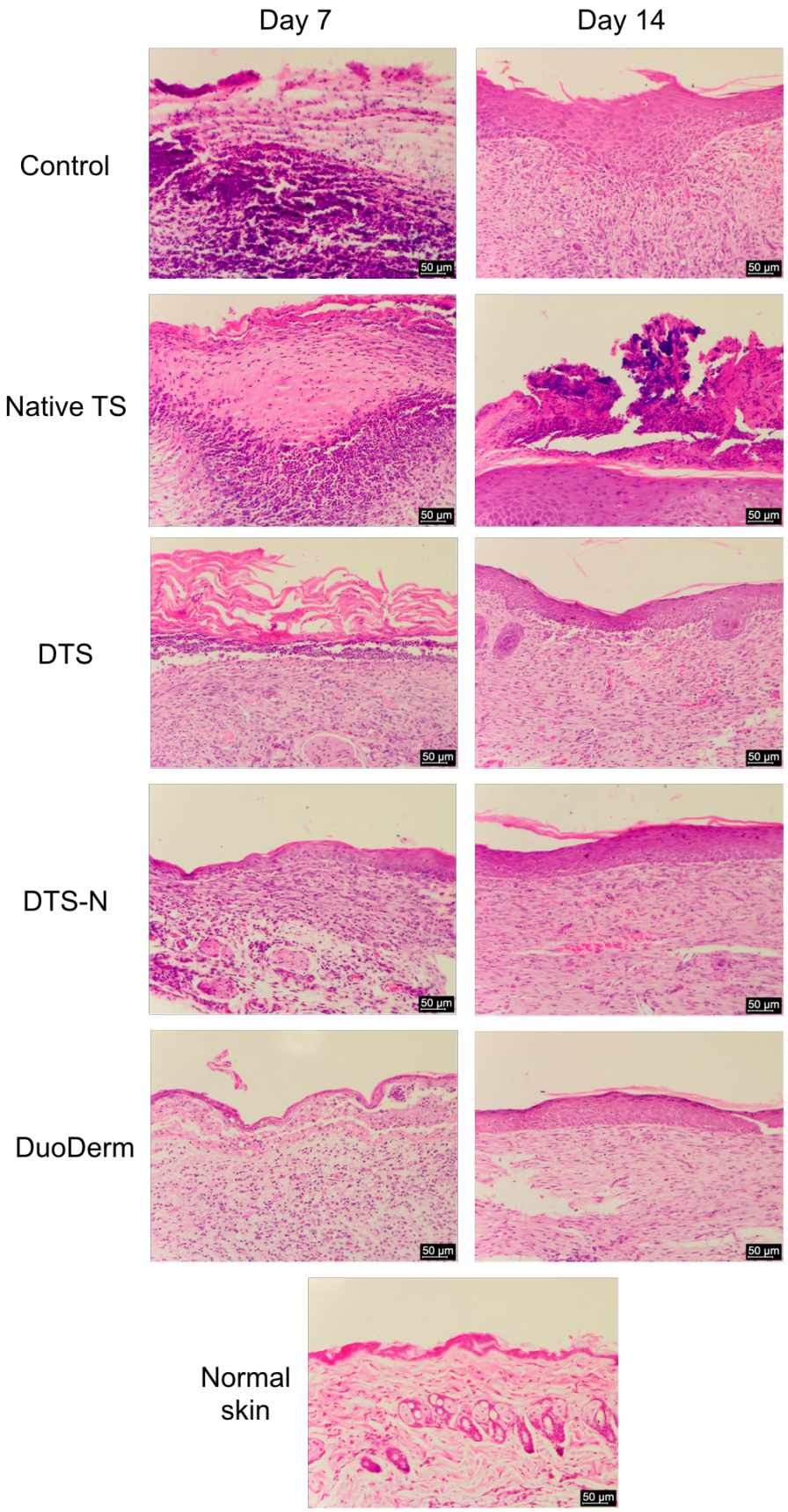

Figure 6.13: Representative images of cross-sectional H&E stained sections of mouse skin wounds covered with native tilapia skin, DTS (decellularized tilapia skin), DTS-N (alkali-treated decellularized tilapia skin) or DuoDerm, with untreated wounds as control (n = 3). Scalebar represents 50 µm.

Compared to the control groups, improvement in wound healing was observed for all groups at Day 7 and Day 14, with the exception of the native tilapia skin group at 2 weeks where signs of chronic inflammation were noticed (Figure 6.12A). For DTS, DTS-N and DuoDerm, most of the wound area was covered with a continuous epidermis at Day 14, while the wounds in the control group and native tilapia skin group were not completely healed. The incomplete healing and signs of chronic inflammation for the native tilapia skin group suggested that the healing process was hindered by the presence of antigens in the native tilapia skin, and decellularization of tilapia skin appeared to help in improving the wound healing rate. Interestingly, the addition of sodium hydroxide treatment into the decellularization protocol further improved the wound healing rate, making the healing in the DTS-N group relatively better than that of the DuoDerm group at Day 14, as evident in the smaller mean wound area of DTS-N in Figure 6.12B.

The histology images (Figure 6.13) confirmed that DTS-N induced the lowest degree of inflammatory response and promoted the best growth of new epidermis throughout the process of wound healing. Good epidermal growth and low inflammatory response were also observed for the DTS and DuoDerm groups at both Day 7 and Day 14, but the thickness and continuity of the new epidermis were at a less extent compared to DTS-N. In the DTS, DTS-N and DuoDerm groups, the epidermal cells appeared to be fully differentiated, with the basal cells closely arranged at the epidermis-dermis boundary and the keratinocytes forming dense layers at the outermost portion of the skin. In the control and native tilapia skin groups, the wound area was mainly occupied by inflammatory cells and granulated tissue at Day 7, with the presence of inflammatory cells and granulated tissue present in native tilapia skin continuing to Day 14. In the control group, the boundary between the epidermis and the dermis was not defined and there is a presence of inflammatory cells at Day 14, suggesting that the wound healing was not yet completed.

As the rate of skin regeneration may differ in each mouse, we devised a scoring system where the healing of the sample-covered wound was rated as “worse”, “similar” or “better” than the healing of the non-covered (control) wound on the same mouse. The definition of each term in the scoring system is explained in Table 6-4, and the results are illustrated in Figure 6.14.

Table 6-4: Definition of terms in the scoring system of wound-healing

	Visual inspection	H&E histology
Better	• The sample-covered wound is smaller than the non-covered wound • Minimal scarring	• The regenerated tissue in the sample-covered wound is thicker than that in the non-covered wound. • No inflammation
Similar	• The sample-covered wound has a similar size to that of the non-covered wound	• The regenerated tissue in the sample-covered wound has a similar thickness to that in the non-covered wound.
Worse	• The sample-covered wound is larger than the non-covered wound • Excessive scarring	• The regenerated tissue in the sample-covered wound is thinner than that in the non-covered wound. • Evidence of chronic inflammation

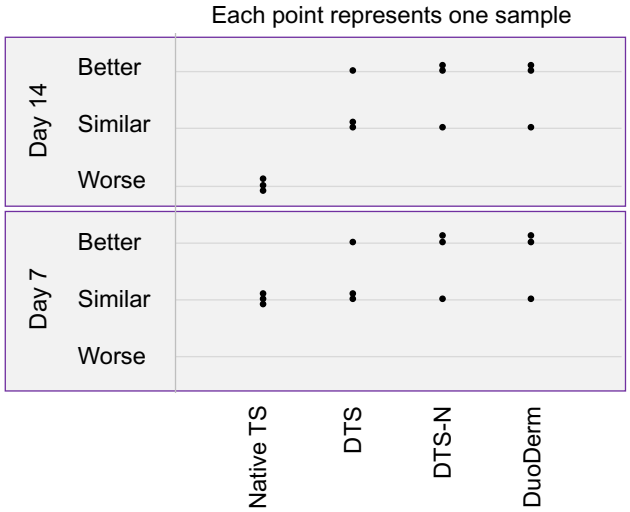

Figure 6.14: Wound healing scores of native tilapia skin, DTS (decellularized tilapia skin), DTS-N (alkali-treated decellularized tilapia skin) and DuoDerm, according to the score system listed in Table 6-4.

From the results, it was evident that native tilapia skin was not favourable to wound healing at Day 14, which was evident in the high level of inflammation observed in the histology images. This was a sign of adverse foreign body reaction, which was likely caused by the high immunogenic potential of native tilapia skin. After decellularization, the inflammatory

response was remarkably reduced and DTS managed to induce new epidermis growth. With an additional sodium hydroxide treatment, there was a further improvement in *in vivo* biocompatibility, as more samples in the DTS-N group have better performance than the control, compared to the DTS group. The performance of DTS-N is similar to that of DuoDerm, an established hydro-colloid dressing used for the management of chronic wounds. DuoDerm is known for its ability to maintain a moist environment in the wound, to provide occlusion that is beneficial for collagen synthesis, and to not damage the newly formed epithelium when the dressing is removed [323]. These beneficial properties were observed in the DTS-N group, as shown by the low water permeability which helped to retain moisture, the positive regeneration of the dermis during the healing process, and the preservation of the epidermis after the sample is removed from the wound. The results of this study suggested that DTS-N is an effective scaffold for skin wound regeneration.

6.4 Conclusion

In this chapter, the suitability of decellularized tilapia skin (DTS) and crosslinked electrospun tilapia collagen (CETC) as tissue engineering scaffolds were investigated. Physical properties which could influence tissue-scaffold interactions, such as water contact angle, porosity, and water permeability were characterized for DTS and CETC. The *in vitro* degradation profiles of the scaffolds were also assessed to predict the stability and the rate of biodegradation *in vivo*. From the physical characterisations, DTS was found to be less hydrophilic and less porous than CETC, and both materials have an extremely low water permeability. DTS was also highly durable in sterile PBS, losing only 19.0% of its weight after 8 weeks of immersion, but it degraded rapidly in the presence of collagenase. It was hypothesized that the low hydrophilicity, low porosity and low water permeability of DTS were attributed to the multiple layers of tightly packed collagen fibres in the skin and contributed to the high mechanical strength and slow

degradation by hydrolysis. In the presence of collagenase, the tightly packed collagen fibres started to break down, leading to a rapid degradation of DTS. For CETC, the higher hydrophilicity contributes to its better biological performance than DTS, as hydrophilic surfaces favour cell attachment.

Next, we evaluated the suitability of our tilapia-derived scaffolds in two clinical applications. In the first application, decellularized tilapia skin (DTS) and crosslinked electrospun tilapia collagen (CETC) were evaluated for their suitability as barrier membranes in guided bone regeneration. Both DTS and CETC were found to be biocompatible to murine pre-osteogenic MC3T3-E1 cells, and support the osteogenic differentiation and mineralization of MC3T3-E1 cells in the presence of the osteogenic media, with CETC exhibiting a better performance. In the rat calvarial defect model, both DTS and CETC supported bone regeneration and did not induce chronic inflammation within the defect. However, fibrous tissues were observed in the defects in the CETC group, suggesting that the CETC degraded *in vivo*, allowing fibroblasts to enter the defect. To combine the benefits of the two scaffolds, namely the high mechanical strength of DTS and the positive biological performance of CETC, we proposed to combine the two scaffolds into a bi-layer membrane for GBR, with DTS facing the exterior to provide mechanical support and prevent the entry of fibroblasts, and CETC facing the defect to provide a biocompatible surface for osteoinduction.

In the second application, DTS was evaluated for its suitability as a skin wound dressing. As DTS was found to be inferior to CETC in terms of immunogenic potential, *in vivo* immune responses, and *in vitro* and *in vivo* osteoinduction, an additional acid or alkali treatment step was added to the decellularization protocol to reduce the water contact angle and reduce the antigen content the skin. It was observed that an additional 3 hour treatment in 0.5 M sodium hydroxide was able to reduce the immunogenic potential of DTS and improve its cellular

biocompatibility to human dermal fibroblasts (HDFs). The alkali-treated DTS (DTS-N) was then compared with native tilapia skin, DTS and DuoDerm, an established hydrocolloid wound dressing, in the murine full-thickness skin wound model. It was observed that decellularization of tilapia skin improved the wound healing rate in mice. An addition of sodium hydroxide treatment further improved the wound healing rate, making the healing in the DTS-N group relatively better than that of the DuoDerm group. The results of this study suggested that DTS-N is a potentially effective scaffold for skin wound regeneration.

7 Conclusion and future work

7.1 Conclusions

This thesis started with a goal to develop the skin of Nile tilapia (*Oreochromis niloticus*), a tropical fish popularly cultivated as food, into acellular scaffolds to provide an economical and safe alternative to mammalian-derived scaffolds in tissue engineering applications. The motivation to develop scaffolds from tilapia skin was driven by the huge demand for tissue constructs to restore non-functional tissues in patients and the huge amount of collagen-rich fish waste generated by the fishing industry, as mentioned in Chapter 1. The choice of fish skin as the source of biomaterials was also prompted by the limitations of current mammalian products, which include the risks of disease transmission from mammals to humans, the rejection of mammalian products by religious patients, and the high immunogenicity of mammalian tissues. This thesis focused on Nile tilapia due to its rapid growth and wide distribution, and also due to the numerous benefits possessed by tilapia collagen, as reported in previous studies and reviewed in Chapter 2.

As collagen is the main constituent of tilapia skin, the properties of tilapia collagen were studied in Chapter 3 by bioinformatics analysis and physio-chemical characterisation. The high level of conservation between tilapia collagen and mammalian collagen revealed in the bioinformatics characterisation suggested that tilapia collagen would be well-tolerated by mammals. In the same chapter, a crosslinked electrospun tilapia collagen (CETC) scaffold was successfully developed with a novel benign PBS/ethanol solvent, which was non-toxic and more environmentally friendly than the traditional electrospinning solvent HFIP. The data obtained in Chapter 3 addressed the first hypothesis that tilapia collagen can be electrospun and crosslinked into a scaffold which is highly biocompatible.

With the knowledge gained from the development and characterisations of CETC scaffolds, tilapia skin was then decellularized to yield acellular scaffolds, which were termed as decellularized tilapia skin (DTS). Chapter 4 demonstrated that a combination of enzyme and detergent treatments were effective in decellularizing tilapia skin, with almost all DNA (99.6%) removed and relatively high amount of collagen (69.3%) retained. The optimized decellularization protocol did not adversely affect the mechanical properties and denaturation temperature of DTS, although the mechanical properties of tilapia skin were discovered to be dependent on the location of the skin and the direction of pull. Electricity was also introduced as a novel medium for decellularization, with preliminary data suggesting the effectiveness of electroporation and electrolysis in the removal of DNA and the preservation of the ECM in treated tissues. In summary, the results in Chapter 4 addressed the second hypothesis that tilapia skin can be decellularized using appropriate treatments to yield an acellular scaffold.

DTS was further subjected to a series of biological assessments to evaluate its biological safety and performance in Chapter 5, using CETC as a comparing scaffold. The human serum based assays revealed that native tilapia skin has a lower immunogenic potential than porcine tissues and decellularization significantly reduced the immunogenic potential of tilapia skin further. Cell culture results demonstrated the low cytotoxicity and high cellular biocompatibility of DTS and CETC towards murine fibroblasts L929, while the *in vivo* immune responses of both scaffolds indicated the lack of chronic inflammation after implantation in rats. Together with the results in Chapter 4, the findings in Chapter 5 addressed the third hypothesis that DTS possesses favourable physical and biological properties, and is less immunogenic than native tilapia skin.

The suitability of DTS as a tissue engineering scaffold was investigated in Chapter 6, where further physical characterization revealed that DTS had low hydrophilicity, low porosity and

low water permeability, all of which are plausible factors that contribute to the slow degradation rate of DTS in sterile PBS. Although DTS lost only 19.0% of its weight after 8 weeks of immersion in sterile PBS, it degraded rapidly in the presence of collagenase, indicating the importance of collagen in the structural integrity of DTS.

The clinical applications of DTS were evaluated in two studies. In the first study, where DTS and CETC were assessed as barrier membranes in guided bone regeneration, *in vitro* results demonstrated the biocompatibility of DTS and CETC towards murine pre-osteogenic MC3T3-E1 cells and the ability of both scaffolds to support osteogenic differentiation and mineralization. In the rat calvarial defect model, both DTS and CETC supported bone regeneration and did not induce chronic inflammation within the defect. However, DTS was found to be inferior to CETC in terms of *in vitro* and *in vivo* osteoinduction, while CETC degraded rapidly *in vivo* and failed to prevent fibroblast infiltration. To combine the benefits of the two scaffolds, we proposed to develop a bi-layer membrane comprising of DTS as the outer layer to prevent fibroblasts infiltration and CETC as the inner layer to support osteoinduction in the defect. In the second study, DTS was assessed for its suitability as a skin wound dressing. DTS was subjected to additional alkali treatment in an attempt to improve its biocompatibility, and the alkali-treated DTS (termed as DTS-N) was shown to have a reduced immunogenic potential and improved cellular biocompatibility to human dermal fibroblasts (HDFs), compared to DTS. Results from the murine full-thickness skin wound model revealed that DTS induced a better healing rate than native tilapia skin, and an additional alkali treatment further improved the wound healing rate, making the healing in the DTS-N group relatively better than that of the DuoDerm group. The findings in Chapter 6, together with the data from Chapter 4 and 5, addressed the fourth hypothesis that DTS is suitable as a scaffold in tissue regeneration, with favourable tissue-scaffold interactions.

In conclusion, the capability of tilapia skin as a biomaterial for tissue engineering applications has been demonstrated in this thesis. While a previous study reported the effectiveness of CETC in skin regeneration, there have been no known prior studies on DTS, making this thesis one of the firsts to report on the development, evaluation and application of DTS for tissue engineering applications. The high mechanical strength, long degradation time and favourable biological properties of DTS would render this novel biomaterial useful for tissue engineering applications requiring strong protective membranes for long term tissue regeneration.

7.2 Recommendations for future work

7.2.1 *Further characterisation of fish skin components*

In this thesis, we only focused on selected substances in the tilapia skin to determine the extent of decellularization. The removal of cellular components was measured by DNA content and immunogenic potential without focusing on individual antigens, while the preservation of the extracellular matrix (ECM) was measured by collagen content, elastin content and glycosaminoglycan (GAG) content. There are many bioactive substances in tilapia skin that can contribute to favourable or adverse cellular response and tissue-implant interaction, and it is a challenge to isolate and identify every substance in tilapia skin. When section 6.3.5 – 6.3.7 reported that an additional sodium hydroxide treatment in the decellularization protocol improved the biocompatibility of tilapia skin, we could only make educated guesses on what the sodium hydroxide did without knowing the actual reasons.

Looking ahead, we would like to perform a more detailed analysis of the biochemical composition of tilapia skin before and after decellularization, to identify substances that are beneficial to tissue-implant interactions and also substances that provoke adverse response. Proteins and peptides from tilapia skin can be separated and identified by immunoproteomic

approaches such as two-dimensional gel electrophoresis, liquid chromatography and mass spectrometry, and the separated proteins can be analysed individually for their cytotoxicity and antigenicity [94, 352, 353]. As fish peptides have been reported to exhibit potent biological activities beyond their nutritional value (as mentioned in section 2.5.2), it would be interesting to investigate whether decellularized tilapia skin would possess any of these biological activities. Beside proteins and peptides, the fat content of tilapia skin would also be worth investigating, as certain fish oils, especially omega-3 polyunsaturated fatty acids, have been reported to regulate inflammatory activities and facilitate wound healing [354, 355]. Fish oils can be isolated from tilapia skin by extraction with organic solvents and purification with liquid chromatography and mass spectrometry. If certain fish oils were found to be beneficial to tissue regeneration, the decellularization protocol could be amended to minimise the loss of the fish oils in tilapia skin.

7.2.2 *Investigation of antimicrobial properties*

In addition to adverse foreign body reaction, another major challenge in the use of scaffolds in tissue engineering is the risk of bacterial infection. As scaffold-associated infection has been increasing identified as a major failure mechanism in scaffolds, there is an urgency to address the challenge on how to create scaffolds that promote tissue-scaffold interactions while concurrently inhibiting bacterial colonization [356]. Despite advances in sterilisation techniques, it is impossible to eliminate all trace of pathogens when implanting a biomaterial due to the ubiquitous presence of opportunistic pathogens in the environment and also in the body of the implant recipient. Normally weakly virulent due to the suppression by the immune system of a healthy individual, opportunistic pathogens can become virulent when there is a loss of innate or adaptive immune responses in a immunocompromised individual [357]. In some patients, adverse FBR to an implant may require the suppression of the patient's immune

system, creating an opportunity for opportunistic pathogens to proliferate. To make things more complicated, the three-dimensional architecture of many tissue engineering scaffolds can enhance bacterial colonization by allowing small-sized bacteria to penetrate into remote parts that are inaccessible to larger mammalian cells. To address this issue, there is a motivation to develop scaffolds with inherent antimicrobial properties to reduce the risk of scaffold-associated infections.

The antimicrobial properties of tilapia skin were briefly studied through a preliminary bacterial adherence assay. Native and decellularized tilapia skins, cut into discs with 6 mm diameter, were incubated in broths containing gram-positive *Staphylococcus aureus* (#25923, ATCC, USA) or gram-negative *Pseudomonas aeruginosa* (PA01, ATCC, USA) at 37°C for 1 hour. The skin samples were washed gently with PBS twice to remove non-adhering bacteria, and adhered bacteria were dislodged by vortexing the samples in 1 ml PBS for 1 minute. The solutions containing the dislodged bacteria were plated on agar and the colonies were counted after 24 hour incubation at 37°C. From the results, no colonies were observed for both native tilapia skin and decellularized tilapia skin, suggesting that tilapia skin prevented the adhesion of *S. aureus* and *P. aeruginosa*, and the anti-adhesion property was retained after decellularization.

To validate the antimicrobial properties of tilapia skin, we would like to propose performing this assay with other species of microbes, as well as performing other tests such as disc diffusion assay and endotoxin assay. In the event that our tilapia scaffolds do not possess sufficient antimicrobial properties, we would like to propose the addition of antimicrobial substances into the scaffolds to minimise the risk of infection during implantation and tissue regeneration.

7.2.3 *Further optimisation of electric decellularization*

In section 4.4, electricity was introduced as a novel decellularization medium. Preliminary results suggested that electroporation was effective in the removal of DNA and the preservation of the ECM. As we only assessed the effect of electric decellularization on tilapia skin based on DNA content, collagen content and histology, we would like to propose more characterisations to validate the effectiveness of electric decellularization. In particular, the mechanical properties, immunogenic potential and biocompatibility of the electricity-treated samples would be of significant interest to us. The setup of the electric decellularization can also be optimised to enable scaling up without excessive heat generation.

7.2.4 *Decellularization using supercritical carbon dioxide*

In section 2.2.3, supercritical carbon dioxide was introduced as a method of sterilization and decellularization. The term supercritical fluid refers to a fluid held above its critical temperature and critical pressure, having a viscosity and diffusion coefficient intermediate between a gas and a liquid [358]. The high transfer rate and high permeability, which can be adjusted by varying the temperature and pressure, allows supercritical carbon dioxide to be used as a versatile, cheap and non-toxic solvent in a variety of applications [359]. Traditionally used as a solvent to extract compounds from plants and remove contaminants from food, supercritical carbon dioxide is now used for tissue decellularization, as it is compatible with biological materials, do not react with ECM components, and do not leave toxic residues [104].

Another advantage of using supercritical carbon dioxide is its capability as a sterilization medium. According to stringent safety regulations, scaffolds often require terminal sterilization methods such as gamma irradiation and ethylene oxide exposure to achieve absolute sterility, but such methods often affect ECM structure and mechanical properties of biologic scaffolds

[98, 99]. Supercritical carbon dioxide is seen as a novel alternative for terminal sterilization, as it can dissolve a low amount of chemical sterilant to form a very effective and yet gentle medium for sterilization of sensitive biomaterials [105]. Hence, supercritical carbon dioxide has the benefit of achieving both decellularization and sterilisation in one treatment, saving substantial amount of time and resources.

Despite the numerous advantages of supercritical carbon dioxide, this medium is not commonly used due to the serious drawback of high investment costs, which is the main reason why this technique was not employed in this thesis. Looking forward, we would like to propose doing a preliminary study of using supercritical carbon dioxide to decellularize and sterilize tilapia skin for tissue engineering applications. If supercritical carbon dioxide is proven to be effective in this preliminary study, the investment on the supercritical carbon dioxide system and a larger-scale study would be justified.

7.2.5 *Decellularization of tissues from other fish species*

Beside tilapia, we would like to look into decellularizing tissues from other fish species. According to the statistics from the Food and Agriculture Organization of the United Nations, global fish production peaked at about 171 million tonnes in 2016, with aquaculture representing 47 percent of the total production [360]. As the harvest level of wild fish remains relatively static since the late 1980s, aquaculture is becoming more important in the supply of fish for human consumption. As for 2016, a total of 598 marine species were cultivated for consumption, but the aquaculture industry is dominated by a small number of staple species, with the 20 most produced species accounting for 84.2 % of the total production (Table 7-1).

Table 7-1: The 20 most produced fish species in global aquaculture and their production levels in 2010 and 2016 (in 1000 tonnes) [360]

Species	2010 production (1000 tonnes)	2016 production (1000 tonnes)	% of total, 2016
Grass carp, *Ctenopharyngodan idellus*	4 362	6 068	11
Silver carp, *Hypophthalmichthys molitrix*	4 100	5 301	10
Common carp, *Cyprinus carpio*	3 421	4 557	8
Nile tilapia, *Oreochromis niloticus*	2 537	4 200	8
Bighead carp, *Hypophthalmichthys nobilis*	2 587	3 527	7
Carassius spp.	2 216	3 006	6
Catla, *Catla catla*	2 977	2 961	6
Freshwater fishes nei, *Osteichthyes*	1 378	2 362	4
Atlantic salmon, *Salmo salar*	1 437	2 248	4
Roho labeo, *Labeo rohita*	1 133	1 843	3
Pangas catfishes nei, *Pangasius spp.*	1 307	1 741	3
Milkfish, *Chanos chanos*	809	1 188	2
Tilapias nei, *Oreochromis (=Tilapia) spp.*	628	1 177	2
Torpedo-shaped catfishes nei, *Claria spp.*	353	979	2
Marine fishes nei, *Osteichthyes*	477	844	2
Wuchang bream, *Megalobrama amblycephala*	652	826	2
Rainbow trout, *Oncorhynchus mykiss*	752	814	2
Cyprinids nei, *Cyprinidae*	719	670	1
Black carp, *Mylopharyngodon piceus*	424	632	1
Snakehead, *Channa argus*	377	518	1
Other fishes	5 849	8 629	16
Total	**38 494**	**54 091**	**100**

This thesis has demonstrated the biomedical benefits of collagen and decellularized skin from Nile tilapia, the second most cultivated fish after the carp family. As Nile tilapia only made up 8 % of the total aquaculture production in 2016, and there is currently very little information on decellularized fish tissues (Table 1-1), there are huge potentials in deriving decellularized tissues and beneficial bioactive substances from the other commonly cultivated species, especially from the carp family.

Extrapolating from the positive results of decellularized tilapia skin from this thesis, we would expect the decellularization of tissues from other fish species to contribute to the production of biocompatible, economical and sustainable scaffolds for tissue engineering, as well as the reduction of fish waste in the fish processing industry and the increase in value for fish by-products.

7.2.6 *Investigation of mechanisms behind enhanced healing*

In section 6.3.7, DTS was evaluated for its suitability as a skin wound dressing, and DTS showed an improved wound healing rate in mice compared to native tilapia skin. After an addition of sodium hydroxide treatment, the DTS-N (sodium hydroxide treated DTS) exhibited further improvement in the *in vivo* wound healing rate, matching the performance of DuoDerm, an established hydro-colloid dressing used for the management of chronic wounds.

Although the process of skin wound healing has been extensively studied, the mechanism of how DTS and DTS-N contributed to enhanced healing of the skin has not been investigated. In the results and discussion, we suggested that the reduction of immunogenic potential by the decellularization process contributed to the enhanced healing. However, there are many other factors that play a role in the wound healing process, which has not been thoroughly studied in this thesis. In chapter 1, I mentioned that the development of a successful tissue construct depends on one or a combination of these five tenets: scaffolds, cells, growth factors, bioreactors, and bioimaging. For my future work, I would like to investigate each of these tenets in more detail, to understand the mechanism behind the enhanced healing by DTS and DTS-N:

1) Scaffolds – The tilapia skin may contain bioactive substances and surface properties that can contribute to favourable or adverse cellular response and tissue-implant interaction. Such substances and surface properties have not been studied in detail in my thesis. As mentioned in section 7.2.1, we would like to perform a more detailed analysis of the biochemical composition of tilapia skin before and after decellularization, to identify substances that contribute to beneficial tissue-implant interactions and also substances provoking adverse response. As surface morphology and stiffness could also influence cellular behaviour [361], it would be useful to

investigate the surface properties of tilapia skin before and after decellularization, to find out whether the modified surface properties of DTS and DTS-N affect cell and tissue response *in vivo*.

2) Cells – Among the five tenets of tissue engineering, cells play the most crucial role in skin regeneration as they are responsible for the inflammatory and healing response, as well as the formation of new tissues. The tremendous ability of the skin to regenerate is due to the presence of fibroblasts that create new ECM to contract the wound, and the presence of keratinocytes that undergo terminal differentiation to a keratinized layer forming the skin's outermost barrier [362, 363]. In my thesis, we only investigated the metabolic activity and viability of human dermal fibroblasts on the tilapia skin for the *in vitro* study and performed H&E histology for the *in vivo* study. For my future work, I would study the cellular behaviour of keratinocytes on tilapia skin, and study how the tilapia skin affects the terminal differentiation of keratinocytes via *in vitro* gene expression study, immunohistochemical analysis of keratinocytic markers in histological sections, and *in vivo* quantitative assay of wound healing related biomarkers, similar to the work done in section 5.3.5.
3) Growth factors – As a biological tissue, the fish skin could contain inherent growth factors which could influence cellular behaviour. Growth factors involved in skin regeneration include platelet-derived growth factor (PDGF), fibroblast growth factor (FGF), and insulin-like growth factor (IGF) [364]. However, the identification and quantification of growth factors in the fish skin have not been carried out within the scope of my thesis. The similarities and differences between human growth factors and fish growth factors are also not well-understood. For my future work, I would compare human growth factors and fish growth factors via bioinformatic analysis (similar to the work done in section 3.3.1) to predict the effects of fish growth factors

on human cells. I would also perform ELISA to isolate and quantify the relevant growth factors from fish skin, to study whether the decellularization process would affect the quantify of these growth factors, and how these growth factors affect skin regeneration.

4) Bioreactors – Although bioreactors are beyond the scope of my thesis, they would be useful to investigate cellular behaviour on the tilapia skin in a dynamic environment. For example, cells can be seeded on a piece of tilapia skin undergoing cyclic strains and/or temperature fluctuations, to mimic the conditions experienced by cells in a real wound.
5) Bioimaging – My thesis contains some simple forms of bioimaging such as scanning electron microscope (SEM), brightfield microscopy, live/dead cytotoxicity fluorescent imaging and microcomputed-tomography (μCT). In my future work, it will be definitely very helpful to include more advanced forms of bioimaging such as fluorescent tagging of skin cells and/or wound healing markers,

8 Reference

[1] R.S. Katari, A. Peloso, G. Orlando, Tissue Engineering, Advances in Surgery 48(1) (2014) 137-154.

[2] G. Orlando, K.J. Wood, P. De Coppi, P.M. Baptista, K.W. Binder, K.N. Bitar, C. Breuer, L. Burnett, G. Christ, A. Farney, M. Figliuzzi, J.H.I. Holmes, K. Koch, P. Macchiarini, S.-H.M. Sani, E. Opara, A. Remuzzi, J. Rogers, J.M. Saul, D. Seliktar, K. Shapira-Schweitzer, T. Smith, D. Solomon, M. Van Dyke, J.J. Yoo, Y. Zhang, A. Atala, R.J. Stratta, S. Soker, Regenerative Medicine as Applied to General Surgery, Annals of Surgery 255(5) (2012) 867-880.

[3] R.M. Nerem, Chapter Two - The Challenge of Imitating Nature, in: R. Lanza, R. Langer, J. Vacanti (Eds.), Principles of Tissue Engineering (Third Edition), Academic Press, Burlington, 2007, pp. 7-14.

[4] R. Langer, J.P. Vacanti, Tissue engineering, Science (New York, N.Y.) 260(5110) (1993) 920-6.

[5] R. Langer, J. Vacanti, Advances in tissue engineering, Journal of pediatric surgery 51(1) (2016) 8-12.

[6] S.H. Teoh, Engineering materials for biomedical applications, Singapore ; Hackensack, N.J. : World Scientific Pub. Co., c2004.2004.

[7] M.S.F. Kurtis Kasper, A.G. Mikos, Chapter II.6.3 - Tissue Engineering Scaffolds, in: B.D. Ratner, A.S. Hoffman, F.J. Schoen, J.E. Lemons (Eds.), Biomaterials Science (Third Edition), Academic Press2013, pp. 1138-1159.

[8] B. Dhandayuthapani, Y. Yoshida, T. Maekawa, D.S. Kumar, Polymeric Scaffolds in Tissue Engineering Application: A Review, International Journal of Polymer Science 2011(Article ID 290602) (2011).

[9] D. Sarkar, W. Zhao, S. Schaefer, J.A. Ankrum, G.S.L. Teo, M.N. Pereira, L. Ferreira, J.M. Karp, Chapter II.6.2 - Overview of Tissue Engineering Concepts and Applications, in: B.D. Ratner, A.S. Hoffman, F.J. Schoen, J.E. Lemons (Eds.), Biomaterials Science (Third Edition), Academic Press2013, pp. 1122-1137.

[10] S.F. Badylak, T.W. Gilbert, J. Myers-Irvin, Chapter 5 - The extracellular matrix as a biologic scaffold for tissue engineering, in: C.v. Blitterswijk, P. Thomsen, A. Lindahl, J. Hubbell, D.F. Williams, R. Cancedda, J.D.d. Bruijn, J. Sohier (Eds.), Tissue Engineering, Academic Press, Burlington, 2008, pp. 121-143.

[11] S. Yi, F. Ding, L. Gong, X. Gu, Extracellular Matrix Scaffolds for Tissue Engineering and Regenerative Medicine, Current stem cell research & therapy 12(3) (2017) 233-246.

[12] M. van der Rest, R. Garrone, Collagen family of proteins, FASEB journal : official publication of the Federation of American Societies for Experimental Biology 5(13) (1991) 2814-23.

[13] G.A. Di Lullo, S.M. Sweeney, J. Korkko, L. Ala-Kokko, J.D. San Antonio, Mapping the ligand-binding sites and disease-associated mutations on the most abundant protein in the human, type I collagen, The Journal of biological chemistry 277(6) (2002) 4223-31.

[14] Y. Pranoto, C.M. Lee, H.J. Park, Characterizations of fish gelatin films added with gellan and κ-carrageenan, LWT - Food Science and Technology 40(5) (2007) 766-774.

[15] S. Yamada, K. Yamamoto, T. Ikeda, K. Yanagiguchi, Y. Hayashi, Potency of Fish Collagen as a Scaffold for Regenerative Medicine, Biomed Research International (2014).

[16] T.H. Silva, J. Moreira-Silva, A.L.P. Marques, A. Domingues, Y. Bayon, R.L. Reis, Marine Origin Collagens and Its Potential Applications, Marine Drugs 12(12) (2014) 5881-5901.

[17] K. Fitzsimmons, R. Martinez-Garcia, P. Gonzalez-Alanis, Why tilapia is becoming the most important food fish on the planet, Proceedings of the 9th International Symposium on tilapia in Aquaculture, Shanghai (2011) 1-8.

[18] C.C. Lin, R. Ritch, S.M. Lin, M.-H. Ni, Y.-C. Chang, Y.L. Lu, H.J. Lai, F.-H. Lin, A New Fish Scale-Derived Scaffold for Corneal Regeneration, European Cells & Materials 19 (2010) 50-57.

[19] K. Yamamoto, K. Igawa, K. Sugimoto, Y. Yoshizawa, K. Yanagiguchi, T. Ikeda, S. Yamada, Y. Hayashi, Biological Safety of Fish (Tilapia) Collagen, Biomed Research International (2014).

[20] T. Zhou, N. Wang, Y. Xue, T. Ding, X. Liu, X. Mo, J. Sun, Electrospun tilapia collagen nanofibers accelerating wound healing via inducing keratinocytes proliferation and differentiation, Colloids Surf B Biointerfaces 143 (2016) 415-422.

[21] J. Chen, L. Li, R. Yi, N. Xu, R. Gao, B. Hong, Extraction and characterization of acid-soluble collagen from scales and skin of tilapia (Oreochromis niloticus), LWT - Food Science and Technology 66 (2016) 453-459.

[22] Q.P. Pham, U. Sharma, A.G. Mikos, Electrospinning of Polymeric Nanofibers for Tissue Engineering Applications: A Review, Tissue Engineering 12(5) (2006) 1197-1211.

[23] J. Baek, S. Sovani, N.E. Glembotski, J. Du, S. Jin, S.P. Grogan, D.D. D'Lima, Repair of Avascular Meniscus Tears with Electrospun Collagen Scaffolds Seeded with Human Cells, Tissue Eng Part A 22(5-6) (2016) 436-48.

[24] B.S. Jha, C.E. Ayres, J.R. Bowman, T.A. Telemeco, S.A. Sell, G.L. Bowlin, D.G. Simpson, Electrospun Collagen: A Tissue Engineering Scaffold with Unique Functional Properties in a Wide Variety of Applications, Journal of Nanomaterials 2011(Article ID 348268) (2011) 15.
[25] S.F. Badylak, B.N. Brown, T.W. Gilbert, Chapter II.6.16 - Tissue Engineering with Decellularized Tissues, in: B.D.R.S.H.J.S.E. Lemons (Ed.), Biomaterials Science (Third Edition), Academic Press2013, pp. 1316-1331.
[26] P.M. Crapo, T.W. Gilbert, S.F. Badylak, An overview of tissue and whole organ decellularization processes, Biomaterials 32(12) (2011) 3233-3243.
[27] T.W. Gilbert, T.L. Sellaro, S.F. Badylak, Decellularization of tissues and organs, Biomaterials 27(19) (2006) 3675-3683.
[28] G.F. Sigurjonsson, D.H. Gisladottir, G. Gudmundsson, Scaffold material for wound care and/or other tissue healing applications, Kerecis EHF, USA, 2013.
[29] N. Mieszkowska, M.J. Genner, S.J. Hawkins, D.W. Sims, Chapter 3 Effects of Climate Change and Commercial Fishing on Atlantic Cod Gadus morhua, Advances in Marine Biology, Academic Press2009, pp. 213-273.
[30] H. Sugiura, S. Yunoki, E. Kondo, T. Ikoma, J. Tanaka, K. Yasuda, In Vivo Biological Responses and Bioresorption of Tilapia Scale Collagen as a Potential Biomaterial, Journal of Biomaterials Science-Polymer Edition 20(10) (2009) 1353-1368.
[31] C. Hackett, D. McClendon, Christians remain world's largest religious group, but they are declining in Europe, 2017. http://pewrsr.ch/2o5CXFL. (Accessed 01 Feb 2019.
[32] S.P. Commins, T.A.E. Platts-Mills, Tick bites and red meat allergy, Current opinion in allergy and clinical immunology 13(4) (2013) 354-359.
[33] R. Parenteau-Bareil, R. Gauvin, F. Berthod, Collagen-Based Biomaterials for Tissue Engineering Applications, Materials 3(3) (2010) 1863.
[34] A.M. Ferreira, P. Gentile, V. Chiono, G. Ciardelli, Collagen for bone tissue regeneration, Acta Biomaterialia 8(9) (2012) 3191-3200.
[35] J. Glowacki, S. Mizuno, Collagen scaffolds for tissue engineering, Biopolymers 89(5) (2008) 338-344.
[36] W. Wagermaier, P. Fratzl, 9.03 - Collagen, in: M. Möller (Ed.), Polymer Science: A Comprehensive Reference, Elsevier, Amsterdam, 2012, pp. 35-55.
[37] A.N. Keen, A.J. Fenna, J.C. McConnell, M.J. Sherratt, P. Gardner, H.A. Shiels, Macro- and micromechanical remodelling in the fish atrium is associated with regulation of collagen 1 alpha 3 chain expression, Pflügers Archiv - European Journal of Physiology 470(8) (2018) 1205-1219.
[38] M.G. Patino, M.E. Neiders, S. Andreana, B. Noble, R.E. Cohen, Collagen: An Overview, Implant Dentistry 11(3) (2002) 280-285.
[39] K. Gelse, E. Pöschl, T. Aigner, Collagens—structure, function, and biosynthesis, Advanced Drug Delivery Reviews 55(12) (2003) 1531-1546.
[40] B. Brodsky, J.A. Ramshaw, The collagen triple-helix structure, Matrix biology : journal of the International Society for Matrix Biology 15(8-9) (1997) 545-54.
[41] W. Friess, Collagen – biomaterial for drug delivery, European Journal of Pharmaceutics and Biopharmaceutics 45(2) (1998) 113-136.
[42] B. Alberts, A. Johnson, J. Lewis, D. Morgan, M. Raff, K. Roberts, P. Walter, Molecular Biology of the Cell, Garland Science, New York, NY, USA, 2015.
[43] M.D. Shoulders, R.T. Raines, Collagen structure and stability, Annual review of biochemistry 78 (2009) 929-58.
[44] M. Saito, K. Marumo, Collagen cross-links as a determinant of bone quality: a possible explanation for bone fragility in aging, osteoporosis, and diabetes mellitus, Osteoporosis international : a journal established as result of cooperation between the European Foundation for Osteoporosis and the National Osteoporosis Foundation of the USA 21(2) (2010) 195-214.
[45] S. Ricard-Blum, F. Ruggiero, The collagen superfamily: from the extracellular matrix to the cell membrane, Pathologie-biologie 53(7) (2005) 430-42.
[46] J. Rossert, B. Decrombrugghe, Type I Collagen: Structure, Synthesis, and Regulation, in: J.P. Bilezkian, L.G. Raisz, G.A. Rodan (Eds.), Principles in Bone Biology, Academic Press, Orlando, FL, USA, 2002, pp. 189-210.
[47] N.T. Wright, J.D. Humphrey, Denaturation of collagen via heating: An irreversible rate process, Annual Review of Biomedical Engineering 4 (2002) 109-128.
[48] M. Gauza-Włodarczyk, L. Kubisz, S. Mielcarek, D. Włodarczyk, Comparison of thermal properties of fish collagen and bovine collagen in the temperature range 298–670K, Materials Science and Engineering: C 80 (2017) 468-471.
[49] I.V. Yannas, J.F. Burke, C. Huang, P.L. Gordon, Correlation of in vivo collagen degradation rate with in vitro measurements, J Biomed Mater Res 9(6) (1975) 623-8.

[50] T. Okada, T. Hayashi, Y. Ikada, Degradation of collagen suture in vitro and in vivo, Biomaterials 13(7) (1992) 448-54.
[51] I.V. Yannas, J.F. Burke, D.P. Orgill, E.M. Skrabut, Wound tissue can utilize a polymeric template to synthesize a functional extension of skin, Science (New York, N.Y.) 215(4529) (1982) 174-6.
[52] G.B. Fields, A model for interstitial collagen catabolism by mammalian collagenases, Journal of Theoretical Biology 153(4) (1991) 585-602.
[53] J.L. Lauer-Fields, G.B. Fields, Triple-helical peptide analysis of collagenolytic protease activity, Biological chemistry 383(7-8) (2002) 1095-105.
[54] A.M. Diamond, S.D. Gorham, D.J. Etherington, J.G. Robertson, N.D. Light, The effect of modification on the susceptibility of collagen to proteolysis: I. Chemical modification of amino acid side chains, Matrix (Stuttgart, Germany) 11(5) (1991) 321-9.
[55] R.F. Oliver, H. Barker, A. Cooke, R.A. Grant, Dermal collagen implants, Biomaterials 3(1) (1982) 38-40.
[56] E.A. Abou Neel, L. Bozec, J.C. Knowles, O. Syed, V. Mudera, R. Day, J.K. Hyun, Collagen — Emerging collagen based therapies hit the patient, Advanced Drug Delivery Reviews 65(4) (2013) 429-456.
[57] L. Rittie, Type I Collagen Purification from Rat Tail Tendons, Methods in molecular biology (Clifton, N.J.) 1627 (2017) 287-308.
[58] J. Parkinson, K.E. Kadler, A. Brass, Simple physical model of collagen fibrillogenesis based on diffusion limited aggregation, Journal of Molecular Biology 247(4) (1995) 823-831.
[59] C.H. Lee, A. Singla, Y. Lee, Biomedical applications of collagen, International journal of pharmaceutics 221(1-2) (2001) 1-22.
[60] N.E. Fedorovich, J. Alblas, J.R. de Wijn, W.E. Hennink, A.J. Verbout, W.J. Dhert, Hydrogels as extracellular matrices for skeletal tissue engineering: state-of-the-art and novel application in organ printing, Tissue Eng 13(8) (2007) 1905-25.
[61] G.D. Nicodemus, S.J. Bryant, Cell encapsulation in biodegradable hydrogels for tissue engineering applications, Tissue engineering. Part B, Reviews 14(2) (2008) 149-65.
[62] P.K. Sehgal, A. Srinivasan, Collagen-coated microparticles in drug delivery, Expert opinion on drug delivery 6(7) (2009) 687-95.
[63] J.L. Brown, L.S. Nair, C.T. Laurencin, Solvent/non-solvent sintering: a novel route to create porous microsphere scaffolds for tissue regeneration, Journal of biomedical materials research. Part B, Applied biomaterials 86(2) (2008) 396-406.
[64] A.G. Mikos, A.J. Thorsen, L.A. Czerwonka, Y. Bao, R. Langer, D.N. Winslow, J.P. Vacanti, Preparation and characterization of poly(l-lactic acid) foams, Polymer 35(5) (1994) 1068-1077.
[65] S.R. Chowdhury, M.F. Mh Busra, Y. Lokanathan, M.H. Ng, J.X. Law, U.C. Cletus, R. Binti Haji Idrus, Collagen Type I: A Versatile Biomaterial, Advances in experimental medicine and biology 1077 (2018) 389-414.
[66] R.A. Brown, M. Wiseman, C.B. Chuo, U. Cheema, S.N. Nazhat, Ultrarapid Engineering of Biomimetic Materials and Tissues: Fabrication of Nano- and Microstructures by Plastic Compression, Advanced Functional Materials 15(11) (2005) 1762-1770.
[67] B. Liu, X. Zhou, Freeze-drying of proteins, Methods in molecular biology (Clifton, N.J.) 1257 (2015) 459-76.
[68] M.G. Haugh, C.M. Murphy, F.J. O'Brien, Novel freeze-drying methods to produce a range of collagen-glycosaminoglycan scaffolds with tailored mean pore sizes, Tissue engineering. Part C, Methods 16(5) (2010) 887-94.
[69] F. Mb, S. Chowdhury, A. Bs, R. Idrus, Fabrication of collagen type I scaffold for skin tissue engineering, Regenerative Research 3(2) (2014) 59.
[70] T.J. Sill, H.A. von Recum, Electrospinning: Applications in drug delivery and tissue engineering, Biomaterials 29(13) (2008) 1989-2006.
[71] K.S. Weadock, E.J. Miller, L.D. Bellincampi, J.P. Zawadsky, M.G. Dunn, Physical crosslinking of collagen fibers: comparison of ultraviolet irradiation and dehydrothermal treatment, J Biomed Mater Res 29(11) (1995) 1373-9.
[72] K.S. Weadock, E.J. Miller, E.L. Keuffel, M.G. Dunn, Effect of physical crosslinking methods on collagen-fiber durability in proteolytic solutions, J Biomed Mater Res 32(2) (1996) 221-6.
[73] A. Oryan, A. Kamali, A. Moshiri, H. Baharvand, H. Daemi, Chemical crosslinking of biopolymeric scaffolds: Current knowledge and future directions of crosslinked engineered bone scaffolds, Int J Biol Macromol 107(Pt A) (2018) 678-688.
[74] F.H. Lin, C.H. Yao, J.S. Sun, H.C. Liu, C.W. Huang, Biological effects and cytotoxicity of the composite composed by tricalcium phosphate and glutaraldehyde cross-linked gelatin, Biomaterials 19(10) (1998) 905-17.

[75] L.M. Delgado, K. Fuller, D.I. Zeugolis, Collagen Cross-Linking: Biophysical, Biochemical, and Biological Response Analysis, Tissue Eng Part A 23(19-20) (2017) 1064-1077.
[76] H.G. Sundararaghavan, G.A. Monteiro, N.A. Lapin, Y.J. Chabal, J.R. Miksan, D.I. Shreiber, Genipin-induced changes in collagen gels: Correlation of mechanical properties to fluorescence, Journal of Biomedical Materials Research Part A 87A(2) (2008) 308-320.
[77] R.-N. Chen, H.-O. Ho, M.-T. Sheu, Characterization of collagen matrices crosslinked using microbial transglutaminase, Biomaterials 26(20) (2005) 4229-4235.
[78] W. Schloegl, A. Klein, R. Fürst, U. Leicht, E. Volkmer, M. Schieker, S. Jus, G.M. Guebitz, I. Stachel, M. Meyer, M. Wiggenhorn, W. Friess, Residual transglutaminase in collagen – Effects, detection, quantification, and removal, European Journal of Pharmaceutics and Biopharmaceutics 80(2) (2012) 282-288.
[79] L. Ma, C. Gao, Z. Mao, J. Zhou, J. Shen, X. Hu, C. Han, Collagen/chitosan porous scaffolds with improved biostability for skin tissue engineering, Biomaterials 24(26) (2003) 4833-4841.
[80] M.S. Hahn, B.A. Teply, M.M. Stevens, S.M. Zeitels, R. Langer, Collagen composite hydrogels for vocal fold lamina propria restoration, Biomaterials 27(7) (2006) 1104-1109.
[81] D.J. Choi, S.M. Choi, H.Y. Kang, H.-J. Min, R. Lee, M. Ikram, F. Subhan, S.W. Jin, Y.H. Jeong, J.-Y. Kwak, S. Yoon, Bioactive fish collagen/polycaprolactone composite nanofibrous scaffolds fabricated by electrospinning for 3D cell culture, J. Biotechnol. (0) (2015).
[82] Q. Zhang, S. Lv, J. Lu, S. Jiang, L. Lin, Characterization of polycaprolactone/collagen fibrous scaffolds by electrospinning and their bioactivity, International Journal of Biological Macromolecules 76(0) (2015) 94-101.
[83] T.J. Keane, L.T. Saldin, S.F. Badylak, 4 - Decellularization of mammalian tissues: Preparing extracellular matrix bioscaffolds A2 - Tomlins, Paul, Characterisation and Design of Tissue Scaffolds, Woodhead Publishing2016, pp. 75-103.
[84] M.P. Bernard, M.L. Chu, J.C. Myers, F. Ramirez, E.F. Eikenberry, D.J. Prockop, Nucleotide sequences of complementary deoxyribonucleic acids for the pro alpha 1 chain of human type I procollagen. Statistical evaluation of structures that are conserved during evolution, Biochemistry 22(22) (1983) 5213-23.
[85] F. Causa, P.A. Netti, L. Ambrosio, A multi-functional scaffold for tissue regeneration: the need to engineer a tissue analogue, Biomaterials 28(34) (2007) 5093-9.
[86] H.S. Koh, T. Yong, C.K. Chan, S. Ramakrishna, Enhancement of neurite outgrowth using nano-structured scaffolds coupled with laminin, Biomaterials 29(26) (2008) 3574-82.
[87] T.J. Keane, I.T. Swinehart, S.F. Badylak, Methods of tissue decellularization used for preparation of biologic scaffolds and in vivo relevance, Methods 84 (2015) 25-34.
[88] D.A. Taylor, L.C. Sampaio, Z. Ferdous, A.S. Gobin, L.J. Taite, Decellularized matrices in regenerative medicine, Acta Biomaterialia 74 (2018) 74-89.
[89] I. Prasertsung, S. Kanokpanont, T. Bunaprasert, V. Thanakit, S. Damrongsakkul, Development of acellular dermis from porcine skin using periodic pressurized technique, Journal of Biomedical Materials Research Part B-Applied Biomaterials 85B(1) (2008) 210-219.
[90] T.J. Keane, R. Londono, N.J. Turner, S.F. Badylak, Consequences of ineffective decellularization of biologic scaffolds on the host response, Biomaterials 33(6) (2012) 1771-81.
[91] M.H. Zheng, J. Chen, Y. Kirilak, C. Willers, J. Xu, D. Wood, Porcine small intestine submucosa (SIS) is not an acellular collagenous matrix and contains porcine DNA: possible implications in human implantation, J Biomed Mater Res B Appl Biomater 73(1) (2005) 61-7.
[92] M.T. Kasimir, E. Rieder, G. Seebacher, E. Wolner, G. Weigel, P. Simon, Presence and elimination of the xenoantigen gal (alpha1, 3) gal in tissue-engineered heart valves, Tissue Eng 11(7-8) (2005) 1274-80.
[93] S.F. Badylak, T.W. Gilbert, Immune response to biologic scaffold materials, Seminars in immunology 20(2) (2008) 109-16.
[94] L.G. Griffiths, L.H. Choe, K.F. Reardon, S.W. Dow, E. Christopher Orton, Immunoproteomic identification of bovine pericardium xenoantigens, Biomaterials 29(26) (2008) 3514-20.
[95] A. Daugs, N. Lehmann, D. Eroglu, M.C. Meinke, A. Markhoff, O. Bloch, In Vitro Detection System to Evaluate the Immunogenic Potential of Xenografts, Tissue engineering. Part C, Methods 24(5) (2018) 280-288.
[96] K. Takagi, S. Fukunaga, A. Nishi, T. Shojima, K. Yoshikawa, H. Hori, H. Akashi, S. Aoyagi, In vivo recellularization of plain decellularized xenografts with specific cell characterization in the systemic circulation: histological and immunohistochemical study, Artificial organs 30(4) (2006) 233-41.
[97] O. Gorschewsky, A. Puetz, K. Riechert, A. Klakow, R. Becker, Quantitative analysis of biochemical characteristics of bone-patellar tendon-bone allografts, Bio-medical materials and engineering 15(6) (2005) 403-11.

[98] D.O. Freytes, R.M. Stoner, S.F. Badylak, Uniaxial and biaxial properties of terminally sterilized porcine urinary bladder matrix scaffolds, J Biomed Mater Res B Appl Biomater 84(2) (2008) 408-14.
[99] W.Q. Sun, P. Leung, Calorimetric study of extracellular tissue matrix degradation and instability after gamma irradiation, Acta Biomater 4(4) (2008) 817-26.
[100] G.C.C. Mendes, T.R.S. Brandão, C.L.M. Silva, Ethylene oxide sterilization of medical devices: A review, American Journal of Infection Control 35(9) (2007) 574-581.
[101] M.F. Moreau, Y. Gallois, M.F. Basle, D. Chappard, Gamma irradiation of human bone allografts alters medullary lipids and releases toxic compounds for osteoblast-like cells, Biomaterials 21(4) (2000) 369-76.
[102] A. Md Sikin, S. S.H. Rizvi, Recent Patents on the Sterilization of Food and Biomaterials by Super-critical Fluids, Recent Patents on Food, Nutrition & Agriculture 3(3) (2011) 212-225.
[103] A.K. Dillow, F. Dehghani, J.S. Hrkach, N.R. Foster, R. Langer, Bacterial inactivation by using near- and supercritical carbon dioxide, Proceedings of the National Academy of Sciences 96(18) (1999) 10344.
[104] K. Sawada, D. Terada, T. Yamaoka, S. Kitamura, T. Fujisato, Cell removal with supercritical carbon dioxide for acellular artificial tissue, Journal of Chemical Technology & Biotechnology 83(6) (2008) 943-949.
[105] A. Bernhardt, M. Wehrl, B. Paul, T. Hochmuth, M. Schumacher, K. Schütz, M. Gelinsky, Improved Sterilization of Sensitive Biomaterials with Supercritical Carbon Dioxide at Low Temperature, PloS one 10(6) (2015) e0129205-e0129205.
[106] R. Parenteau-Bareil, R. Gauvin, S. Cliche, C. Gariépy, L. Germain, F. Berthod, Comparative study of bovine, porcine and avian collagens for the production of a tissue engineered dermis, Acta Biomaterialia 7(10) (2011) 3757-3765.
[107] H. Yang, Z. Shu, The extraction of collagen protein from pigskin, Journal of Chemical and Pharmaceutical Research 6(2) (2014) 683-687.
[108] Y.K. Lin, D.C. Liu, Comparison of physical–chemical properties of type I collagen from different species, Food Chemistry 99(2) (2006) 244-251.
[109] H. Li, B.L. Liu, L.Z. Gao, H.L. Chen, Studies on bullfrog skin collagen, Food Chemistry 84(1) (2004) 65-69.
[110] F.-Y. Cheng, F.-W. Hsu, H.-S. Chang, L.-C. Lin, R. Sakata, Effect of different acids on the extraction of pepsin-solubilised collagen containing melanin from silky fowl feet, Food Chemistry 113(2) (2009) 563-567.
[111] P. Hashim, M. Ridzwan, J. Bakar, Isolation and Characterization of Collagen from Chicken Feet, International Journal of Biological, Food, Veterinary and Agricultural Engineering 8(3) (2014) 242-246.
[112] S. Addad, J.Y. Exposito, C. Faye, S. Ricard-Blum, C. Lethias, Isolation, characterization and biological evaluation of jellyfish collagen for use in biomedical applications, Mar Drugs 9(6) (2011) 967-83.
[113] L.T. Minh Thuy, E. Okazaki, K. Osako, Isolation and characterization of acid-soluble collagen from the scales of marine fishes from Japan and Vietnam, Food Chemistry 149(0) (2014) 264-270.
[114] P. Kittiphattanabawon, S. Benjakul, W. Visessanguan, H. Kishimura, F. Shahidi, Isolation and Characterisation of collagen from the skin of brownbanded bamboo shark (Chiloscyllium punctatum), Food Chemistry 119(4) (2010) 1519-1526.
[115] S. Vesentini, A. Redaelli, A. Gautieri, Nanomechanics of collagen microfibrils, Muscles, ligaments and tendons journal 3(1) (2013) 23-34.
[116] M.C. Gómez-Guillén, B. Giménez, M.E. López-Caballero, M.P. Montero, Functional and bioactive properties of collagen and gelatin from alternative sources: A review, Food Hydrocolloids 25(8) (2011) 1813-1827.
[117] F.H. Silver, G. Pins, Cell growth on collagen: a review of tissue engineering using scaffolds containing extracellular matrix, Journal of long-term effects of medical implants 2(1) (1992) 67-80.
[118] A.A. Karim, R. Bhat, Fish gelatin: properties, challenges, and prospects as an alternative to mammalian gelatins, Food Hydrocolloids 23(3) (2009) 563-576.
[119] J.W. Steinke, T.A.E. Platts-Mills, S.P. Commins, The alpha-gal story: Lessons learned from connecting the dots, The Journal of allergy and clinical immunology 135(3) (2015) 589-596.
[120] G. Crispell, S.P. Commins, S.A. Archer-Hartman, S. Choudhary, G. Dharmarajan, P. Azadi, S. Karim, Discovery of Alpha-Gal-Containing Antigens in North American Tick Species Believed to Induce Red Meat Allergy, Frontiers in immunology 10 (2019) 1056.
[121] M. Kwak, C. Somerville, S. van Nunen, A novel Australian tick Ixodes (Endopalpiger) australiensis inducing mammalian meat allergy after tick bite, Asia Pac Allergy 8(3) (2018) e31-e31.
[122] F. DeLustro, S.T. Smith, J. Sundsmo, G. Salem, S. Kincaid, L. Ellingsworth, Reaction to injectable collagen: results in animal models and clinical use, Plastic and reconstructive surgery 79(4) (1987) 581-94.

[123] C. Yang, P.J. Hillas, J.A. Báez, M. Nokelainen, J. Balan, J. Tang, R. Spiro, J.W. Polarek, The Application of Recombinant Human Collagen in Tissue Engineering, BioDrugs 18(2) (2004) 103-119.
[124] O. Shoseyov, Y. Posen, F. Grynspan, Human recombinant type I collagen produced in plants, Tissue Eng Part A 19(13-14) (2013) 1527-33.
[125] X. Xu, Q. Gan, R.C. Clough, K.M. Pappu, J.A. Howard, J.A. Baez, K. Wang, Hydroxylation of recombinant human collagen type I alpha 1 in transgenic maize co-expressed with a recombinant human prolyl 4-hydroxylase, BMC biotechnology 11 (2011) 69.
[126] W. Liu, J.A. Burdick, G.J. van Osch, Plant-derived recombinant human collagen: a strategic approach for generating safe human ECM-based scaffold, Tissue Eng Part A 19(13-14) (2013) 1489-90.
[127] K.V. Kumar, K.P. Sai, M. Babu, Application of frog (Rana tigerina Daudin) skin collagen as a novel substrate in cell culture, J Biomed Mater Res 61(2) (2002) 197-202.
[128] Y. Yang, C. Li, G. Qian, [Isolation, purification of collagen from soft-shelled turtle calipash for application in biomaterial], Sheng wu gong cheng xue bao = Chinese journal of biotechnology 32(6) (2016) 819-830.
[129] T.J.C. Beebee, R.A. Griffiths, The amphibian decline crisis: A watershed for conservation biology?, Biological Conservation 125(3) (2005) 271-285.
[130] M.W. Klemens, J.B. Thorbjarnarson, Reptiles as a food resource, Biodiversity & Conservation 4(3) (1995) 281-298.
[131] L. Day, Protein: Food Sources, in: B. Caballero, P.M. Finglas, F. Toldrá (Eds.), Encyclopedia of Food and Health, Academic Press, Oxford, 2016, pp. 530-537.
[132] J.A. Arnesen, A. Gildberg, Extraction of muscle proteins and gelatine from cod head, Process Biochemistry 41(3) (2006) 697-700.
[133] S. Kimura, X.-P. Zhu, R. Matsui, M. Shijoh, S. Takamizawa, Characterization of Fish Muscle Type I Collagen, Journal of Food Science 53(5) (1988) 1315-1318.
[134] I.J. Haug, K.I. Draget, O. Smidsrød, Physical and rheological properties of fish gelatin compared to mammalian gelatin, Food Hydrocolloids 18(2) (2004) 203-213.
[135] N. Nagai, K. Mori, Y. Satoh, N. Takahashi, S. Yunoki, K. Tajima, M. Munekata, In vitro growth and differentiated activities of human periodontal ligament fibroblasts cultured on salmon collagen gel, Journal of Biomedical Materials Research Part A 82A(2) (2007) 395-402.
[136] M.A. Moore, B. Samsell, G. Wallis, S. Triplett, S. Chen, A.L. Jones, X. Qin, Decellularization of human dermis using non-denaturing anionic detergent and endonuclease: a review, Cell and Tissue Banking 16(2) (2015) 249-259.
[137] J.-C. Luo, W. Chen, X.-H. Chen, T.-W. Qin, Y.-C. Huang, H.-Q. Xie, X.-Q. Li, Z.-Y. Qian, Z.-M. Yang, A multi-step method for preparation of porcine small intestinal submucosa (SIS), Biomaterials 32(3) (2011) 706-713.
[138] D.C. Sullivan, S.-H. Mirmalek-Sani, D.B. Deegan, P.M. Baptista, T. Aboushwareb, A. Atala, J.J. Yoo, Decellularization methods of porcine kidneys for whole organ engineering using a high-throughput system, Biomaterials 33(31) (2012) 7756-7764.
[139] D.W. Courtman, C.A. Pereira, V. Kashef, D. McComb, J.M. Lee, G.J. Wilson, Development of a Pericardial Acellular Matrix Biomaterial - Biochemical and Mechanical Effects of Cell Extraction, Journal of Biomedical Materials Research 28(6) (1994) 655-666.
[140] L. Mancuso, A. Gualerzi, F. Boschetti, F. Loy, G. Cao, Decellularized ovine arteries as small-diameter vascular grafts, Biomedical Materials 9(4) (2014) 045011.
[141] J.M. Wilson, T.A.E. Platts-Mills, Meat allergy and allergens, Molecular Immunology 100 (2018) 107-112.
[142] S.A. Safley, H. Cui, S.M.D. Cauffiel, B.Y. Xu, J.R. Wright, C.J. Weber, Encapsulated piscine (tilapia) islets for diabetes therapy: studies in diabetic NOD and NOD-SCID mice, Xenotransplantation 21(2) (2014) 127-139.
[143] D.J. White, Fish islet xenografts, Xenotransplantation 21(2) (2014) 124-126.
[144] J.R. Wright, Jr., S. Polvi, H. MacLean, Experimental transplantation with principal islets of teleost fish (Brockmann bodies). Long-term function of tilapia islet tissue in diabetic nude mice, Diabetes 41(12) (1992) 1528-32.
[145] J.R. Wright, Jr., H. Yang, O. Hyrtsenko, B.Y. Xu, W. Yu, B. Pohajdak, A review of piscine islet xenotransplantation using wild-type tilapia donors and the production of transgenic tilapia expressing a "humanized" tilapia insulin, Xenotransplantation 21(6) (2014) 485-95.
[146] D. Hos, T.H. van Essen, F. Bock, C.H. Chou, H.A. Pan, C.C. Lin, M.C. Huang, S.C. Chen, C. Cursiefen, M.J. Jager, Decellularized collagen matrix from tilapia fish scales for corneal reconstruction (BioCornea), Ophthalmologe 111(11) (2014) 1027-1032.

[147] T.H. van Essen, C.C. Lin, A.K. Hussain, S. Maas, H.J. Lai, H. Linnartz, T.J.T.P. van den Berg, D.C.F. Salvatori, G.P.M. Luyten, M.J. Jager, A Fish Scale-Derived Collagen Matrix as Artificial Cornea in Rats: Properties and Potential, Investigative Ophthalmology & Visual Science 54(5) (2013) 3224-3233.
[148] F. Yuan, L. Wang, C.-C. Lin, C.-H. Chou, L. Li, A Cornea Substitute Derived from Fish Scale: 6-Month Followup on Rabbit Model, Journal of Ophthalmology (2014).
[149] C.-H. Chou, Y.-G. Chen, C.-C. Lin, S.-M. Lin, K.-C. Yang, S.-H. Chang, Bioabsorbable Fish Scale for the Internal Fixation of Fracture: A Preliminary Study, Tissue Engineering Part A 20(17-18) (2014) 2493-2502.
[150] B.T. Baldursson, H. Kjartansson, F. Konradsdottir, P. Gudnason, G.F. Sigurjonsson, S.H. Lund, Healing Rate and Autoimmune Safety of Full-Thickness Wounds Treated With Fish Skin Acellular Dermal Matrix Versus Porcine Small-Intestine Submucosa: A Noninferiority Study, International Journal of Lower Extremity Wounds 14(1) (2015) 37-43.
[151] S. Magnusson, B.T. Baldursson, H. Kjartansson, O. Rolfsson, G.F. Sigurjonsson, Regenerative and Antibacterial Properties of Acellular Fish Skin Grafts and Human Amnion/Chorion Membrane: Implications for Tissue Preservation in Combat Casualty Care, Military Medicine 182 (2017) 383-388.
[152] E.M. Lima Júnior, M.O.d. Moraes Filho, M.J.B.d. Miranda, N.S. Piccolo, Tilapia skin processing method and use thereof for covering skin injuries, Companhia Energética Do Ceará - Coelce, Brazil, 2017.
[153] V. Reyma, N. Kumar, A. Sharma, D.D. Mathew, M. Negi, S. Maiti, S. Shrivastava, N. Kurade, Bone marrow derived cell-seeded extracellular matrix: a novel biomaterial in the field of wound management, Veterinary World 7(11) (2014) 1019-1025.
[154] W.C.W. Chen, Z. Wang, M.A. Missinato, D.W. Park, D.W. Long, H.-J. Liu, X. Zeng, N.A. Yates, K. Kim, Y. Wang, Decellularized zebrafish cardiac extracellular matrix induces mammalian heart regeneration, Science Advances 2(11) (2016).
[155] R.F. Sîrbulescu, G.K.H. Zupanc, Spinal cord repair in regeneration-competent vertebrates: Adult teleost fish as a model system, Brain Research Reviews 67(1) (2011) 73-93.
[156] D.D. Manning, N.D. Reed, C.F. Shaffer, MAINTENANCE OF SKIN XENOGRAFTS OF WIDELY DIVERGENT PHYLOGENETIC ORIGIN ON CONGENITALLY ATHYMIC (NUDE) MICE, The Journal of Experimental Medicine 138(2) (1973) 488-494.
[157] K. Jacyniak, R.P. McDonald, M.K. Vickaryous, Tail regeneration and other phenomena of wound healing and tissue restoration in lizards, The Journal of experimental biology 220(Pt 16) (2017) 2858-2869.
[158] S.J. Shieh, T.C. Cheng, Regeneration and repair of human digits and limbs: fact and fiction, Regeneration (Oxford, England) 2(4) (2015) 149-68.
[159] P.W. Whitlock, T.L. Smith, G.G. Poehling, J.S. Shilt, M. Van Dyke, A naturally derived, cytocompatible, and architecturally optimized scaffold for tendon and ligament regeneration, Biomaterials 28(29) (2007) 4321-4329.
[160] F.K. Farahani, H. Fattahian, A.-M. Kajbafzade, Experimental Study on Ostrich Acellular Dermal Matrix in Repair of Full-Thickness Wounds of Guinea Pig, Kafkas Universitesi Veteriner Fakultesi Dergisi 21(5) (2015) 697-702.
[161] A. Mahara, S. Somekawa, N. Kobayashi, Y. Hirano, Y. Kimura, T. Fujisato, T. Yamaoka, Tissue-engineered acellular small diameter long-bypass grafts with neointima-inducing activity, Biomaterials 58(Supplement C) (2015) 54-62.
[162] X.N. Liu, X.P. Zhu, J. Wu, Z.J. Wu, Y. Yin, X.H. Xiao, X. Su, B. Kong, S.Y. Pan, H. Yang, Y. Cheng, N. An, S.L. Mi, Acellular ostrich corneal stroma used as scaffold for construction of tissue-engineered cornea, International journal of ophthalmology 9(3) (2016) 325-31.
[163] S. HOSSEINI, S. HASANZADEH, R. SHAHROOZ, TISSUE ENGINEERING AND HISTOLOGY OF OSTRICH TENDON, (2015).
[164] J.B. West, R.R. Watson, Z. Fu, The human lung: did evolution get it wrong?, European Respiratory Journal 29(1) (2007) 11.
[165] D.J. Weiss, S. Wrenn, 158 - Avian Lung Decellularization, Cytotherapy 18(6, Supplement) (2016) S94.
[166] Q. Bone, Biology of fishes, 3rd ed., Taylor & Francis, New York, NY, USA, 2008.
[167] T.M. Berra, Freshwater Fish Distribution, University of Chicago Press, Chicago, IL, USA, 2008.
[168] P. Alestrom, H.C. Winther-Larsen, 7 - Zebrafish offer aquaculture research their services, in: S. MacKenzie, S. Jentoft (Eds.), Genomics in Aquaculture, Academic Press, San Diego, 2016, pp. 165-194.
[169] J. Bakar, K.W. Tan, M. R. Umi Hartina, A. Ahmad, Gelatins from three cultured freshwater fish skins obtained by liming process, 2011.
[170] S. Rakers, M. Gebert, S. Uppalapati, W. Meyer, P. Maderson, A.F. Sell, C. Kruse, R. Paus, 'Fish matters': the relevance of fish skin biology to investigative dermatology, Experimental dermatology 19(4) (2010) 313-24.

[171] D.G. Elliott, Microscopic functional anatomy: Integumentary system: Chapter 17, in: K.O. Gary (Ed.), The laboratory fish, Academic Press2000, pp. 271-306.
[172] S. Rakers, L. Niklasson, D. Steinhagen, C. Kruse, J. Schauber, K. Sundell, R. Paus, Antimicrobial peptides (AMPs) from fish epidermis: perspectives for investigative dermatology, The Journal of investigative dermatology 133(5) (2013) 1140-9.
[173] T. Ikoma, H. Kobayashi, J. Tanaka, D. Walsh, S. Mann, Microstructure, mechanical, and biomimetic properties of fish scales from Pagrus major, Journal of structural biology 142(3) (2003) 327-33.
[174] Y.S. Lin, C.T. Wei, E.A. Olevsky, M.A. Meyers, Mechanical properties and the laminate structure of Arapaima gigas scales, J Mech Behav Biomed Mater 4(7) (2011) 1145-56.
[175] N. Suzuki, K.-i. Kitamura, A. Hattori, Fish scale is a suitable model for analyzing determinants of skeletal fragility in type 2 diabetes, Endocrine 54(3) (2016) 575-577.
[176] D.G. Elliott, Gross functional anatomy: Integumentary system: Chapter 5, in: K.O. Gary (Ed.), The laboratory fish, Academic Press2000, pp. 95-108.
[177] S. Subramanian, S.L. MacKinnon, N.W. Ross, A comparative study on innate immune parameters in the epidermal mucus of various fish species, Comparative biochemistry and physiology. Part B, Biochemistry & molecular biology 148(3) (2007) 256-63.
[178] J. Ruangsri, J.M. Fernandes, M. Brinchmann, V. Kiron, Antimicrobial activity in the tissues of Atlantic cod (Gadus morhua L.), Fish & shellfish immunology 28(5-6) (2010) 879-86.
[179] Y. Iger, M. Abraham, The process of skin healing in experimentally wounded carp, Journal of Fish Biology 36(3) (1990) 421-437.
[180] S.H. Zigmond, Recent quantitative studies of actin filament turnover during cell locomotion, Cell motility and the cytoskeleton 25(4) (1993) 309-16.
[181] G. Csucs, K. Quirin, G. Danuser, Locomotion of fish epidermal keratocytes on spatially selective adhesion patterns, Cell motility and the cytoskeleton 64(11) (2007) 856-67.
[182] M.Á. Esteban, A. Cuesta, E. Chaves-Pozo, J. Meseguer, Phagocytosis in Teleosts. Implications of the New Cells Involved, Biology 4(4) (2015) 907-922.
[183] A.P. Summers, J.H. Long Jr, Skin and Bones, Sinew and Gristle: the Mechanical Behavior of Fish Skeletal Tissues, Fish Physiology, Academic Press2005, pp. 141-177.
[184] L. Szewciw, F. Barthelat, Mechanical properties of striped bass fish skin: Evidence of an exotendon function of the stratum compactum, Journal of the Mechanical Behavior of Biomedical Materials 73 (2017) 28-37.
[185] S.W.A. Himaya, S.-K. Kim, Functional Proteins and Peptides from Fish Skin, in: S.-K. Kim (Ed.), Seafood Processing By-Products: Trends and Applications, Springer New York, New York, NY, 2014, pp. 197-205.
[186] J. Venkatesan, S. Anil, S.-K. Kim, M.S. Shim, Marine Fish Proteins and Peptides for Cosmeceuticals: A Review, Marine drugs 15(5) (2017) 143.
[187] S.W.A. Himaya, B. Ryu, D.-H. Ngo, S.-K. Kim, Peptide Isolated from Japanese Flounder Skin Gelatin Protects against Cellular Oxidative Damage, Journal of Agricultural and Food Chemistry 60(36) (2012) 9112-9119.
[188] S.K. Kim, Marine cosmeceuticals, J Cosmet Dermatol 13(1) (2014) 56-67.
[189] S.-K. Kim, Y.D. Ravichandran, S.B. Khan, Y.T. Kim, Prospective of the cosmeceuticals derived from marine organisms, Biotechnology and Bioprocess Engineering 13(5) (2008) 511-523.
[190] E. Xhauflaire-Uhoda, K. Fontaine, G.E. Pierard, Kinetics of moisturizing and firming effects of cosmetic formulations, International journal of cosmetic science 30(2) (2008) 131-8.
[191] S.-K. Kim, I. Wijesekara, Development and biological activities of marine-derived bioactive peptides: A review, Journal of Functional Foods 2(1) (2010) 1-9.
[192] B. Ryu, Z.J. Qian, S.K. Kim, SHP-1, a novel peptide isolated from seahorse inhibits collagen release through the suppression of collagenases 1 and 3, nitric oxide products regulated by NF-kappaB/p38 kinase, Peptides 31(1) (2010) 79-87.
[193] B. Ryu, Z.J. Qian, S.K. Kim, Purification of a peptide from seahorse, that inhibits TPA-induced MMP, iNOS and COX-2 expression through MAPK and NF-kappaB activation, and induces human osteoblastic and chondrocytic differentiation, Chemico-biological interactions 184(3) (2010) 413-22.
[194] B.-H. Li, Y.-B. Zhou, S.-B. Guo, C.-b. Wang, Polypeptide from Chlamys farreri inhibits UVB-induced HaCaT cells apoptosis via inhibition CD95 pathway and reactive oxygen species, 2007.
[195] H. Hou, B. Li, Z. Zhang, C. Xue, G. Yu, J. Wang, Y. Bao, L. Bu, J. Sun, Z. Peng, S. Su, Moisture absorption and retention properties, and activity in alleviating skin photodamage of collagen polypeptide from marine fish skin, Food Chem 135(3) (2012) 1432-9.
[196] R. Song, R.-B. Wei, H.-Y. Luo, D.-F. Wang, Isolation and characterization of an antibacterial peptide fraction from the pepsin hydrolysate of half-fin anchovy (Setipinna taty), Molecules (Basel, Switzerland) 17(3) (2012) 2980-2991.

[197] B. Pena-Mendoza, J.L. Gomez-Marquez, I.H. Salgado-Ugarte, D. Ramirez-Noguera, Reproductive biology of Oreochromis niloticus (Perciformes: Cichlidae) at Emiliano Zapata dam, Morelos, Mexico, Revista de biologia tropical 53(3-4) (2005) 515-22.
[198] M.J. Armstrong, H.D. Gerritsen, M. Allen, W.J. McCurdy, J.A.D. Peel, Variability in maturity and growth in a heavily exploited stock: cod (Gadus morhua L.) in the Irish Sea, ICES Journal of Marine Science 61(1) (2004) 98-112.
[199] S.-k. Zeng, C.-h. Zhang, H. Lin, P. Yang, P.-z. Hong, Z. Jiang, Isolation and characterisation of acid-solubilised collagen from the skin of Nile tilapia (Oreochromis niloticus), Food Chemistry 116(4) (2009) 879-883.
[200] A.A. El-Rashidy, A. Gad, A.E.-H.G. Abu-Hussein, S.I. Habib, N.A. Badr, A.A. Hashem, Chemical and biological evaluation of Egyptian Nile Tilapia (Oreochromis niloticas) fish scale collagen, International Journal of Biological Macromolecules 79 (2015) 618-626.
[201] C.-Y. Huang, J.-M. Kuo, S.-J. Wu, H.-T. Tsai, Isolation and characterization of fish scale collagen from tilapia (Oreochromis sp.) by a novel extrusion–hydro-extraction process, Food Chemistry 190 (2016) 997-1006.
[202] J. Tang, T. Saito, Biocompatibility of Novel Type I Collagen Purified from Tilapia Fish Scale: An In Vitro Comparative Study, Biomed Research International (2015).
[203] H.-H. Hsu, T. Uemura, I. Yamaguchi, T. Ikoma, J. Tanaka, Chondrogenic differentiation of human mesenchymal stem cells on fish scale collagen, Journal of Bioscience and Bioengineering 122(2) (2016) 219-225.
[204] J. Lee, G. Tae, Y.H. Kim, I.S. Park, S.-H. Kim, S.H. Kim, The effect of gelatin incorporation into electrospun poly(l-lactide-co-ε-caprolactone) fibers on mechanical properties and cytocompatibility, Biomaterials 29(12) (2008) 1872-1879.
[205] B. Ghorani, N. Tucker, Fundamentals of electrospinning as a novel delivery vehicle for bioactive compounds in food nanotechnology, Food Hydrocolloids 51 (2015) 227-240.
[206] D.H. Reneker, A.L. Yarin, Electrospinning jets and polymer nanofibers, Polymer 49(10) (2008) 2387-2425.
[207] A. Formhals, Process and apparatus for preparing artificial threads, Richard Schreiber Gastell, USA, 1934.
[208] T. Subbiah, G.S. Bhat, R.W. Tock, S. Parameswaran, S.S. Ramkumar, Electrospinning of nanofibers, Journal of Applied Polymer Science 96(2) (2005) 557-569.
[209] D. Annis, A. Bornat, R.O. Edwards, A. Higham, B. Loveday, J. Wilson, AN ELASTOMERIC VASCULAR PROSTHESIS, ASAIO Journal 24(1) (1978) 209-214.
[210] J.A. Matthews, G.E. Wnek, D.G. Simpson, G.L. Bowlin, Electrospinning of collagen nanofibers, Biomacromolecules 3(2) (2002) 232-238.
[211] L. Huang, K. Nagapudi, R.P. Apkarian, E.L. Chaikof, Engineered collagen-PEO nanofibers and fabrics, Journal of Biomaterials Science-Polymer Edition 12(9) (2001) 979-993.
[212] C.M. Timperley, Chapter 29 - Highly-toxic fluorine compounds, in: R.E. Banks (Ed.), Fluorine Chemistry at the Millennium, Elsevier Science Ltd, Oxford, 2000, pp. 499-538.
[213] T. Liu, W.K. Teng, B.P. Chan, S.Y. Chew, Photochemical crosslinked electrospun collagen nanofibers: synthesis, characterization and neural stem cell interactions, Journal of biomedical materials research. Part A 95(1) (2010) 276-82.
[214] A. Fiorani, C. Gualandi, S. Panseri, M. Montesi, M. Marcacci, M.L. Focarete, A. Bigi, Comparative performance of collagen nanofibers electrospun from different solvents and stabilized by different crosslinkers, J Mater Sci Mater Med 25(10) (2014) 2313-21.
[215] V.Y. Chakrapani, A. Gnanamani, V.R. Giridev, M. Madhusoothanan, G. Sekaran, Electrospinning of type I collagen and PCL nanofibers using acetic acid, Journal of Applied Polymer Science 125(4) (2012) 3221-3227.
[216] B. Dong, O. Arnoult, M.E. Smith, G.E. Wnek, Electrospinning of collagen nanofiber scaffolds from benign solvents, Macromolecular rapid communications 30(7) (2009) 539-42.
[217] S.Y. Bak, G.J. Yoon, S.W. Lee, H.W. Kim, Effect of humidity and benign solvent composition on electrospinning of collagen nanofibrous sheets, Materials Letters 181 (2016) 136-139.
[218] F. Pati, B. Adhikari, S. Dhara, Isolation and characterization of fish scale collagen of higher thermal stability, Bioresource Technology 101(10) (2010) 3737-3742.
[219] P. Timpson, E.J. McGhee, Z. Erami, M. Nobis, J.A. Quinn, M. Edward, K.I. Anderson, Organotypic collagen I assay: a malleable platform to assess cell behaviour in a 3-dimensional context, Journal of visualized experiments : JoVE (56) (2011) e3089.
[220] J.H. Highberger, The Isoelectric Point of Collagen, Journal of the American Chemical Society 61(9) (1939) 2302-2303.

[221] H.X. Liu, R.S. Zhang, X.J. Yao, M.C. Liu, Z.D. Hu, B.T. Fan, Prediction of the isoelectric point of an amino acid based on GA-PLS and SVMs, Journal of chemical information and computer sciences 44(1) (2004) 161-7.
[222] C. Gistelinck, R. Gioia, A. Gagliardi, F. Tonelli, L. Marchese, L. Bianchi, C. Landi, L. Bini, A. Huysseune, P.E. Witten, A. Staes, K. Gevaert, N. De Rocker, B. Menten, F. Malfait, S. Leikin, S. Carra, R. Tenni, A. Rossi, A. De Paepe, P. Coucke, A. Willaert, A. Forlino, Zebrafish Collagen Type I: Molecular and Biochemical Characterization of the Major Structural Protein in Bone and Skin, Scientific Reports 6 (2016) 21540.
[223] T. Potaros, N. Raksakulthai, J. Runglerdkreangkrai, W. Worawattanamateekul, Characteristics of collagen from Nile Tilapia (Oreochromis niloticus) skin isolated by two different methods, Kasetsart J (Nat Sci) 43(3) (2009) 584-593.
[224] T. Ikoma, H. Kobayashi, J. Tanaka, D. Walsh, S. Mann, Physical properties of type I collagen extracted from fish scales of Pagrus major and Oreochromis niloticas, International Journal of Biological Macromolecules 32(3–5) (2003) 199-204.
[225] P. Chandika, S.C. Ko, G.W. Oh, S.Y. Heo, V.T. Nguyen, Y.J. Jeon, B. Lee, C.H. Jang, G. Kim, W.S. Park, W. Chang, I.W. Choi, W.K. Jung, Fish collagen/alginate/chitooligosaccharides integrated scaffold for skin tissue regeneration application, Int J Biol Macromol 81 (2015) 504-13.
[226] D.R. Eyre, M. Weis, D.M. Hudson, J.-J. Wu, L. Kim, A Novel 3-Hydroxyproline (3Hyp)-rich Motif Marks the Triple-helical C Terminus of Tendon Type I Collagen, Journal of Biological Chemistry 286(10) (2011) 7732-7736.
[227] Phosphate-buffered saline (PBS), Cold Spring Harbor Protocols 2006(1) (2006) pdb.rec8247.
[228] A. Bigi, G. Cojazzi, S. Panzavolta, K. Rubini, N. Roveri, Mechanical and thermal properties of gelatin films at different degrees of glutaraldehyde crosslinking, Biomaterials 22(8) (2001) 763-768.
[229] A.J. Kuijpers, G.H.M. Engbers, J. Feijen, S.C. De Smedt, T.K.L. Meyvis, J. Demeester, J. Krijgsveld, S.A.J. Zaat, J. Dankert, Characterization of the Network Structure of Carbodiimide Cross-Linked Gelatin Gels, Macromolecules 32(10) (1999) 3325-3333.
[230] D.I. Zeugolis, S.T. Khew, E.S.Y. Yew, A.K. Ekaputra, Y.W. Tong, L.Y.L. Yung, D.W. Hutmacher, C. Sheppard, M. Raghunath, Electro-spinning of pure collagen nano-fibres - Just an expensive way to make gelatin?, Biomaterials 29(15) (2008) 2293-2305.
[231] A. Ozcelikkale, B. Han, Thermal Destabilization of Collagen Matrix Hierarchical Structure by Freeze/Thaw, PLOS ONE 11(1) (2016) e0146660.
[232] E. Leikina, M.V. Mertts, N. Kuznetsova, S. Leikin, Type I collagen is thermally unstable at body temperature, Proc Natl Acad Sci U S A 99(3) (2002) 1314-8.
[233] A. Gopinath, S.M. Reddy, B. Madhan, G. Shanmguam, J.R. Rao, Effect of aqueous ethanol on the triple helical structure of collagen, European biophysics journal : EBJ 43(12) (2014) 643-52.
[234] K.I. Kivirikko, Chapter 9 Posttranslational processing of collagens, in: E.E. Bittar, N. Bittar (Eds.), Principles of Medical Biology, Elsevier1996, pp. 233-254.
[235] B. Standards, Biological evaluation of medical devices - Part 5: Tests for in vitro cytotoxicity (ISO 10993-5:2009), 2009.
[236] C.G. Scanes, P. Chengzhong, Chapter 11 - Animals and Religion, Belief Systems, Symbolism and Myth, in: C.G. Scanes, S.R. Toukhsati (Eds.), Animals and Human Society, Academic Press2018, pp. 257-280.
[237] A.K. Chakravarti, Regional Preference for Food: Some Aspects of Food Habit Patterns in India, The Canadian Geographer / Le Géographe canadien 18(4) (1974) 395-410.
[238] S. Boylan, Zoonoses Associated with Fish, Veterinary Clinics of North America: Exotic Animal Practice 14(3) (2011) 427-438.
[239] V. Kumar, N. Kumar, A.K. Gangwar, H. Singh, R. Singh, Comparative histologic and immunologic evaluation of 1,4-butanediol diglycidyl ether crosslinked versus noncrosslinked acellular swim bladder matrix for healing of full-thickness skin wounds in rabbits, Journal of Surgical Research 197(2) (2015) 436-446.
[240] A.H. Fischer, K.A. Jacobson, J. Rose, R. Zeller, Hematoxylin and eosin staining of tissue and cell sections, CSH protocols 2008 (2008) pdb.prot4986.
[241] F. Rusconi, E. Valton, R. Nguyen, E. Dufourc, Quantification of sodium dodecyl sulfate in microliter-volume biochemical samples by visible light spectroscopy, Anal Biochem 295(1) (2001) 31-7.
[242] C.M. Morrison, K. Fitzsimmons, J.R.J. Wright, Atlas of Tilapia Histology, The World Aquaculture Society, Baton Rouge, Louisiana, United States, 2006.
[243] K.S. Stenn, R. Link, G. Moellmann, J. Madri, E. Kuklinska, Dispase, a neutral protease from Bacillus polymyxa, is a powerful fibronectinase and type IV collagenase, The Journal of investigative dermatology 93(2) (1989) 287-90.
[244] A. Mansour, M.A. Mezour, Z. Badran, F. Tamimi, Extracellular Matrices for Bone Regeneration: A Literature Review, Tissue Eng Part A 23(23-24) (2017) 1436-1451.

[245] H. Yan, V. Solozobova, P. Zhang, O. Armant, B. Kuehl, G. Brenner-Weiss, C. Blattner, p53 is active in murine stem cells and alters the transcriptome in a manner that is reminiscent of mutant p53, Cell death & disease 6(2) (2015) e1662-e1662.
[246] S. Hamm, A. Heit, M. Koffler, K.M. Huster, S. Akira, D.H. Busch, H. Wagner, S. Bauer, Immunostimulatory RNA is a potent inducer of antigen-specific cytotoxic and humoral immune response in vivo, International Immunology 19(3) (2007) 297-304.
[247] D. Bastian, H. Borel, T. Sasaki, A.D. Steinberg, Y. Borel, Immune response to nucleic acid antigens and native DNA by human peripheral blood lymphocytes in vitro, Journal of immunology (Baltimore, Md. : 1950) 135(3) (1985) 1772-7.
[248] L.J. White, A.J. Taylor, D.M. Faulk, T.J. Keane, L.T. Saldin, J.E. Reing, I.T. Swinehart, N.J. Turner, B.D. Ratner, S.F. Badylak, The impact of detergents on the tissue decellularization process: A ToF-SIMS study, Acta biomaterialia 50 (2017) 207-219.
[249] M.X. Pan, P.Y. Hu, Y. Cheng, L.Q. Cai, X.H. Rao, Y. Wang, Y. Gao, An efficient method for decellularization of the rat liver, Journal of the Formosan Medical Association 113(10) (2014) 680-687.
[250] P.F. Gratzer, R.D. Harrison, T. Woods, Matrix alteration and not residual sodium dodecyl sulfate cytotoxicity affects the cellular repopulation of a decellularized matrix, Tissue Eng 12(10) (2006) 2975-83.
[251] A. Gilpin, Y. Yang, Decellularization Strategies for Regenerative Medicine: From Processing Techniques to Applications, BioMed research international 2017 (2017) 9831534-9831534.
[252] S.M. Mithieux, A.S. Weiss, Elastin, Advances in Protein Chemistry, Academic Press2005, pp. 437-461.
[253] D.A.D. Parry, J.M. Squire, Fibrous Proteins: New Structural and Functional Aspects Revealed, Advances in Protein Chemistry, Academic Press2005, pp. 1-10.
[254] D.H. Lee, J.-H. Oh, J.H. Chung, Glycosaminoglycan and proteoglycan in skin aging, Journal of Dermatological Science 83(3) (2016) 174-181.
[255] S.G. Wise, A.S. Weiss, Tropoelastin, The International Journal of Biochemistry & Cell Biology 41(3) (2009) 494-497.
[256] G.C. Yeo, F.W. Keeley, A.S. Weiss, Coacervation of tropoelastin, Advances in colloid and interface science 167(1-2) (2011) 94-103.
[257] S. Ghatak, E.V. Maytin, J.A. Mack, V.C. Hascall, I. Atanelishvili, R. Moreno Rodriguez, R.R. Markwald, S. Misra, Roles of Proteoglycans and Glycosaminoglycans in Wound Healing and Fibrosis, International Journal of Cell Biology 2015 (2015) 20.
[258] R.C. Hill, E.A. Calle, M. Dzieciatkowska, L.E. Niklason, K.C. Hansen, Quantification of extracellular matrix proteins from a rat lung scaffold to provide a molecular readout for tissue engineering, Mol Cell Proteomics 14(4) (2015) 961-973.
[259] M.D. Naresh, V. Arumugam, R. Sanjeevi, Mechanical behaviour of shark skin, Journal of Biosciences 22(4) (1997) 431-437.
[260] E. Jacquet, J. Chambert, J. Pauchot, P. Sandoz, Intra- and inter-individual variability in the mechanical properties of the human skin from in vivo measurements on 20 volunteers, Skin research and technology : official journal of International Society for Bioengineering and the Skin (ISBS) [and] International Society for Digital Imaging of Skin (ISDIS) [and] International Society for Skin Imaging (ISSI) 23(4) (2017) 491-499.
[261] H.G. Vogel, Directional variations of mechanical parameters in rat skin depending on maturation and age, The Journal of investigative dermatology 76(6) (1981) 493-7.
[262] M.E. Grear, M.R. Motley, S.B. Crofts, A.E. Witt, A.P. Summers, P. Ditsche, Mechanical properties of harbor seal skin and blubber − a test of anisotropy, Zoology 126 (2018) 137-144.
[263] C. Escoffier, J. de Rigal, A. Rochefort, R. Vasselet, J.L. Leveque, P.G. Agache, Age-related mechanical properties of human skin: an in vivo study, The Journal of investigative dermatology 93(3) (1989) 353-7.
[264] D.M. Adelman, J.C. Selber, C.E. Butler, Bovine versus Porcine Acellular Dermal Matrix: A Comparison of Mechanical Properties, Plast Reconstr Surg Glob Open 2(5) (2014) e155.
[265] A. Ní Annaidh, K. Bruyère, M. Destrade, M.D. Gilchrist, M. Otténio, Characterization of the anisotropic mechanical properties of excised human skin, Journal of the Mechanical Behavior of Biomedical Materials 5(1) (2012) 139-148.
[266] P.A. Norowski, S. Mishra, P.C. Adatrow, W.O. Haggard, J.D. Bumgardner, Suture pullout strength and in vitro fibroblast and RAW 264.7 monocyte biocompatibility of genipin crosslinked nanofibrous chitosan mats for guided tissue regeneration, Journal of biomedical materials research. Part A 100(11) (2012) 2890-6.
[267] H. Su, K.Y. Liu, A. Karydis, D.G. Abebe, C. Wu, K.M. Anderson, N. Ghadri, P. Adatrow, T. Fujiwara, J.D. Bumgardner, In vitro and in vivo evaluations of a novel post-electrospinning treatment to improve

the fibrous structure of chitosan membranes for guided bone regeneration, Biomed Mater 12(1) (2016) 015003.
[268] T.R. Cox, J.T. Erler, Remodeling and homeostasis of the extracellular matrix: implications for fibrotic diseases and cancer, Disease models & mechanisms 4(2) (2011) 165-178.
[269] R.V. Davalos, Irreversible Electroporation to Create Tissue Scaffolds, Virginia Tech Intellectual Properties Inc, 2009.
[270] A.R. Deipolyi, A. Golberg, M.L. Yarmush, R.S. Arellano, R. Oklu, Irreversible electroporation: evolution of a laboratory technique in interventional oncology, Diagnostic and interventional radiology (Ankara, Turkey) 20(2) (2014) 147-54.
[271] E.L. Sandvik, B.R. McLeod, A.E. Parker, P.S. Stewart, Direct electric current treatment under physiologic saline conditions kills Staphylococcus epidermidis biofilms via electrolytic generation of hypochlorous acid, PLoS One 8(2) (2013) e55118.
[272] D.F. Williams, Tissue-biomaterial interactions, Journal of Materials Science 22(10) (1987) 3421-3445.
[273] J.M. Morais, F. Papadimitrakopoulos, D.J. Burgess, Biomaterials/tissue interactions: possible solutions to overcome foreign body response, AAPS J 12(2) (2010) 188-96.
[274] J.M. Anderson, A.K. McNally, Biocompatibility of implants: lymphocyte/macrophage interactions, Semin Immunopathol 33(3) (2011) 221-33.
[275] D.T. Luttikhuizen, M.C. Harmsen, M.J. Van Luyn, Cellular and molecular dynamics in the foreign body reaction, Tissue Eng 12(7) (2006) 1955-70.
[276] J.M. Anderson, Biological Responses to Materials, Annual Review of Materials Research 31(1) (2001) 81-110.
[277] M.T. Kasimir, E. Rieder, G. Seebacher, A. Nigisch, B. Dekan, E. Wolner, G. Weigel, P. Simon, Decellularization does not eliminate thrombogenicity and inflammatory stimulation in tissue-engineered porcine heart valves, J Heart Valve Dis 15(2) (2006) 278-86; discussion 286.
[278] W. Li, J. Zhou, Y. Xu, Study of the in vitro cytotoxicity testing of medical devices, Biomedical reports 3(5) (2015) 617-620.
[279] X. Liu, D.P. Rodeheaver, J.C. White, A.M. Wright, L.M. Walker, F. Zhang, S. Shannon, A comparison of in vitro cytotoxicity assays in medical device regulatory studies, Regulatory Toxicology and Pharmacology 97 (2018) 24-32.
[280] Z. Xia, J.T. Triffitt, A review on macrophage responses to biomaterials, Biomed Mater 1(1) (2006) R1-9.
[281] M. Viney, L. Lazarou, S. Abolins, The laboratory mouse and wild immunology, Parasite Immunology 37(5) (2015) 267-273.
[282] L. Tao, T.A. Reese, Making Mouse Models That Reflect Human Immune Responses, Trends in Immunology 38(3) (2017) 181-193.
[283] R.J. Schutte, L. Xie, B. Klitzman, W.M. Reichert, In vivo cytokine-associated responses to biomaterials, Biomaterials 30(2) (2009) 160-168.
[284] S.W. Kim, J. Roh, C.S. Park, Immunohistochemistry for Pathologists: Protocols, Pitfalls, and Tips, Journal of pathology and translational medicine 50(6) (2016) 411-418.
[285] H.W. Schroeder, Jr., L. Cavacini, Structure and function of immunoglobulins, The Journal of allergy and clinical immunology 125(2 Suppl 2) (2010) S41-52.
[286] U. Galili, The alpha-Gal epitope (Galalpha1-3Galbeta1-4GlcNAc-R) in xenotransplantation, Biochimie 83(7) (2001) 557-63.
[287] F. Naso, A. Gandaglia, L. Iop, M. Spina, G. Gerosa, Alpha-Gal detectors in xenotransplantation research: a word of caution, Xenotransplantation 19(4) (2012) 215-20.
[288] I.M. McMorrow, C.A. Comrack, D.H. Sachs, H. DerSimonian, Heterogeneity of human anti-pig natural antibodies cross-reactive with the Gal(alpha1,3)Galactose epitope, Transplantation 64(3) (1997) 501-10.
[289] S.N. Rampersad, Multiple applications of Alamar Blue as an indicator of metabolic function and cellular health in cell viability bioassays, Sensors (Basel, Switzerland) 12(9) (2012) 12347-60.
[290] J.A. Jansen, J.E. Deruijter, P.T.M. Janssen, Y.G.G.J. Paquay, Histological-Evaluation of a Biodegradable Polyactive(R)/Hydroxyapatite Membrane, Biomaterials 16(11) (1995) 819-827.
[291] W. Ji, F. Yang, H. Seyednejad, Z. Chen, W.E. Hennink, J.M. Anderson, J.J.J.P. van den Beucken, J.A. Jansen, Biocompatibility and degradation characteristics of PLGA-based electrospun nanofibrous scaffolds with nanoapatite incorporation, Biomaterials 33(28) (2012) 6604-6614.
[292] S. Zhao, E.M. Pinholt, J.E. Madsen, K. Donath, Histological evaluation of different biodegradable and non-biodegradable membranes implanted subcutaneously in rats, J Craniomaxillofac Surg 28(2) (2000) 116-22.
[293] N.U. Zitzmann, R. Naef, P. Scharer, Resorbable versus nonresorbable membranes in combination with Bio-Oss for guided bone regeneration, The International journal of oral & maxillofacial implants 12(6) (1997) 844-52.

[294] A. Tincani, L. Andreoli, C. Bazzani, D. Bosiso, S. Sozzani, Inflammatory molecules: A target for treatment of systemic autoimmune diseases, Autoimmunity Reviews 7(1) (2007) 1-7.
[295] S.A. JONES, S. HORIUCHI, N. TOPLEY, N. YAMAMOTO, G.M. FULLER, The soluble interleukin 6 receptor: mechanisms of production and implications in disease, The FASEB Journal 15(1) (2001) 43-58.
[296] O. Boyman, J. Sprent, The role of interleukin-2 during homeostasis and activation of the immune system, Nat Rev Immunol 12(3) (2012) 180-190.
[297] S.L. Deshmane, S. Kremlev, S. Amini, B.E. Sawaya, Monocyte Chemoattractant Protein-1 (MCP-1): An Overview, Journal of Interferon & Cytokine Research 29(6) (2009) 313-326.
[298] G. Lopez-Castejon, D. Brough, Understanding the mechanism of IL-1β secretion, Cytokine & Growth Factor Reviews 22(4) (2011) 189-195.
[299] K.N. Couper, D.G. Blount, E.M. Riley, IL-10: The Master Regulator of Immunity to Infection, The Journal of Immunology 180(9) (2008) 5771-5777.
[300] A. Bhattacharjee, M. Shukla, V.P. Yakubenko, A. Mulya, S. Kundu, M.K. Cathcart, IL-4 and IL-13 employ discrete signaling pathways for target gene expression in alternatively activated monocytes/macrophages, Free Radical Biology and Medicine 54 (2013) 1-16.
[301] M. Shibuya, Vascular Endothelial Growth Factor (VEGF) and Its Receptor (VEGFR) Signaling in Angiogenesis: A Crucial Target for Anti- and Pro-Angiogenic Therapies, Genes & Cancer 2(12) (2011) 1097-1105.
[302] C. Gretzer, L. Emanuelsson, E. Liljensten, P. Thomsen, The inflammatory cell influx and cytokines changes during transition from acute inflammation to fibrous repair around implanted materials, Journal of biomaterials science. Polymer edition 17(6) (2006) 669-87.
[303] M.L. Jarman-Smith, T. Bodamyali, C. Stevens, J.A. Howell, M. Horrocks, J.B. Chaudhuri, Porcine collagen crosslinking, degradation and its capability for fibroblast adhesion and proliferation, J Mater Sci Mater Med 15(8) (2004) 925-32.
[304] G.T. Richter, J.E. Smith, H.J. Spencer, C.Y. Fan, E. Vural, Histological comparison of implanted cadaveric and porcine dermal matrix grafts, Otolaryngology--head and neck surgery : official journal of American Academy of Otolaryngology-Head and Neck Surgery 137(2) (2007) 239-42.
[305] J.M. Anderson, Chapter II.2.2 - Inflammation, Wound Healing, and the Foreign-Body Response, in: B.D. Ratner, A.S. Hoffman, F.J. Schoen, J.E. Lemons (Eds.), Biomaterials Science (Third Edition), Academic Press2013, pp. 503-512.
[306] M.L. Wong, L.G. Griffiths, Immunogenicity in xenogeneic scaffold generation: antigen removal vs. decellularization, Acta Biomater 10(5) (2014) 1806-16.
[307] Y. Liu, J. Lim, S.-H. Teoh, Review: Development of clinically relevant scaffolds for vascularised bone tissue engineering, Biotechnology Advances 31(5) (2013) 688-705.
[308] A. Khojasteh, L. Kheiri, S.R. Motamedian, V. Khoshkam, Guided Bone Regeneration for the Reconstruction of Alveolar Bone Defects, Annals of maxillofacial surgery 7(2) (2017) 263-277.
[309] M. Retzepi, N. Donos, Guided Bone Regeneration: biological principle and therapeutic applications, Clin Oral Implants Res 21(6) (2010) 567-76.
[310] T.B. Johnson, B. Siderits, S. Nye, Y.-H. Jeong, S.-H. Han, I.-C. Rhyu, J.-S. Han, T. Deguchi, F.M. Beck, D.-G. Kim, Effect of guided bone regeneration on bone quality surrounding dental implants, Journal of Biomechanics 80 (2018) 166-170.
[311] M.C. Bottino, V. Thomas, G. Schmidt, Y.K. Vohra, T.-M.G. Chu, M.J. Kowolik, G.M. Janowski, Recent advances in the development of GTR/GBR membranes for periodontal regeneration—A materials perspective, Dent Mater 28(7) (2012) 703-721.
[312] Y.D. Rakhmatia, Y. Ayukawa, A. Furuhashi, K. Koyano, Current barrier membranes: Titanium mesh and other membranes for guided bone regeneration in dental applications, Journal of Prosthodontic Research 57(1) (2013) 3-14.
[313] N.D. Evans, R.O.C. Oreffo, E. Healy, P.J. Thurner, Y.H. Man, Epithelial mechanobiology, skin wound healing, and the stem cell niche, Journal of the Mechanical Behavior of Biomedical Materials 28 (2013) 397-409.
[314] A.S. Halim, T.L. Khoo, S.J. Mohd. Yussof, Biologic and synthetic skin substitutes: An overview, Indian Journal of Plastic Surgery : Official Publication of the Association of Plastic Surgeons of India 43(Suppl) (2010) S23-S28.
[315] J.S. Boateng, K.H. Matthews, H.N.E. Stevens, G.M. Eccleston, Wound healing dressings and drug delivery systems: A review, Journal of Pharmaceutical Sciences 97(8) (2008) 2892-2923.
[316] A.G. Haddad, G. Giatsidis, D.P. Orgill, E.G. Halvorson, Skin Substitutes and Bioscaffolds: Temporary and Permanent Coverage, Clinics in Plastic Surgery 44(3) (2017) 627-634.
[317] H. Debels, M. Hamdi, K. Abberton, W. Morrison, Dermal matrices and bioengineered skin substitutes: a critical review of current options, Plast Reconstr Surg Glob Open 3(1) (2015) e284.

[318] Q.P. Pham, U. Sharma, A.G. Mikos, Electrospun poly(epsilon-caprolactone) microfiber and multilayer nanofiber/microfiber scaffolds: characterization of scaffolds and measurement of cellular infiltration, Biomacromolecules 7(10) (2006) 2796-805.
[319] S. Sell, C. Barnes, D. Simpson, G. Bowlin, Scaffold permeability as a means to determine fiber diameter and pore size of electrospun fibrinogen, Journal of biomedical materials research. Part A 85(1) (2008) 115-26.
[320] K.J. Livak, T.D. Schmittgen, Analysis of relative gene expression data using real-time quantitative PCR and the 2(-Delta Delta C(T)) Method, Methods 25(4) (2001) 402-8.
[321] P.P. Spicer, J.D. Kretlow, S. Young, J.A. Jansen, F.K. Kasper, A.G. Mikos, Evaluation of bone regeneration using the rat critical size calvarial defect, Nature protocols 7(10) (2012) 1918-29.
[322] L. Dunn, H.C. Prosser, J.T. Tan, L.Z. Vanags, M.K. Ng, C.A. Bursill, Murine model of wound healing, Journal of visualized experiments : JoVE (75) (2013) e50265.
[323] M.H.E. Hermans, R.P. Hermans, Duoderm, an alternative dressing for smaller burns, Burns 12(3) (1986) 214-219.
[324] R. Vasita, I.K. Shanmugam, D.S. Katt, Improved biomaterials for tissue engineering applications: surface modification of polymers, Current topics in medicinal chemistry 8(4) (2008) 341-53.
[325] L. Vikingsson, B. Claessens, J.A. Gomez-Tejedor, G. Gallego Ferrer, J.L. Gomez Ribelles, Relationship between micro-porosity, water permeability and mechanical behavior in scaffolds for cartilage engineering, J Mech Behav Biomed Mater 48 (2015) 60-69.
[326] A. Basu, J. Lindh, E. Alander, M. Stromme, N. Ferraz, On the use of ion-crosslinked nanocellulose hydrogels for wound healing solutions: Physicochemical properties and application-oriented biocompatibility studies, Carbohydr Polym 174 (2017) 299-308.
[327] M.S. Agren, C.J. Taplin, J.F. Woessner, Jr., W.H. Eaglstein, P.M. Mertz, Collagenase in wound healing: effect of wound age and type, The Journal of investigative dermatology 99(6) (1992) 709-14.
[328] A. Kozlovsky, G. Aboodi, O. Moses, H. Tal, Z. Artzi, M. Weinreb, C.E. Nemcovsky, Bio-degradation of a resorbable collagen membrane (Bio-Gide®) applied in a double-layer technique in rats, Clinical Oral Implants Research 20(10) (2009) 1116-1123.
[329] D.F. Williams, On the mechanisms of biocompatibility, Biomaterials 29(20) (2008) 2941-2953.
[330] T. Angwarawong, S.T. Dubas, M. Arksornnukit, P. Pavasant, Differentiation of MC3T3-E1 on poly(4-styrenesulfonic acid-co-maleic acid)sodium salt-coated films, Dent Mater J 30(2) (2011) 158-69.
[331] T.A. Owen, M. Aronow, V. Shalhoub, L.M. Barone, L. Wilming, M.S. Tassinari, M.B. Kennedy, S. Pockwinse, J.B. Lian, G.S. Stein, Progressive development of the rat osteoblast phenotype in vitro: reciprocal relationships in expression of genes associated with osteoblast proliferation and differentiation during formation of the bone extracellular matrix, Journal of cellular physiology 143(3) (1990) 420-30.
[332] S. Chen, L. Chen, A. Jahangiri, B. Chen, Y. Wu, H.H. Chuang, C. Qin, M. MacDougall, Expression and processing of small integrin-binding ligand N-linked glycoproteins in mouse odontoblastic cells, Archives of oral biology 53(9) (2008) 879-89.
[333] P.V. Hauschka, J.B. Lian, D.E. Cole, C.M. Gundberg, Osteocalcin and matrix Gla protein: vitamin K-dependent proteins in bone, Physiological reviews 69(3) (1989) 990-1047.
[334] G.R. Beck, Jr., B. Zerler, E. Moran, Phosphate is a specific signal for induction of osteopontin gene expression, Proceedings of the National Academy of Sciences of the United States of America 97(15) (2000) 8352-8357.
[335] Z.-K. Kuo, P.-L. Lai, E.K.-W. Toh, C.-H. Weng, H.-W. Tseng, P.-Z. Chang, C.-C. Chen, C.-M. Cheng, Osteogenic differentiation of preosteoblasts on a hemostatic gelatin sponge, Scientific Reports 6 (2016) 32884.
[336] K.G. Lee, K.S. Lee, Y.J. Kang, J.H. Hwang, S.H. Lee, S.H. Park, Y. Park, Y.S. Cho, B.K. Lee, Rabbit Calvarial Defect Model for Customized 3D-Printed Bone Grafts, Tissue engineering. Part C, Methods 24(5) (2018) 255-262.
[337] J.P. Schmitz, J.O. Hollinger, The critical size defect as an experimental model for craniomandibulofacial nonunions, Clinical orthopaedics and related research (205) (1986) 299-308.
[338] Z. Han, M. Bhavsar, L. Leppik, K.M.C. Oliveira, J.H. Barker, Histological Scoring Method to Assess Bone Healing in Critical Size Bone Defect Models, Tissue engineering. Part C, Methods 24(5) (2018) 272-279.
[339] Z.S. Patel, S. Young, Y. Tabata, J.A. Jansen, M.E. Wong, A.G. Mikos, Dual delivery of an angiogenic and an osteogenic growth factor for bone regeneration in a critical size defect model, Bone 43(5) (2008) 931-40.
[340] G.M. Harris, I. Raitman, J.E. Schwarzbauer, Chapter 5 - Cell-derived decellularized extracellular matrices, in: R.P. Mecham (Ed.), Methods in Cell Biology, Academic Press2018, pp. 97-114.

[341] L. Yang, J.D. Harding, A.V. Ivanov, N. Ramasubramanyan, D.D. Dong, Effect of cleaning agents and additives on Protein A ligand degradation and chromatography performance, Journal of chromatography. A 1385 (2015) 63-8.
[342] S. Onder, E. David, O. Tacal, L.M. Schopfer, O. Lockridge, Hupresin Retains Binding Capacity for Butyrylcholinesterase and Acetylcholinesterase after Sanitation with Sodium Hydroxide, Frontiers in pharmacology 8 (2017) 713.
[343] M.V. Clement, J. Ramalingam, L.H. Long, B. Halliwell, The in vitro cytotoxicity of ascorbate depends on the culture medium used to perform the assay and involves hydrogen peroxide, Antioxidants & redox signaling 3(1) (2001) 157-63.
[344] P.L. Roberts, D. Lloyd, Virus inactivation by protein denaturants used in affinity chromatography, Biologicals : journal of the International Association of Biological Standardization 35(4) (2007) 343-7.
[345] D. Liu, G. Wei, T. Li, J. Hu, N. Lu, J.M. Regenstein, P. Zhou, Effects of alkaline pretreatments and acid extraction conditions on the acid-soluble collagen from grass carp (Ctenopharyngodon idella) skin, Food Chem 172 (2015) 836-43.
[346] I. Pastar, O. Stojadinovic, M. Tomic-Canic, Role of keratinocytes in healing of chronic wounds, Surgical technology international 17 (2008) 105-12.
[347] I.A. Darby, B. Laverdet, F. Bonte, A. Desmouliere, Fibroblasts and myofibroblasts in wound healing, Clinical, cosmetic and investigational dermatology 7 (2014) 301-11.
[348] B. Li, J.H. Wang, Fibroblasts and myofibroblasts in wound healing: force generation and measurement, J Tissue Viability 20(4) (2011) 108-20.
[349] H. Sengyoku, T. Tsuchiya, T. Obata, R. Doi, Y. Hashimoto, M. Ishii, H. Sakai, N. Matsuo, D. Taniguchi, T. Suematsu, M. Lawn, K. Matsumoto, T. Miyazaki, T. Nagayasu, Sodium hydroxide based non-detergent decellularizing solution for rat lung, Organogenesis 14(2) (2018) 94-106.
[350] K. Jarbrink, G. Ni, H. Sonnergren, A. Schmidtchen, C. Pang, R. Bajpai, J. Car, Prevalence and incidence of chronic wounds and related complications: a protocol for a systematic review, Systematic reviews 5(1) (2016) 152.
[351] P. Zahedi, I. Rezaeian, S.-O. Ranaei-Siadat, S.-H. Jafari, P. Supaphol, A review on wound dressings with an emphasis on electrospun nanofibrous polymeric bandages, Polymers for Advanced Technologies 21(2) (2010) 77-95.
[352] U. Boer, A. Lohrenz, M. Klingenberg, A. Pich, A. Haverich, M. Wilhelmi, The effect of detergent-based decellularization procedures on cellular proteins and immunogenicity in equine carotid artery grafts, Biomaterials 32(36) (2011) 9730-7.
[353] K.V. Gates, A.J. Dalgliesh, L.G. Griffiths, Antigenicity of Bovine Pericardium Determined by a Novel Immunoproteomic Approach, Scientific Reports 7(1) (2017) 2446.
[354] W.W. So, W.N. Liu, K.N. Leung, Omega-3 Polyunsaturated Fatty Acids Trigger Cell Cycle Arrest and Induce Apoptosis in Human Neuroblastoma LA-N-1 Cells, Nutrients 7(8) (2015) 6956-73.
[355] J.W. Alexander, D.M. Supp, Role of Arginine and Omega-3 Fatty Acids in Wound Healing and Infection, Advances in wound care 3(11) (2014) 682-690.
[356] A. Trampuz, A.F. Widmer, Infections associated with orthopedic implants, Current opinion in infectious diseases 19(4) (2006) 349-56.
[357] R.J. José, J.S. Brown, Opportunistic bacterial, viral and fungal infections of the lung, Medicine 44(6) (2016) 378-383.
[358] E. Reverchon, I. De Marco, Supercritical fluid extraction and fractionation of natural matter, The Journal of Supercritical Fluids 38(2) (2006) 146-166.
[359] G. Brunner, Supercritical fluids: technology and application to food processing, Journal of Food Engineering 67(1) (2005) 21-33.
[360] FAO, The State of World Fisheries and Aquaculture 2018 - Meeting the sustainable development goals, Food and Agriculture Organization of the United Nations, Rome, 2018.
[361] A.J. Engler, S. Sen, H.L. Sweeney, D.E. Discher, Matrix Elasticity Directs Stem Cell Lineage Specification, Cell 126(4) (2006) 677-689.
[362] M. Chen, M. Przyborowski, F. Berthiaume, Stem cells for skin tissue engineering and wound healing, Critical reviews in biomedical engineering 37(4-5) (2009) 399-421.
[363] P. Bainbridge, Wound healing and the role of fibroblasts, Journal of wound care 22(8) (2013) 407-8, 410-12.
[364] J.W. Park, S.R. Hwang, I.-S. Yoon, Advanced Growth Factor Delivery Systems in Wound Management and Skin Regeneration, Molecules (Basel, Switzerland) 22(8) (2017) 1259.